

April 2009

# Design of Low Cost Modular Robotic Manipulator Joints

Colin McCarthy

*Worcester Polytechnic Institute*

Jonathan D. Baldiga

*Worcester Polytechnic Institute*

Shivahn M. Fitzell

*Worcester Polytechnic Institute*

Thomas Branton Watson

*Worcester Polytechnic Institute*

Follow this and additional works at: <https://digitalcommons.wpi.edu/mqp-all>

---

## Repository Citation

McCarthy, C., Baldiga, J. D., Fitzell, S. M., & Watson, T. B. (2009). *Design of Low Cost Modular Robotic Manipulator Joints*. Retrieved from <https://digitalcommons.wpi.edu/mqp-all/2295>

This Unrestricted is brought to you for free and open access by the Major Qualifying Projects at Digital WPI. It has been accepted for inclusion in Major Qualifying Projects (All Years) by an authorized administrator of Digital WPI. For more information, please contact [digitalwpi@wpi.edu](mailto:digitalwpi@wpi.edu).

Design of Low Cost Modular Robotic Manipulator Joints

A Major Qualifying Project Report

Submitted to the Faculty

of the

WORCESTER POLYTECHNIC INSTITUTE

in partial fulfillment of the requirements for the

Degree of Bachelor of Science

in Mechanical Engineering

by

---

Jonathan Baldiga

---

Shivahn Fitzell

---

Colin McCarthy

---

Thomas Watson

Date: April 28<sup>th</sup>, 2009

Approved:

---

Prof. Cobb, Major Advisor

---

Prof. Looft, Co-Advisor

---

Prof. Looft, Co-Advisor

Keywords:

1. Modular joints
2. Inexpensive robotics
3. Infinite rotation

## **Abstract**

The goal of this project was to design and manufacture robotic joints that are inexpensive and capable of being used in a variety of applications. In order to maximize the number of applications in which our design could be utilized, research was done on optimal strength, size, communications, modularity, and price. This project includes the research and design development necessary to engineer such a joint, including part selection, motor control, manufacturing processes, and strength analysis. Two Joints were constructed and tested: a rotator joint and a elbow-joint. The joints performed well under testing conditions and overall prices were kept low. With future development, these joints could be used in fields where size and price are critical.

## Acknowledgements

We would like to thank the following individuals for their contributions to this report:

Professor Cobb (ME)

For his assistance and feedback throughout the project

Professor Looft (ECE)

For his motivation and creation of this project

Professor Padir (RBE)

For his contributions and dedication to feedback

Professor Ciaraldi (CS)

For his wealth of fresh ideas and extensive help with programming

Adam Sears

For machining many of our parts

Neil Whitehouse

For aiding in the construction of our prototypes

Russ Morin

For his help with rapid prototyping and Solidworks expertise

# Contents

<b>ABSTRACT</b> .....	<b>I</b>
<b>ACKNOWLEDGEMENTS</b> .....	<b>II</b>
<b>1 INTRODUCTION</b> .....	<b>7</b>
1.1 MODULARITY.....	7
1.2 COST VS CAPABILITY .....	8
1.3 GOAL.....	9
<b>2 BACKGROUND</b> .....	<b>11</b>
2.1 MOTION OF JOINTS .....	11
2.1.1 <i>RoboFlex</i> .....	12
2.1.2 <i>Robotic Wrist Patent</i> .....	13
2.1.3 <i>Double Universal Joint</i> .....	14
2.1.4 <i>Ultrasonic Motors</i> .....	16
2.2 MODULARITY AND COMMUNICATION .....	18
2.2.1 <i>Development of Modular Robot Joint</i> .....	18
2.2.2 <i>Unidrive Modular Joint</i> .....	20
2.2.3 <i>Snake Robot</i> .....	22
2.2.4 <i>Electrical Component/Communication Research</i> .....	23
2.2.5 <i>Manipulability and Redundancy Control of Robotic Mechanisms</i> .....	23
2.3 MARKET FEASIBILITY .....	24
2.3.1 <i>PowerCube</i> .....	24
2.3.2 <i>Research Robotics</i> .....	25
2.3.3 <i>Unimate Mark II PUMA Robot</i> .....	26
<b>3 PROJECT OBJECTIVES</b> .....	<b>33</b>
<b>4 DESIGN SPECIFICATIONS</b> .....	<b>34</b>
<b>5 PRELIMINARY DESIGN CONCEPTS</b> .....	<b>35</b>
5.1 ELBOW-JOINT ITERATION 01 .....	37
5.1.1.....	37
5.1.2 <i>Kinematics</i> .....	38
5.1.3 <i>Iteration 01 Torque Analysis</i> .....	39
5.1.5 <i>Iteration 01 Stress Analysis</i> .....	41
5.1.6 <i>Iteration 01 Part Selection</i> .....	51
5.1.7 <i>Iteration 01 Discussion</i> .....	54
5.2 ROTATOR-JOINT ITERATION 01 .....	55
5.2.1 <i>Kinematics</i> .....	55
5.2.2 <i>Iteration 01 Components</i> .....	56
5.2.3 <i>Iteration 01 Inertia Calculations and Motor Selection</i> .....	57
5.2.4 <i>Iteration 01 Stress Analysis</i> .....	57
5.2.5 <i>Iteration 01 Part Selection</i> .....	62
5.3 ELECTRICAL SYSTEMS ITERATION 01 .....	64
5.4 ELBOW-JOINT PRE-PROTOTYPING .....	67
5.5 ELBOW-JOINT ITERATION 02 .....	69
5.5.1 <i>Kinematics</i> .....	70
5.5.2 <i>Iteration 02 Stress Analysis</i> .....	70
5.5.3 <i>Iteration 02 Part Selection</i> .....	76
5.5.4 <i>Construction of Prototype</i> .....	78
5.5.5 <i>Iteration 02 Discussion</i> .....	78
5.6 ROTATOR-JOINT ITERATION 02 .....	79
5.6.1 <i>Kinematics</i> .....	80
5.6.2 <i>Iteration 02 Components</i> .....	80
5.6.3 <i>Iteration 02 Stress Analysis</i> .....	81
5.6.4 <i>Iteration 02 Part Selection</i> .....	86

5.6.6	Construction of Prototype.....	88
5.7	ELECTRICAL SYSTEMS ITERATION 02 .....	90
<b>6</b>	<b>DETAILED DESIGN .....</b>	<b>93</b>
6.1	ELBOW-JOINT ITERATION 03 .....	93
6.1.1	Kinematics .....	95
6.1.2	Iteration 03 Stress Analysis.....	96
6.1.3	Iteration 03 Motion Analysis.....	106
6.1.4	Iteration 03 Part Selection.....	108
6.1.5	Iteration 03 Cost Estimate .....	110
6.1.6	Iteration 03 Discussion .....	113
6.2	ROTATOR-JOINT ITERATION 03 .....	114
6.2.1	Kinematics .....	114
6.2.2	Iteration 03 Components.....	115
6.2.3	Iteration 03 Stress Analysis.....	116
6.2.4	Iteration 03 Motion Analysis.....	123
6.2.5	Iteration 03 Part Selection.....	125
6.2.6	Iteration 03 Cost Estimate .....	125
6.2.7	Iteration 03 Discussion .....	128
6.3	ELECTRICAL SYSTEMS ITERATION 03 .....	129
6.3.1	Optical Encoder Module .....	131
6.3.2	Communications .....	133
6.3.3	IrDA Communications.....	136
6.4	POWER SUPPLY .....	138
<b>7</b>	<b>PROTOTYPE CONSTRUCTION.....</b>	<b>140</b>
7.1	ELBOW CONSTRUCTION.....	140
7.2	ROTATOR CONSTRUCTION.....	140
<b>8</b>	<b>PROTOTYPE TESTING.....</b>	<b>142</b>
8.1	TESTING PROCEDURE .....	142
8.1.1	Accuracy/Repeatability .....	142
8.1.2	Strength.....	143
8.1.3	Product Life.....	145
8.1.4	IR communication .....	145
8.1.5	Power Transmission .....	145
8.2	TESTING RESULTS .....	146
8.2.1	Strength Testing.....	146
8.2.2	Accuracy/Repeatability and Product Life Testing.....	150
<b>9</b>	<b>CONCLUSIONS.....</b>	<b>151</b>
9.1	PROJECT SUMMARY .....	151
<b>10</b>	<b>RECOMMENDATIONS.....</b>	<b>152</b>
10.1	ELBOW-JOINT .....	152
10.2	ROTATOR-JOINT .....	153
10.3	BASE FIXTURE .....	157
10.4	ELECTRONIC CONTROL SYSTEMS .....	157
10.5	PARTS/MANUFACTURING .....	162
10.5.1	Elbow Joint .....	164
10.5.2	Rotator Joint.....	165
10.6	TESTING.....	165
<b>11</b>	<b>BIBLIOGRAPHY.....</b>	<b>166</b>
	<b>APPENDIX A – WEIGHTED TASK SPECIFICATIONS .....</b>	<b>168</b>
	<b>APPENDIX B – MOTOR SELECTION MATRIX.....</b>	<b>172</b>
	<b>APPENDIX C – CALCULATIONS FOR SECURING THE MITER GEAR .....</b>	<b>176</b>
	<b>APPENDIX D – FULL TESTING DATA .....</b>	<b>177</b>
	<b>ROTATOR-JOINT TEST RESULTS .....</b>	<b>177</b>

<b><i>ELBOW-JOINT TEST RESULTS</i></b> .....	<b>180</b>
<b>APPENDIX E – PRELIMINARY INFORMATION GATHERING:</b> .....	<b>181</b>
<b>APPENDIX F – VENDOR SPEC SHEETS (ELECTRICAL SYSTEMS ITERATION 01) :</b> .....	<b>182</b>
<b>APPENDIX G – VENDOR SPEC SHEETS (ELECTRICAL SYSTEMS ITERATION 02):</b> .....	<b>186</b>
<b>APPENDIX H – VENDOR SPEC SHEETS (ELECTRICAL SYSTEMS FINAL) :</b> .....	<b>190</b>
<b>APPENDIX I – CODE LISTINGS :</b> .....	<b>199</b>
<b>APPENDIX J – ELBOW JOINT ITERATION 01 EXPLODED/SECTIONED VIEW</b> .....	<b>217</b>
<b>APPENDIX K – ELBOW JOINT ITERATION 02 EXPLODED/SECTIONED VIEW</b> .....	<b>218</b>
<b>APPENDIX L – ELBOW JOINT ITERATION 03 LABELED ISOMETRIC VIEW</b> .....	<b>220</b>
<b>APPENDIX M –ELBOW JOINT ITERATION 03 LABELED SECTIONED VIEW</b> .....	<b>221</b>
<b>APPENDIX N – ELBOW JOINT ITERATION 03 LABELED EXPLODED VIEW</b> .....	<b>222</b>
<b>APPENDIX O – ELBOW JOINT ITERATION 03 COMPONENTS</b> .....	<b>223</b>
<b>APPENDIX P – ROTATOR JOINT ITERATION 01 EXPLODED VIEW</b> .....	<b>231</b>
<b>APPENDIX Q – ROTATOR JOINT ITERATION 02 EXPLODED VIEW</b> .....	<b>232</b>
<b>APPENDIX R – ROTATOR JOINT ITERATION 03 ISOMETRIC VIEW</b> .....	<b>233</b>
<b>APPENDIX S – ROTATOR JOINT ITERATION 03 EXPLODED VIEW</b> .....	<b>234</b>
<b>APPENDIX T – ROTATOR JOINT ITERATION 03 SECTION VIEW</b> .....	<b>235</b>
<b>APPENDIX U – ROTATOR JOINT ITERATION 03 COMPONENTS</b> .....	<b>236</b>
<b>APPENDIX V – MACHINING PROCESS CALCULATION SHEET (WPI FSAE TEAM)</b> .....	<b>243</b>
<b>APPENDIX W – DETAILED COST ESTIMATE (ELBOW)</b> .....	<b>247</b>
<b>APPENDIX X – DETAILED COST ESTIMATE (ROTATOR)</b> .....	<b>248</b>

## Table of Figures

FIGURE 1: ELEVATION AND AZIMUTH (5) .....	11
FIGURE 2: WERNER MERLO'S ROBO-FLEX JOINT (6).....	12
FIGURE 3: ROBOTIC WRIST PATENT .....	13
FIGURE 4: THE YAW AND PITCH MOTION GENERATED BY A HUMAN FINGER (RYEW 2001).....	14
FIGURE 5: THE DOUBLE ACTIVE UNIVERSAL JOINT (DAUJ) (RYEW AND CHOI 2001).....	15
FIGURE 6: INSPECTION ROBOT (RYEW AND CHOI 2001). .....	16
FIGURE 7: USE OF POTENTIOMETER AND ULTRASONIC MOTOR TO SENSE FORCE EXERTED,.....	17
FIGURE 8: DETAIL DESIGN OF FINGER USING ULTRASONIC MOTORS (YAMANO, TAKEMURA AND MAENO) .....	17
FIGURE 9: THE MODULAR JOINT ACHIEVING 1 DEGREE OF MOTION (9).....	19
FIGURE 10: COMMUNICATION SYSTEM FOR THE MODULAR ROBOTIC JOINT (9). .....	20
FIGURE 11: UNIDRIVE SYSTEM (10). .....	21
FIGURE 12: CARNEGIE MELLON'S HERCULES (11) .....	22
FIGURE 13: POWERCUBE WRIST (13). .....	24
FIGURE 14: MODULAR ROBOTIC MANIPULATOR (14).....	26
FIGURE 15: MARK II PUMA 200 ROBOTIC ARM.....	27
FIGURE 16: SHOULDER JOINT MECHANICAL DRAWING AND DETAILED MECHANICAL DRAWING OF WRIST .....	28
FIGURE 17: GRIPPER MOUNTING .....	29
FIGURE 18: PUMA CONTROL SYSTEM BLOCK DIAGRAM .....	30
FIGURE 19: ELECTRONIC FLOW DIAGRAM.....	31
FIGURE 20: TEACH PENDANT MECHANICAL .....	32
FIGURE 21: MODULAR PLATFORM DESIGN .....	35
FIGURE 22: ELBOW-JOINT ITERATION 01.....	37
FIGURE 23: JOINT SET-UP FOR INERTIA CALCULATIONS.....	40
FIGURE 24: ELBOW BASE .....	42
FIGURE 25: FULLY CONSTRAINED FACE AND APPLIED FORCED LOCATION OF THE ELBOW BASE .....	42
FIGURE 26: INTERNAL STRESSES AND DISPLACEMENT OF THE ELBOW BASE.....	43
FIGURE 27: BOTTOM COLLAR .....	44
FIGURE 28: FULLY CONSTRAINED FACE AND APPLIED FORCE LOCATION OF THE BOTTOM COLLAR .....	45
FIGURE 29: INTERNAL STRESSES AND DISPLACEMENT OF THE BOTTOM COLLAR .....	45
FIGURE 30: ROTATOR PIN .....	46
FIGURE 31: FULLY CONSTRAINED FACE AND APPLIED FORCE LOCATION OF THE ROTATOR PIN.....	47
FIGURE 32: INTERNAL STRESSES AND DISPLACEMENT OF THE ROTATOR PIN.....	47
FIGURE 33:TOP COLLAR .....	48
FIGURE 34: FULLY CONSTRAINED FACE AND FORCE LOCATION OF THE TOP COLLAR .....	49
FIGURE 35: INTERNAL STRESSES AND DISPLACEMENT OF THE TOP COLLAR.....	50
FIGURE 36: ITERATION ONE ROTATOR-JOINT.....	56
FIGURE 37: JOINT SET-UP FOR INERTIA CALCULATIONS.....	57
FIGURE 38: TOP SHELL MODEL.....	58
FIGURE 39: RESTRAINT SURFACE AND LOAD SURFACE FOR TOP SHELL.....	59
FIGURE 40: STRESS DISTRIBUTION AND DISPLACEMENT OF TOP SHELL WITH 80 N LOAD.....	59
FIGURE 41: BOTTOM SHELL MODEL.....	60
FIGURE 42: RESTRAINT SURFACE AND LOAD SURFACE FOR BASE SHELL .....	60
FIGURE 43: STRESS AND DISPLACEMENT DISTRIBUTIONS FOR BASE SHELL .....	61
FIGURE 44: ITERATION 1 ELECTRICAL SCHEMATIC.....	65
FIGURE 45: ITERATION 1 PROTOTYPE.....	66
FIGURE 46: ELBOW PRE-PROTOTYPE #1 .....	67
FIGURE 47: ELBOW PRE-PROTOTYPE #2.....	68
FIGURE 48: ELBOW-JOINT ITERATION 02.....	69
FIGURE 49: DRIVEN COLLAR.....	72
FIGURE 50: FULLY CONSTRAINED FACE AND APPLIED FORCE LOCATION OF THE DRIVEN COLLAR .....	73
FIGURE 51: INTERNAL STRESSES OF THE DRIVEN COLLAR.....	73



FIGURE 52: BOTTOM COLLAR .....	74
FIGURE 53: FULLY CONSTRAINED FACE AND APPLIED FORCE LOCATION OF THE BOTTOM COLLAR .....	75
FIGURE 54: INTERNAL STRESSES OF THE BOTTOM COLLAR.....	75
FIGURE 55: ITERATION TWO ROTATOR-JOINT, ISOMETRIC AND TRANSPARENT TRIMETRIC VIEWS .....	79
FIGURE 56: BASE SHELL MODEL.....	82
FIGURE 57: RESTRAINT SURFACE AND LOAD SURFACE FOR BASE SHELL .....	83
FIGURE 58: STRESS AND DISPLACEMENT DISTRIBUTIONS FOR THE BASE SHELL. ....	83
FIGURE 59: ISOMETRIC TOP AND BOTTOM VIEWS OF TOP SHELL. ....	84
FIGURE 60: RESTRAINT SURFACE AND LOAD SURFACE FOR TOP SHELL.....	84
FIGURE 61: STRESS AND DISPLACEMENT DISTRIBUTIONS FOR TOP SHELL.....	85
FIGURE 62: SECTION VIEW OF THE SECOND ITERATION ROTATOR-JOINT.....	88
FIGURE 63: TYPICAL H-BRIDGE CIRCUIT (NATIONAL SEMICONDUCTOR).....	91
FIGURE 64: H-BRIDGE LOGIC TABLE (STMICROELECTRONICS).....	91
FIGURE 65: ITERATION 2 SCHEMATIC.....	92
FIGURE 66: ELBOW-JOINT ITERATION 03.....	93
FIGURE 67: ELBOW SLEEVE .....	98
FIGURE 68: FULLY CONSTRAINED FACE AND APPLIED FORCE LOCATION OF THE ELBOW SLEEVE.....	99
FIGURE 69: INTERNAL STRESSES AND DISPLACEMENT OF THE ELBOW SLEEVE.....	99
FIGURE 70: BOTTOM COLLAR .....	100
FIGURE 71: FULLY CONSTRAINED FACE AND APPLIED FORCE LOCATION OF THE BOTTOM COLLAR .....	101
FIGURE 72: INTERNAL STRESSES AND DISPLACEMENT OF THE BOTTOM COLLAR .....	102
FIGURE 73: DRIVEN COLLAR.....	103
FIGURE 74: FULLY CONSTRAINED FACE AND APPLIED FORCE LOCATION OF THE DRIVEN COLLAR .....	104
FIGURE 75: INTERNAL STRESSES AND DISPLACEMENT OF THE DRIVEN COLLAR .....	104
FIGURE 76: WORM/DRIVE SHAFT.....	106
FIGURE 77: FULLY CONSTRAINED FACE AND APPLIED TORQUE OF THE WORM/SHAFT .....	107
FIGURE 78: INTERNAL STRESSES AND DISPLACEMENT OF THE WORM/DRIVE SHAFT .....	108
FIGURE 79: THIRD ITERATION OF ROTATOR-JOINT MODEL.....	114
FIGURE 80: THE BASE SHELL AND BASE TOP.....	115
FIGURE 81: BASE SHELL .....	117
FIGURE 82: RESTRAINT SURFACE AND LOAD SURFACE FOR BASE SHELL. ....	118
FIGURE 83: STRESS AND DISPLACEMENT DISTRIBUTIONS IN BASE SHELL .....	118
FIGURE 84: ITERATION THREE BASE TOP.....	119
FIGURE 85: RESTRAINT AND LOAD SURFACES FOR THE BASE TOP. ....	120
FIGURE 86: STRESS, DISPLACEMENT, AND SAFETY FACTOR DISTRIBUTIONS FOR BASE TOP. NOTE, FOR THE SAFETY FACTOR ANALYSIS, AREAS IN BLUE ARE PORTIONS OF PART WHERE SF>15, WHILE RED AREAS ARE WHERE SF<15.....	120
FIGURE 87: ISOMETRIC TOP AND BOTTOM VIEWS OF THE TOP SHELL. ....	121
FIGURE 88: RESTRAINT AND LOAD SURFACES FOR TOP SHELL. ....	121
FIGURE 89: STRESS AND DISPLACEMENT DISTRIBUTION FOR TOP SHELL. ....	122
FIGURE 90: MAIN SHAFT FOR ROTATOR-JOINT.....	123
FIGURE 91: RESTRAINT AND LOAD SURFACES FOR MAIN SHAFT.....	123
FIGURE 92: STRESS AND DISPLACEMENT DISTRIBUTIONS FOR MAIN SHAFT. ....	124
FIGURE 93: ROBOJOINT CONTROL SYSTEM .....	130
FIGURE 94: OPTICAL ENCODER FUNCTIONALITY (US DIGITAL) .....	133
FIGURE 95: BASE TO JOINT PACKET STRUCTURE.....	135
FIGURE 96: JOINT TO BASE PACKET STRUCTURE.....	135
FIGURE 97: IRDA PROTOCOL (TEXAS INSTRUMENTS).....	138
FIGURE 98: BASE FIXTURE PROPOSED.....	157

## Table of Tables

TABLE 1: MOTOR SELECTION MATRIX FOR ELEVATOR JOINT .....	52
TABLE 2: MOTOR SELECTION MATRIX FOR ROTATOR-JOINT .....	63
TABLE 3: PROPERTIES OF RAPID PROTOTYPE ABS PLASTIC.....	96
TABLE 4: GEAR ANCHORING ANALYSIS RESULTS.....	109
TABLE 5: COST CALCULATIONS FOR MACHINED PARTS OF ELBOW-JOINT .....	111
TABLE 6: ELBOW-JOINT COST ESTIMATE BREAKDOWN.....	112
TABLE 7: PROPERTIES OF RAPID PROTOTYPE ABS PLASTIC.....	117
TABLE 8: COST CALCULATIONS FOR MACHINED PARTS OF ROTATOR-JOINT .....	126
TABLE 9: COST ESTIMATE FOR ROTATOR-JOINT .....	127
TABLE 10: COMMANDS (BASE TO JOINT) .....	135
TABLE 11: COMMANDS (JOINT TO BASE) .....	136
TABLE 12: SPECIAL DATA VALUES.....	136
TABLE 13: SPECIAL ADDRESS VALUES .....	136
TABLE 14: ROTATOR-JOINT TEST RESULTS.....	147
TABLE 15: ELEVATOR-JOINT TEST RESULTS.....	148

## 1 Introduction

Robotics is a diverse and promising field with numerous opportunities and challenges. For example, the Defense Advanced Research Projects Agency (DARPA), a division of the United States Department of Defense, has sponsored two autonomous robotics competitions with one million to two million dollar prizes in order to support robotics research and development(1).

iRobot's Roomba, an autonomous vacuum, has successfully made robotics available to the consumers, selling over two million units as of January 2008(2). Applications of robotics are numerous and varied, therefore it would be beneficial to design robots that are capable of being adapted to serve multiple functions. Designing robotic components to be modular, or able to integrate easily with other parts or machines, while still being affordable, would facilitate flexibility of robots.

### 1.1 Modularity

The ability to create motion gives robotic joints the potential for modular development and would be useful in a variety of applications if inexpensive enough. For a part to be modular, it must be an individual working unit, but able to interface with a variety of other parts and systems to create a more complex machine. Modularity allows for versatility in design and machine capabilities, the ability to adapt according to the needs of the user, and ease of assembly(3). Mechanically, a part would need to be able to attach to other parts or surfaces using common materials, such as clamps or bolts. Electronically, it would need to be able to plug into a standard power source, battery, or outlet. In the case of a robotic joint, it would also need to be able to transfer both electrical power and communication signals to another part or joint.

In order for a joint to be modular and be commercially viable, some challenges must be overcome and criteria must be met. A feasible design would have to:

1. Have comparable properties to commercially available joints, such as torque capabilities and power requirements
2. Keep price per unit below industry standard
3. Be capable of transferring power, either electrical or mechanical, as well as data
4. Rotate about one or more axes

There are currently many robot kits available that allow for motor and component reconfiguration; however, their basic abilities hinder their capacity to be used in professional applications. High quality modular joints are often packaged in manipulators, such as arms, consisting of five or more joints. This becomes an issue if a user only has a need for two joints, yet they must purchase the entire kit of five joints. With a modular joint a user can obtain only the joints they need, which cuts back on both the cost and complexity of any robotic applications.

## **1.2 Cost vs Capability**

One of the predominant challenges in this project is to find a balance between joint capabilities and cost. Currently there is a gap in the market for a midrange robotic joint. On the low end is the \$19.99 wrist kit, which VEX manufactures for their robotics kits, capable of producing only a few in-lbs of torque(4). Successful high load joints are capable of lifting several kilograms and are produced by major manufacturers such as Fanuc and Mitsubishi, but there is a cost increase of several thousand dollars.

Although an inexpensive robotic joint can be designed to perform similar to high priced joints, it is essential to produce it at a low cost. The first step in achieving low cost

production is to minimize the cost of each individual part. Precision and durability are often lost when cheaper components are chosen, so a balance, determined by the task specifications, must be achieved. Another way to reduce component cost is to construct a robotic joint using common and readily available parts. Custom components are typically more expensive than mass produced or commonly stocked items. In addition, if the parts used in a joint are carried by multiple vendors production of the joints would less likely to be hindered by shortages or discontinuations.

Since this project focuses on developing a joint that is inexpensive to manufacture, all facets of the design are affected by the need to keep the final cost low. This limitation will require all aspects of the joint to be efficient and thoroughly researched in order to ensure that a balance between price and technical ability is reached.

### **1.3 Goal**

The goal of this project is therefore to develop, manufacture, test, and evaluate a modular joint or series of joints that have comparable design specifications and technical capabilities with similar commercially available products and that can be manufactured for under \$1000. The steps to achieve this goal are to:

1. Assess the needs of the joint and develop a series of task specifications
2. Design the joint based on the task specifications
3. Test the design for:
  - a. Durability, or environments it can function safely in
  - b. Fatigue Life Analysis, or how long it can run continuously before failing
  - c. Torque, Force, and Stress Specifications, or how much it can safely lift

- d. Precision and Accuracy, or how accurate and precise the joint's response is to data input
4. Make recommendations for design improvements based on test results
5. Market the design

Achieving these goals and objectives would result in a marketable and potentially profitable design for a robotic joint.

## 2 Background

### 2.1 Motion of Joints

When designing a robotic joint it is important to note which planes or axes this joint will move in. While there is a large range of motions available, the two that have been selected are elevation and azimuth, as depicted by the blue and red arrows, respectively, in Figure 1.

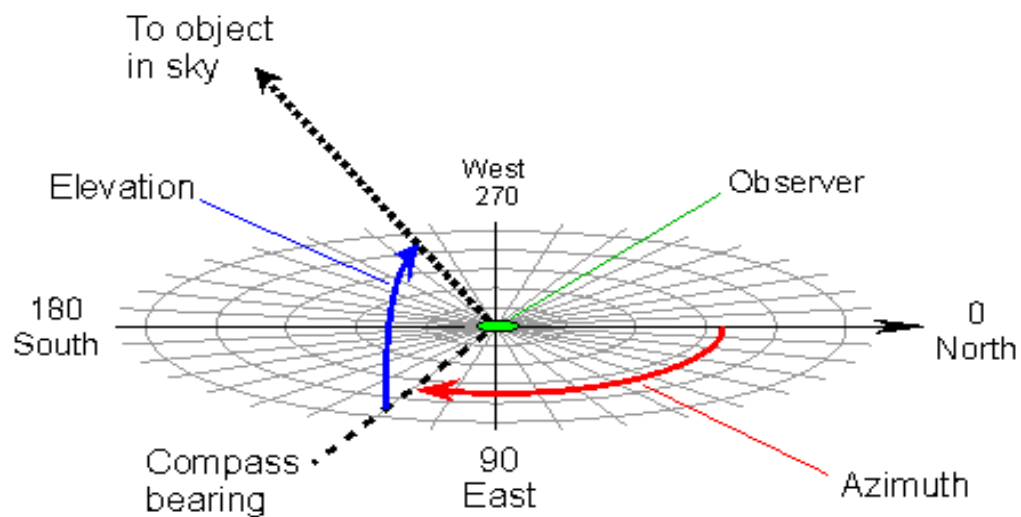


Figure 1: Elevation and Azimuth (5)

Elevation, as seen in Figure 1 is the motion in the direction above the horizon. It most closely matches the motion of a human elbow. Azimuth, also shown in Figure 1, is rotational translation. It resembles the motion of a human wrist while rotating(5). These two movements, when combined, are capable of a full range of motion that will give the joints the freedom necessary for a joint that will be used in a variety of applications. The following is a discussion of commercial products that produce a range of motion similar to that which is desired.

### 2.1.1 RoboFlex

Although the robotics industry is filled with numerous joints built for many applications, it is important to find a joint that is capable of handling a diverse set of tasks. Inventor Werner Merlo developed a ball-joint that uses a system of locking pins to either allow movement or restrict it.

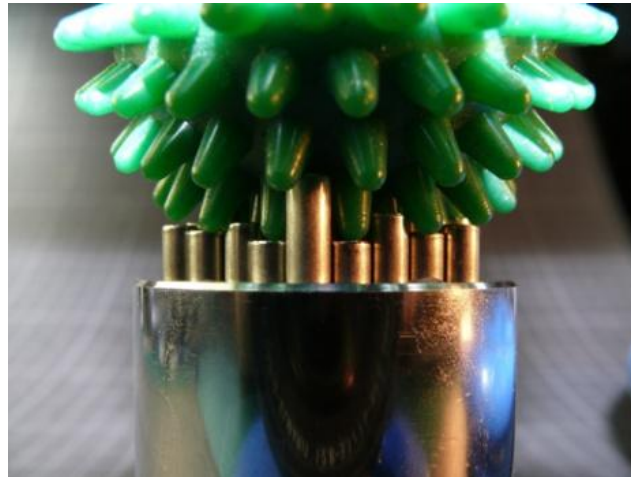


Figure 2: Werner Merlo's Robo-Flex Joint (6)

This joint, called Robo-Flex and shown in Figure 2 allows for the free-range movement of a ball joint, without the drawbacks of load support, meaning the joint can support a load without drawing power from an outside source(6). The joint uses a ball covered in pins that roll freely over the lower pin-heads. His prototypes are capable of holding up to 500 pounds before the pins begin to slip. The Robo-Flex joint is already gaining interest for a range of applications from bomb-defusing robots to the robotic arm on the space-shuttle(6). Although Werner Merlo has solved the problem of a joint's range and load-carrying ability, the fact that his joint requires an outside energy source and is incapable of moving on its own is a limiting factor.



### 2.1.2 Robotic Wrist Patent

Another key aspect of the robotic joint is its kinematics, or mechanical motion. Initial design gives the opportunity to explore different mechanical methods of creating the same motion, in our case rotation or elevation, while the details of how that motion will be driven can be determined later in the design. A patent filed by inventor Nathan Ulrich outlines only the mechanical aspect of a robotic “wrist” joint.

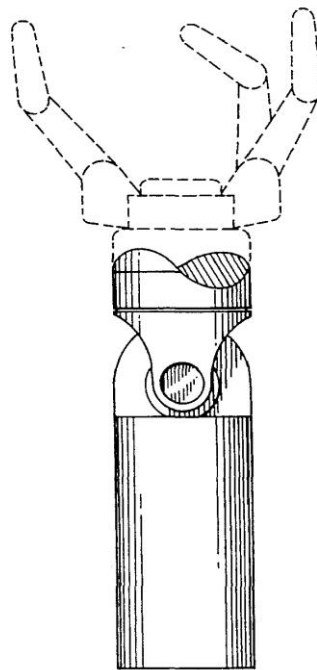


Figure 3: Robotic Wrist Patent

While his design does not provide any information on the electrical components of such a joint, the patent provided insight into the basic level mechanics of the joint. Although, this joint is for aesthetic purposes only, and does not include any components to drive its movement, it explained techniques to tackle the various movements mechanically.

### 2.1.3 Double Universal Joint

Ryew and Choi developed a unique joint to transfer mechanical power through rotating half-spheres(7). This joint, the Double Active Universal Joint (DAUJ), incorporates two active universal joints to create two degrees of motion, pitch and yaw, as depicted by Figure 4.

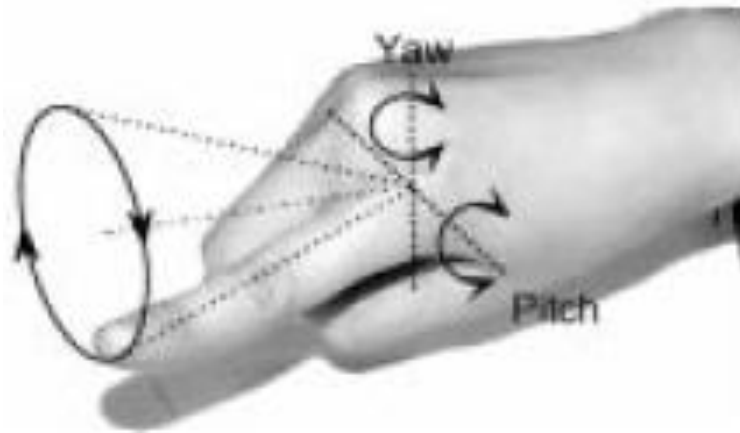


Figure 4: The yaw and pitch motion generated by a human finger (Ryew 2001).

The motivation for developing this joint was to create motion similar to that in a human finger. Traditionally, two small joints are incorporated to produce the motion of the joint created in the first knuckle of a human finger, but the orientation is restricted to create pitch and rotation about the axis of the finger. While this motion is appropriate in a variety of applications, the mimicking of human motion requires pitch and yaw, as shown in Figure 4.

The DAUJ joint created by Ryew and Choi, shown in Figure 5, relies on the idea of two concentric universal joints.

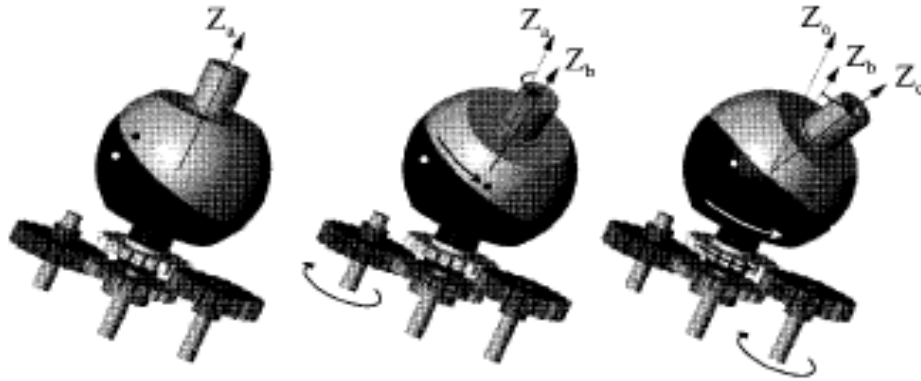
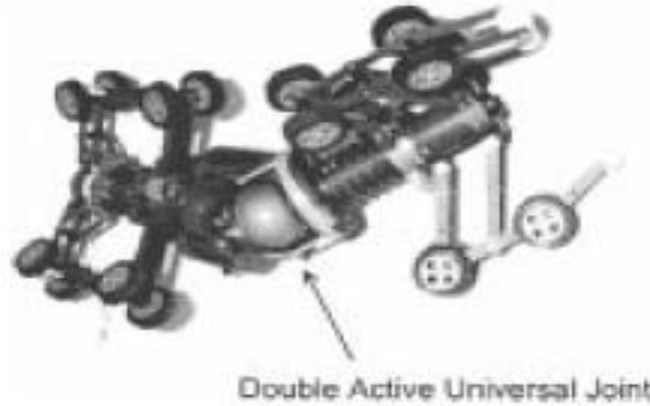


Figure 5: The Double Active Universal Joint (DAUJ) (Ryew and Choi 2001).

Each joint is driven by an individual actuator, and rotates a sphere, slanted at an angle. The induced angle of the spheres allows for the pitch and yaw motion to be generated. This motion generation is shown in Figure 5.

The angle between the two hemispheres allows the joint to articulate in both elevation and azimuth directions. Rotation of the top cylinder induces a change in pitch while the rotation of the bottom sphere would create rotational translation. While the DAUJ offers a unique solution to create two degrees of motion, it also has some disadvantages. One of these drawbacks is that the elevation motion is dependent upon the rotation of the top hemisphere. This causes a slight rotation about the  $Z_a$  axis. The bottom sphere would have to be used to compensate for the slight rotation induced by the top sphere. Human fingers, on the other hand, are capable of generating solely yaw motion. Additionally, due to the utilization of rotating spheres and the angle,  $\Phi$ , the DAUJ joint has a smaller physical range of motion than other two degrees of motion mechanisms.



**Figure 6: Inspection robot (Ryew and Choi 2001).**

The Double Active Universal Joint has been successfully implemented in robotic hands, as well as other applications. One of the robotic fingers developed was able to generate 30 degrees of yaw angle and 88 degrees of pitch angle. The DAUJ has been used in a “steering mechanism of the articulated in pipe inspection robot”(7). The joint in this application, shown in Figure 6, allowed the robot to both “twist” and “bend” as needed to provide adequate forces to the inside of a pipe.

The DAUJ is a new approach for the generation of two degrees of motion. Additionally, it has been effectively implemented in mimicking motion of human fingers, as well as in robotic assemblies. The unique motion generated is appropriate for mimicking the human finger, though is too limited for broad use.

#### **2.1.4 Ultrasonic Motors**

An interesting method of actuating a joint is to use ultrasonic motors, which are essentially tiny motors that use friction caused by vibration of a stator, or elastic body, to turn the rotor(8).

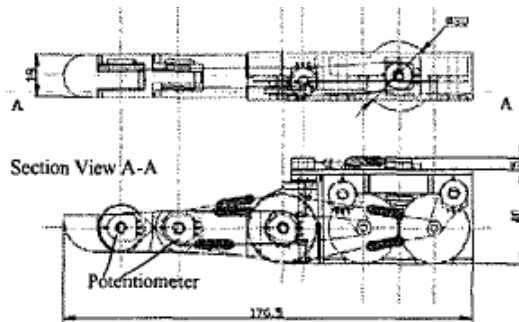


Figure 7: Use of Potentiometer and Ultrasonic Motor to Sense Force Exerted,

Inventors of a robotic hand used ultrasonic motors to actuate the joints because they have a high driving and holding torque at low speeds, and are also compact and light in weight. They used rubber wires with elastic spring attached to pulleys on either side of the joint, driven by the ultrasonic motors, to move the joint itself. A potentiometer was used to measure the change in joint angle, which they also used to sense the force exerted on a surface by each finger. This eliminated the need for a force sensor, saving weight and space.

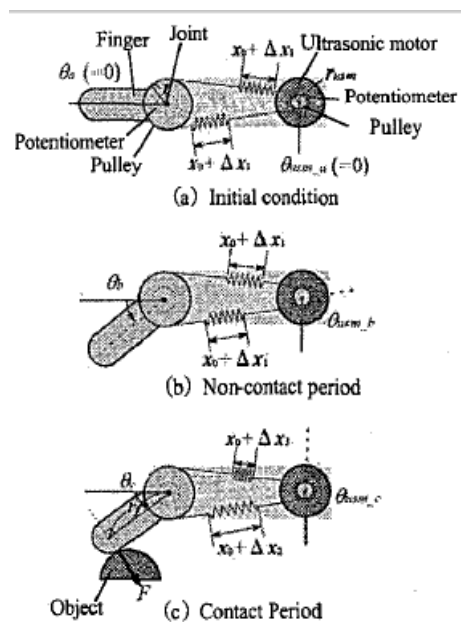


Figure 8: Detail Design of Finger Using Ultrasonic Motors (Yamano, Takemura and Maeno)

The combination of lightweight, multipurpose parts is appealing considering a target goal of this project is to create a compact joint. Ultrasonic motors did not appear to be commercially available, therefore they may not meet another goal of being cost effective, as custom parts tend to be more expensive.

## **2.2 Modularity and Communication**

Industry has proven it is possible to create a single joint with multiple degrees of freedom, or being able to move in more than one axis. Utilizing a series of modular joints will allow for the same, if not greater, degree of freedom while reducing the complexity of each joint. However, including modular characteristics in the design brings many new problems and challenges such as:

1. Transferring either electrical or mechanical power through the joint
2. Transferring either electrical or mechanical power between joints
3. Communicating data between multiple joints
4. Assuring mechanical strength of mechanical connection between joints

Although these factors present difficult problems to overcome, the capabilities of multiple modular joints will exceed those of a more complex single joint.

### **2.2.1 Development of Modular Robot Joint**

Jia Qing-xuan et al worked to develop a modular robotic joint. Their paper, "Development of Modular Robot Joint" discussed the advantages of a modular design, as well as the methods for communication between the modules, using a master-slave approach with a base processor acting as the master(9).

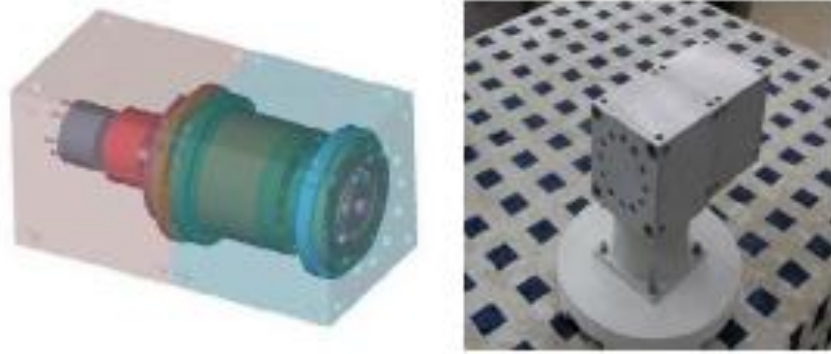


**Figure 9: The modular joint achieving 1 degree of motion (9).**

The designers outlined the advantages of a modular design as “convenient reconstruction; good redundancy; easy to assemble; good agility; easy to maintenance” (Jia Qing-xuan 2006, 827), which were similar to this Robojoint project. Their research led to a design as shown in Figure 9, of a simple rotating joint, that when a series of rotators were linked, it resulted in numerous degrees of freedom. The authors also discuss the importance of a back-drive system, to prevent unnecessary motion by utilizing one of the following systems; “The planetary gearing decelerator, the gear worm decelerator, cup-type harmonic-driver and pancake-type harmonic-driver” (9).

In addition to selecting a back-drive system, the designers also rigorously tested their module using finite element analysis. Since modular joints, such as this, undergo stresses in nearly every possible axis, thorough analyses must be completed in order to reliably design the module. The designers recognized that their joint would induce the most stress on the casing and the bearings. After prototyping and testing, they determined that their design was comparable with commercially available modular joints, with the added benefit of greater precision and less cost

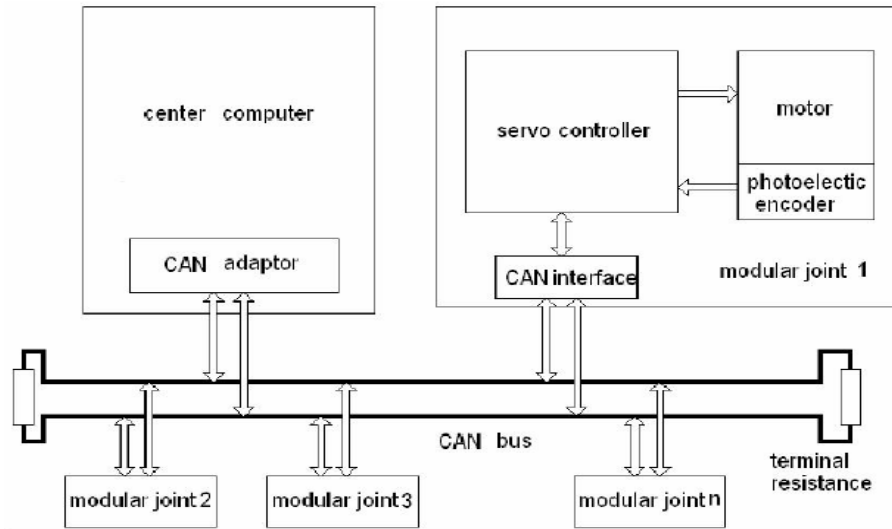


Figure 10: Communication system for the modular robotic joint (9).

Lastly, the authors continue to explain the method in which the modules are controlled. This process utilizes a master-slave approach, with a central PC being the master and incorporating other processors for controlling each servo. Each module is powered by an external source, and signal is transmitted to each joint via wires. The central PC sends signal to each of the modules, as appropriate, which then each convert this signal to drive the motor. Feedback sensors then relay information back to the central computer. This arrangement is shown in Figure 10. The communication between modules is an essential aspect of this paper. In order to properly function, a series of joint modules must be able to have at least rudimentary communication in order to be considered modular. Due to the similar goals and objectives of the joint created by the Beihang University students, the Robojoint project can learn from their methods and compare the results.

### 2.2.2 Unidrive Modular Joint

Karbasi, Khajepour, and Paul developed a system to deliver mechanical power through a series of joints, rather than electrical power or signal (10). The “Unidrive



Modular Robot” incorporates a flexible shaft to power a series of joints, as shown in Figure 11.

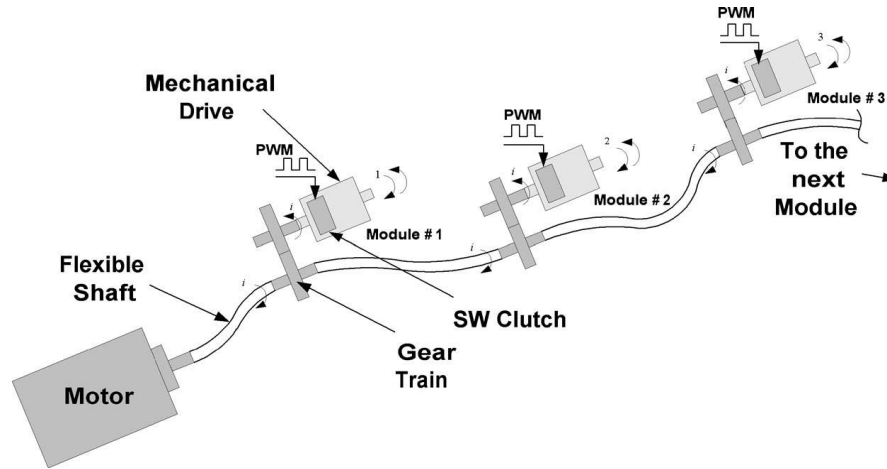


Figure 11: Unidrive System (10).

Each joint node would attach to the shaft utilizing gears. Figure 11 shows the Unidrive system connected to modular joints in a series arrangement. Similar to electrical circuits, this system may also be implemented in a parallel configuration, where a “Distributor” would split the mechanical power into numerous shafts. Each node consists of gears and a clutch assembly to adjust the torque generated by the mechanical shaft. Without a clutch mechanism, the node would always be activated; implementing the clutch allows control over when the joint actuates.

The idea of a mechanical shaft delivering power is essentially analogous to electrical wires delivering electrical power. The primary advantage of this arrangement is to centralize the electrical power storage and actuators, both of which traditionally account for most of a module’s weight and size. However, this approach also complicates many aspects of delivering power to individual joint modules. Utilizing a single flexible drive shaft introduces a lot of noise vibration into the system, which results in non-uniform

motion. Additionally, the clutch assembly controlling the node motion may be required to be digitally controlled, which would necessitate wiring and circuitry. Regardless, the idea of a flexible shaft to deliver power is a unique way to create modular joints.

### 2.2.3 Snake Robot

One potential lead on how to make the joints modular can be found in the research the Biorobotics division at Carnegie Mellon University has done on creating modular snake robots.



Figure 12: Carnegie Mellon's Hercules (11)

Using commercially available products and simple designs, their team has been able to make extremely capable robots. Their design looked to solve two main problems: movement and modularity. The biorobotics team devised a modular joint called a “gait”. Their design gave the robot locomotion in a large range of applications, “Our gaits enable snake robots to maneuver through a variety of three-dimensional terrains and include swimming and climbing (11). This modular design provides insight to how to solve many of the design problems a modular joint presents. However, significant research will have to be done to ensure that this design is suitable for other applications.

#### **2.2.4 Electrical Component/Communication Research**

One key area of development is the electronic and communication components of the joint. Internal standards and protocols must be developed to allow for power and data transmission across modules. Additionally, industry standards must be taken into consideration to allow integration of the robot as a whole into a larger environment. These standards are directly influenced by the intended use of the unit. For example, a highly portable application may necessitate the ability to utilize a 12 volt battery and utilization of the USB communications protocol, while an industrial application would suggest compliance for 120/208 volt operation and compatibility with existing RS-232 or RS-485 technology.

#### **2.2.5 Manipulability and Redundancy Control of Robotic Mechanisms**

The degrees of freedom (DOF) a robotic joint possesses, both individually and in series, is important to calculate in order to determine the sphere of reach. A series of three joints theoretically have three DOF and should be able to touch any point within their combined spheres of reach. However, in reality the three DOF degenerates into two conical regions of freedom, limiting the orientation of the end joint (12). Four DOF or more increases the true sphere of reach of the joint series and is useful in more applications. In order to maximize utility, the robotic joint created in this project will be designed to operate with at least four joints connected in series.

## 2.3 Market feasibility

Prior discussion focused on the creation of a robust, modular joint. However, this joint must be able to compete in the commercial market with similar products, as outlined below. By providing a reliable product at a reasonable price, the group is confident that the manufactured joint will be a viable product in today's market.

### 2.3.1 PowerCube

Modular robotic components are currently available on the market. For example, Amtec Robotics, a branch of the Schunk Group, is a European modular robotics component designer and manufacturer.



Figure 13: PowerCube Wrist (13).

Their product line, PowerCube, has parts that pivot like a door hinge, rotate like a wheel, and linearly translate. The PowerCube swiveling joints, as shown in Figure 13, are the most similar to the joint this project aims to develop and are, thus, a standard for comparison. These joints are able to generate up to a maximum 425 Nm (313.65 lb-ft)

torque with a maximum mass of 5.4kg (0.0308bl or 0.3699slugs or 11.88lbs), values that are equivalent to the Robojoint design specifications. Consultation with the manufacturer suggested that the cost of an individual unit, or a single PowerCube joint, would cost between \$4,000 and \$5,000, even if purchased in large quantities. That \$3,000 to \$4,000 price difference makes the joint created in this project, far more appealing to buyers. Some applications in which PowerCube joints are used and which this project should take into consideration include inspection systems, service and personal robots, machine vision and projectors, factory automation (CNC, industrial robotics), and lab automation (pharmaceutical, chemistry) (13).

### **2.3.2 Research Robotics**

Another modular joint manufacturer is Robotics Research Corporation. This company markets its joints as modular parts that make up an industrial arm or manipulator, limiting customers to buying a set number of components while still allowing them to select joints with different specifications (i.e. they can buy whatever types they want but they have to buy enough to make an arm of some sort).

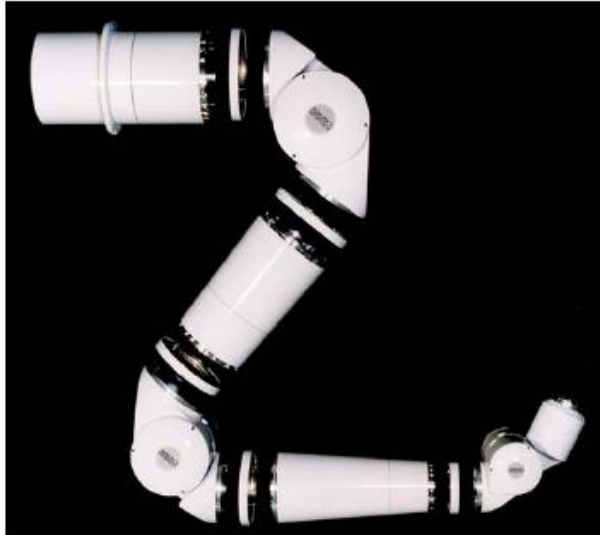


**Figure 14: Modular Robotic Manipulator (14).**

They use a patented torque-loop servo control in order to exert a high torque, which is then measured and controlled by an array of semiconductor strain-gages. Each joint is comprised of a DC brushless motor, a harmonic drive gear reducer, a power-off brake, axis bearings that are sealed, transducers to measure drive output position and torque, and a wiring harness. The wiring harness runs down the centerline of the joints and connectors, eliminating the risk of snags and reducing wear. In addition, they have developed a modular software package, R2 Control Software™, which supports control development and application. Specific design specifications are not available to the public, however dimensions are given, and one of the smallest joint components they manufacture is a rotator that is 3.2 inches in diameter and can output a torque of approximately 25 in-lbs(14).

### **2.3.3 Unimate Mark II PUMA Robot**

In order to obtain more information about the construction and operation of robotic joints, an older robotic arm was obtained for inspection and experimentation.

Manufactured in the late 1980s by Unimate, the 29 lb robot utilizes 6 DC servomotors to obtain 6 degrees of freedom in a work envelope, or complete 3D work space, of just under half a meter.

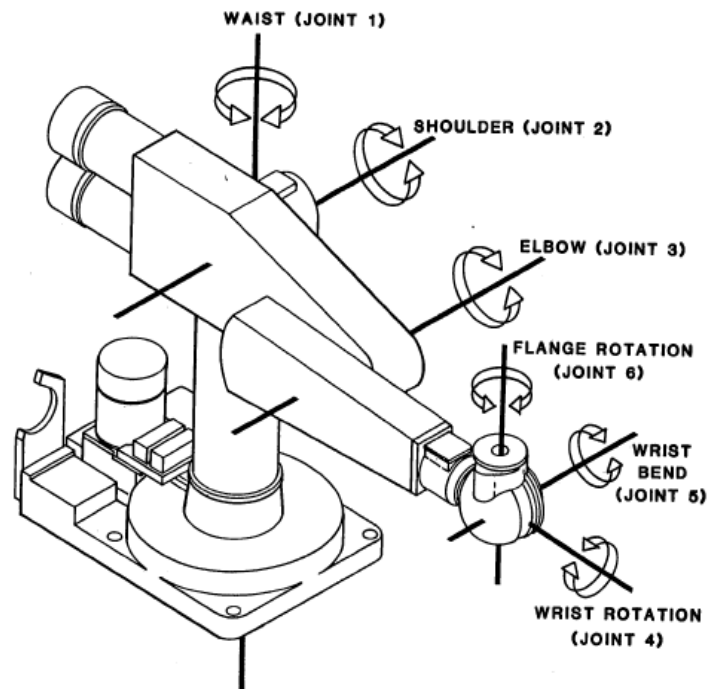
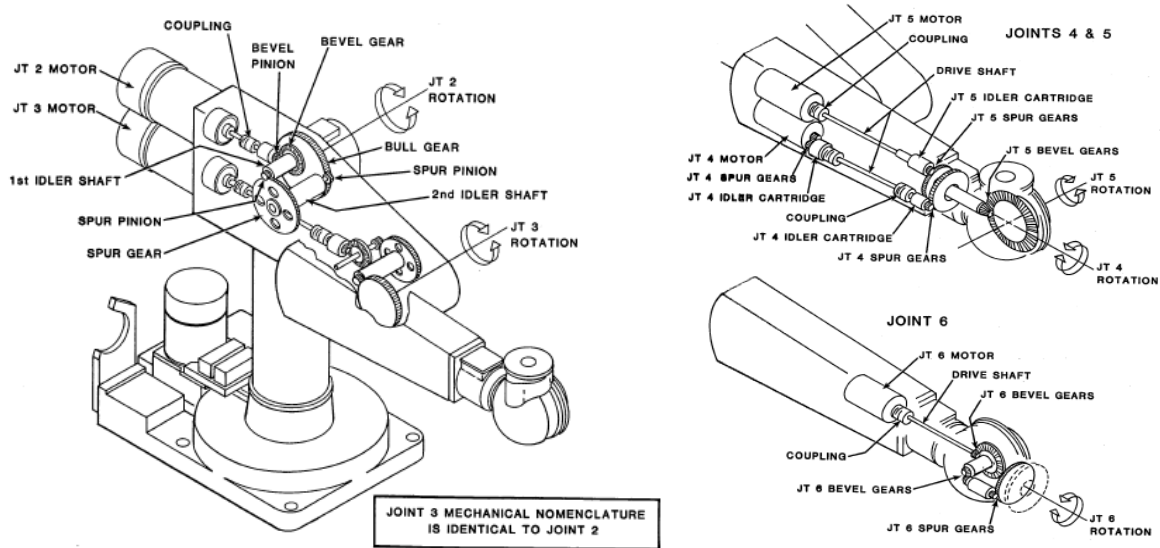


Figure 15: Mark II PUMA 200 Robotic Arm

Although outdated, the robot still provided a vast amount of information pertaining to industrial communication standards, and common mechanical configurations used on robotic manipulators.



**Figure 16: Shoulder Joint Mechanical Drawing and Detailed Mechanical Drawing of Wrist**

As shown in Figure 16, the power is transferred mechanically through the arm. While the waist joint is straightforward mechanically, the shoulder joint begins to introduce complexity as the motor has to transfer power from its location to the pivot point of the arm. Additionally, this point has to support the weight of the remaining arm, in addition to any payload. As a result the joint has a significant torque capacity, which can also be accounted for by the large size of the spur and bevel gears. The elbow-joint similarly transfers mechanical power from the motor location to a remote area, in this case the opposite side of the arm, in order to drive the rotation of the final arm segment. This last arm segment is by far the most complex. Motors for joints 4-6 are centrally located. Drive shafts run to the extent of the arm. A set of simple spur gears provide rotation to joint 4. A bevel gear inside the wrist ball allows for the bend motion of joint 5. A second set of bevel gears transfer power within the wrist ball to a spur gear which causes the flange to rotate. This unit provided valuable information about proven techniques that was utilized both in design and construction of the robot joints.



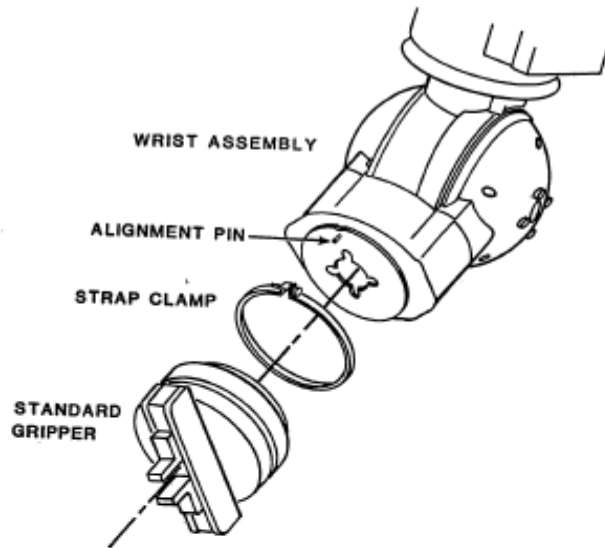


Figure 17: Gripper Mounting

Additionally, the PUMA robot provides an example of a common wrist mounting flange, a part that could be replicated so that this project's joint is capable of mating to a standard gripper. This would vastly increase the project joint's modularity with existing industry grippers and tooling.

From an electrical standpoint, it is useful to see the control hardware utilized in the robot controller. In the past 15 years, the size of components has drastically reduced, allowing for the controller to be potentially mounted within the base of the joint, instead of within an adjacent computer. Several harnesses are run along the inside of the robot, connecting each joint directly to the controller. The wires to each joint carry the direct electrical signals for the joint servos. There is no additional circuitry between the controller and the joint servo, as shown in Figure 18.

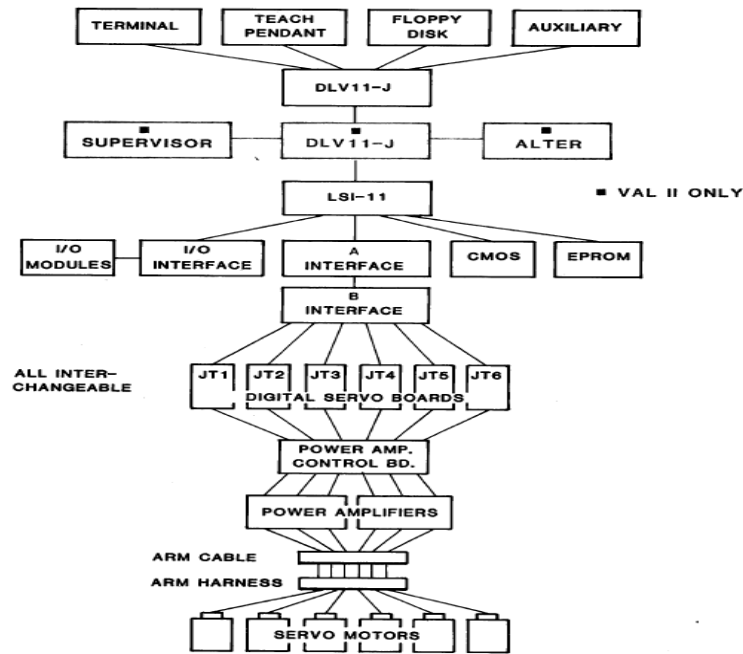


Figure 18: PUMA Control System Block Diagram

The controller also is responsible for converting all movements to the coordinate system the robot is currently operating in. Figure 19 shows an attached rotary encoder that is connected directly back to the digital servo board in the controller. Also shown in the Block Diagram is the relationship of the teach pendant and terminal.

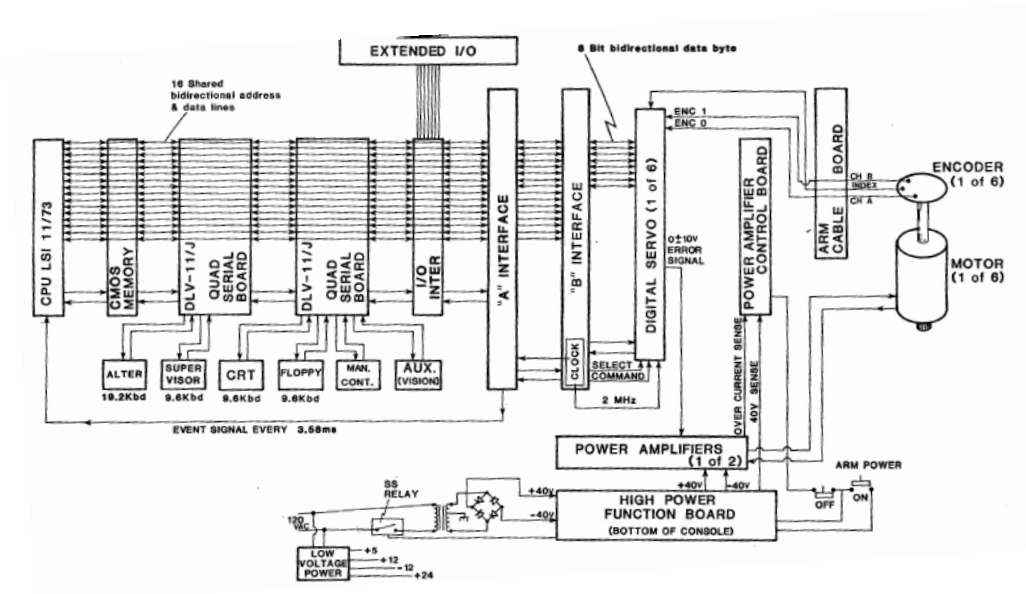


Figure 19: Electronic Flow Diagram

The Teach Pendant, shown in Figure 20 provides for direct user control of the PUMA robot. It also allows for the operator to program points and movements, to be later recalled when running the robot. More complex operations and programming is performed through a terminal attached to the controller. Routines are then stored in the controllers onboard memory to be executed when called upon by the user.



### 3 Project Objectives

From the previous section, it is evident that adequate research was done in robotic joints, or electromechanical articulators that are capable of being controlled with an outlined degree of accuracy. Additionally, a few of these joints were modular and were able to connect in a variety of configurations. However, these joints were expensive (upwards of \$4000), though the functionality of the modules was high-quality. Therefore, the goal of this project was to develop, manufacture, test, and evaluate a modular joint or series of joints that were extremely capable and were able to be manufactured for under \$1000. The objectives to achieve this goal were to:

1. Assess the needs of the joint and develop a series of task specifications
2. Design the joint based on the task specifications
3. Test the design for:
  - a. Durability
  - b. Cycle and Life Analysis
  - c. Torque, Force, and Stress Specifications
  - d. Precision and Accuracy
4. Improve the design based on test results

A successful design would be able to connect to multiple modules while still maintaining communication and power transmission. Additionally, the module must be able to withstand stresses in any arbitrary plane, since any number of joints could be connected in a variety of different configurations. Lastly, the robotics joint modules must be commercially viable. By creating a truly modular joint, these mechanisms would be an affordable option to implement in a greater range of commercial and academic applications than existing modular joints currently reach.

## 4 Design Specifications

Certain task specifications were identified to ensure that the robotic joint design met the needs established in the problem statement. These specifications were then quantified using previous background research and their level of importance, according to the project team's goals, and was weighted on a scale of zero to ten, with zero being the least important and ten being absolutely essential. Using a weighted average allowed for easy design comparisons using a mathematical means. Those specifications that were identified as most important included cost, modularity, movement, and safety. These specifications related directly to the need described in the problem statement, and thus were essential elements of the Robojoint design. Safety was critical, as a lack of it could result in legal and health consequences. Specifications that were recognized as important to consider during ideation and design of the joint included durability, ease of maintenance, materials needed, manufacturability, ease of operation, power requirements, applications, and dimensions. Details on the weighted specifications can be found in Appendix A.

## 5 Preliminary Design Concepts

Using these specifications, the group was able to objectively compare five different preliminary designs. The designs, as shown in Figure 21, each have strengths and weaknesses, as outlined in the task specifications in Appendix A. After calculating the weights and ranking each design, it was determined Design #1 would become the focus of the project. It was estimated that it would have a much greater

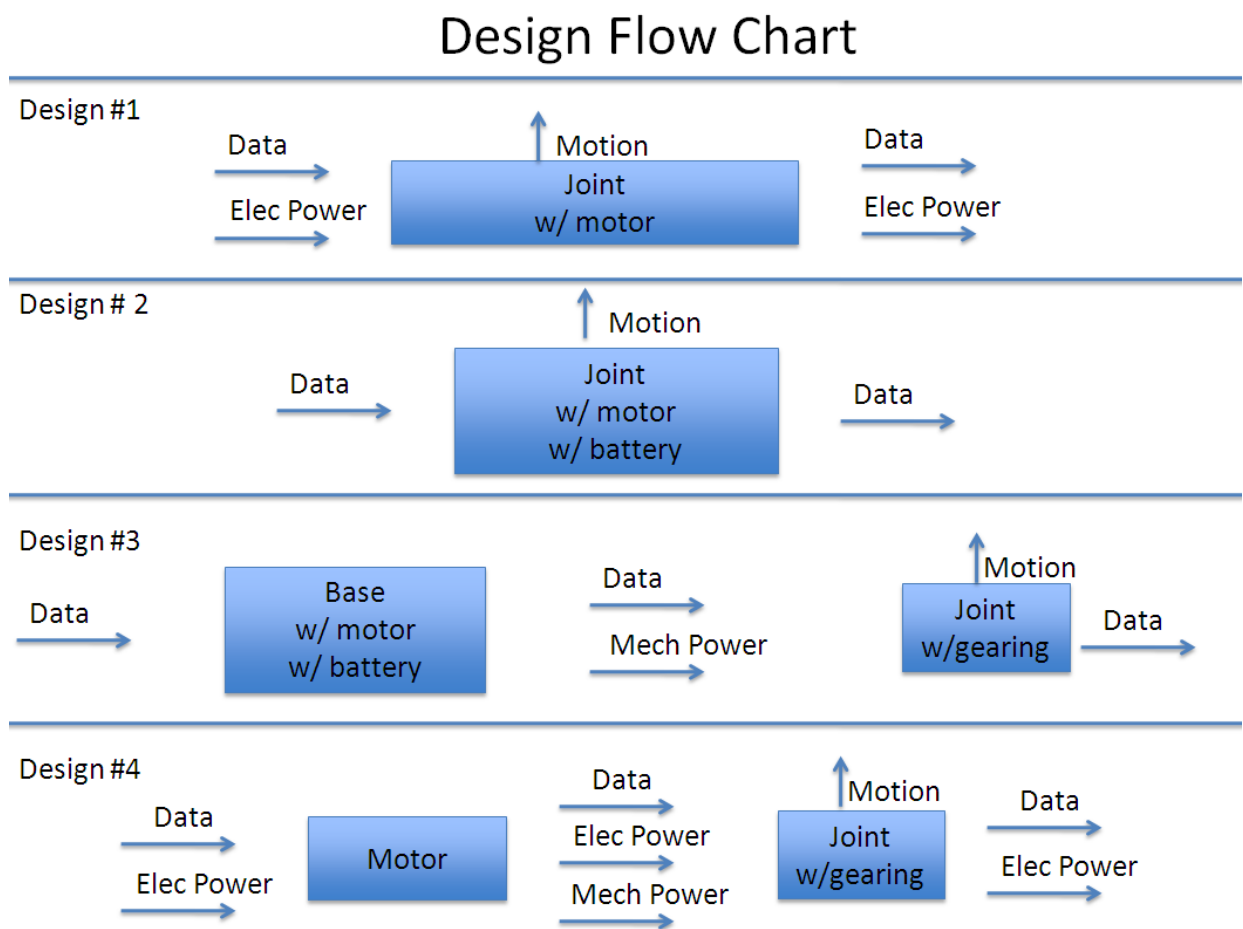


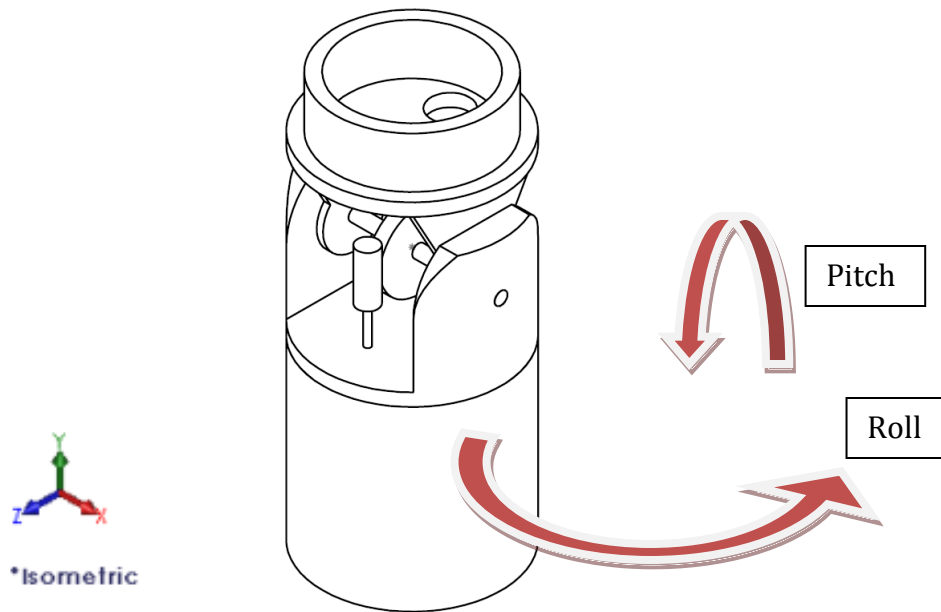
Figure 21: Modular Platform Design

cycle life and required the least maintenance, due to the few moving parts in the actual joint. This was in contrast to Designs 3 and 4, which relied heavily on mechanical linkages. Also, it was determined having multiple batteries in the system (i.e. on each joint) would

complicate maintenance, as well increase the frequency of repairs. This was a major detriment to designs 3 and 4. Between just these few critical specifications, it was clear that design #1 would have all the necessary capabilities, without the significant drawbacks associated with the other designs.



## 5.1 Elbow-joint Iteration 01



### 5.1.1

Figure 22: Elbow-joint Iteration 01

Iteration one of the elbow-joint was the first design based on the finalized task specifications. The design was composed of the elbow sleeve, bottom collar, driven collar, rotator pin, and the drive gears.

At this point both the motor and specific gear ratios had not been determined. This first iteration focused on the structure of the joint as well as the size and the modularity. The elbow sleeve and driven collar provided mounting points where another joint could be attached in series. Also, this design employed a worm gear drive system that would allow the joint to hold its position without requiring power from the motor.

### 5.1.2 Kinematics

Although the elbow-joint was designed to be an inexpensive yet capable device, the complexity of the structure and drive system require explanation in order to understand the overall function. A labeled drawing is included in Appendix J.

The overall structure of the elbow-joint was designed to maximize strength and minimize weight. The three major components that made up the structure were; the base, and the bottom and top collar. The base acted as the anchor of the device. Between the base and bottom collar was a fixed connection which allowed no motion between the bottom collar and base. This connection eliminated any roll motion in the design. As a result, the bottom collar became an extension of the base and anchored many of the other components. However, between the bottom and top collar there was a revolute joint with an axis of rotation about the X-axis. The rotator pin connected the two components. The rotator pin was allowed to move freely in relation to the bottom collar. However, the rotator pin was anchored to the top collar and the rotator pin would be unable to move in relation to the top collar. This freedom allowed the joint to be capable of pitch motion.

### 5.1.3 Iteration 01 Torque Analysis

To determine the required output of a motor for use in the elbow-joint, basic inertia calculations were performed. For analysis, four elbow-joints were connected in series. These elbow-joints are labeled as link one through four and joints one through four. These joints included the weight of: the base, bottom and top collar, rotator pin, as well as a rudimentary motor (modeled as a 75 gram block of commercial steel). Also a 2 kg weight was attached at the end (labeled as link five). The overall weight of the joint train was calculated to be about 3.89 kg. This configuration was expected to provide the maximum torque requirements for the joint. The analysis assumed that material the used in the model was Aluminum 6061. Additionally, to determine the maximum required output torque, the rotator pin of the bottom joint was driven at 13 RPM. This speed was determined to be the average speed a human arm moves during a 90 degree sweep. The full procedure for determining this speed is in Appendix D. It is important to note that for the following calculations, friction was ignored.

For this analysis, link one was fully constrained at the base and only joint number one was driven. Joints two, three, and four were locked and assumed no independent motion. The entire joint train would perform a sweeping motion in a clock-wise direction until reaching the ending position shown in Figure 23. This motion required the maximum amount of torque in order to move the joint train. Also, as outlined previously it was assumed that there would be no motion within any of the links. The links were support structures that were designed to not move or deform. Also, gravity was assumed to be acting in the negative y-axis direction with a magnitude of  $9.8 \frac{m}{s^2}$ . This resulted in a maximum required torque of 12 N-m.

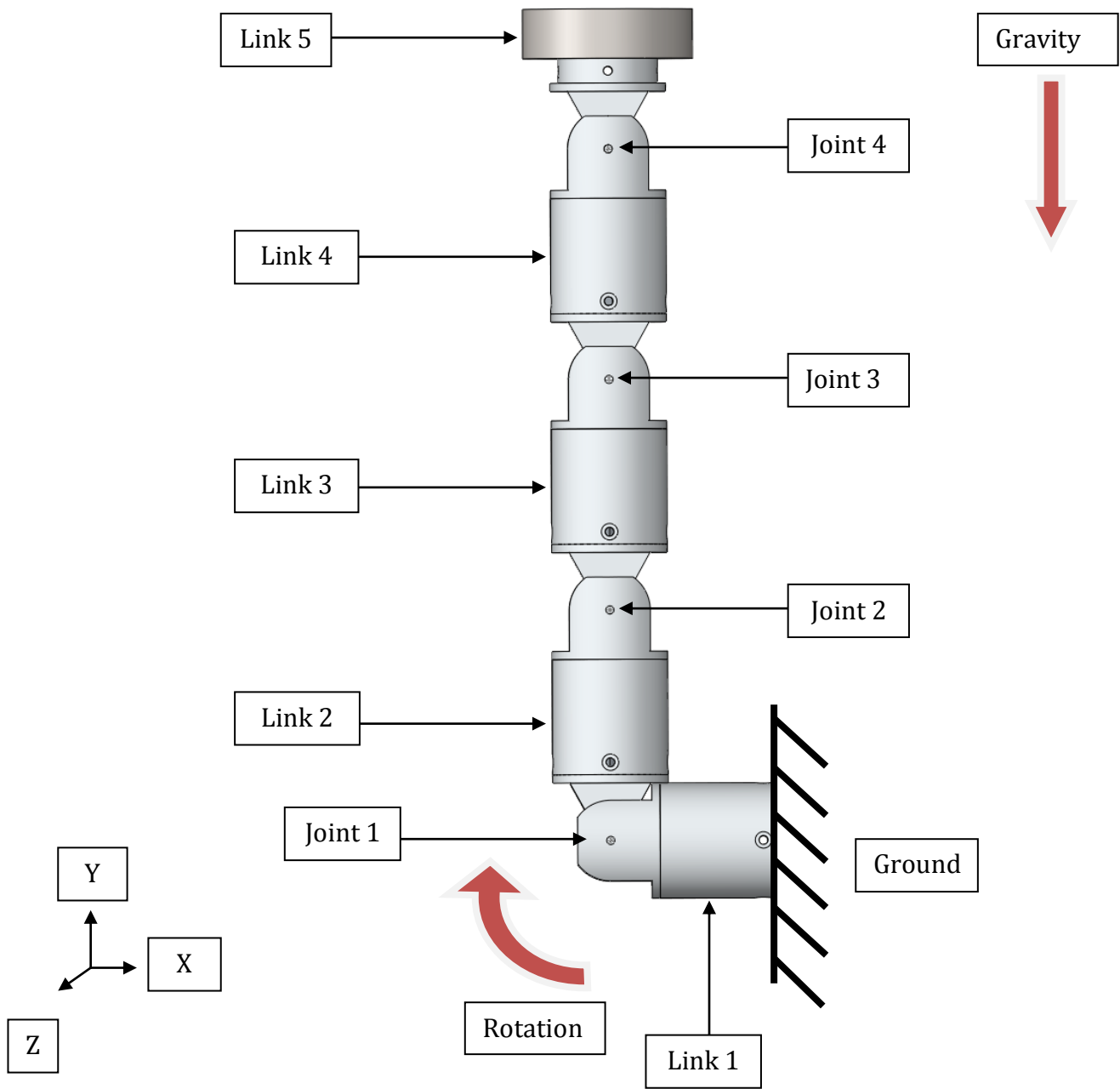


Figure 23: Joint Set-Up for Inertia Calculations

### 5.1.5 Iteration 01 Stress Analysis

While the finalized task specifications provided the necessary material to begin the design process, in order to improve the overall design and ensure it would operate in the manner outlined, preliminary stress of the structural components analysis was necessary. Although, many components were not fully defined, general properties such as materials and loads were used in order to conduct preliminary analysis. It was important to note that future designs may not employ the same properties, however, these factors were selected by the group to be both feasible and a good representation of what would be used in future designs.

The first assumption was that the entire joint would be made out of Aluminum 6061. This was a readily available commercial material that was very inexpensive, easy to work with and relatively strong. Secondly, the forces being used for joint analysis were the equivalent of four joints connected in series with a 2 kg weight attached to the end. This was beyond what was outlined in the finalized task specifications however; since overall strength was very important to the design and very little was known about how the joint would react to the forces applied, it was necessary to over-test this preliminary design. With these general properties implemented, preliminary testing could begin. All preliminary analysis was done electronically using the models created in SolidWorks.

### 5.1.5.1 Base

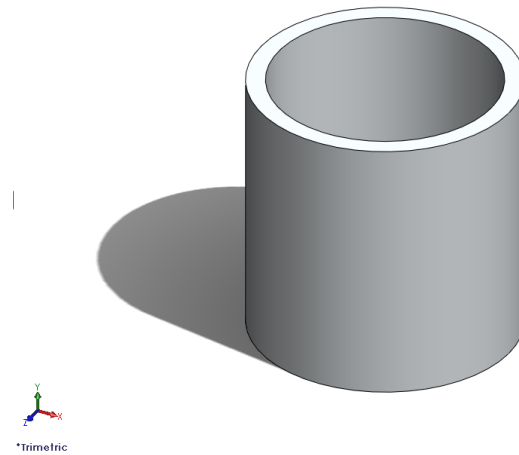


Figure 24: Elbow Base

The Elbow base was a simple component composed of a shaft with an outer diameter of 70 mm and an inner diameter of 60 mm and a length of 70 mm. This early component was only used as a structural anchor for the rest of the joint. It was extremely important that this part be strong enough to support the joint and the forces of operation. For preliminary stress analysis the bottom face of the Elbow base was fully constrained (Figure 25). In order to determine if the part was sufficient a force of 60 Newtons was applied to the top face.

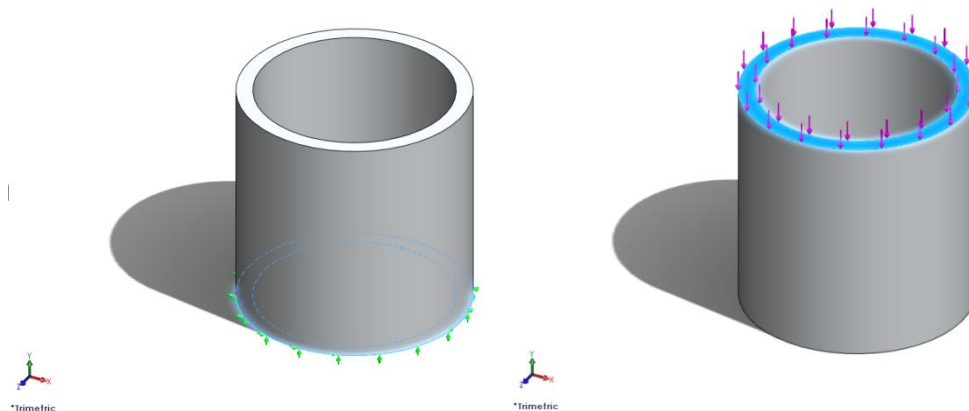


Figure 25: Fully Constrained Face and Applied Forced Location of the Elbow Base

The dimensions of this part were initially chosen using an educated guess as to what would be required to cope with the loads this device would encounter during normal use. However, the results that were calculated from the analysis showed that this part was highly over-engineered.

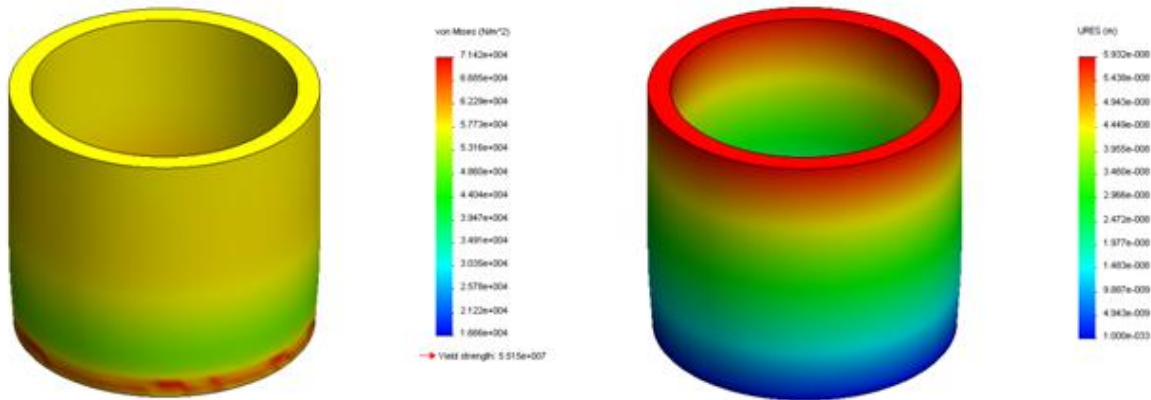


Figure 26: Internal Stresses and Displacement of the Elbow Base

With a maximum internal stress of  $7.142 \times 10^4 \text{ N/m}^2$ , a maximum displacement of  $5.932 \times 10^{-8} \text{ m}$ , and a minimum safety factor of 772.139, this component was a perfect candidate for a new iteration. The new design would allow for weight optimization. However, caution would have to be taken in order to ensure this part would not be under-engineered to the point where the component would be in danger of damage if the device was hit or impacted by its environment. A safety factor of 20 or more would cope with such a situation while also greatly reducing the overall weight and robustness of the component.

### 5.1.5.2 Bottom Collar

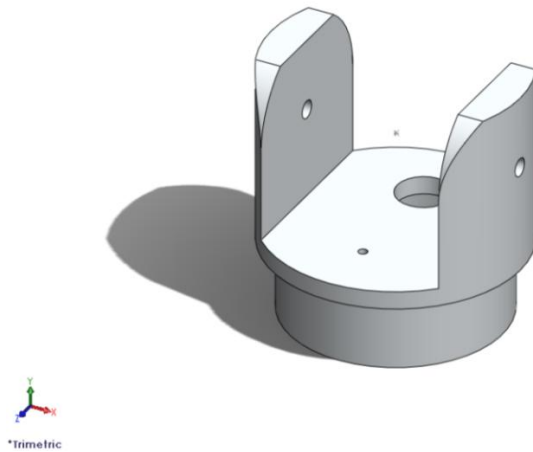
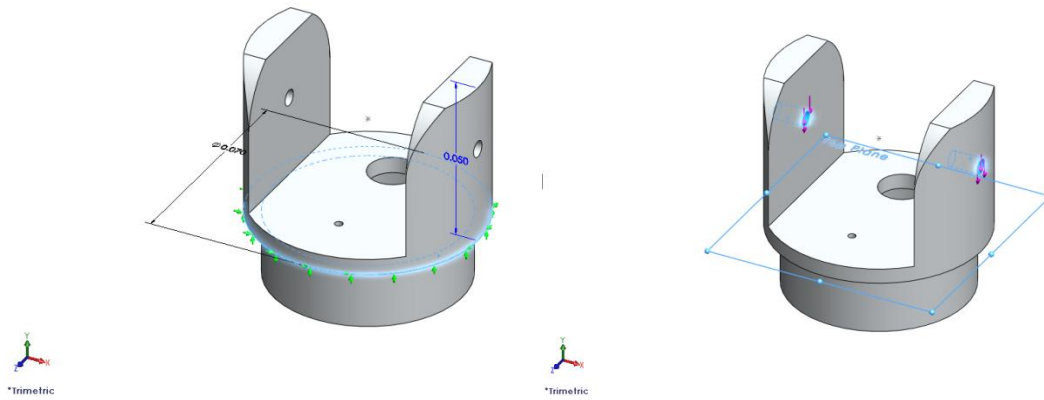


Figure 27: Bottom Collar

The Bottom Collar was one of the more complex designs on the elbow-joint. This part was designed to allow 180 degrees of movement while also allowing electrical power and communications connections to pass through the joint. The Bottom Collar also supported the worm drive system that was to be employed in this design. Also, the Bottom Collar featured a flange that would be used to attach it to the Elbow Base. During this analysis, it was assumed that it would be either welded or attached with screws to the Elbow Base. The structure itself would bear the load rather than rely on screws or welds to support the applied forces.

Analysis was done by fully constraining the bottom flange of the collar and then applying a force of 60 Newtons to the rotator pin mounts Figure 28.





**Figure 28: Fully Constrained Face and Applied Force Location of the Bottom Collar**

Much like the Elbow Base, the Bottom Collar was a preliminary design that was over-engineered in a few areas. The results of the analysis Figure 29 shows the Bottom Collar achieved a maximum internal stress of  $6.615 \times 10^5 \text{ N/m}^2$ , a maximum displacement of  $3.329 \times 10^{-7} \text{ m}$ , and a minimum safety factor of 83.3643.

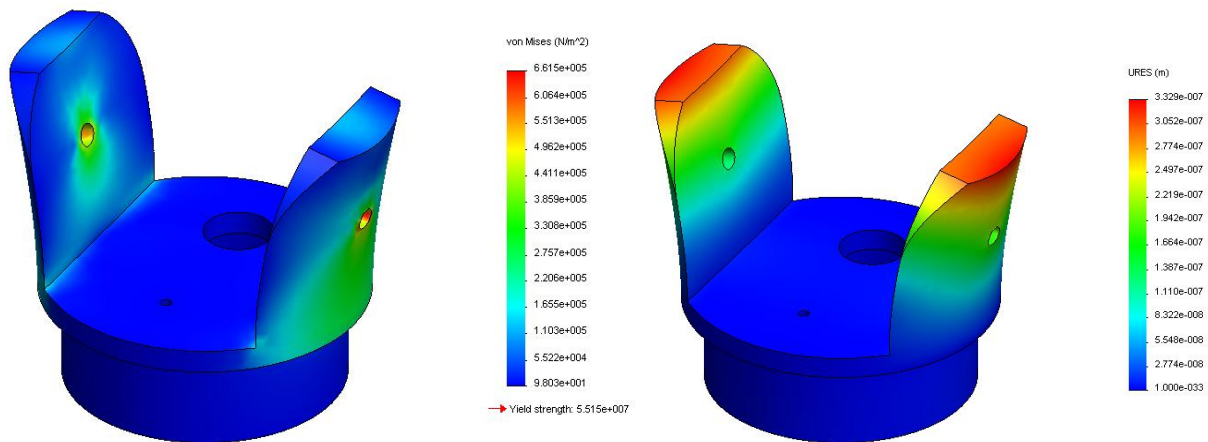


**Figure 29: Internal Stresses and Displacement of the Bottom Collar**

Also, the design featured some characteristics that could be altered in the next iteration. The radius of the Rotator Pin mount, Drive Shaft support and the communications opening were all subject to change if the following iteration required it. Although overall strength

was extremely important to the design of this device, this design could afford the loss of some strength in order to reduce overall weight and price.

### 5.1.5.3 Rotator Pin

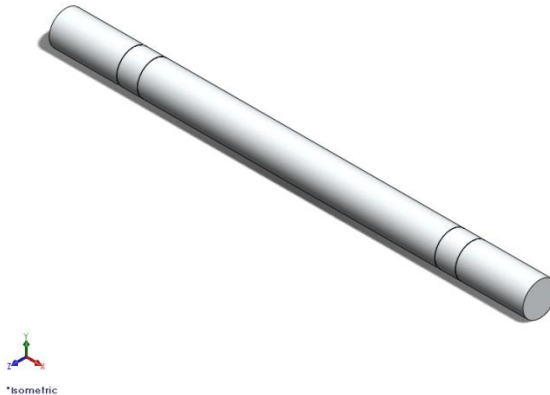
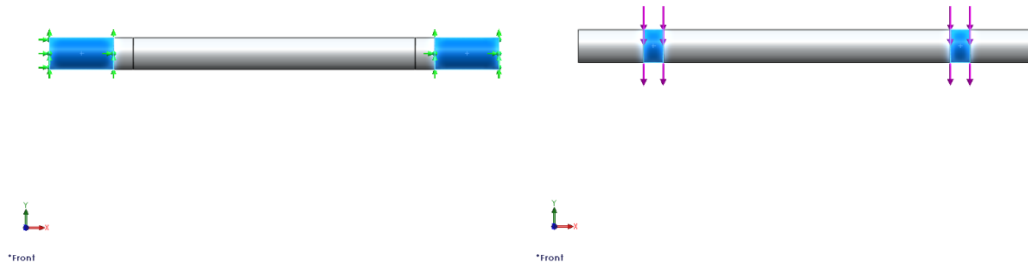


Figure 30: Rotator Pin

Although the rotator pin was one of the more simple parts of this design, it played a crucial role in both transferring mechanical power and supporting the whole joint. For this reason it was extremely important that preliminary analysis was done in order to ensure this component would not fail under operational loads. Also, it was important to note that at this point in the design phase, the rotator pin was thought to be the weakest point in the design.

Unfortunately, due to the way Solidworks conducts stress analysis, small grooves were needed to divide the rotator pin into sections. While this would have an effect on the stress analysis results, the grooves were made so small that they were nearly negligible, and it was determined that a smooth rod would yield higher safety factors, since there would be less stress concentration areas. First, the outer section of the pin was fully constrained (Figure 31). This was created to simulate the reactionary forces the bottom

collar would apply. Also a force of 60 Newtons was applied to simulate the weight of four joints and a 2 kg weight (Figure 31).



**Figure 31: Fully Constrained Face and Applied Force Location of the Rotator Pin**

After the results of the preliminary analysis were gathered, it was found that indeed the rotator pin was one of the weakest parts of the design. The analysis found that the rotator pin achieved a maximum internal stress of  $8.782 \times 10^6 \text{ N/m}^2$  (Figure 32), a maximum displacement of  $7.977 \times 10^{-7} \text{ m}$  (Figure 32) and a minimum safety factor of 6.27959.

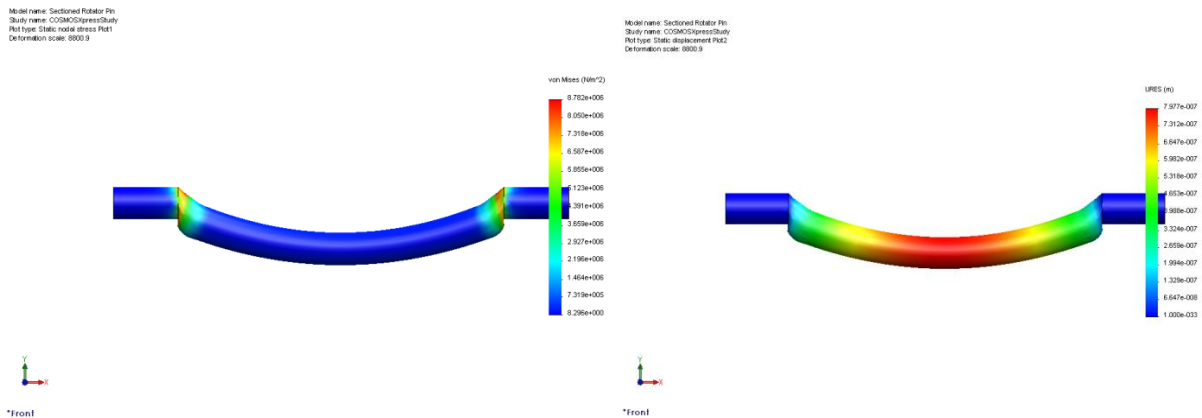


**Figure 32: Internal Stresses and Displacement of the Rotator Pin**

While this may still seem as though the part was needlessly over engineered, it was important to conserve some of the strength, such that in case of impact, the components

would be able to handle the forces they would encounter. For this reason, it was important to either preserve the strength of the rotator pin or increase it in all of the following designs.

#### 5.1.5.4 Top Collar

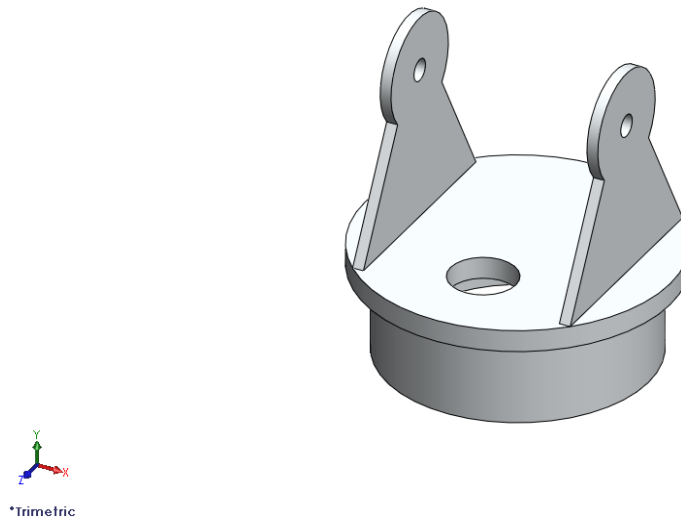
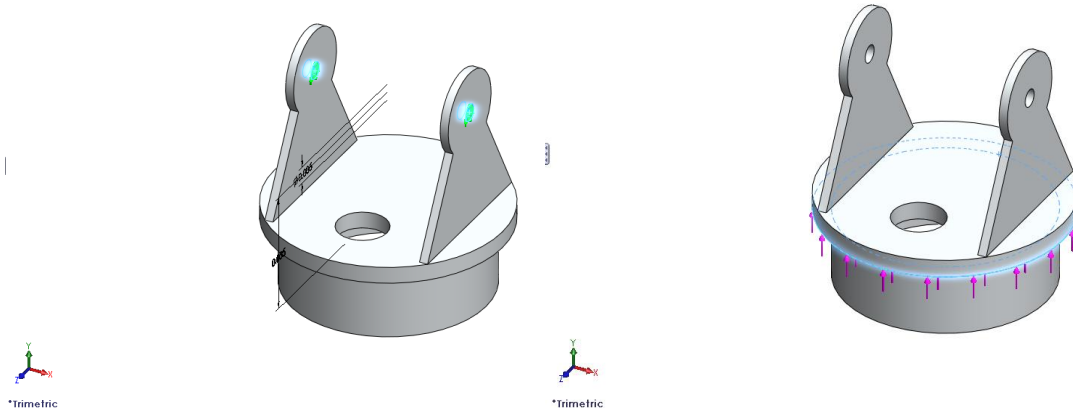


Figure 33:Top Collar

The Top Collar component was very similar to the Bottom Collar. However, the Rotator Pin mounts featured thinner supports to cut down the overall size of the design. Also, the Rotator Pin supports were shaped to ensure the joint would be able to achieve a full 180 degrees of rotation. However, since the mount members were thinner, it was expected that this design would require more robust components. The Top Collar features the same flange design as the Bottom Collar; however, this flange would be used to allow other joints to be attached to this design.

Much like the Bottom Collar, the Top Collar would be constrained in a few areas. The Top Collar would be fully constrained at its Rotator Pin mounts, as shown in Figure 34. Unlike the Bottom Collar, the reactionary forces within the Top Collar would be coming

from the Rotator Pin Mounts. Also, a force of 60 Newtons was applied to the flange of the Top Collar to simulate operational forces. The reaction and load surfaces are shown in Figure 34.



**Figure 34: Fully Constrained Face and Force Location of the Top Collar**

It was important to note that at this point in the design process, no decision had been made as to how adjacent joints would be connected. For preliminary analysis purposes it was assumed that this joint would either be welded or attached with screws to the following joint. For now analysis would be done to determine if the design could withstand the forces it would be subjected to.

The results of the preliminary analysis were very similar to the Bottom Collar. Although the thinner Rotator Pin supports played a large role in how this component reacted to forces. The different design accounted for a maximum internal stress of  $1.24 \times 10^6 \text{ N/m}^2$ , a maximum displacement of  $6.157 \times 10^{-7} \text{ m}$  (Figure 35), and safety factor of 44.4808, which was nearly half of what was achieved with the Bottom Collar.

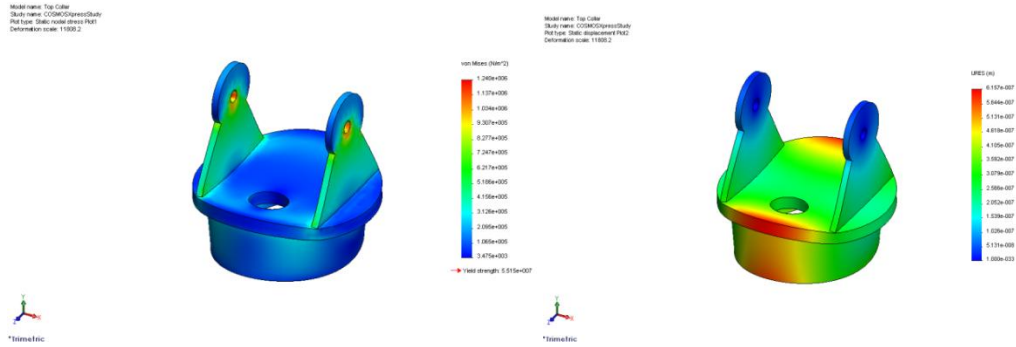


**Figure 35: Internal Stresses and Displacement of the Top Collar**

While a safety factor of 44.4808 meant it was weaker than the Bottom Collar, it did not mean this component was insufficient for the application. This was still a large safety factor which showed that this component could also benefit from a new iteration that required less material and possibly a more intricate design to help the component cope with the forces it would be subjected to.

### 5.1.6 Iteration 01 Part Selection

The first parts to be researched were the motor and worm/worm gear combination. During the creation of iteration one, the necessary motor torque and rpm for both joints were estimated by both computer analysis of iteration one (described in section 0) and tests to find an average speed for a human arm to move back and forth Appendix D.

Using the information gathered from the torque analysis in section 0, the necessary motor torque could be calculated. Torque specifications for motors are normally given in either rated torque, which is the torque a motor can output without overheating, or stall torque, the maximum torque at no speed. Stall torque is typically twice the rated torque for DC motors. If the rated torque for the elevator joint was 12 Nm, the stall torque would be approximately 24 Nm.

Once the desired rated and stall torque and rpm were determined, a motor could be selected. The task specifications placed significant importance on a compact, low cost joint, therefore research focused on small and affordable parts. A motor selection matrix comparing power, speed, cost, and size was developed to aid in motor selection, which is included in Appendix B. Compact, high torque motors were either difficult to find, expensive, or could not be sold in single units. Merkle-Korff Industries, for example, manufactures a small motor that met our requirements (Table 1), however they are only sold in batches of 250 units. Another small motor manufacturer, MicroMo, quoted an approximate cost of \$14,000, which was considerably outside the desired price range of this project.

To adjust the motor requirements of both joints, an estimated gear ratio between the worm and worm gear was introduced, which effectively reduced the required motor torque and made an appropriate motor easier to find. With a gear ratio of 20:1, motors with stall torque capabilities and speeds around and above 1.2 Nm and 260 RPM, respectively, were researched.

Motor Selection Matrix for Elevator Joint		
	Elevator	Units
Required Torque	24000	mNm
Required RPM	13	rpm
Gear Ratio	20	:1
Motor Torque	1200	mNm
Motor RPM	260	rpm

**Table 1: Motor Selection Matrix for Elevator Joint**

Motor manufacturers typically had two forms of presenting the motor specifications. They simply listed the stall torque and no-load speed, or they had a line graph showing the relationship between the torque and speed of their motor. When only listed values were given, the stall torque was already accounted for; however the no-load speed had to be significantly higher than the desired speed because no-load assumes there is no torque on the motor. Torque and speed are inversely related, where as torque increases, speed decreases and vice versa. The elevator joint would be having at least a 12 Nm torque acting on it, therefore the actual speed of the motor would be significantly less than the no-load speed given by the manufacturer. In the case of a graph given by a manufacturer, the speed corresponding to the desired torque had to fall below or on the line to meet the desired specifications.

A motor with a stall torque of 2.2 Nm and no-load speed of 120 rpm was found for \$26.95, a reasonable price, at robotmarketplace.com. The standard gear ratio to reach the



24 Nm requirement was 10, so worm gears with a 10:1 ratio were considered instead of 20:1 ratio. A little speed was lost in order to reach the desired torque, however the difference between 12 and 13 rpm was insignificant for the scope of this project.

Similar to the motor, a small, affordable worm that could handle the torque output of the motor was either difficult to find, expensive, or was not sold individually. Common suppliers, such as McMaster-Carr, MSC Direct, and Stock Drive Products/Sterling Instruments, were identified as the most reasonable sources of worms and worm gears. However, the final motor was selected after suppliers were identified. This was a problem because the shaft of this motor was measured in metric units. For the sake of continuity, all other parts had to be in metric units. Small metric parts proved more difficult to find than English unit parts. Neither McMaster-Carr, nor MSC Industrial Supply, carried metric worms or worm gears, which left only Stock Drive Products/Sterling Instrument to choose from. The smallest worms sold were either integral to a shaft, required a press fit onto a shaft, or needed a keyway. A press fit and a keyway would have contradicted the ease of manufacturing and maintenance task specifications, as they would have been difficult to disassemble, whereas worms integral to the shaft met both task specifications. In addition, according to the mechanical design of iteration one, the worm would require a coupler between its shaft and the shaft of the motor. A worm that needed to be mounted on a shaft would mean a 4-part assembly: the motor, the coupler, the shaft and the worm. An integral shaft worm would only be a 3-part assembly: motor, coupler, and worm. An integral shaft worm was thus determined as the best option for the elevator joint due to its ease of manufacturing, maintenance, and assembly qualities.

The smallest integral worms were expensive, at approximately \$68 each when bought individually. In order to compromise between size and cost, a larger than desired, yet reasonably priced, worm was selected and purchased for approximately \$26. The worm gear corresponding to the chosen worm that created a 10:1 gear ratio was also purchased.

### **5.1.7 Iteration 01 Discussion**

Although this first iteration provided many of the necessary details needed to complete the other designs, there were a few areas where the design needed improvement. After analysis was done on the elevator joint components, it was found that many of the parts were needlessly over engineered. Since it was unknown how the elevator joint would react to loads, most of the parts were designed to be robust to ensure no structural failures were present. This design also did not include the motor or a means of securing the motor to the elevator joint. Analysis would need to be done in order to find the power necessary to move the elevator joint in the manner outlined in the task specifications.

## 5.2 Rotator-Joint Iteration 01

The rotator-joint was designed to allow for continuous rotation. Continuous rotation allows for the joint to rotate in either direction indefinitely. Though this allow for further applications, it also presented many technical challenges in order to allow for modularity. Specifically, since the rotator-joint would be able to rotate infinitely in either direction, traditional means of transferring power and signal via wires would not work, since they would twist and eventually break. Therefore, most of the following iterations focused on determining a solution to transferring power and signal across the rotator-joint.

The first iteration of the rotator-joint included basic components to achieve the rotation function, as well as defined the basic size and shape of the rotator-joint. For simplicity in the first design, the communication and electronic system were neglected. The focus of the design was on the exterior of the rotator-joint as well as the modularity of the system.

### 5.2.1 Kinematics

The rotator-joint was designed to be an inexpensive device, but capable of continuous rotation. This allowed for numerous complexities in the design. Drawings of iteration one may be found in Appendix P.

The rotator-joint was designed to transfer the mechanical power of the motor to the rotating top, while supporting the load of the next joints and any applied load. The major components were the bottom and top shells and the rotating shaft. These components created a simple revolute joint, rotating about the y-axis as shown in Figure 36. For

simplification, the base shell was considered fixed, while the shaft and top shell were fixed together and rotate about the base shell.

## 5.2.2 Iteration 01 Components

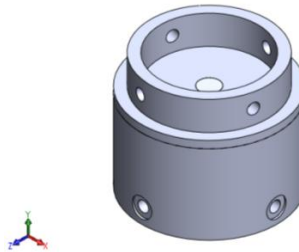


**Figure 36: Iteration One Rotator-Joint**

Iteration one contained four basic components, the base shell, top shell, main shaft, and bearing, as shown in Figure 36. The base shell was designed to be the housing for the motor, shaft, circuits and wires. Additionally, the base shell would be the main structure used for securing the rotator-joint to other joints or fixtures. The base shell also had to be designed to withstand the compressive load, and included machine screw holes in the bottom to allow for attaching to the next module.

The top shell was the rotating part in the assembly. This part was driven by the main shaft, and included screw holes for attachment to the next joint. A flange was included to allow for the top shell to fit inside of the next module to create a secure fit. The top shell had to be able to support a load and transfer the load down to the base shell. The main shaft was designed to transfer the mechanical power from the motor to the top shell. The first iteration design of the main shaft was a simple cylinder to be detailed later in this report.

### 5.2.3 Iteration 01 Inertia Calculations and Motor Selection

Basic inertia calculations were completed to determine the required output of a motor for use in the rotator-joint. The analysis assumed that material used in the model was Aluminum 6061. Additionally, to determine the maximum required output torque, the analysis assumed that the rotator-joint was placed on its side, rotating three elevator-joints, as shown in Figure 37. This resulted in a maximum required torque of 9 N-m, as shown in the calculations in Appendix E. This inertia analysis assumed that the rotator-joint was rotating the load at approximately 1.4 degrees per second, roughly the speed of a human arm.

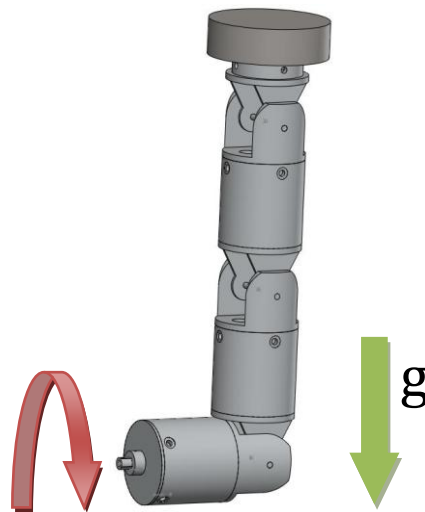


Figure 37: Joint Set-Up for Inertia Calculations

### 5.2.4 Iteration 01 Stress Analysis

In order to determine the strength of the rotator-joint, stress analysis using SolidWorks analysis was performed. Each load bearing part was analyzed assuming simple compression. These load bearing parts analyzed included the top shell and base shell.

Though simplified, this allowed the group to determine if the rotator-joint was strong enough to perform successfully in a variety of configurations. The load was set at 80N, which was determined by the approximate weight of three elevator-joints and a 2 kg load.

#### 5.2.4.1 Top Shell

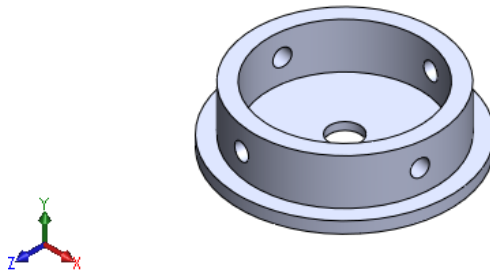


Figure 38: Top Shell Model

The top shell, as shown in Figure 38, needed to support the load of adjacent joints as well as any applied load. The total load was therefore assumed to be around eight kilograms, or approximately 80 Newtons. This analysis also assumed that the part was made from Aluminum 6061. For the analysis, the restraint chosen was the bottom surface of the part, while the load surface was chosen as the outer collar, as shown in Figure 39. The restraint surface chosen assumed that all applied load to the top shell was transferred directly to the base shell, and that no compressive force was transferred through the shaft. Similarly, the load surface chosen assumed that the next joint in the series applies the load through the base shell onto the flange of the top shell.

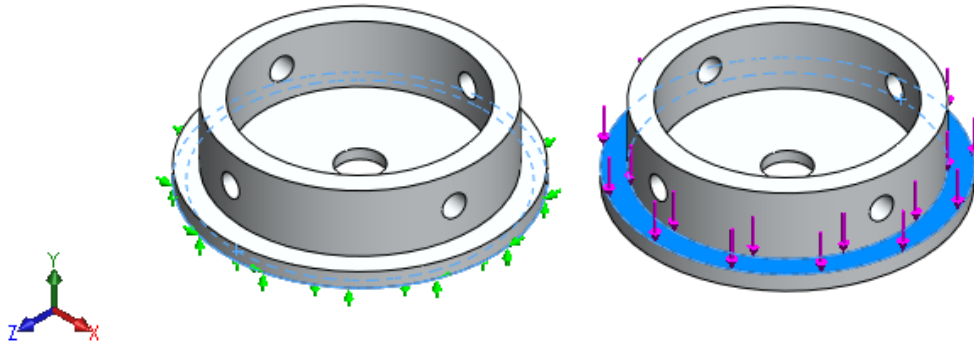


Figure 39: Restraint Surface and Load Surface for Top Shell

The stress analysis solved for the following values: minimum safety factor of 181, maximum stress of  $3.046 \times 10^5 \text{ N}/\text{m}^2$ , and a maximum displacement of  $2.692 \times 10^{-8} \text{ m}$ .

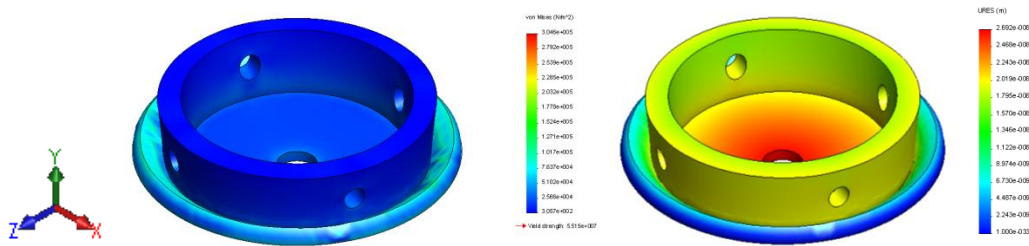


Figure 40: Stress Distribution and Displacement of Top Shell With 80 N Load.

The large safety factor shows that the top shell was strong enough assuming this load and material. If Aluminum 6061 was chosen as the final material, this part could have been redesigned to use less material. Additionally, the stress distribution and displacement models behaved as expected, and showed no potential problems for the part under a compression load. This analysis allowed the group to determine that Aluminum 6061 may be too strong of a material for this part; therefore the group researched other lighter materials such as plastics to be used in the next iteration.

### 5.2.4.2 Bottom Shell

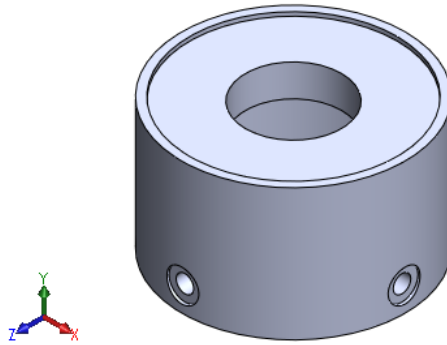


Figure 41: Bottom Shell Model

The base shell, shown in Figure 41, supported the force of the base top, as well as the weights of any other joint and the added load. Again, the total load applied to the base shell was 80 Newtons, approximately the force three additional joints and a 2kg load would create. This analysis also assumes that Aluminum 6061 was used for the bottom shell material. The restraint force was applied to be the bottom surface of the shell, while the applied force was along the top outer edge, both shown in Figure 42. This loading assumed that all the force creates simple compression of the base shell, and that no load was transferred through the shaft, bearing, or motor.

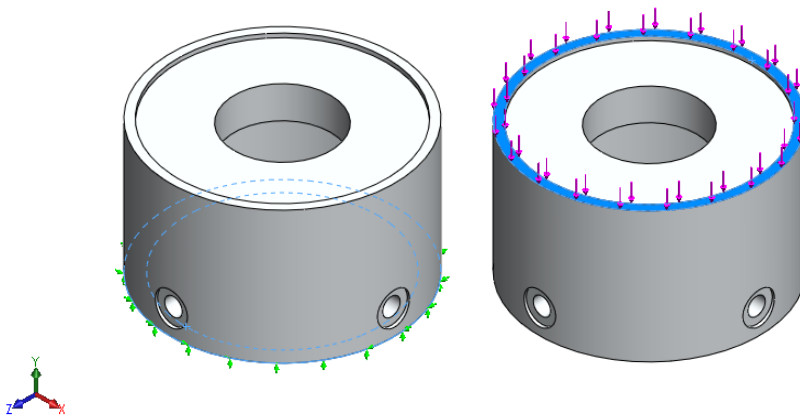
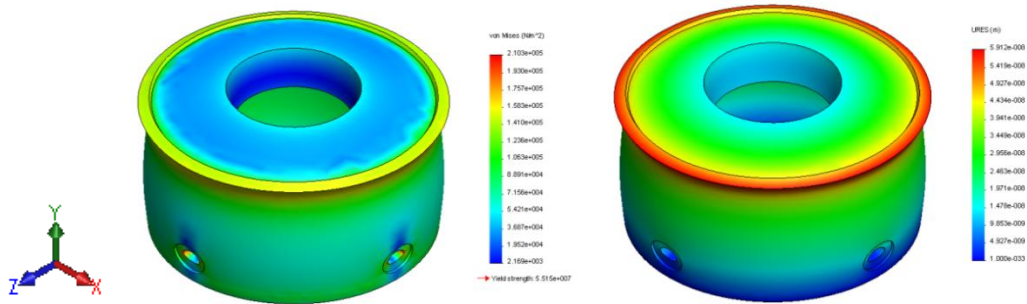


Figure 42: Restraint Surface and Load Surface for Base Shell



This analysis yielded the following values: minimum safety factor of 262, maximum stress of  $2.103 \times 10^5 \text{ N}/\text{m}^2$ , and a maximum displacement of  $5.912 \times 10^{-8} \text{ m}$ . The stress and displacement distributions are shown in Figure 43.



**Figure 43: Stress and Displacement Distributions for Base Shell**

The safety factor of the base shell was much larger than that of the top shell, therefore the top shell would be the first structural part to fail under a compressive load. This large safety factor shows that the part was over-engineered for an aluminum material, and therefore allowed the group to consider plastics as an alternative option. The stress and displacement distribution of the base shell was adequate for these loading conditions, however the cuff on top of the base shell was the weakest point and could be easily improved by making it thicker or adding a chamfer.

### 5.2.5 Iteration 01 Part Selection

Parts selection for iteration one of the rotator was similar to iteration one of the elevator, with the first parts researched being the motor and worm/worm gear combination. The only differences were that the computer analysis to determine the torque required by the rotator placed it as the base, rather than the elevator, and the subsequent torque requirement proved to be different. The necessary speed, determined in section 5.2.3 as 13 rpm, was assumed to be the same as the elevator.

The computer analyzed four joints in series with the rotator as the first joint and four other joints directly connected and a 2 kg weight on the end. The rotator was orientated at a right angle, its length parallel to the ground with an elbow-joint as the second joint. The driven collar of the elbow-joint was oriented all the way to the side, or at a 90 degree angle, and the subsequent joints and weights were positioned linearly. This orientation required the most torque, compared to other orientations, for the rotator-joint to lift the following three joints and would therefore be the maximum torque required by the rotator-joint to successfully function. Computer analysis showed that for iteration one of the rotator to operate without stalling or burning the motor, its torque output needed to be about 9 Nm, making the DC motor stall torque approximately 18 Nm.

After the desired rated and stall torque were determined, a selection of a motor was possible. As discussed in the task specifications, the ideal end product was a compact, low cost joint, and therefore small and affordable parts were prioritized. A motor selection matrix comparing power, speed, cost, and size was developed to aid in motor selection for the rotator, as shown in Appendix B. Finding a motor that met the rotator-joint requirements was equally as difficult as finding one to fit the elevator-joint, therefore, an

estimated 20:1 gear ratio between the worm and worm gear was introduced, effectively reducing the required motor torque to 1.8 Nm and increasing the required speed to 260 RPM (shown in Table 2).

Motor Selection Matrix for Rotator Joint		
	Rotator	Units
Required Torque	18000	mNm
Required RPM	13	rpm
Gear Ratio	20	:1
Motor Torque	900	mNm
Motor RPM	260	rpm

**Table 2: Motor Selection Matrix for Rotator-Joint**

A motor with a stall torque of 2.6 Nm and no-load speed of 70 rpm was found on robotmarketplace.com for \$39.99, which was considered very affordable compared to the \$1400 motors with comparable capabilities sold by MicroMo. The standard gear ratio required to reach the 18 Nm requirement was 10, which was the same ratio as the worm in the elevator. The downside to this motor was that a significant amount of speed was given up in order to reach the desired torque, as it would be 7 rpm with a 10:1 gear ratio, however the cost savings and added torque were considered worth the loss in speed.

### 5.3 Electrical Systems Iteration 01

The initial electrical design consisted of a microcontroller to supervise all functions of the motor control as well as provide an interface to the user's computer. This interface was in the form of RS-232 serial communication to the host PC. At the time, the system was designed to drive a stepper motor, and as a result, a MSP430 microcontroller was chosen, as it had on-board peripherals designed explicitly to interface with servo and stepper motors, as well as a UART capable of serial and IrDA communications (to accommodate the needs of the rotator-joint). The MCU chosen was an MSP430F2132 and had the capability, in addition to IrDA functionality, to provide serial communications using its hardware UART. Although this would not be an issue for production, when it came to prototyping it proved to be problematic. As a result, the processor was mounted on a surface-mount interface board. A preliminary prototype was assembled to establish serial communications between the host and the control board, and to test the functionality of the IR transceiver. Although work had begun on implementing stepper motor control, it was never completed due to electromechanical design changes which resulted in a change from stepper motors to conventional brushed DC motors.



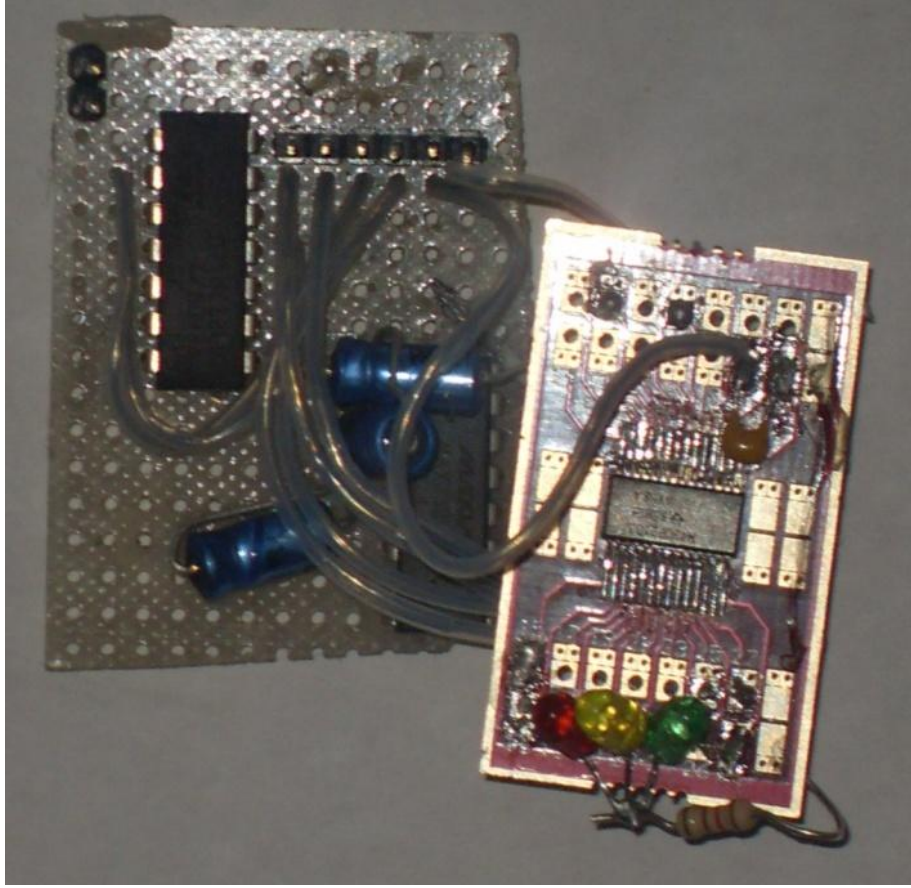


Figure 45: Iteration 1 Prototype

## 5.4 Elbow-joint Pre-Prototyping

Although Erector Set™ products are often used as toys, they provided a unique experience of being able to partially build the Elbow-joint and provide insight to possible problems that could arise during assembly of the prototype, shown in Figure 46.

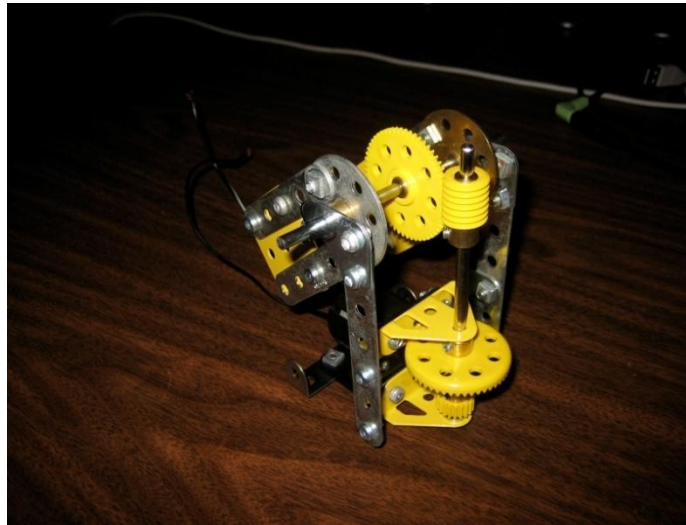


Figure 46: Elbow Pre-Prototype #1

Although this design successfully operated, it revealed a few problems with the initial design concepts. The elevator-joint utilized the vertical worm drive system outlined in iteration one Figure 46. While theoretically this system configuration was acceptable, in reality, the elevator-joint failed to perform. An argument can be made that since Erector Set™ parts were not designed for this application, it was not an appropriate means of building a pre-prototype, however, the elbow-joint was incapable of lifting its own weight which was viewed to be unacceptable. Also, in this design the motor was oriented horizontally. While this was not a problem when using the motor supplied with the Erector Set™, the purchased motors that were purchased were usually longer axially. In order to

accommodate the purchased motors in the current orientation the diameter of the elbow-joint would have to be expanded which was considered unreasonable.

Using what was learned from the first pre-prototype, a new design was created in order to change the worm orientation. This new design featured a worm that was orientated horizontally. The worm shaft could now be anchored in two locations rather than one, as outlined in the first pre-prototype design, as shown in Figure 47.



**Figure 47: Elbow Pre-Prototype #2**

Also, a right-angle gear was used in order to change the orientation of the motor and position it vertically. This new design proved to be more capable than the previous design and very little tooth slip was noted in operation. Using the information gathered during the pre-prototyping process, more capable designs could be made in future iterations.



## 5.5 Elbow-joint Iteration 02

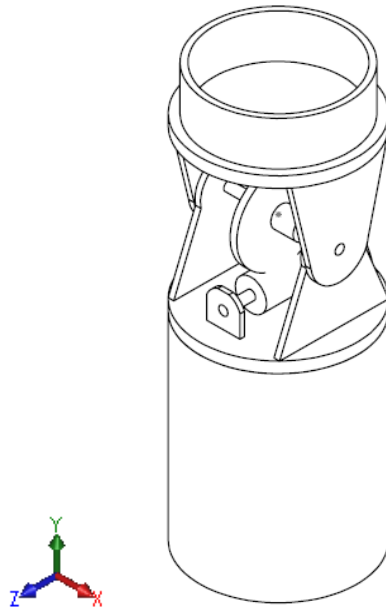


Figure 48: Elbow-joint Iteration 02

Iteration two of the elbow-joint was designed to improve some key areas of the previous design, and to begin including purchased parts. One of the largest changes between iteration one and two was the reorientation of the worm gear drive system. The worm gear in the prototype of iteration one was prone to tooth slip because the shaft was poorly anchored. Design iteration two addressed this problem by changing the orientation of the worm gear from vertical to horizontal, which allowed it to be anchored in two locations, reducing the likelihood of tooth slip. Also, the collar orientation was adjusted in order to accommodate the changes in the worm gear orientation. Finally, in this design iteration, more attention was paid to the drive system. An Hsiang Neng Geared Motor was included in the design of iteration two. The inclusion of the commercial motor generated the problem of how the motor was going to be positioned and mounted within the elevator-

joint. To solve this problem a series of motor mount disks were created in order to ensure perfect placement and provide a means of anchoring the motor.

### **5.5.1 Kinematics**

Although the design of the elbow-joint changed with iteration two, fundamentally the joints operate on the same kinematic assumptions. The overall structure of the elbow-joint was designed to maximize strength and minimize weight. The three major components that made up the structure were; the base, and the bottom and top collar as shown in Appendix K. The base acted as the anchor of the device. Between the base and bottom collar was a fixed connection which allowed no motion between the bottom collar and base. This connection eliminated any roll motion in the design. As a result, the bottom collar became an extension of the base and was in charge of anchoring many of the other components. However, between the bottom and top collar there was a revolute joint. The rotator pin connected the two components. The rotator pin was allowed to move freely in relation to the bottom collar. However, the rotator pin was anchored to the top collar and the rotator pin would be unable to move in relation to the top collar. This freedom allowed the elevator-joint to be capable of pitch motion.

### **5.5.2 Iteration 02 Stress Analysis**

With the inclusion of more parts, the analysis done on the second iteration provided more accurate results. Analysis had previously assumed that all the parts were made of Aluminum, however the prototype was being rapid prototyped out of ABS plastic. Analysis of the parts using ABS plastic would determine whether it was necessary to use metal or not. All the components of the elbow-joint are represented in Appendix K. The following components were made out of rapid prototype ABS:

1. Bottom Collar - ABS Plastic
2. Driven Collar - ABS Plastic
3. Elbow Sleeve - ABS Plastic
4. Motor Mounts - ABS Plastic

Iteration two included the drive system components which were previously left out of the analysis. The motor, gears, and shafts were now included in all models. The gears had been acquired from an erector set and were modeled using ABS plastic. The shafts were also from erector sets but were made of unknown steel. Cast alloy steel would be assumed for the shafts. Using the physical properties provided by the manufacturer, the motor would be modeled as a solid cast alloy steel to mimic the weight of the motor and the geared transmission.

The analysis procedure was very similar to that of iteration one. The forces applied would be the equivalent of four joints being connected in series with a 2 kg weight at the end. However, the change in materials caused a drastic change in overall design weight. As a result, the applied forces were calculated to be 37 Newtons. All the analysis would be done electronically using SolidWorks. It was important to note that SolidWorks did not have ABS plastic registered in its material database; the program was unable to calculate maximum displacement and safety factors. However, by reviewing the internal stress results, one could determine if the design was insufficient. Finally, since the Driven Collar and the Bottom Collar were the two designs that had the most drastic changes, they would be analyzed first.

### 5.5.2.1 Driven Collar

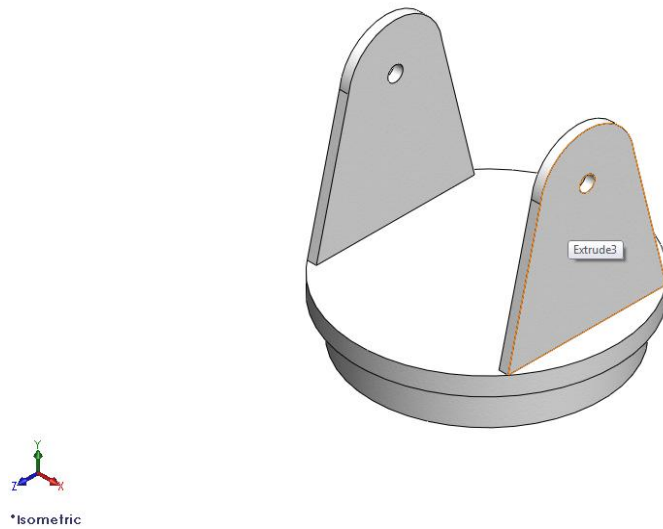
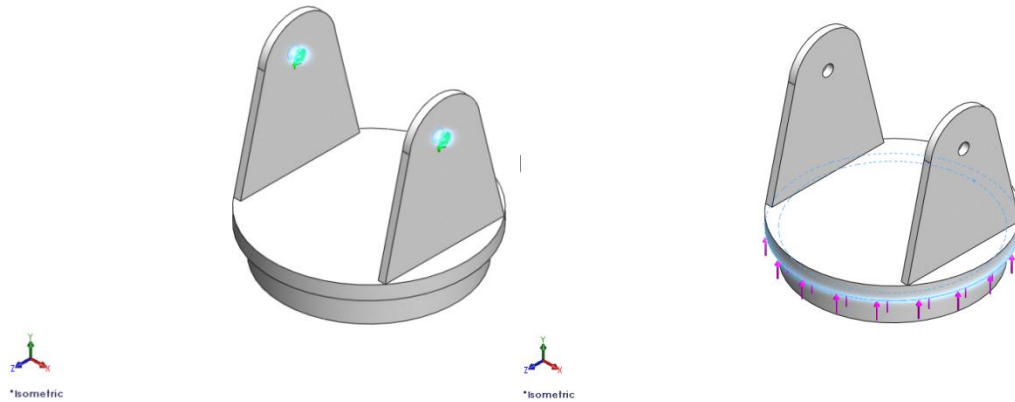


Figure 49: Driven Collar

The Driven Collar was the moving portion of the elbow-joint. This new design minimized the material required for the design as well as preserved the 180 degree freedom that the first iteration was capable of. However, this decrease in material meant that the joint would react differently to loads.

Due to the orientation of the Driven Collar the forces of the following joints would be acting on the top flange. For analysis purposes it was assumed that the operational force of 37 Newtons would be applied to the top flange of Driven Collar. To simulate the reactionary forces, the joint was fully constrained at the Rotator Pin mounts (Figure 50).



**Figure 50: Fully Constrained Face and Applied Force Location of the Driven Collar**

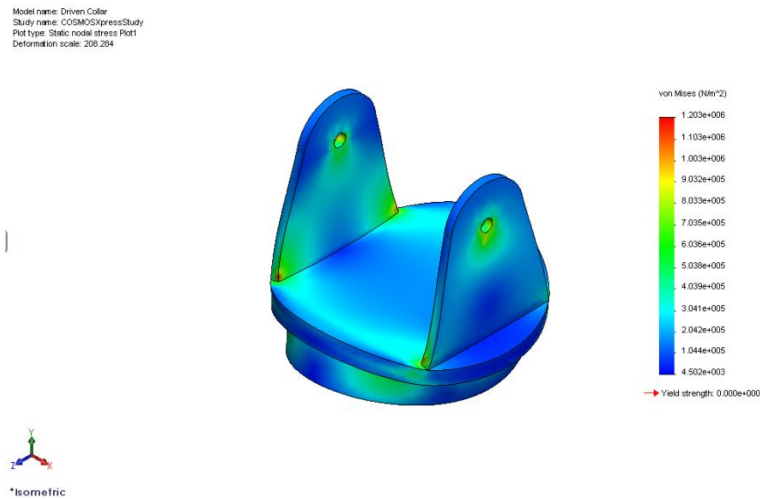


**Figure 51: Internal Stresses of the Driven Collar**

Unfortunately, due to the reduction in overall dimensions, this part achieved larger overall internal stresses. The Driven Collar attained a maximum internal stress of  $1.203 \times 10^6 \text{ N/m}^2$ . These results meant that the new design had posted higher internal stresses than the previous iteration. Had the building material still been Aluminum 6061 these results may have been acceptable. However, the overall strength of ABS plastic was significantly less than aluminum. These results meant that the following design would need more emphasis on strength if ABS plastic was going to be used in the future as the building material.

### 5.5.2.2 Bottom Collar

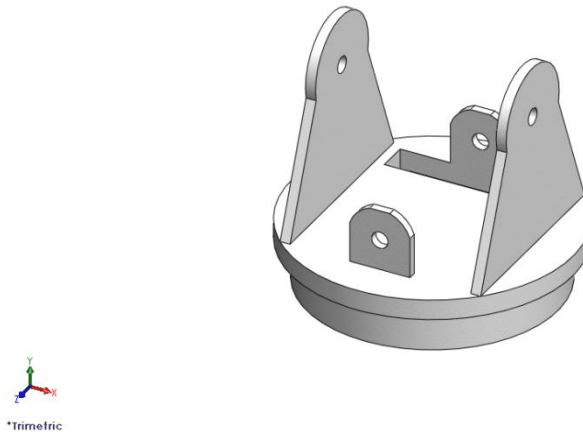
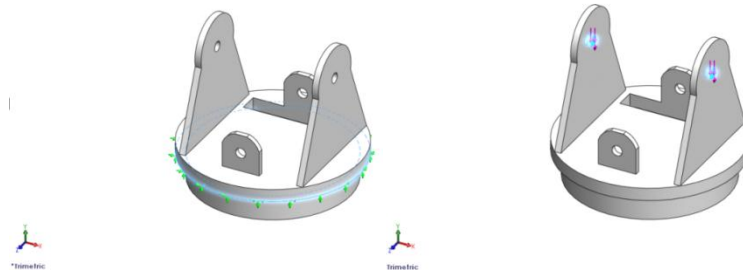


Figure 52: Bottom Collar

The Bottom Collar was the anchoring structure for the driven collar as well as the mounting system for the worm gear. This iteration was designed with the knowledge that was gained during the Pre-Prototyping phase of the design Process. The new orientation of the drive worm would ensure a stronger and smoother drive system, minimizing tooth slip and overall worm displacement. Much like the Driven Collar, the Bottom Collar featured thinner Rotator Pin mounts. After the results of the Driven Collar had found the design to be insufficient, special attention was paid to the Bottom Collar to see if it suffered from the same short-comings.

Analysis was done by fully constraining the bottom flange of the collar to simulate the reactionary forces. Also, the operational force of 37 Newtons was applied at the Rotator Pin mounts (Figure 53).



**Figure 53: Fully Constrained Face and Applied Force Location of the Bottom Collar**

It was important to note that, in the future, the collar would be bolted to the elbow sleeve. The affects of the screws were ignored because they were designed only for positioning, not load carrying.

Unfortunately, much like the Driven Collar, the Bottom Collar was found to have large internal stresses. With a maximum internal stress of  $1.808 \times 10^6 \text{ N/m}^2$  this component also suffered from internal stresses that were too high for the material. This design of the Bottom Collar would need to be visited in the next iteration to ensure it would cope with operational forces. It was important to note that since these two crucial components failed their analysis, it was deemed unnecessary to continue analysis since it was apparent that a large design overhaul was needed.

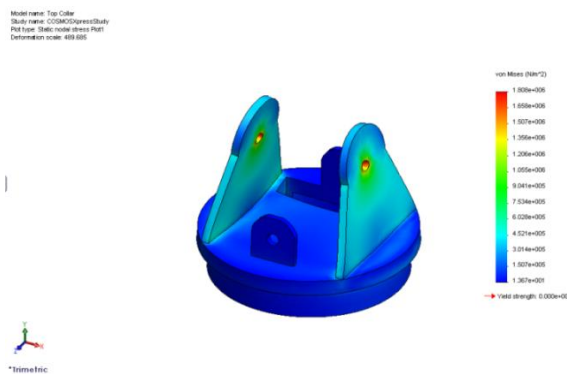


**Figure 54: Internal Stresses of the Bottom Collar**

### 5.5.3 Iteration 02 Part Selection

Changes to iteration one brought additions to part selection in iteration two. The orientation of the worm in iteration one proved to be considerably unsteady in the first prototype, so it was reoriented to provide more stability. This new orientation required a right-angle gear to translate the mechanical energy of the motor shaft from vertical to horizontal. Miter, bevel, and differential gears were considered options, however the gearing needed a 1:1 gear ratio which is satisfied by a miter gear. A differential gear would have been ideal due to its increased stability; unfortunately, most were too expensive or were only sold in English units.

It was determined that iteration one could be redesigned to have a smaller package size, thus a greater emphasis was placed on more compact parts in iteration two. To minimize increased length due to the added gears, the smallest miter gears that could reasonably be attached to a shaft or to the worm were identified. A miter gear with a set screw would have been the ideal option, however the metric consumer off the shelf miter gears with set screws or keyways had an overall width of 32 mm or greater. Therefore a small miter gear without a set-screw or keyway was chosen and it was decided that it could be modified to include a pin or smaller set-screw in order to secure it to a shaft. The smallest pins available were found to be 1 mm in diameter, on smallparts.com, and the smallest set screws at 1.6 and 2 mm in diameter, from smallparts.com and Stock Drive Products/Sterling Instrument, respectively. Therefore a hub length of at least 4 mm was considered necessary for both strength and ease of manufacturing; anything smaller would have been difficult to drill a small hole into. The smallest miter gears with a >4 mm hub length were compared for overall diameter and hub diameter, and the smallest was chosen



with an overall diameter of 10.7 mm and hub diameter of 8 mm. Calculations to determine whether a pin, set screw, or possibly a press fit would be most effective for the prototype were done during iteration three.

A consequence to the use of such a small miter gear was that the integral shaft of the worm would need to be turned down to the miter gear's bore size. In the case of the selected miter gear, the bore size was 3 mm, which was simple to create in solid modeling, however in manufacturing, it later proved to be extremely difficult, and is discussed during iteration three, 6.1.

Iteration two also included the worm, worm gear, and motor chosen during iteration one. This then allowed for a more detailed mechanical design, and the identification of additional parts, such as shafts and bearings. The bore size of the worm gear was 6 mm, therefore a 6 mm stainless steel shaft was selected from the cheapest supplier. Bearings for the shaft of the worm would receive little thrust force, therefore flanges were not necessary to hold them in place. Also, to minimize dust getting into the bearings and lubricant getting out, bearings were limited to being either doubled shielded or double sealed. Cheap, unflanged, double-shielded bearings, with a 3 mm bore, were finally purchased on smallparts.com for \$4.00 each.

#### **5.5.4 Construction of Prototype**

Although the computer analysis of iteration two indicated that the rotator-joint would not be as functional as the group intended, a prototype of the design was constructed. The prototyping process provided insight into the many problems of the design that could not be recognized during the computer design process. The most difficult problem was the positioning and anchoring of the motor mount disks. These thin features were created to anchor the motor to the Elbow Base however, with no system of attachment the motor often shifted its position or fell out. The group learned that these motor mount disks would need to be improved and include some form of physical attachment to the Elbow Base such as screws. Also, although the Erector Set™ parts proved to be easy to use, their overall strength and functionality was greatly limited. It was clear that the decision to use Erector Set™ parts limited the second iteration of the Elbow-joint. In the future the group would need to research more robust parts in order to create a stronger rotator-joint.

#### **5.5.5 Iteration 02 Discussion**

Although the second iteration utilized many of the improvements that were discovered during the first iteration of design and the pre-prototyping phase, it was clear that the overall design was not strong enough for the applications it was designed to operate in. The decision to use ABS plastic instead of Aluminum 6061 had more of an impact than was expected. As a result, future designs would need to consider the adverse affects of this new building material in order to produce a design that would be strong, functional, and inexpensive.

## 5.6 Rotator-Joint Iteration 02

Though structurally the first design of the rotator-joint was sufficient, there were many aspects that needed improvement. Iteration one was designed for conceptual purposes and allowed the group to determine other components that were necessary to include. Additionally, the first iteration motivated most of the part selection for the prototype design. The motor selected required the base shell to be lengthened. Additionally, iteration one did not allow for electrical power and signal to be transmitted across the rotator-joint, as required in the design specifications. Lastly, the rotator-joint had no means to securely fasten the motor to the base shell. These missing features required design changes for iteration two, as shown in Figure 55.

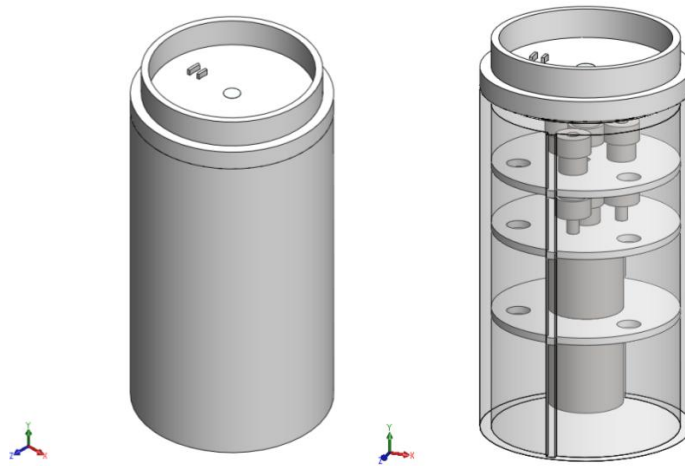


**Figure 55: Iteration Two Rotator-Joint, Isometric and Transparent Trimetric Views**

To allow for electrical power transmission, the second iteration rotator-joint included a custom slip ring joint. The rotator-joint was also required to transmit signal, so the shaft was designed to be hollow to allow IR beams to transmit signal from each end of the rotator-joint. While this was a feasible idea, it required a space for the IR transmitter in between the motor and main shaft, which was created by a gearing system.

### **5.6.1 Kinematics**

The second iteration rotator-joint was kinematically similar to the previous iteration; however, the inclusion of the gear train complicated the system. A drawing of the second iteration is included in Appendix Q.

The simple revolute joint in iteration one was expanded to include several revolute joints, since each gear train would rotate. The carrier plates were assumed fixed to the base shell, and allowed for rotation of the main shaft as well the gear shafts. The mechanical power was transferred from a gear fixed to the motor, to three gears evenly spaced. These gears were fixed to shafts, with three other gears on the opposite end. These gears then transferred the mechanical power to the main shaft.

### **5.6.2 Iteration 02 Components**

Iteration two included a large number of new parts, mostly due to the inclusion of the slip ring and gearing assembly associated with the IR transmitter. Additional changes included the addition of carrier plates that would support the motor and gear assemblies.

The slip ring was designed to allow for maximum electrical power transmission while minimizing mechanical friction. The system included two sets of concentric rings, one for electrical power and one for ground. Each set contained two rings, one on top of the other. The rings would be recessed into the base shell and top shell. Additionally, the rings would have small tabs on them that would prevent them from rotating as well and allow the conductive rings to be connected to the electrical system. The contact rings were constructed of brass, which is both highly conductive and has a low friction coefficient.

To allow for signal transmission, IR transmitters and receivers would be fixed to each end of the rotator-joint. The signal would pass through the center of the shaft, so the IR mechanisms had to be centered in the rotator-joint. This required creating space in between the motor and the shaft, and therefore required gears.

The gear assembly created was designed to transmit the mechanical power of the motor to the outside of the main shaft. Gears of the same diameter and number of teeth were used to maintain constant speed and torque as desired. Three sets of gear trains were used at equal circumferential spacing to minimize wobble of the main shaft.

Carrier plates were also included in the second iteration. These carrier plates were thin disks that stabilized the motor and gear assemblies. Holes were included in the plates to allow for correct positioning of the motor and gear shafts, as well as extra holes to allow for circuit wires. Additionally, two tabs were added to match grooves in the base shell. These tabs and grooves prevented rotation of the assemblies in the base shell.

### **5.6.3 Iteration 02 Stress Analysis**

The analysis performed on the second iteration was similar to the previous. The SolidWorks analysis program Cosmos was utilized to analyze each load bearing part in compression. The analyzed parts included the base shell, the base top, and the top shell. Though simplified, this allowed the group to determine if the rotator-joint was strong enough to perform successfully in a variety of configurations. The load was set at 80N, which was determined by the approximate weight of three joints and a 2 kg load.

### 5.6.3.1 Base Shell

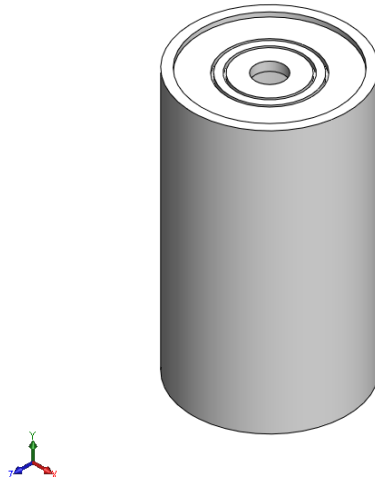


**Figure 56: Base Shell Model**

The base shell was designed to house the motor and electrical components, as well as support the gear assembly. The base shell needed to be able to support the weight of the next joints in series as well as any applied load. Since the safety factors in the previous iterations were significantly large when assuming aluminum, this analysis assumes ABS plastic to save on weight while hopefully still falling with a reasonable range for the safety factor. For this analysis, the bottom surface was constrained, while the upper outer edge of the base shell has the applied load, as shown in Figure 57.

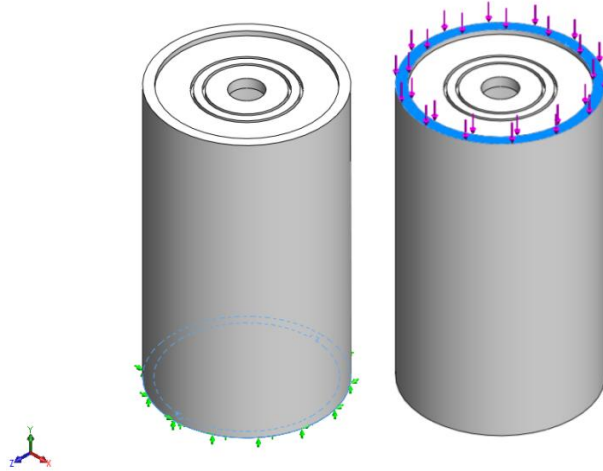


**Figure 57: Restraint Surface and Load Surface for Base Shell**

The stress analysis solved for the following values: maximum stress of  $1.389 \times 10^5 \text{ N/m}^2$ , and a maximum displacement of  $36.741 \times 10^{-6} \text{ m}$ . The stress and displacement distributions are shown in Figure 58.

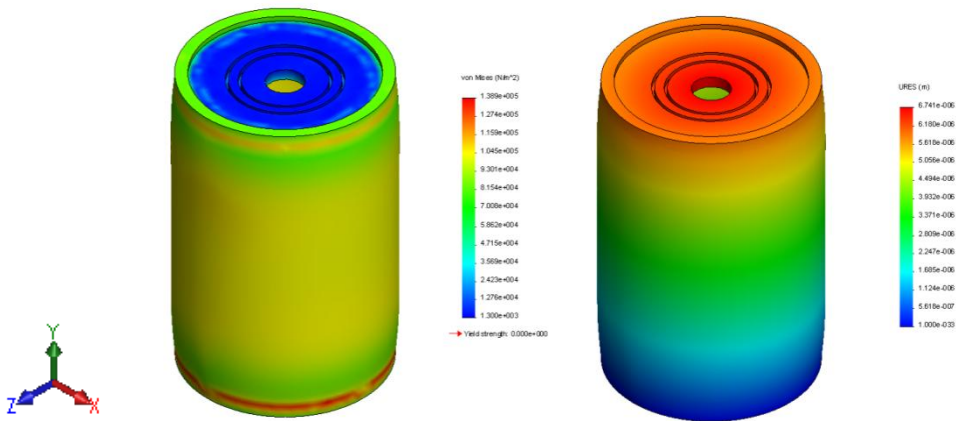


**Figure 58: Stress and Displacement Distributions for the Base Shell.**

This iteration also behaved well with the stress analysis. However, the analysis was unable to determine a safety factor for this type of ABS plastic. Nonetheless, the maximum stresses in these models were comparable to the previous iteration. The analysis also showed that the bottom and top edges of the shell were still the limiting factors of the

design. Though these areas should have been strengthened, the analysis allowed the group to determine that the shell dimensions were adequate for the compression load.

### 5.6.3.2 Top Shell

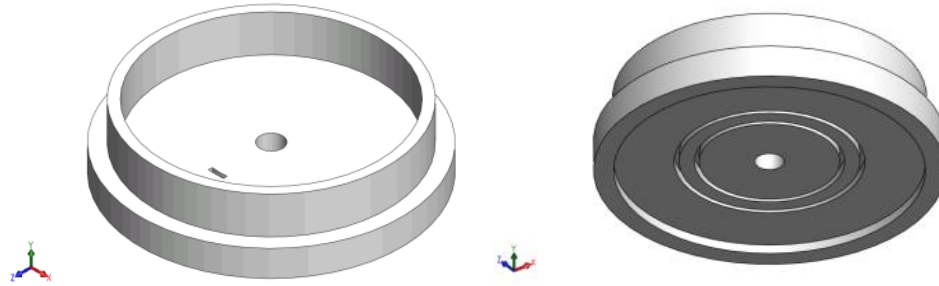


Figure 59: Isometric Top and Bottom Views of Top Shell.

The top shell was designed to support the weight of the next joints as well as any applied load in compression. Since the previous iteration top shell was made of aluminum and had large safety factors, this analysis assumed ABS plastic for the material. For this analysis, the bottom surface was constrained, while the outer collar of the top shell had the applied load, as shown in Figure 60.

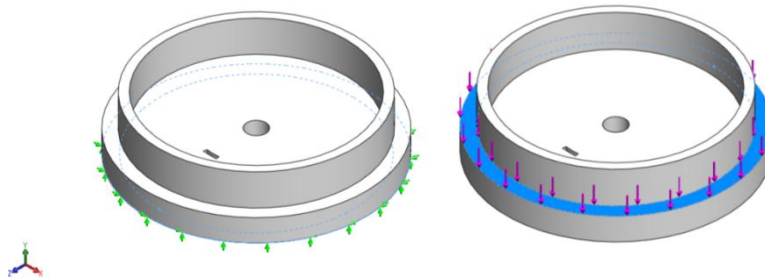
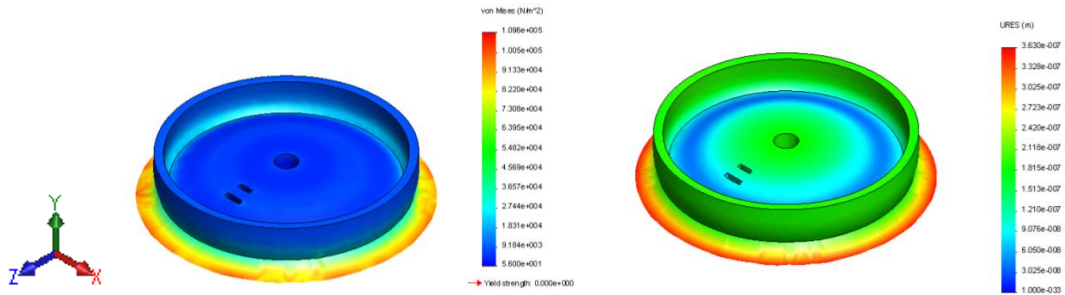


Figure 60: Restraint Surface and Load Surface for Top Shell.



The stress analysis solved for the following values: maximum stress of  $1.096 \times 10^5 \text{ N}/\text{m}^2$ , and a maximum displacement of  $3.630 \times 10^{-7} \text{ m}$ . The stress and displacement distributions are shown in Figure 61.



**Figure 61: Stress and Displacement Distributions for Top Shell.**

This analysis allowed the group to determine that this rotator-joint was strong enough to withstand the expected loading. Though a safety factor was not calculated, the stress distribution was comparable to the previous iteration. The weakness of this part was the small ridge on the bottom surface. By increasing the thickness of this feature, this would no longer become a limiting feature.

#### 5.6.4 Iteration 02 Part Selection

Initially, a hollow shaft for the IR transmitter was researched, which would have also required calculations on the necessary strength of the hollow shaft. However, iteration two was determined to be overly complicated before these values were determined. Similarly, the design change from iteration two to three that removed the complex planetary gearing system came prior to commercial parts research, thus analysis and selection of them did not occur.

Another crucial aspect of iteration two was the electrical transmission, which required conductive plates. Two methods, either using conductive circular disks or inlaying copper wire, were investigated. Manufacturing of conductive disks would have required punching a thin copper or brass sheet; however the tooling costs alone for the four punches it would require (inside and outside edges of two rings) would have exceeded \$100, therefore that option was determined unreasonable for the prototype. Copper wire inlay would create more friction, and consequently more heat and noise, than smooth copper disks, however it was significantly cheaper at \$20 for a 1 lb spool from McMaster-Carr. Therefore, copper wire was used as the conductor for electrical transmission from the bottom collar to the driven collar of the joint.

In order to avoid the costs of punches, a prototype was assembled using copper wire coated with solder in place of the rings. On the opposite place springs were inserted with a wire run through it. The wire was soldered so that the force of the spring would maintain contact between the wire and the simulated plate. However, in testing this design, it was discovered that any change in direction had a tendency to snag the spring/wire assembly and deform it. To solve this, the wire, instead of sitting normal to the surface, forms a loop

re-entering the joint. A large spring remains and is soldered to the wire to maintain contact. Since there is a rounded contact surface, however, the spring no longer is deformed during rotation.

### 5.6.6 Construction of Prototype

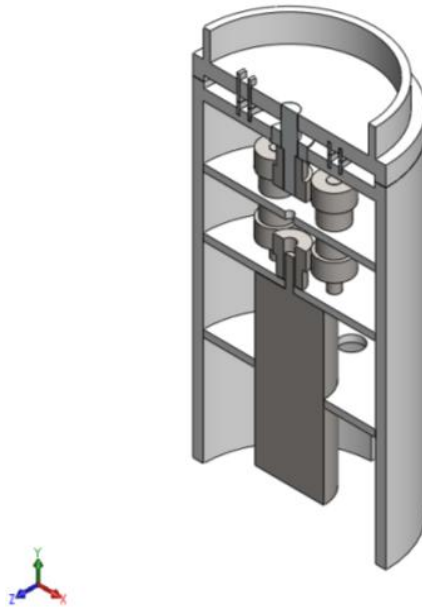


**Figure 62: Section View of the Second Iteration Rotator-Joint.**

After fully designing iteration two and performing preliminary stress analysis, the group decided that it was essential to create a basic prototype to further test the design. The base and top shells, as well as the carrier plates, were manufactured using a rapid prototyping machine. This device creates three dimensional models of the parts using ABS plastic. Though they are weaker than molded ABS plastic due to a natural grain, this prototype was being constructed to test the manufacturability and function of the design, not the strength. The selected motor, bearing, shafts and gears were also included in this prototype, while the IR and slip ring assemblies were neglected.

Construction of this preliminary prototype allowed insight into many issues associated with manufacturing and assembling the rotator-joint. One of the largest flaws in the design was the design of the carrier plates. Though they properly secured the motor and gears from wobble, there was no way to fix these plates to the case, and the motor

could spin within the carrier plates. The prototype also allowed the group to realize that the current IR configuration and gear train assembly unnecessarily complicated the rotator-joint. The addition of the gear assembly increased the number of parts by 18; this included the eight gears, seven set screws, and three shafts added to the design. Each part added increased the cost of the rotator-joint, as well as assembly time, replacement costs, and more opportunities for misaligned parts.

## 5.7 Electrical Systems Iteration 02

Upon selection of a standard brushed DC motor, it was decided to completely redesign the controller instead of adapting the MSP430 design. Instead, a PIC microcontroller was chosen due to its simplicity and ease of interface with a brushed DC motor. Like the MSP430 design, a serial link was created to communicate commands to the host PC. While the emphasis of the first iteration was on communications and creating a reliable method of delivering the commands to the joint module, iteration two was primarily focused on motor control, as shown in Figure 65 . While the project as a whole focused on communication from the host to a number of joints, for simplicity and to encourage design on the motor controller, this iteration provided the capacity to communicate with a sole joint through an RS-232 interface.

Communication with the module was achieved through a serial terminal, which enabled the user to access a text-based prompt system to issue relevant commands for manipulating the joint. This prompt allowed the user to move the joint either forwards or backwards for a set amount of time or to a rough location. The relevant commands were formed from these text responses and executed by the joint.

The PIC microcontroller used in this iteration is a 16F876. This microcontroller is a TTL based device, powered by a 5v regulated source. An PWM (Pulse-Width Modulation) interface integrated into the PIC is utilized to vary the duty cycle of a TTL drive signal. This drive signal is fed to an H-Bridge driver onboard the controller, in this case a SN75441. This H-bridge driver contains a series of MOSFETs which utilizing the TTL input logic, switches the high voltage, high current source provided separately for the purpose of driving the

motor. Figure 63 shows a simplified depiction of an H-bridge circuit, while Figure 64 shows the common logic states and their accompanying function.

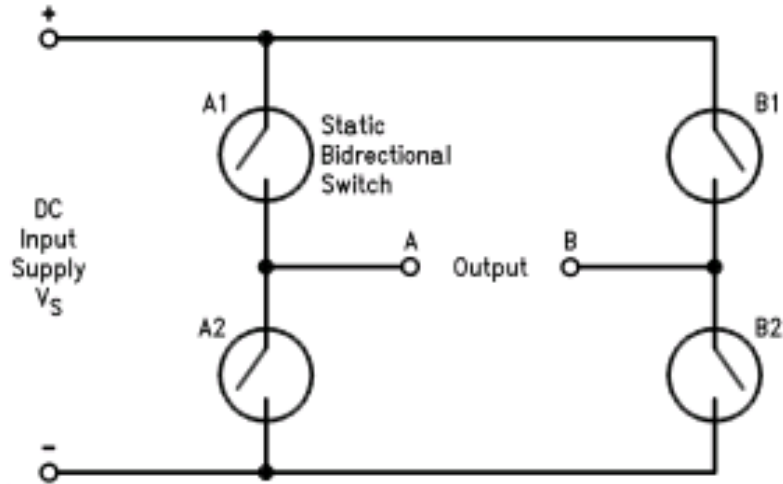


Figure 63: Typical H-Bridge Circuit (National Semiconductor)

$C = H ; D = L$	Forward
$C = L ; D = H$	Reverse
$C = D$	Fast Motor Stop
$C = X ; D = X$	Free Running Motor Stop

Figure 64: H-Bridge Logic Table (STMicroelectronics)

Figure 65 also shows the external RS232 transceiver which translated the TTL (0volts , 5volts) levels to true RS-232 (-15volts, 15volts) allowing for the circuit's direct interface with the PC. The code programmed on this microcontroller is available in Appendix H.

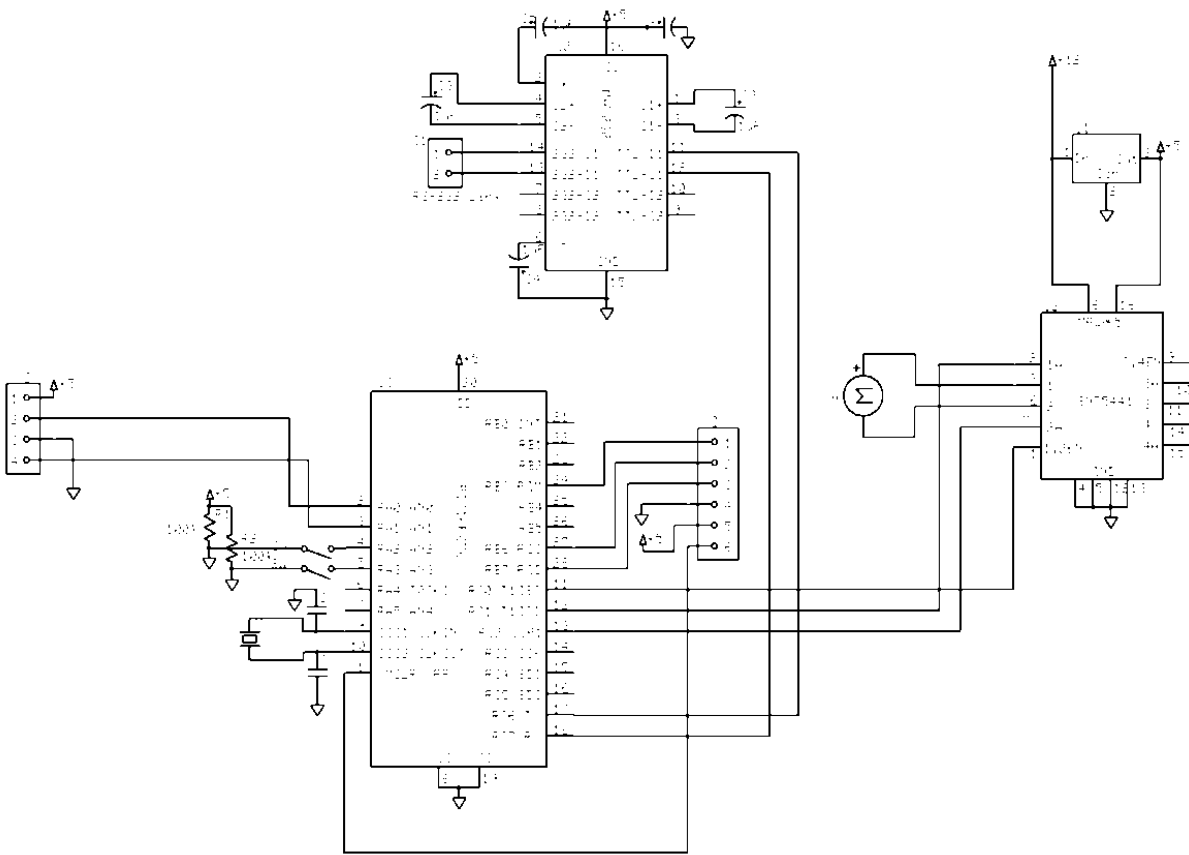


Figure 65: Iteration 2 Schematic



## 6 Detailed Design

### 6.1 Elbow-joint Iteration 03

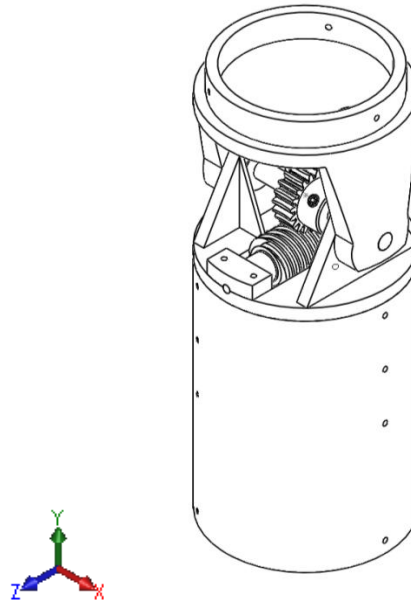


Figure 66: Elbow-joint Iteration 03

The majority of the development of the elbow-joint was improving the previous designs. Iteration one and two provided information that was crucial to developing the third and final iteration. The third iteration of the elbow-joint was designed to improve some key areas of the two previous design iterations. Unlike the previous iterations, the final design included the electrical components that had previously not been included. A printed circuit board (PCB) was added to the overall design. This component was made to be the same size as the motor mount plate. This would allow the PCB to be positioned around the motor ensuring a smaller package. Also, an Encoder was attached directly to the motor and allowed for a finer degree of control and feedback.

The final design also marked significant changes to the mechanical drive system. A new worm drive system was included. The purchased worm and drive shaft are made out

of one piece of metal meaning that the worm was permanently attached to the shaft. This means that the new design would have to allow the worm to be easily installed and removed as one piece. Included with the worm was the mating worm gear. This worm required a six-millimeter rotator pin, which was not only larger than the one used in previous designs but also made of commercial grade stainless steel. This meant that the new six-millimeter rotator pin would be able to cope with operational forces better than the three-millimeter forged steel shaft that was used in iteration two. This design change had the added effect of increasing the overall strength of the elevator-joint. In addition, a set of miter gears were added to transfer the mechanical power from the motor to the worm shaft. Finally, drive bearings were added to all moving components to reduce overall friction.

Another key area explored in the final iteration was manufacturing/assembly. Previous iterations of the design were extremely difficult to assemble and repair. In many cases, it was impossible to disassemble the elevator-joint afterwards without damaging crucial parts. To alleviate this problem, a system of locking screws was devised. All structural components benefitted from being locked in place by screws, including the motor mount plates. This eliminated the possibility of the motor shifting and also provided a means of correctly and precisely position components. The rotator pin was physically locked to the driven collar by two locking pins. This meant the system was stronger compared to the press-fit system that was relied on in the past. Finally, screw holes were created to lock joints together. This ensured a very strong attachment that was also easily disconnected if needed.

Similar to the second iteration, this design was made out of rapid prototyped ABS plastic. This greatly reduced the manufacturing time since the rapid prototype machine took under a few hours to complete most parts. Also, the rapid prototype machine was capable of making parts that would be impossible to machine. However, since the components in the second iteration failed during analysis, the final design needed to be strengthened. Most of the parts were bolstered during their redesign.

### **6.1.1 Kinematics**

Although the design of the elbow-joint changed with iteration three, the joints operate on the same fundamental kinematic assumptions. The overall structure of the elbow-joint was designed to maximize strength and minimize weight. The three major components that made up the structure were; the base, and the bottom and top collar as shown in Appendix K. The base acted as the anchor of the device. Between the base and bottom collar was a fixed connection which allowed no motion between the bottom collar and base. This connection eliminated any roll motion in the design. As a result, the bottom collar became an extension of the base and was in charge of anchoring many of the other components. However, between the bottom and top collar there was a revolute joint. The rotator pin connected the two components. The rotator pin was allowed to move freely in relation to the bottom collar. However, the rotator pin was anchored to the top collar and the rotator pin would be unable to move in relation to the top collar. This freedom allowed the joint to be capable of pitch motion.

### 6.1.2 Iteration 03 Stress Analysis

The analysis done on the third iteration was by far the most important due to the fact that this joint was going to be subjected to testing and real world applications. The final design includes all of the commercially purchased parts as well as the machined components. The analysis done on this joint was very similar to what was utilized for previous joints; however, a new material database was created to model the rapid prototyped plastic. Due to the rapid prototyping process, it was believed that this plastic was weaker than ABS plastic that has been injection molded. However, the extent to which this plastic was weaker was, at the time, unknown. As a result, it was decided that the team would construct a custom material database that would use weaker material characteristics (Information obtained from the CES EduPack 2008). This material featured reduced values for many of the strength characteristics, shown in Table 3.

ABS Plastic	
Property	Value
Elastic Modulus	$1.1 \times 10^9 N/m^2$
Poisson's Ratio	.391
Shear Modulus	$3.19 \times 10^8 N/m^2$
Thermal Expansion Coefficient	$2.4 \times 10^{-5}$
Density	$1010 kg / m^3$
Thermal Conductivity	$0.2256 W / (m * K)$
Specific Heat	$1386 J / (kg * K)$
Tensile Strength	$2.76 \times 10^7 N/m^2$
Yield Strength	$1.85 \times 10^7 N/m^2$

Table 3: Properties of Rapid Prototype ABS Plastic

Also, in previous analysis iterations, all gears were modeled as ABS plastic. However, with the inclusion of commercial parts, the components were made of varied materials. The miter gears were commercial grade brass, the Worm and shaft assembly was made of A303 steel and the worm gear was made of acetyl.

### 6.1.2.1 Elbow Sleeve Analysis

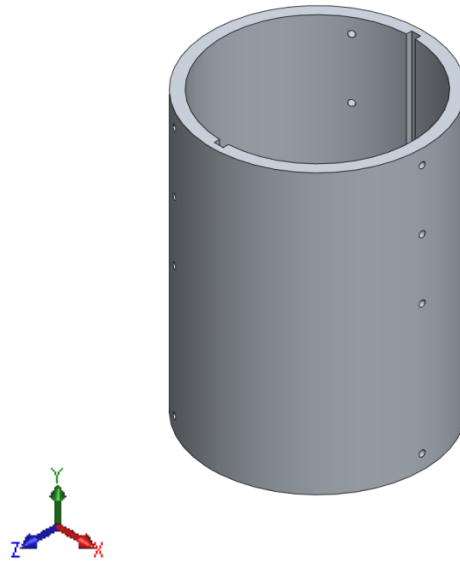
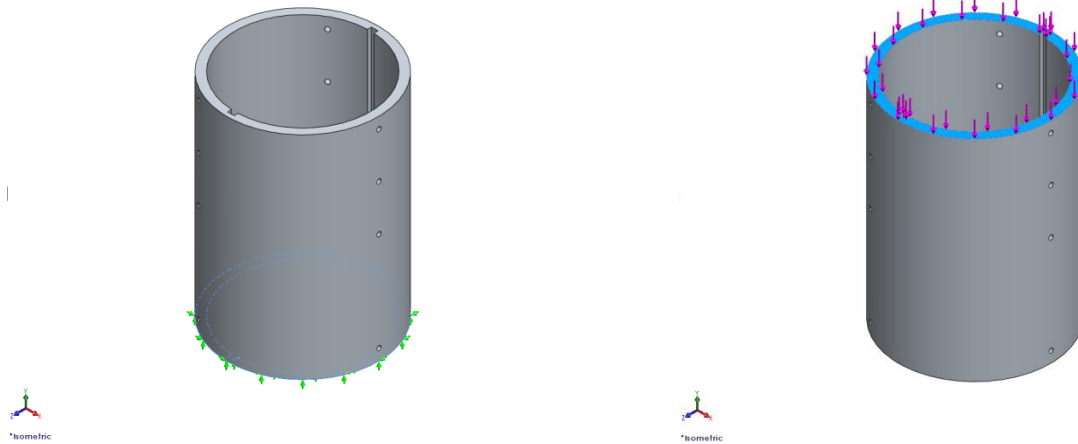


Figure 67: Elbow Sleeve

The Elbow Sleeve was a component that evolved from the original base. Previously this component was only used for supporting the elevator-joint. However, it played a major role in both supporting the elevator-joint, and the positioning of components being mounted within. Grooves and screw holes were added to work in conjunction with motor mount plates and the bottom collar as well as being attached to other joints. This would ensure both perfect positioning of the components as well as providing a means of securely anchoring them to the structure

Although, the overall design has changed since previous iterations, the analysis process was very similar. The component was fully constrained on the lower face to simulate the reactionary forces of being attached to a base or another joint. Also, an operational force of 60 Newtons was applied at the top face Figure 68. This force was to simulate the weight of four joints connected in series and a 2 kg weight on the end.



**Figure 68: Fully Constrained Face and Applied Force Location of the Elbow Sleeve**

The analysis provided the following results: a maximum internal stress of  $2.252 \times 10^5 \text{ N/m}^2$ , a maximum displacement of  $6.836 \times 10^{-6} \text{ m}$  and an overall safety factor of 82.1588.

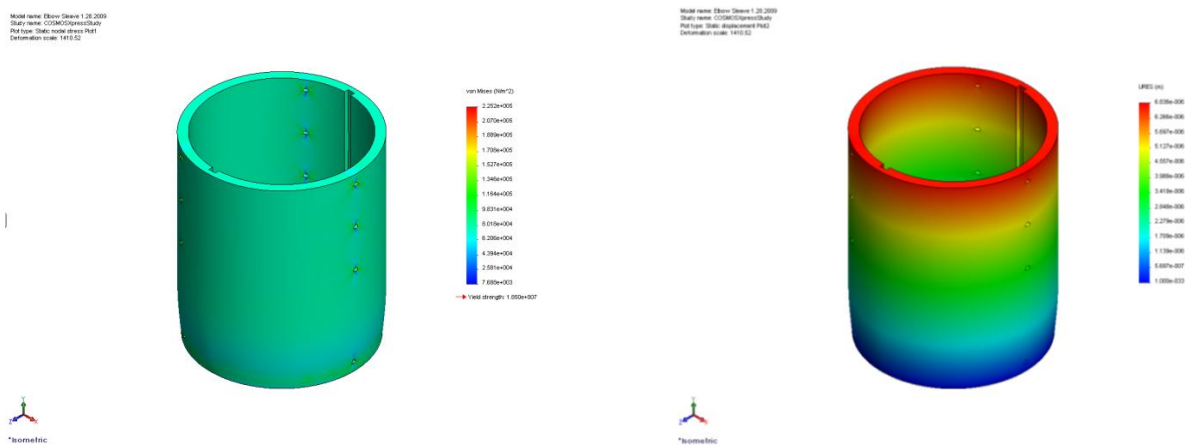


**Figure 69: Internal Stresses and Displacement of the Elbow Sleeve**

In previous designs this component was getting safety factors in excess of 772. This was extremely large and unnecessary especially in a design that was looking to limit both weight and price. This new design achieves a safety factor of 82.1588. While this number was also extremely high, it was important to note that due to the rapid prototyping process,

it was extremely difficult to estimate what the actual strength of the component is. However, the benefit of this process was that with a safety factor this high, it was safe to assume that this part would be able to cope with the operational forces that it would be subjected to. Also, components made though injection molding would most certainly be stronger in which case they would be capable of a higher safety factor.

### **6.1.2.2 Bottom Collar Analysis**

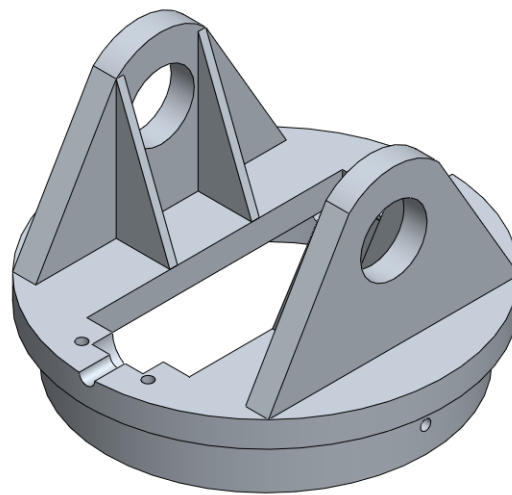


**Figure 70: Bottom Collar**

The Bottom Collar continued to be one of the more complex parts. This part was designed to allow 180 degrees of movement while also allowing electrical power and communications connections to pass through the joint. Also, in the final iteration a few key changes were made to improve the overall functionality of the Bottom Collar. The overall strength of the component was increased by including thicker members and ribs. Also, this component was designed to have four bearings installed to reduce friction between the collar and rotator pin and the worm shaft. In addition, the worm assembly has been



recessed into the structure to decrease the overall package size. Finally, a new system was put in place to ensure easy installation of the worm assembly.

First the collar must be fully constrained on the bottom flange Figure 71. Although there are screw holes on this design, these are put in place for positioning and locking only. They would not be used to bear structural load. Next, a load of 60 Newtons was applied to the Rotator Pin bearing mounts Figure 71.

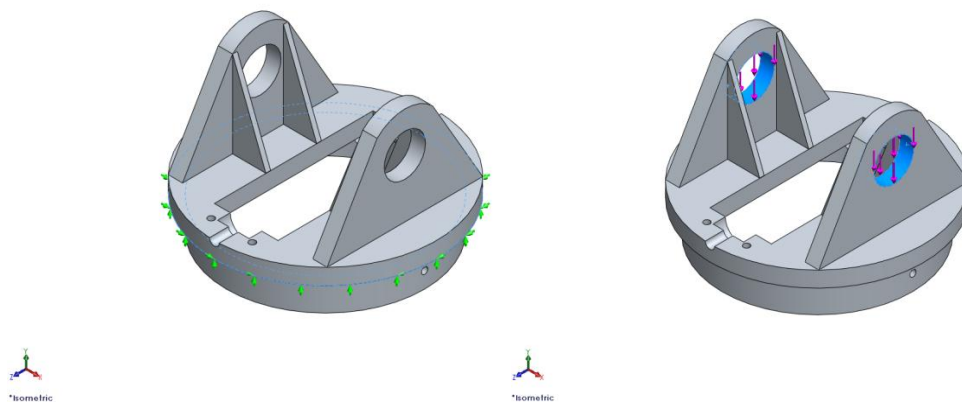


**Figure 71: Fully Constrained Face and Applied Force Location of the Bottom Collar**

The analysis provided the following results: a maximum internal stress of  $1.086 \times 10^6 \text{ N}/\text{m}^2$ , a maximum displacement of  $2.335 \times 10^{-5} \text{ m}$  and an overall safety factor of 17.0364 Figure 72.

Model name: Bottom Collar 1.26.2020  
Study name: COEIMCOComponent040  
Plot type: Stress: vonMises (Pa)  
Deformation scale: 302.703

Model name: Bottom Collar 1.26.2020  
Study name: COEIMCOComponent040  
Plot type: Displacement (mm)  
Deformation scale: 302.703

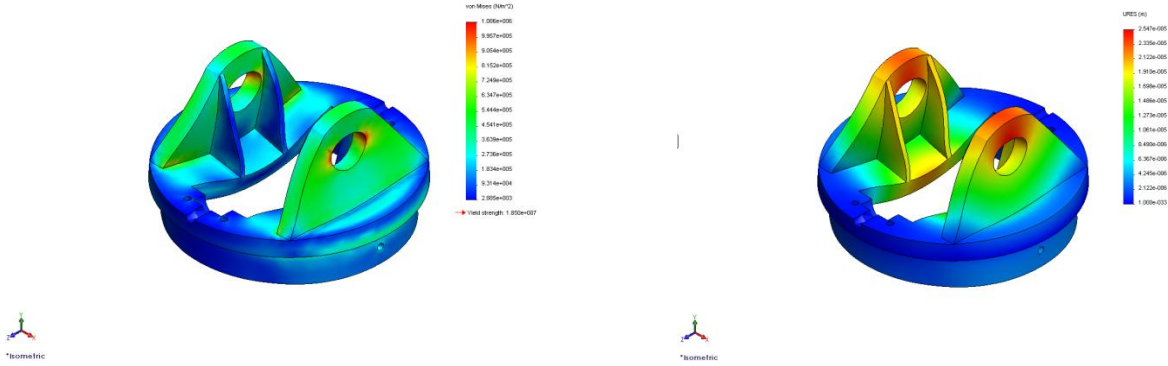


**Figure 72: Internal Stresses and Displacement of the Bottom Collar**

After it was found that previous components did not have the strength necessary to cope with operational forces, it was extremely important to determine if the new components would be strong enough. With a minimum safety factor of 17.0364, it was safe to say this component would be sufficient. Although it was unknown how the rapid prototype material would react during operation, it was safe to assume that the components would be strong enough for testing purposes.

### 6.1.2.3 Driven Collar Analysis

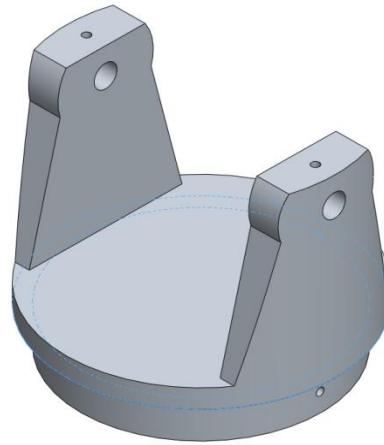


**Figure 73: Driven Collar**

Although, the Driven Collar component has changed greatly over the three iterations, like in the previous designs, strength and range were always paramount to the design. While this new part was capable of the same range as previous design, there are a few areas that have been changed to greatly improve strength. This final design includes more robust pin supports. Since the previous was found to be insufficient after analysis was completed, more strength was required to ensure the part would be able to cope with operational forces. Also included was a system that allows a lock screw to be set through the rotator pin and then anchored in the collar itself.

Much like the Bottom Collar, The Driven Collar would be constrained in a few areas. Although there are screw holes on this design, these are put in place for positioning and locking purposes. They would not be used to bear structural load. The Driven Collar would be fully constrained in the Rotator Pin Bearing Mounts due to the fact that this was the

location that would be the components ground. Then a force 60 Newton was applied to the bottom rim to simulate operational forces Figure 74.

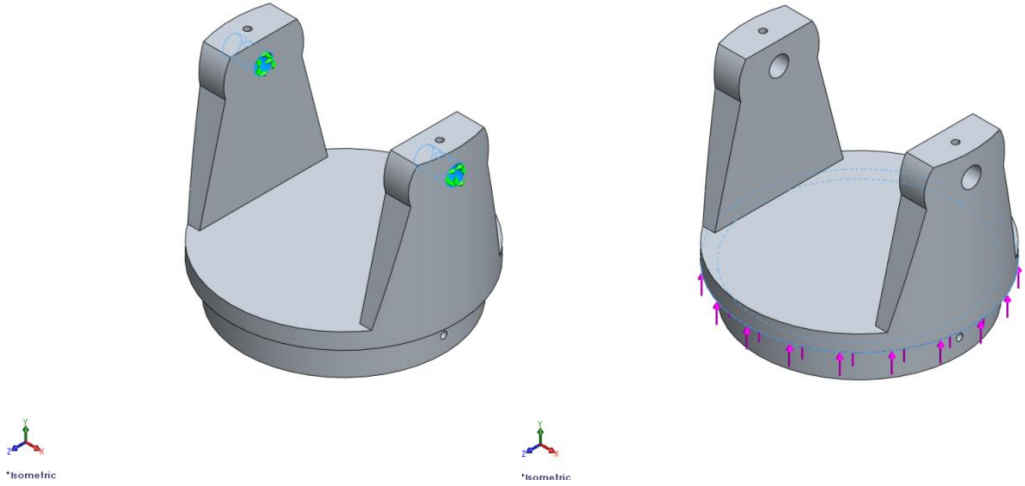


Figure 74: Fully Constrained Face and Applied Force Location of the Driven Collar

The analysis provided the following results: a maximum internal stress of  $1.434 \times 10^6 \text{ N/m}^2$ , a maximum displacement of  $5.960 \times 10^{-5} \text{ m}$  and an overall safety factor of 12.8992 Figure 75.

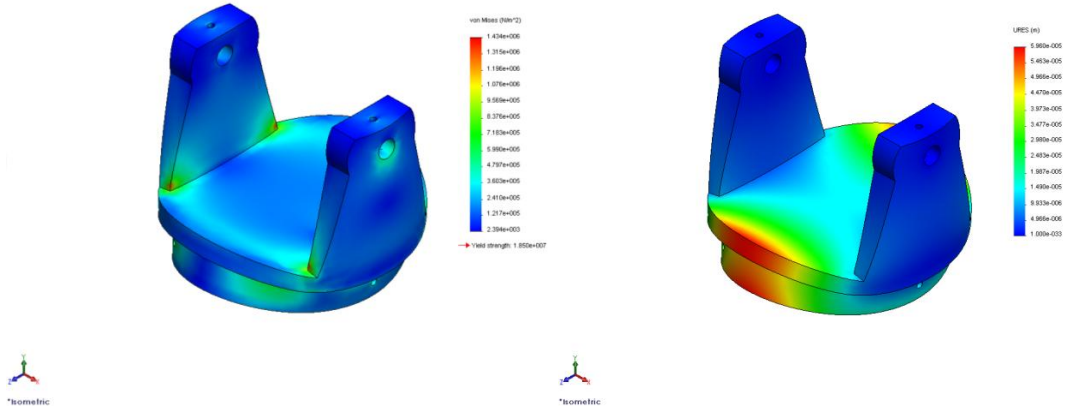


Figure 75: Internal Stresses and Displacement of the Driven Collar

After it was found that previous components did not have the strength necessary to cope with operational forces, it was extremely important to determine if the new

components would be strong enough. With a minimum safety factor of 12.8992, it was safe to say this component would be sufficient. Although it was unknown how the rapid prototype material would react during operation, it was safe to assume that the components would be strong enough for testing purposes.

### 6.1.3 Iteration 03 Motion Analysis

Although the structural analysis of iteration three was similar to the previous designs, one key area that needed to be considered was the forces due to motion and applied torque. This joint needed to be able to cope with operational forces. Also, with the inclusion of small commercially purchased and machined parts, analysis was necessary to ensure the elevator-joint could operate without damage.

#### 6.1.3.1 Worm/Shaft Analysis

The worm/shaft component plays a huge role in mechanical power transmission. Although the component was manufactured with a large shaft, it needed to be turned down to a diameter of three millimeters in order for the miter gears to be mounted on it. This large change in design proved to be a manufacturing hurdle. Also, there was concern as to whether or not a shaft of this size would be able to cope with the operational forces. Analysis was necessary to ensure this small component would not fail under operation.

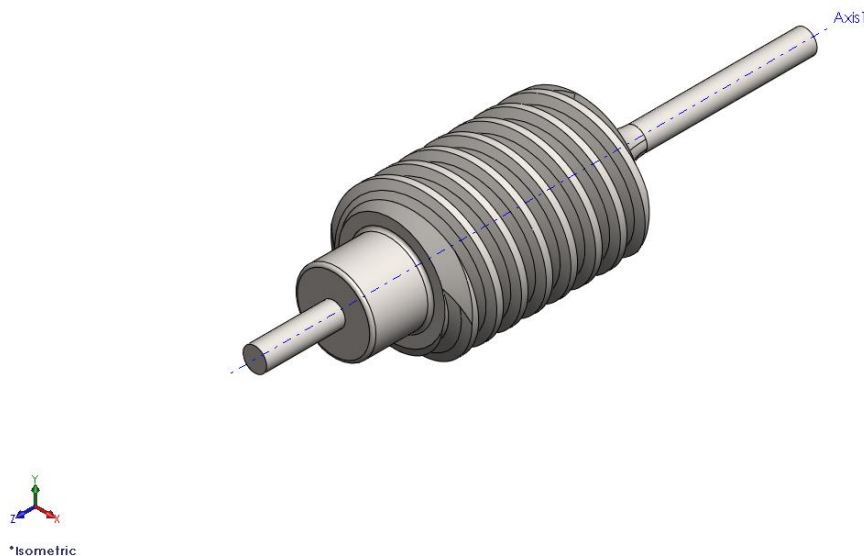
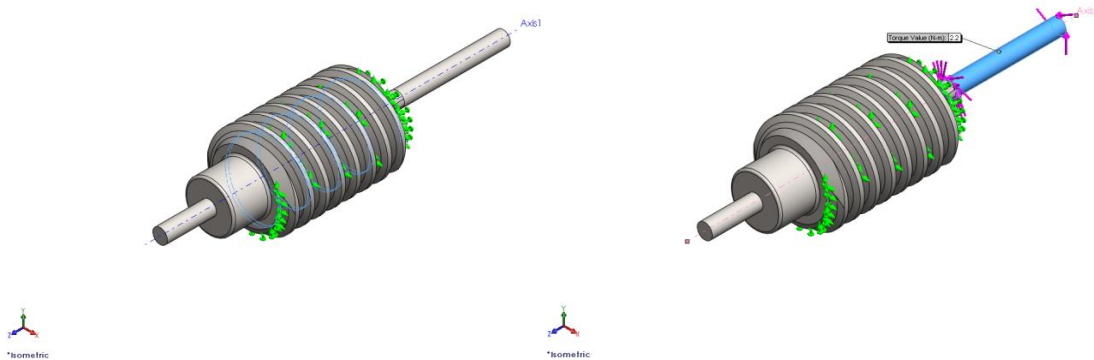


Figure 76: Worm/Drive Shaft

The torque analysis was done using a COSMOSWorks study in Solidworks as well as a modified version of the Solidworks model the manufacturer provided for the worm. Since the maximum output of the motor being used was 2.2 Newtons, this was the value that would be used for the calculation. First, the worm was fully constrained Figure 77. This would simulate the forces of weight lifting during operation. Then, a torque of 2.2 Newton-meters was applied to simulate the maximum torque of the motor being transferred to the worm shaft by the miter gears Figure 77.



**Figure 77: Fully Constrained Face and Applied Torque of the Worm/Shaft**

Unfortunately after the analysis was completed, it was found that this component would likely fail during full operation. The maximum internal stresses  $7.566 \times 10^8 \text{ N/m}^2$  far exceeds the materials yield strength of  $2.069 \times 10^8 \text{ N/m}^2$  as shown in Figure 78 and provided a safety factor of 0.273. Although it is impossible to fully represent the all the forces acting during operation, this safety was still too low to deem this part strong enough for the application. In the future stronger materials or larger geometry should be used in order to ensure no part failure

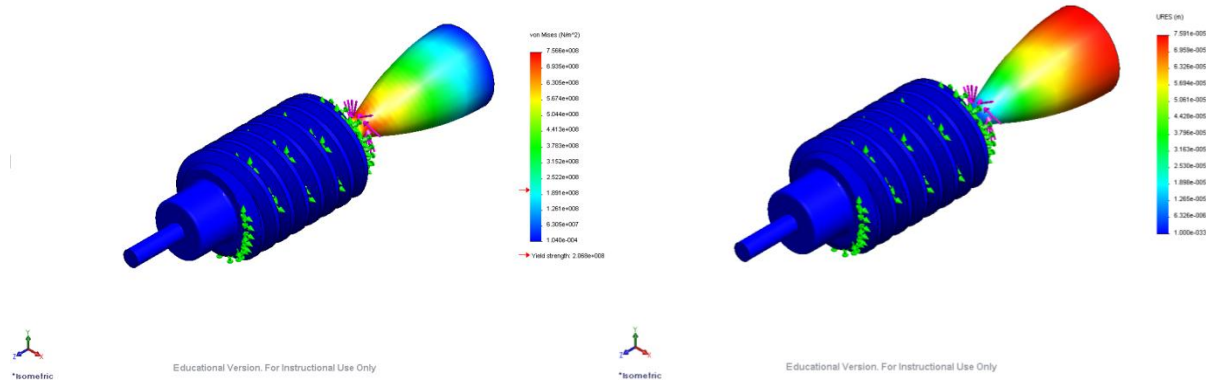


Figure 78: Internal Stresses and Displacement of the Worm/Drive Shaft

### 6.1.4 Iteration 03 Part Selection

Manufacturing was the main focus of iteration three of the elbow-joint. Turning the shaft of the worm down to a smaller diameter had the potential for detrimental vibrations that could break the shaft. The natural frequency equation,  $\omega_n = \sqrt{\frac{k}{m}}$ , indicates that an increase in stiffness (k) and decrease in mass (m) would increase the natural frequency ( $\omega_n$ ), which would minimize vibrations. Adding a fillet with a large radius would add some mass, however the increase in stiffness would be significantly greater than the increased mass, ultimately increasing the natural frequency. Therefore a large fillet was included between the edge of the worm and the reduced diameter shaft in the design. The curve of the fillet, in addition to the increased stiffness, gave the shaft more stability during turning than a right angle connection would have. Also, the turning blade began at the tip of the shaft by cutting deep and then gradually moved away to make a shallower cut, creating a taper to the shaft that was later removed. This taper essentially acted as a large, shallow fillet, which increased the natural frequency and reduced vibrations, making the shaft less likely to shear.



The method of securing the miter gear to this shaft was researched in depth and was limited to using either a pin through the gear and the shaft, a set screw, or interference fit. Calculations, included in Appendix C, indicated that using a 1.5 mm diameter stainless steel dowel pin could result in a sheared pin or worm shaft, but was still feasible (see Table 4). However, calculation (Appendix C) also indicated that a set screw was feasible, but the set screw might slip before reaching the maximum torque (see Table 4). A press fit would have been the best option, as it met the necessary holding power requirements, however the exact position of the miter gear on the shaft could not be determined using SolidWorks, and would have made assembling the elevator-joint difficult. The worm would have needed to be cooled to shrink and the brass miter gear heated to expand in order to press the miter gear on without breaking the shaft. This also meant that the miter gear would have been far more difficult to remove if adjustments needed to be made or the miter gear needed to be replaced. A compromise was made to reduce the torque capacity of the system and increase the ease of assembly and disassembly by using a small, M2 diameter set screw.

<b>Form of Securing</b>	<b>Holding Power (Nm)</b>
1.5 mm pin	0.364
M2 setscrew	0.179
Medium drive interference fit	11.780

**Table 4: Gear Anchoring Analysis Results**

The pin for the driven collar, also acting as the shaft for the worm gear, required two holes drilled into each end, which was accomplished by milling. The coupler between motor shaft and miter gear also needed to be machined. It was created from 8 mm diameter stainless steel stock material by a combined process of milling and turning.

### 6.1.5 Iteration 03 Cost Estimate

The cost estimate calculated the estimated costs of producing both a single elbow-joint by itself and a single elbow-joint out of one thousand total joints. The comparison of the two showed how much it cost to produce the prototype alone and then the savings of creating one thousand at a time. It also gave an idea as to the feasibility of mass producing the elbow-joint and the potential profit from selling them.

Prices for the purchased parts came directly from supplier websites. In the case of the motor, bearings, encoder, and H-bridge, only the single individual unit price was given and that was used in the cost estimate calculations; however it can be assumed that if a thousand were purchased, the unit price would decrease. Hardware, such as screws and set screws, that was purchased in groups was included in the '1 of 1' elbow-joint column (see Table 6) as the cost of the fewest number of individual pieces that could be bought in a pack. For the '1 of 1000' calculations (see Table 6), hardware was calculated as the cost of the maximum number of individual pieces in a package multiplied by the number needed per elbow-joint. The cost of rapid prototyping was measured by material volume used, at \$0.27 per cubic cm. The manufacturing processes costs were determined from a spreadsheet of standard prices, complements of the Worcester Polytechnic Institute FSAE team, and are included in Appendix V. Table 5 includes the calculations to determine the cost for the manufacturing processes and Table 6 shows the calculations for the entire cost to manufacture the elbow-joint.

<b>Cost Calculations for Machined Parts of Elbow Joint</b>						
Machining						
Joint	Part	Process	Cost (\$)	Per Unit	Quantity	Sub-total
Elbow	Coupler	Drill holes	0.35	hole	2	0.70
Elbow	Miter Gears (2)	Drill holes	0.35	hole	2	0.70
Elbow	Pin	Drill holes	0.35	hole	2	0.70
Elbow	Coupler	End mill	0.04	cm <sup>3</sup>	0.6	0.02
Elbow	Coupler	Lathe-turn finish	0.04	cm <sup>3</sup>	0.2	0.01
Elbow	Worm	Lathe-turn finish	0.04	cm <sup>3</sup>	9	0.36
Elbow	All	setup, install, remove	1.3	# setups	5	6.50
Subtotal:						8.99
Material						
Joint	Part	Material	Cost	Per Unit	Quantity	Sub-total
Elbow	Coupler	Stock - Stainless Steel	1.17	6 inch	1	1.17
Elbow	Coupler	Stock - Stainless Steel	15.59	72 inch	11	0.17
					1 of 1	1 of 1000
				<b>Total</b>	<b>10.16</b>	<b>9.16</b>

**Table 5: Cost Calculations for Machined Parts of Elbow-joint**

The cost of the motor ended up being \$26.95 individually. The combined 1 of 1000 cost of all the mechanical purchased parts came to \$94.39. Electrical parts, both purchased and the printed circuit board, came to \$70.20 for 1 of 1000 elbow joints. The cost of manufacturing, both machining and abs printing, came to a subtotal of \$53.69.

<b>Cost Estimate for Elbow Joint</b>							
<b>Purchased Parts</b>							
<b>Part</b>	<b>Supplier</b>	<b>Price of 1</b>	<b>Price of 1000 units</b>	<b># parts needed</b>		<b>Cost of 1 of 1</b>	<b>Cost of 1 of 1000</b>
Elevator Motor	RobotMarketPlace	\$26.95	\$26.95	1		\$26.95	\$26.95
Shaft: 6mm	SDP-SI	\$4.44	\$3.08	1		\$4.44	\$3.08
Bearings: 6mm bore	McMaster-Carr	\$9.10	\$9.10	2		\$18.20	\$18.20
Bearings: 3mm bore	SmallParts	\$6.00	\$6.00	1		\$6.00	\$6.00
Miter gear	SDP-SI	\$15.73	\$11.33	2		\$31.46	\$22.66
Worm	SDP-SI	\$25.88	\$21.74	1		\$25.88	\$21.74
Worm Gear	SDP-SI	\$24.67	\$20.59	1		\$24.67	\$20.59
Encoder	N/A	\$56.25	\$56.25	1		\$56.25	\$56.25
Passive Electrical Components	N/A	\$3.00	\$2.00	1		\$3.00	\$2.00
MCU	N/A	\$4.96	\$3.78	1		\$4.96	\$3.78
H-Bridge	N/A	\$5.87	\$5.87	1		\$5.87	\$5.87
Voltage Regulator	N/A	\$0.60	\$0.30	1		\$0.60	\$0.30
<b>Grouped Parts</b>	<b>Supplier</b>	<b>Price/pack (minimum)</b>	<b>Price/pack of 1000</b>	<b># packs needed</b>	<b># packs needed per 1000 parts</b>	<b>Cost of 1 of 1</b>	<b>Cost of 1 of 1000</b>
Screw: 10mm L Philips Pan Head M3	SmallParts	\$5.50	\$55.00	1	19	\$5.50	\$1.05
Screw: 20mm L Philips Pan Head M3	SmallParts	\$1.25	\$12.67	1	2	\$1.25	\$0.03
Set Screw	SmallParts	\$1.96	\$261.40	1	4	\$1.96	\$1.05
<b>Purchased Subtotal</b>						<b>\$216.99</b>	<b>\$189.54</b>
<b>Manufactured Parts</b>							
<b>ABS Printing</b>	<b>Supplier</b>	<b>Cost</b>	<b>Per unit</b>	<b>Quantity</b>		<b>Cost of 1 of 1</b>	<b>Cost of 1 of 1000</b>
driven collar	N/A	0.27	cm <sup>3</sup>	47.2		12.74	12.74
bottom collar	N/A	0.27	cm <sup>3</sup>	27.7		7.48	7.48
plates	N/A	0.27	cm <sup>3</sup>	20		5.40	5.40
casing	N/A	0.27	cm <sup>3</sup>	70		18.90	18.90
<b>Machined</b>	<b>Supplier</b>					<b>Cost of 1 of 1</b>	<b>Cost of 1 of 1000</b>
Worm, Coupler, Pin	N/A					\$10.16	\$9.16
<b>Printed Circuit Board</b>	<b>Supplier</b>					<b>Cost of 1 of 1</b>	<b>Cost of 1 of 1000</b>
Board	N/A					\$20.00	\$2.00
<b>Manufactured Subtotal</b>						<b>\$74.69</b>	<b>\$55.69</b>
Total Production Cost		1 of 1 \$291.68	1 of 1000 \$245.22				

**Table 6: Elbow-joint Cost Estimate Breakdown**

The total cost of producing an individual elbow-joint was calculated to be approximately \$291.68, whereas producing one out of a group of one thousand would cost \$245.22. The cost of the grouped elbow-joint is assumed to be less than \$231.27 in reality, as the prices for batched parts would be cheaper than prices given by suppliers for individual parts. Consequently, if sold for \$1000, there would be a profit of approximately \$700-\$750 for each elbow-joint, and \$700,000-750,000 in total for the full 1000.

### **6.1.6 Iteration 03 Discussion**

Overall, the final design utilized many of the improvements that were discovered during the initial iteration phases of the design process. However, it was clear that there were still a few components that need further improvement, most notably the worm/shaft and the miter gears. These two components were used based on the price and size limitations of the project, however, these two components proved to be the largest weak point of the design. Although the group was aware of the difficulties smaller components would inherently cause, the magnitude of the effects were unknown.

## 6.2 Rotator-Joint Iteration 03

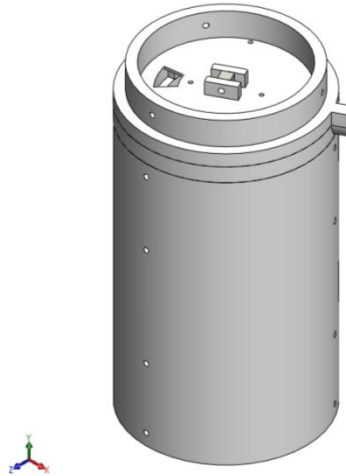


**Figure 79: Third Iteration of Rotator-Joint Model.**

The construction of the second iteration prototype was essential for motivating a third design. The IR created numerous problems that needed to be addressed in order to create a more efficient and reliable design. Additionally, further consideration for securing the motor and carrier plates was necessary. The third iteration, shown above in Figure 79, removed the gear train and redirected the IR path. This design uses fewer parts, as well as reducing the height of the rotator-joint. The carrier plates were modified to allow for more secure fastening, and the base shell was separated into two parts to allow for more access inside the rotator-joint while assembling and repairing.

### 6.2.1 Kinematics

The third iteration of the rotator-joint was similar to the first iteration; the gear train implemented in iteration two was removed for simplification. The detailed drawings of the iteration assembly and parts are outline in the Appendix.

Similar to the first iteration, the third iteration included a simple revolute joint. The base shell, however, was separated into two parts. These parts were fixed to each other,

using machine screws, and are therefore assumed to act as one part. These parts were fixed, and the main shaft would rotate about the base to rotate the top shell. This assembly was much simpler than the previous since the path of mechanical power was transferred across fewer parts.

### 6.2.2 Iteration 03 Components

To provide better access into the rotoat-joint for assembly and repair, the base shell was separated into two distinct parts. The base shell remained the housing for the motor, circuits, and wiring, while the base top became the housing for the slip ring contact plates and the IR transmitter. The base top is also the contact surface for the top shell.

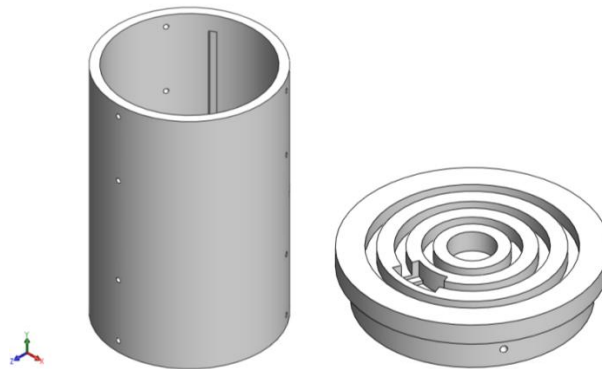


**Figure 80: The Base Shell and Base Top.**

To simplify the third iteration of the rotator design, the IR transmitter system was redirected. Previously, the group relied on direct line of sight communication between the IR transmitter and receiver. However, it was determined that the IR signal would bounce off surfaces and travel around a curved edge. This resulted in a circular channel between the base top and the top shell in which the IR beam would travel. Even as the two parts rotated, the IR beam remained in the channel.

With the removal of the axial IR system, the gear train could also be removed. A shaft was designed to transmit the mechanical power from the motor to the top shell. The shaft was designed with a flat edge on one side to allow set screws to grip the shaft and securely fasten to the coupler. Additionally, the top portion of the shaft was rectangular, such that there was no slippage between the shaft and the top shell. The top shell had a square hole in it, rather than a traditional circular hole. Additionally, the middle was raised such that a pin or machine screw could be inserted through the top shell and into the shaft.

The base shell and carrier plates were altered to allow for the proper fastening of the motor to the shell. The plates included extrusions with holes that would correspond to holes on the base shell. Machine screws would align the carrier plates at the proper height and orientation and secure them. Additionally, the top carrier plate included holes for securing to the motor top, as well as an extrusion in the middle to support an electrical encoder to monitor the output speed and position of the main shaft. This support had to be designed to allow access to the set screws in the coupler.

### **6.2.3 Iteration 03 Stress Analysis**

Stress analysis was performed on the final design similar to the previous iterations. To be more precise, a custom material was defined, similar to the rapid prototyped ABS plastic used in the external parts of the joint, as shown in Table 7. Setting up a custom material also allowed for the calculation of safety factors during the analysis. The analysis was done on the load bearing parts, and assumed basic compression of the parts. The load was set at 80N, which was determined by the approximate weight of three joints and a 2 kg load. Additionally, stress analysis was performed on the main shaft. This analysis assumed



cast stainless steel and an applied torque of 2.6 Nm, equal to the maximum stall torque of the motor.

ABS Plastic	
Property	Value
Elastic Modulus	$1.1 \times 10^9 \text{ N/m}^2$
Poisson's Ratio	.391
Shear Modulus	$3.19 \times 10^8 \text{ N/m}^2$
Thermal Expansion Coefficient	$2.4 \times 10^{-5}$
Density	$1010 \text{ kg/m}^3$
Thermal Conductivity	$0.2256 \text{ W/(m * K)}$
Specific Heat	$1386 \text{ J/(kg * K)}$
Tensile Strength	$2.76 \times 10^7 \text{ N/m}^2$
Yield Strength	$1.85 \times 10^7 \text{ N/m}^2$

Table 7: Properties of Rapid Prototype ABS Plastic.

### 6.2.3.1

### 6.2.3.2 Base Shell

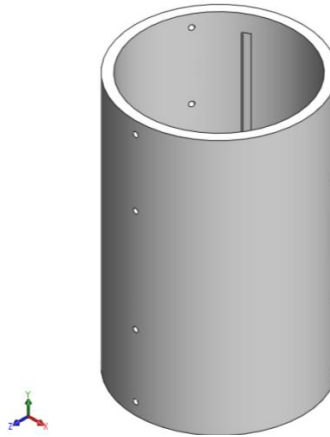
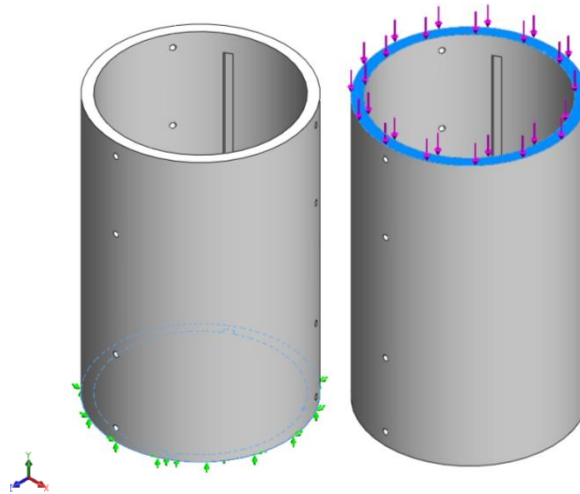


Figure 81: Base Shell

As with previous iterations, the base shell must be capable of transferring the compressive load to the next load or base fixture. However, since the top of the base shell has been removed, this design was essentially a tube with small grooves and holes. The

applied load was 80 Newtons, equivalent of three adjacent joints and a 2 kg load. The restraining surface was defined as the bottom surface while the load was applied to the top surface, as shown in Figure 82.



**Figure 82: Restraint Surface and Load Surface for Base Shell.**

The stress analysis solved for the following values: minimum safety factor of 66.8, maximum stress of  $1.769 \times 10^5 \text{ N/m}^2$ , and a maximum displacement of  $1.035 \times 10^{-5} \text{ m}$ .

The stress and displacement distributions of the part are shown in Figure 83.

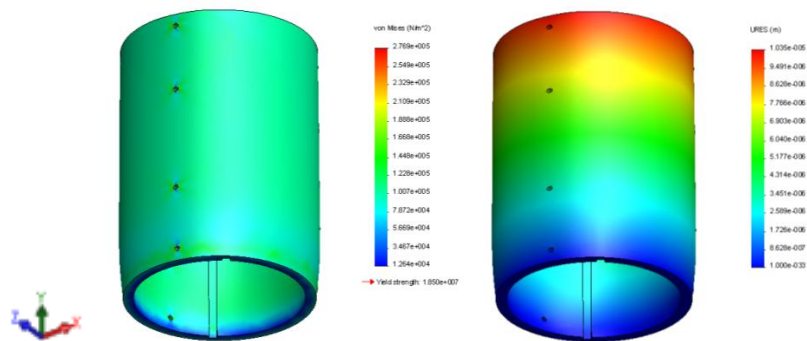


**Figure 83: Stress and Displacement Distributions in Base Shell.**

This analysis still yielded a high safety factor, though reduced from iteration one's safety factor which assumed aluminum material. Additionally, the stress distribution was

mostly uniform throughout the part. Stress concentrations do appear around the screw holes, however, and these areas should be considered the weakest point of the part. Regardless, the analysis determined that the base shell was designed adequately to sustain a simple compressive load of 80 Newtons.

### 6.2.3.3 Base Top

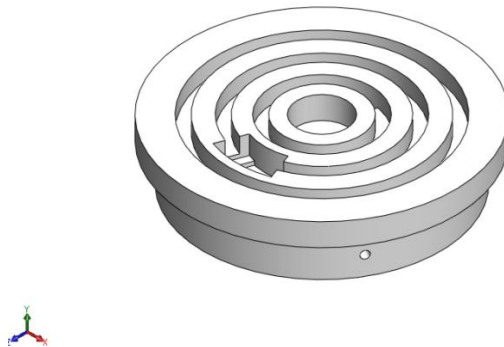
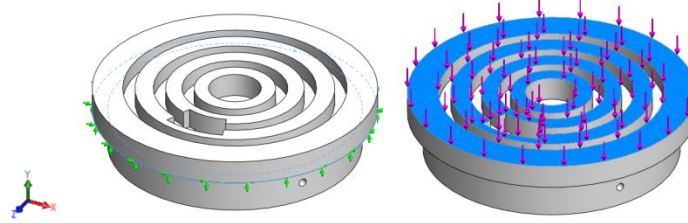


Figure 84: Iteration Three Base Top.

The base top was a new part in the third iteration; it houses the slip ring and IR assemblies. Additionally, it provides additional support to the main shaft through a bearing. The base top also transmits all the compressive force from adjacent joints from the top shell to the base shell. The analysis performed assumed the part was made from ABS plastic, and a compressive load of 80 Newtons. The restraint surface was taken as the bottom surface of the cuff, which will be resting on the base shell. The load surface was all surfaces on the top of the part, which the top shell will be resting on. This analysis assumed that minimal compressive force was transferred through the slip ring assembly or the main shaft. Though this was unrealistic, ideally there should be minimal force onto the slip ring and shaft due to increase wear. The restraint and load surfaces are shown in Figure 85.



**Figure 85: Restraint and Load Surfaces for the Base Top.**

The stress analysis solved for the following values: minimum safety factor of 6.32, maximum stress of  $1.171 \times 10^7 \text{ N}/\text{m}^2$ , and a maximum displacement of  $8.895 \times 10^{-5} \text{ m}$ . The stress and displacement distributions of the part are shown in Figure 86, as well as the safety factor distribution.

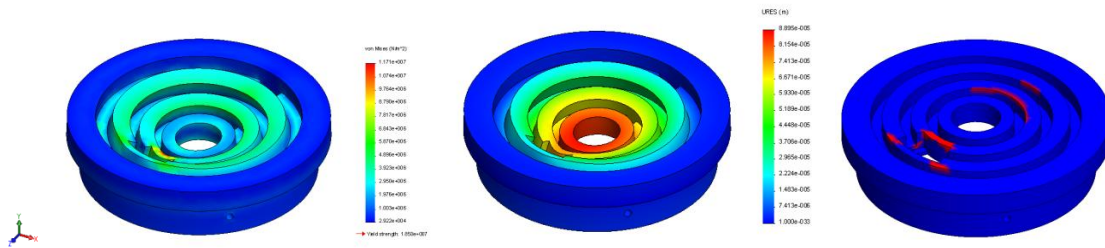


**Figure 86: Stress, Displacement, and Safety Factor Distributions for Base Top. Note, for the Safety Factor analysis, areas in blue are portions of part where SF>15, while red areas are where SF<15.**

The safety factor for this part was significantly lower than any previous part or iteration. There was some concern that this part may fail under a compressive load if too much force is applied. However, as the safety factor analysis in Figure 86 shows, the limiting parts of the part are because the grooves in the base top are too big and there was concern that the extrusions could snap off. The analysis showed that the structural features of the part, specifically the outside surface, would sufficiently transfer the load to the base shell.

### 6.2.3.4 Top Shell

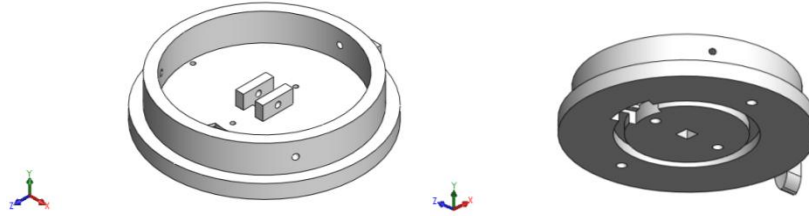


Figure 87: Isometric Top and Bottom Views of the Top Shell.

The top shell part was designed to rotate with the main shaft. Additionally, the piece would either be fixed to the next joint or the external load. Therefore, the top shell must be capable of transferring this load to the base top. This analysis assumed a simple, compressive load and ABS plastic. The restraint surface was selected to be all the surfaces on the bottom of the part, as these surfaces will directly contact the base top. The load surface was chosen as the outer cuff, where the next joint would be fixed and transfer the load to. The restraint and load surfaces are shown in Figure 88.

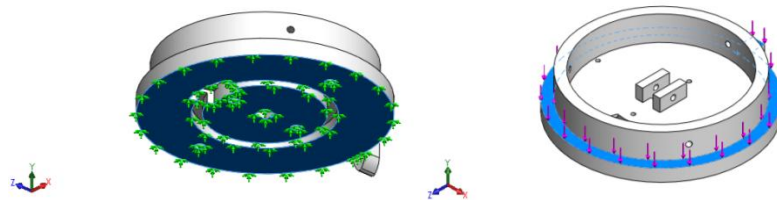
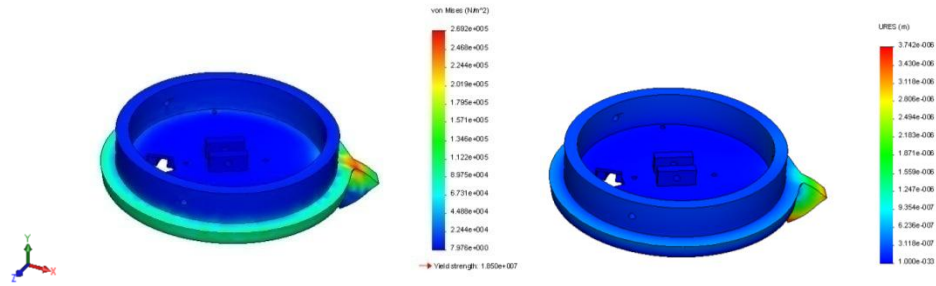


Figure 88: Restraint and Load Surfaces for Top Shell.

The stress analysis solved for the following values: minimum safety factor of 68.715, maximum stress of  $2.695 \times 10^5 \text{ N}/\text{m}^2$ , and a maximum displacement of  $3.742 \times 10^{-6} \text{ m}$ . The stress and displacement distributions of the part are shown in Figure 89.



**Figure 89: Stress and Displacement Distribution for Top Shell.**

The top shell analysis showed that the rotator-joint was successful in handling a load of 80N. The large safety factor, though less than the original parts using aluminum, was quite sufficient, and further engineering would allow for a reduction in size. The limiting feature in the design was a tab created to activate a limit switch. Without this tab, the part would be able to handle even more force.

## 6.2.4 Iteration 03 Motion Analysis

### 6.2.4.1 Main Shaft

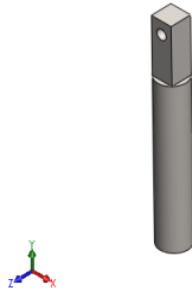


**Figure 90: Main Shaft for Rotator-Joint.**

The main shaft, shown in Figure 90, was designed to transfer the mechanical power from the motor to the top shell. One side of the shaft had a flat edge to allow for a set screw to secure the shaft to the coupler. Additionally, the top had a hole for a pin to secure the shaft to the top shell. The maximum torque applied to the shaft will be 2.6 Nm, which is the stall torque of the motor. Therefore, the analysis assumes a 2.6Nm torque applied to the top, while the bottom edge was constrained. The restraint and load surfaces are shown in Figure 91. The material of the shaft was assumed to be cast stainless steel, which has yield strength of 215MPa. The analysis assumed a fine mesh size of 0.8 by 0.4 mm.

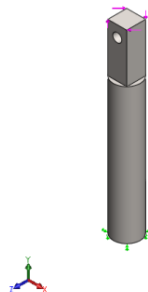


**Figure 91: Restraint and Load Surfaces for Main Shaft.**

The stress analysis solved for the following values: minimum safety factor of 0.361, maximum stress of  $5.953 \times 10^8 \text{ N/m}^2$ , and a maximum displacement of  $5.965 \times 10^{-5} \text{ m}$ . The stress and displacement distributions of the part are shown in Figure 89.

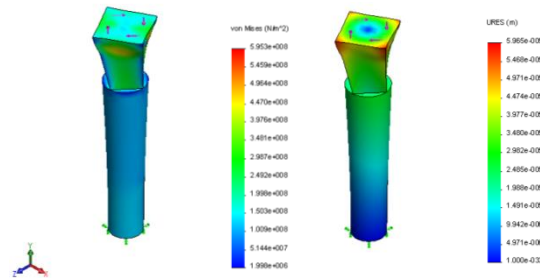


**Figure 92: Stress and Displacement Distributions for Main Shaft.**

This analysis clearly shows the large stresses created when a 2.6 Nm load was applied. The safety factor was much less than 1, which means that the part would fail if this large of a load was applied. This shaft, therefore, becomes the limiting part in the rotator-joint design. However, it was not anticipated that this large of a load would be applied to the rotator-joint, and the loading was assumed to be a worst case scenario. Regardless, the part would fail even if half of the maximum torque is applied. Further consideration and redesign of this shaft was necessary for increasing the acceptable load capacity of the rotator-joint.



### **6.2.5 Iteration 03 Part Selection**

The final iteration required the coupler between motor shaft and drive shaft. The coupler was manufactured by milling down a piece of eight millimeter diameter stainless steel stock material. It was discovered that milling such a small part was difficult, both in setup and in material removal, therefore it was discussed that powder metallurgy, if affordable, could be a better option for manufacturability. A local company, GKN Sinter Metals was contacted about the cost of producing a batch of 100 couplers, however they responded saying that the desired volume created would not offset the setup and tooling costs. However, a volume of 100,000 couplers would be more reasonable.

### **6.2.6 Iteration 03 Cost Estimate**

The cost estimate for the rotator-joint used the same format as the elbow, with different values inputted; however the estimated costs of producing a rotator-joint, both individually and in a group of one thousand, were calculated the same. The cost savings from batching joint production was shown as well, giving an idea as to the feasibility of mass producing turning a profit from the rotator-joint. The cost breakdown of the manufactured processes (Table 8) and the entire cost estimate for the rotator-joint (Table 10) are included below.

<b>Cost Calculations for Machined Parts of Rotator Joint</b>						
<b>Machining</b>						
Joint	Part	Process	Cost (\$)	Per Unit	Quantity	Sub-total
rotator	Coupler	Drill holes	0.35	hole	2	0.70
rotator	Shaft	Drill holes	0.35	hole	1	0.35
rotator	Coupler	End mill	0.04	cm <sup>3</sup>	0.22	0.01
rotator	Shaft	End mill	0.04	cm <sup>3</sup>	0.387	0.02
rotator	All	setup, install, remove	1.3	# setups	4	5.20
Subtotal:						6.27
<b>Material</b>						
Joint	Part	Material	Cost	Per Unit	Quantity	Sub-total
Rotator	Coupler	Stock - Stainless Steel	1.17	6 inch	1	1.17
Rotator	Coupler	Stock - Stainless Steel	15.59	72 inch	12	0.19
					1 of 1	1 of 1000
					<b>Total</b>	<b>7.44</b>
						<b>6.46</b>

**Table 8: Cost Calculations for Machined Parts of Rotator-Joint**

The cost of the motor ended up being \$39.99 individually. The combined 1 of 1000 cost of all the mechanical purchased parts came to \$13.26. Electrical parts, both purchased and the printed circuit board, came to \$72.22 for 1 of 1000 elbow joints. The cost of manufacturing, both machining and abs printing, came to a subtotal of \$47.27.

<b>Cost Estimate for Rotator Joint</b>							
<b>Purchased parts</b>							
<b>Single Parts</b>	<b>Supplier</b>	<b>Price per 1</b>	<b>Price per 1000 units</b>	<b># parts needed</b>		<b>Cost of 1 of 1</b>	<b>Cost of 1 of 1000</b>
Rotator Motor	RobotMarketPlace	\$39.99	\$39.99	1		\$39.99	\$39.99
Shaft: 6mm	SDP-SI	\$4.01	\$2.76	1		\$4.01	\$2.76
Bearings: 6mm bore	McMaster-Carr	\$9.10	\$9.10	1		\$9.10	\$9.10
Encoder		\$56.15	\$56.15	1		\$56.15	\$56.15
Passive Electrical Components	N/A	\$3.00	\$2.00	1		\$3.00	\$2.00
IrDA Transceiver		\$3.65	\$2.12	1		\$3.65	\$2.12
MCU		\$4.96	\$3.78	1		\$4.96	\$3.78
H-Bridge		\$5.87	\$5.87	1		\$5.87	\$5.87
Voltage Regulator		\$0.60	\$0.30	1		\$0.60	\$0.30
<b>Grouped Parts</b>	<b>Supplier</b>	<b>Price/pack (minimum)</b>	<b>Price/pack of 1000</b>	<b># packs needed</b>	<b># packs needed per 1000 parts</b>	<b>Cost of 1 of 1</b>	<b>Cost of 1 of 1000</b>
Screw: Philips Pan Head M3, 10r	SmallParts	\$5.50	\$55.00	1	16	\$5.50	\$0.88
Set Screw	SmallParts	\$1.96	\$261.40	1	2	\$1.96	\$0.52
<b>Purchased Subtotal</b>						<b>\$134.79</b>	<b>\$123.47</b>
<b>Manufactured Parts</b>							
<b>ABS Printing</b>	<b>Supplier</b>	<b>Cost</b>	<b>Per unit</b>	<b>Quantity</b>		<b>Cost of 1 of 1</b>	<b>Cost of 1 of 1000</b>
driven collar	N/A	0.27	cm^3	25.05		6.76	6.76
bottom collar	N/A	0.27	cm^3	24.49		6.61	6.61
plates	N/A	0.27	cm^3	19.29		5.21	5.21
casing	N/A	0.27	cm^3	82.31		22.22	22.22
<b>Machined Parts</b>	<b>Supplier</b>					<b>Cost of 1 of 1</b>	<b>Cost of 1 of 1000</b>
Coupler, Shaft	N/A					\$7.44	\$6.46
<b>Printed Circuit Board</b>	<b>Supplier</b>					<b>Cost of 1 of 1</b>	<b>Cost of 1 of 1000</b>
Board	N/A					\$20.00	\$2.00
<b>Manufactured Subtotal</b>						<b>\$68.25</b>	<b>\$49.27</b>
<b>Total Production Cost</b>		1 of 1	1 of 1000				
		\$203.04	<b>\$172.74</b>				

**Table 9: Cost Estimate for Rotator-Joint**

The total cost of producing an individual rotator-joint was calculated to be approximately \$203.04, whereas producing one out of a group of one thousand would cost \$172.74. As with the elbow, it can be assumed that the cost of the grouped rotator-joint would be less than \$172.74 in reality, since batched parts' prices would be cheaper than what is given by suppliers. Therefore, if sold for \$1000, there would be a profit of approximately \$800-850 for each rotator-joint, and \$800,000-850,000 for the 1000 produced.

### **6.2.7 Iteration 03 Discussion**

The final design of the rotator-joint behaved well, as shown with the above stress analysis. Overall, the rotator-joint fulfilled the primary requirements; the design allowed to easily be attached to adjacent joints, the design minimized custom parts, and infinite rotation was achieved. The analysis also showed that the main shaft was under designed. However, the analysis assumed a maximum torque of 2.6 Nm, which is an extreme load for this joint. Nonetheless, further design of the shaft should be considered in order to increase the maximum load. Additionally, this analysis assumed ABS plastic and created large safety factors on many parts. If this or a stronger material is selected, the components should be redesigned to further minimize part size and weight, and decrease costs.

### 6.3 Electrical Systems Iteration 03

The Final RoboJoint control system is made up of two primary components, the base controller and the joint controller, as shown in Figure 93. The base controller serves as a link between a PC and the RoboJoint system. Receiving commands from the PC via a USB connection, it translates the instructions from the PC into commands the joint controllers can interpret. Additionally, the base controller keeps track of all joint controllers' operations and status, allowing the PC to poll for updated data from the controller when necessary. After reviewing the results of Iteration 2, especially in regards to the terminal based user interface, it was decided that it would be important to provide the user an easily operable interface, which was fulfilled through the use of a Visual Basic program. This program communicates directly with the base controller, which then relays the commands to the appropriate joint.

Joint controllers, which reside in each individual joint, provide the actual motion functionality. An onboard microcontroller controls motor speed and direction, maintains a record of the current shaft position, monitors the status of necessary limit switches and provides two-way communication back to the controller. These controllers are designed to work with both the elbow and rotation joints. In order to accommodate the differences between the joints, a jumper must be set on the PC board, which will trigger the embedded software to react appropriately.

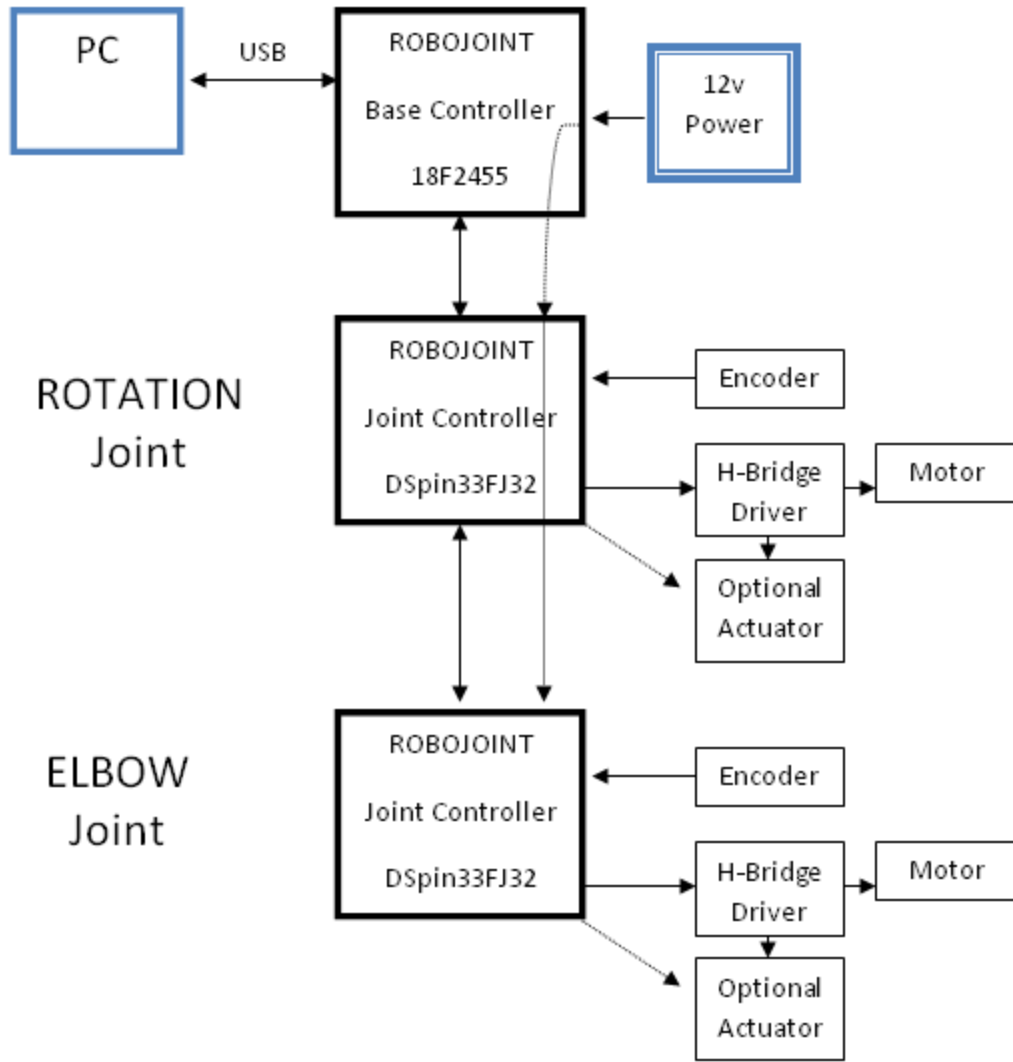


Figure 93: RoboJoint Control System

In addition to the microcontroller, a dual-channel H-bridge driver resides on each board. Both channels of this driver can be utilized by the controller. A set of header pins provide connectivity to the both the output and input of this second channel to any peripherals that may need it. As a result it is possible to use the controller board to drive an end effector. Additionally, these pins could potentially be used as logic level input/outputs, to either activate relays or interface with feedback systems, such as additional limit switches.

Two ports, one each for power and communication, exist on the controller board. This is intended to allow for pass through functionality. The power pins are simply connected together creating a bus, which the onboard regulator and H-bridge driver draw from. Each communication port, however, routes directly to the PIC. This allows the PIC to determine which side commands are being sent from, and to determine where it lies in the chain of joints. This functionality is expanded upon in section 6.3.2 and is critical to allowing the joints to self-address and act in a truly modular fashion.

In order to best utilize the capabilities of the PIC microcontroller, two individual microcontrollers were chosen. The 18F2455, which has extensive support for USB and an on-board transceiver, and a dsPIC, which has both a built-in PWM module and a Quadrature Encoder Interface, were utilized in the final design. To reduce cost and complexity however, the same PC Board is used in both the joint and base controllers. This is accomplished by setting the appropriate jumpers to reroute power to the correct pins, as the dsPIC varies in this manner from the 18F. Additionally, on this board, it is intended that certain components, such as the H-Bridge driver are not populated, as in practice they will most likely go unused and add extra cost. From a technical standpoint, no capabilities of the base controller are compromised by allowing the extra components to be populated.

### **6.3.1 Optical Encoder Module**

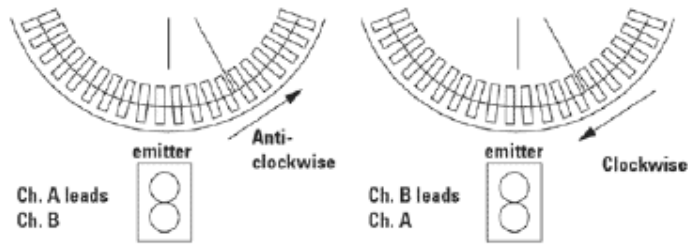
The RoboJoint utilizes off-the-shelf optical encoders to determine the joint's current position. The encoder is made up of a graduated codewheel, fixed to the shaft, and a stationary circuit board with a LED emitter and detector. As the graduations pass over the emitter/detector, a pulse is sent out of the encoder. The encoder is comprised of two channels, which carry pulses corresponding to the detection of black marks and reflective

gaps on the rotary wheel, as shown in Figure 94. Based on the phase between these two channels, and determining which channel is leading, it is possible to determine the direction of rotation in the shaft.

In early iterations and prototypes, the PIC monitored the lines, continually looping through trying to detect changes. Each pulse incremented the appropriate counter, allowing the controller to keep track of the shaft's rotation. Each full rotation of the shaft will produce 256 pulses, as a result of the 256 extremely fine marks on the code wheel. However, in the final prototype, the utilization of the dsPIC brought with it the ability to utilize an internal hardware peripheral that allows the MCU to monitor and keep track of the encoder and its count, while allowing the primary core of the PIC to be devoted to executing the programs code. After the peripheral has been configured correctly, the main program code can simply retrieve the value of the counter on demand.



## Phase Relationship



## Timing Diagram

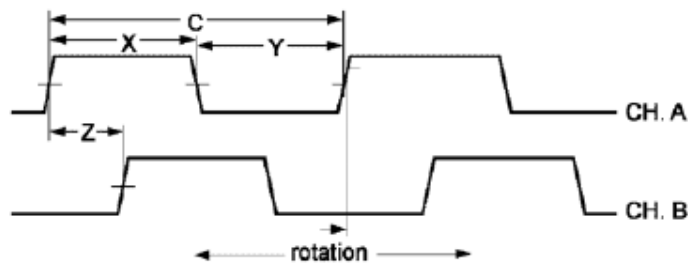


Figure 94: Optical Encoder Functionality (US Digital)

### 6.3.2 Communications

A key feature of the RoboJoint was its ability to interconnect with other joints. The joints are intended to be arranged in a line topology so that joints are able to determine their position in the chain relative to each other. This allowed the modular joints to be moved around without needing to manually set an address on the unit. As a result, each communication module had two serial communication ports, for data both coming into the unit and being forwarded to the next joints in the chain. Additionally, any of these serial connections can be replaced with an IrDA transceiver. This transceiver's primary purpose is to accommodate crossing an infinite rotation joint. This base station provided a USB interface to a user's PC. The PC, which provided a user interface for controlling the joint

system, forwards the commands to the base station, which subsequently translated the instructions sent via USB, or potentially any other common computer interface, to instructions compatible with the joint system.

### ***6.3.2.1 Initialization***

Upon power up the base station will begin a search sequence for all joints. The base will send a 16-bit sync command, consisting of all logic highs. This will be followed by a search command (0xC0) and an address, which for the base station will be 0x00. Any unit receiving this command will immediately return a search acknowledgement command (0xC1), the received address incremented by one, and the type of joint as determined by a mode jumper on the unit. The unit will store this address to identify any future commands intended for it. After this information has been sent back to the base station, the joint module will then reissue the search command (0xC0) to the next units in the chain, this time with the updated address. This process will continue until no response is received, at which time the last joint to initialize will send a search termination (0xC2) command back towards the base followed by a word containing the total number of joints found.

### ***6.3.2.2 Packet Structure***

All data transmitted between the components of the system will follow a predetermined format. Commands can be preceded by a SYNC command consisting solely of logic highs (1's) in order to ensure all units are ready to receive. All commands sent by the base unit will consist of the destination address, followed by a command and data values pertaining to that command. While most commands only require one word of data, position commands require two to allow for additional resolution. These commands will

then use both data words, otherwise the second data word will contain only logic lows (0's). A CRC word will be appended to ensure correct transmission of data.

Data being sent from the joints to the base will be formatted similarly. The address, however, will always be 0x00. After sending the command and data, the address of the joint the message originated from is sent.



Figure 95: Base to Joint Packet Structure

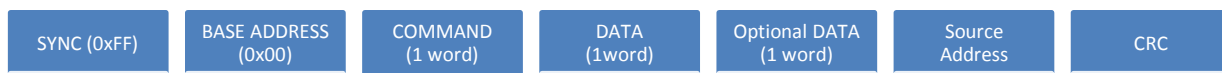


Figure 96: Joint to Base Packet Structure

Value	Command	Description
0x11	Move	Move to absolute position
0x12	Move Rel FWD	Move forward relative distance
0x13	Move Rel BWD	Move backwards relative distance
0x50	Query	Query Status and Position
0x55	Set Speed	Set Speed 0-255
0xC0	Search Start	Starts initialization sequence to address joint
0xE0	Stop	Stop Move
0xEE	Emergency Stop	All Joints Stop
0xFF	SYNC	

Table 10: Commands (Base to Joint)

Value	Command	Description
0x51	Move Started	Joint has started moving, destination in data (confirms any move commands)
0x52	Moving	Joint moving, current position in Data
0x53	Move Complete	Move completed, current position in Data
0x54	Stopped	Joint is stopped, current position
0xC1	Search Return	Joint received search command, returns its address to the base
0xC2	Search End	No additional joint found, returns total number of joints
0xE5	Limit Error	Joint hit limit switch, data may convey which limit switch
0xE6	Move Error	Joint unable to start move, data may have additional error code
0xE7	Current Trip	Joint drew too much current (possible collision)
0xFF	SYNC	

Table 11: Commands (Joint to Base)

Value	Command	Description
0xD1	Rotation Joint	Signals rotation mode jumper set on board
0xD2	Elbow-joint	Signals elbow mode jumper set on board

Table 12: Special Data Values

Value	Command	Description
0x00	Base Station	Designation reserved for Base Station
0xEE	All Units	Command applies to all units (primarily for Emergency Stop)

Table 13: Special Address Values

### 6.3.3 IrDA Communications

In order to reduce the cost of the joint, it was decided that an infrared data link would be used to transmit data across the infinite rotation joint. While it would be possible to integrate a slip-ring device capable of transmitting power and signal through the shaft, the cost of these devices grows as more conductors are added and higher signal integrity is needed. Instead of purchasing a high-quality 4-conductor device, capable of transmitting

both power and signal, the design could utilize a cheaper 2-conductor part. Additionally, by only transmitting power, the device does not need to be of high quality, as voltage regulators and capacitive filtering on each board will be able to flatten out any spikes or dropouts in the power supply. The communication link which would be very sensitive to any interruptions, is then provided through the use of IR transceivers, integrated into the mechanical package of the RoboJoint. The TFDU4300 Infrared Transceiver was chosen due to its small size and high modularity. Capable of an 115.2kbps transmission rate, the module is fully IrDA compliant. As a result, it can be easily integrated into designs using a wide range of microcontrollers, such as the MSP430 and Microchip PICs.

The TFDU4300 at its core, is little more than an IR LED and IR photo detector. It takes logic bits and triggers the LED accordingly and does not have any processing ability of its own. Because of this, serial data streams must be processed before arriving at the device. The IrDA specifications call for the nominal pulse to be  $T/12$ , where  $T$  is the duration of a typical UART bit at that transmission rate. During testing, a 9600 bits/second transmission rate was used. This equates to a bit duration of 104  $\mu\text{S}$  and a resulting IrDA pulse of approximately 19.5  $\mu\text{S}$ . Further calculations, referenced by the IrDA specifications, detail that the pulse length can deviate to a minimum of 1.41  $\mu\text{S}$  and maximum of 22.13  $\mu\text{S}$  and still be considered valid. A diagram comparing a typical UART serial stream to its IrDA compliment is shown in Figure 97. It is also important to note that pulses only occur for logic lows, effectively inverting the signal.

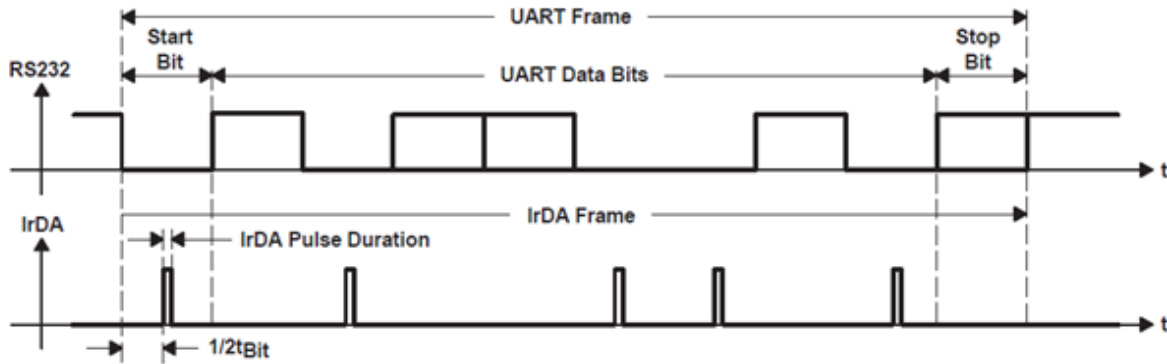


Figure 97: IrDA Protocol (Texas Instruments)

The utilization of the TFDU4300 IR Transceiver began early in the design phase, appearing in the first design iteration. Initial testing consisted of using the MSP430 microcontrollers outfitting with an IR link to toggle LEDs, and progressed to testing the rotary joints' integrated transceivers. The TFDU4300 module proved to be a simple device to use and integrate with both the early MSP4300 microcontroller and the final dsPIC used on the controller board.

## 6.4 Power Supply

The RoboJoint was designed to run primarily off a 12 volt power supply. This value was derived from industry standard and by researching other robotic applications, the vast majority of which function off of a 12 volt power supply if battery operated. The option to power the system off a battery if desired was important, if it is desired to mount the joint on a mobile platform or similar device. Because of the availability and low cost of 12 volt batteries, this is also an extremely economical choice. Additionally, if the joint is to be used in a static location, 12-volt power supplies are exceedingly easy to obtain, and the selection can be customized so that the RoboJoint can utilize any power source from residential to industrial, domestic and international.

However, while the nominal voltage is stated to be 12-volts, the true operating voltage can vary from 3 to 16volts, depending on the electrical specifications of the DC motor utilized in the joint. A 3.3v DC regulator provides the necessary power to the microcontroller and other onboard electronics, and is stable over this range. While any change in voltage will affect the actual speed of the motor, the microcontroller is dependent solely on position, and is not affected by any change in rotational speed. Furthermore, the speed set by the controller is simply a relative value. When the controller sets the speed, it is simply based on a scale from 0-100% which relates to the duty cycle produced by the PWM generator.

It is important to note that the regulator is extremely versatile and recommended for automotive applications, where it routinely sees large spikes and dropouts, while continuing to provide a reliable output. This is critical since the rotation joint, because of its slip ring, introduces an extremely unstable power supply, which must be reliably regulated to prevent damage to the onboard electronics. The power supply to the motor, however, remains unregulated. Because of the current draw, it would consume a large deal of space on the PCB and add unnecessary cost and complexity since filter is not necessary for the DC motor. Although these spikes and dropouts will affect the speed, it will only be for a brief moment, and the inertia of the shaft and attached load will help to keep the motor operating at a fairly continuous speed.

## **7 Prototype Construction**

### **7.1 Elbow Construction**

Once the final iteration design was completed and all the parts were acquired, the prototype construction process could begin. Although, all the parts were designed to be easily assembled, a few unforeseen problems were encountered during the construction process. One of which was attaching the gears. For design purposes it was assumed that the miter gears and coupler would be anchored by means of a set pin. However, there were a few unforeseen problems with this design. First, since set pins required a hole to be drilled through both the miter gear and shaft, there would be no room for error in positioning the gears. Second, once the miter gears had been attached, they could not be removed. Finally, with a worm shaft that was three millimeters in diameter, drilling a one millimeter hole in the shaft would have an adverse effect on the overall strength of the shaft.

### **7.2 Rotator Construction**

Through the construction of a rotator-joint prototype, many weaknesses of the design were discovered. One of the initial design task specifications was to create a joint that was easy to manufacture. However, during prototype construction, it was found that it was difficult to properly align the shaft and coupler. Additionally, the set screws used to fix the shaft to the coupler and the motor were not strong enough to create a permanent hold. The prototype also allowed for determining the success of the IR transmitter and custom slip ring created. Though the slip ring worked, there is much room for improvement. The prototype also confirmed successful design features, such as the carrier plates and the



rotator-joint structure. The motor and circuits were securely held in place, and each part was fixed to each other using machine screws.

## 8 Prototype Testing

Although the Elbow and Rotator-joint were designed to adhere to abilities outlined in the task specifications, testing was required to ensure that these joints would perform as intended. A set of testing regulations were devised that concentrated on Accuracy/Repeatability, Strength, and Product Life. With these testing procedures, it could be determined if the joints performed as outlined.

### 8.1 Testing Procedure

#### 8.1.1 Accuracy/Repeatability

- Record 0-180 degree sweeps.
  - Joint Operating in front of calibrated background.
    - results will be recorded by hand while team members monitor the device.
  - Joints mounted to the base, oriented vertically (length of cylindrical casing is vertical, gravity is acting along the length, opposite the driven collar)
  - Elbow
    - Mount the goniometer vertically to joint (see diagram)
      - will be calibrated to elbow's axis of rotation
      - Home is 0 degrees (as far to one side as joint can go rotate)
    - Test 1 : Home to 90 deg (or vertical)
      - Input command to go 90 deg once
      - Record results (true location) by taking a photograph and measuring angle with the goniometer (calculate absolute degrees)
      - Repeat 25 times
    - Test 2: Home to 180 deg (horizontal to horizontal)
      - Input command to go 180 deg once
      - Record results (true location) by taking a photograph and measuring angle with the goniometer (calculate absolute degrees)
      - Repeat 25 times
  - Rotator
    - Mount goniometer to rotator and ground (ground is a fixed apparatus to that one arm of the goniometer is held constant and the other arm rotates with the joint)

- will be calibrated to rotator's axis of rotation
- Home is 0 degrees (a predetermined point marked by a limit switch)
- Test 1 : Home to 90 deg
  - Input command to go 90 deg once
  - Record results (true location) by taking a photograph and measuring angle with the goniometer (calculate absolute degrees)
  - Repeat 25 times
- Test 2: Home to 180 deg (horizontal to horizontal)
  - Input command to go 180 deg once
  - Record results (true location) by taking a photograph and measuring angle with the goniometer (calculate absolute degrees)
  - Repeat 25 times
- Test 3: Home to 360 deg (horizontal to horizontal)
  - Input command to go 360 deg once
  - Record results (true location) by taking a photograph and measuring angle with the goniometer (calculate absolute degrees)
  - Repeat 25 times
- Calculate standard deviation for each test and record subjective results if necessary

### 8.1.2 Strength

- Joints mounted to the base, orientation as follows:
  - 1: vertically (length of cylindrical casing is vertical, gravity is acting along the length, opposite the driven collar)
  - 2: horizontally (length of cylindrical casing is horizontal, gravity is acting along the diameter of the casing)
- Run with varying speeds and varying loads.
  - Speed varying from 25% to 100% at 25% intervals, with loads.
  - Loads starting at 0 kg and increasing by 0.25 kg.
- Elbow
  - Test 1: 0 kg (no load)
    - run joint at 25% speed from 0 to 180 degrees and back 25 times
    - subjectively record noise, heat, and whether it functions properly
    - repeat first and second bullet point at 50%, 75%, and 100% speeds

- 5 minute break for minor adjustments, not including replacing broken parts
  - Test 2: 0.25 kg
    - mount weight to joint end, centered
    - run joint at 25% speed from 0 to 180 degrees and back 25 times
    - subjectively record noise, heat, and whether it functions properly
    - repeat first and second bullet point at 50%, 75%, and 100% speeds
    - 5 minute break for minor adjustments, not including replacing broken parts
  - Test 3: 0.5 kg
    - mount weight to joint end, centered
    - run joint at 25% speed from 0 to 180 degrees and back 25 times
    - subjectively record noise, heat, and whether it functions properly
    - repeat first and second bullet point at 50%, 75%, and 100% speeds
    - 5 minute break for minor adjustments, not including replacing broken parts
- Rotator
  - Test 1: 0 kg (no load)
    - run joint at 25% speed from 0 to 360 degrees and back 25 times
    - subjectively record noise, heat, and whether it functions properly
    - repeat first and second bullet point at 50%, 75%, and 100% speeds
    - 5 minute break for minor adjustments, not including replacing broken parts
  - Test 2: 0.25 kg
    - mount weight to joint end, centered
    - run joint at 25% speed from 0 to 360 degrees and back 25 times
    - subjectively record noise, heat, and whether it functions properly
    - repeat first and second bullet point at 50%, 75%, and 100% speeds
    - 5 minute break for minor adjustments, not including replacing broken parts
  - Test 3: 0.5 kg
    - mount weight to joint end, centered
    - run joint at 25% speed from 0 to 360 degrees and back 25 times
    - subjectively record noise, heat, and whether it functions properly
    - repeat first and second bullet point at 50%, 75%, and 100% speeds
    - 5 minute break for minor adjustments, not including replacing broken parts

### 8.1.3 Product Life

- Joints mounted to the base, oriented vertically (length of cylindrical casing is vertical, gravity is acting along the length, opposite the driven collar)
- Run continuously with small load.
  - run time 5 hours to start.
    - If necessary, time will be increased.
  - Elbow
    - Test 1: 0.5 kg load
      - attach 1 kg load to end of joint, centered
      - run joint at 50% speed from 0 to 180 degrees and back for 5 hours
      - 5 minute break for minor adjustments, not including replacing broken parts
  - Rotator
    - Test 1: 0.5 kg load
      - attach 1 kg load to end of joint, centered
      - run joint at 50% speed from 0 to 360 and back for 5 hours
      - 5 minute break for minor adjustments, not including replacing broken parts

### 8.1.4 IR communication

- Run with varying speeds, with small load.
  - Speed varying from 25% to 100% at 25% intervals.
- Send data packets through and record number of received.

### 8.1.5 Power Transmission

- Run at varying speeds, with small load.
  - Speed varying from 25% to 100% at 25% intervals.
- Record power loss across the joint while in operation.

## 8.2 Testing Results

### 8.2.1 Strength Testing

After the construction of the rotator and elevator joint prototypes, it was necessary to test the joints to judge the success of the design. Though preliminary stress analysis was performed on the structural parts of the joints, many of the mechanical parts of the project have yet to be tested, including the gears and bearings. Additionally, testing was necessary to determine the maximum load the entire structure could withstand and the motors could handle.

The testing performed on the joint was to determine the maximum load the joint could withstand for a variety of input voltages. Each joint would be loaded with a variety of loads between 0 and 1000g, increasing by 250g each test. Each loading configuration would also be tested at a changing input voltages, from 3V to 12V, increasing by 3V each test. The result is 20 tests for each joint. The full testing procedure may be found in section 8.1. During testing, the team recorded both quantitative and qualitative data, including vibrations, deformations, increase in heat, current draw, and cycle time. For the rotator-joint, one cycle was defined as 720 degrees: 360 degrees clockwise followed by 360 degrees counterclockwise. The elevator-joint cycle was defined as 360 degrees: 180 degrees clockwise followed by 180 counterclockwise. The full results may be found in Appendix C, while a summary of relevant data may be found below in Table 14 and Table 15.

Test	Voltage	Load	Avg. 360 deg time (s)	Avg. current draw	Notes
1	3V	0g	4.67	-	-
2	3V	250g	5.00	-	-
3	3V	500g	5.17	-	-
4	3V	750g	5.03	-	-
5	3V	1000g	5.67	-	-
6	6V	0g	2.33	100 mA	long pause between direction change - loose set screws
7	6V	250g	2.33	100 mA	long pause between direction change - loose set screws
8	6V	500g	2.33	100 mA	long pause between direction change - loose set screws
9	6V	750g	2.33	175 mA	-
10	6V	1000g	2.47	-	only 20 cycles, concerns of grinding
11	9V	0g	1.57	-	lot of play as direction changes- need to tighten set screws
12	9V	250g	1.50	200 mA	-
13	9V	500g	1.50	-	-
14	9V	750g	1.60	-	-
15	9V	1000g	1.53	-	-

Table 14: Rotator-Joint Test Results

Test	Voltage	Load	Avg. 180 deg Time (s)	Avg. Current Draw	Notes
1	3V	0g	9.33	-	-
2	3V	250g	9.30	-	-
3	3V	500g	10.03	-	motor close to stalling?
4	3V	750g	10.83	-	only ran 15 cycles due to concerns of motor
5	3V	1000g	-	-	unsuccessful test- motor strain and gear slip
6	6V	0g	4.60	175 mA	-
7	6V	250g	4.40	200 mA	initial test set screws loosened, fixed and reran 15 times
8	6V	500g	4.63	350 mA left, 250 mA right	-
9	6V	750g	4.57	-	motor strained, only completed 15 cycles, current less issue after letting it rest
10	6V	1000g	-	-	did not complete- gears slipping
11	9V	0g	2.73	-	-
12	9V	250g	2.93	-	-
13	9V	500g	3.23	200 mA	only completed 13 cycles, avg time adjusted here appropriately
14	9V	750g	-	400 mA	failed test- too loud and large current draw

Table 15: Elevator-Joint Test Results

Though the testing did not provide with concrete numerical data, it did provide adequate information regarding the performance of the joints.

The rotator-joint performed well at low speeds at all loads. However, as the speed voltage increased, the rotator-joint was unable to handle large loads. This was primarily due to the slip-joint assembly, and the associated grinding. Concern of additional wear on the contact surfaces limited further testing. However, many of the mechanical and structural parts in the rotator-joint performed quite well during all tests, regardless of



speed or load. The testing did show that another weakness of the assembly were the set screws. As testing progressed, there became continued lag between changing directions. This was attributed to loosened set screws that allowed some play between the shaft and the coupler. Finally, the current draw for the rotator-joint was appropriate for the application, and had no large spikes that could result in circuit problems.

The elevator-joint also performed well during testing. However, despite low and high voltages, the elevator-joint was unable to handle a load of 1000g; this was primarily due to slippage of the miter gears. The motor also had some difficulty with higher loads and created noticeable motor strain. The motor performed well with loads 500g and less, though loads of 750g were also successful but created concerns of motor strain. Primary problems from the elevator-joint were the miter gears slipping, as well as the relevant set screws loosening. Misalignment of the miter gears created further gear slip problems. Additionally, the current drawn during the testing was also of concern. Average current readings of 350 mA were recorded, as well as peaks of up to 500 mA. These current readings are of concern to the circuit and power supply, as the circuit is only rated to 800 mA. If multiple joints were inducing such a high current simultaneously, total current draw could exceed the circuit ratings. Additionally, the power transmission through the rotator-joint slip ring could limit the available current.

Regardless of the concerns outlined above, both the rotator and elevator-joints were successful during testing. The rotator-joint was able to rotate 1000g and both 3V and 9V, while the elevator-joint was able to lift 500g at 3V and 9V. Additionally, the essential components in the joints behaved as expected, with only minimal modifications and

reassembly required during testing. The electronic and structural components behaved well throughout testing, while the testing provided with areas for future improvement.

### **8.2.2 Accuracy/Repeatability and Product Life Testing**

Unfortunately due to time constraints and malfunctions with the electronics the group was unable to finish the testing procedure. Although the accuracy/repeatability of the joints were not tested, it should be noted that during the strength test the joints were running for nearly five hours under different load conditions which would have tested the overall product life. Under none of the testing conditions did any part of the joint fail. These results indicated that the joint was a relatively strong design. However, without the completion of the official product life test, no definitive results can be quantified.

## 9 Conclusions

### 9.1 Project Summary

The goal of this project was to design and manufacture robotic joints that are inexpensive and capable of being used in a variety of applications. In order to accomplish this objective, the group used an iterative design process to devise joints that adhered to a set of task specifications which focused on; Modularity, Communications, and Size. Then, testing procedures were developed and proved that the final designs were proficient in the areas of testing: Accuracy/Repeatability, Strength, and Product Life. Although the short time frame of the project inhibited the group from fully completing the testing procedure, the designs were deemed to be extremely capable.

## 10 Recommendations

Although the group designed two extremely capable joints, due to time restrictions there were a few areas that with more time could have been improved.

### 10.1 Elbow-Joint

Although the final design of the Elbow Joint adhered to many of the original task specifications, due to the short time window for the overall project, there were a few areas that could benefit from improvement with future work.

One of the key areas was to eliminate the need for couplers. The coupler (shown in Appendix O) was fixed to the motor shaft and provided a three-millimeter shaft for the miter gear to mount on. The coupler in the elbow-joint design was notorious for having the incorrect dimensions. This was caused by the machining process used and caused difficulties during operation. Using either a motor with the correct shaft diameter or gears with the proper bore would help improve the drive system and reduce the number of parts.

Another key area for improvement was the anchoring system and electronic connection between joints. Although the design of the interlocking joints was functional for the applications outlined, it is possible to research easier mechanisms. New designs that have electrically connects that were automatically positions and would allow the joints to quickly attached without the need for tools would be a design that would improve the joint connection experience for the end-user.

Throughout the design process there were many situations where the overall size of the joint could be decreased. The diameter of the base, top collar, and bottom collar could be decreased however, this would require re-positioning of the motor, newly designed

motor mounts and printed-circuit-board, and also a complete redesign of the rotator joint in order to match the changes in dimensions and maintain modularity between the joints. The group did not include many of these dimension changes due to the design ramifications and time constraints, with more time many aspects of the joints could be decreased. The smaller size would further increase the applications for the joint and reduce materials cost.

## **10.2 Rotator-Joint**

To create a simpler and more reliable rotator-joint, numerous improvements can be made on the current design. Improvements to the casing, custom manufactured parts, and better selection of commercial parts would result in a less expensive and thorough design.

One recommendation for reducing the number of parts and to simplify the design is to combine the rotator and the shaft. In the current design, these are two distinct parts that must be joined together with set screws. This results in increased machine costs, as well as assembly time. Additionally, it creates another point of failure; during testing the set screws used to join the coupler and shaft often failed. By combining the two parts, total failure of the part would be reduced.

Another weakness in the rotator-joint design is the custom slip ring implemented. Though the assembly successfully transmitted sufficient electrical power, it created numerous problems. The contacts used in the prototype were not the proper height, which misaligned the top shell. This misalignment caused the joint to become unbalanced as it rotated. Additionally, the misalignment raised the top shell off of the base top, such that all

compressive force was transmitted onto the electrical contacts and shaft. This induced significant grinding and friction, creating wear and noticeable noise.

Future development of the rotator-joint should focus on refining the slip joint assembly. Numerous commercial slip joints are available, though were not included in this design because of the prohibitive costs. Nonetheless, the slip joints reliably transfer power across a continuously rotating joint. Additionally, slip joints may transmit numerous channels, allowing it to also replace the IR signal transmitter and further simplifying the design. Commercial slip rings are also available in “pancake” style, similar to what was included in this design, or a “spool” style. The pancake style is flat, but has a large radius, while the spool design has a smaller radius but a larger height. Each type has their advantages in the rotator joint, and both should be equally considered depending on which joint dimension should be minimized. In addition to including commercial slip joints, it is possible to design custom slip joints that would also be appropriate in this application. Though extensive design is necessary, the custom slip joint would lower the total of the joint.

Concerns about the slip ring assembly could be further reduced with the addition of another thrust bearing. The bearing currently used is rated for axial and one direction thrust. However, an additional thrust bearing between the base top and top shell, providing thrust reaction in the opposite direction from the first bearing, would reduce friction between the two parts when rotated. Additionally, with careful alignment of the electrical contacts and shaft position, the thrust bearing would be able to transmit the mechanical load from the next joint without wearing the contacts.

An additional feature of the rotator-joint that could be simplified is the carrier plate that supports the encoder. The extrusion around the center currently supports the encoder in its correct position; however it creates a barrier for accessing the coupler and set screws. It is recommended that the encoder position is moved such that the carrier plate is not required to support it. If the shaft and coupler are combined in one part, there would be space to move the encoder closer to the base top, and perhaps attach it there.

In addition to parts and design features discussed above, there is also room for improvements in the structure of the rotator-joint. The prototype constructed was made large enough for easy assemble and adjustment. However, future design should reduce the size of the joint, both the diameter and height. With many of the changes previously discussed, such as the combination of the coupler and shaft, as well as improving the slip joint, will also reduce part size. Therefore, the entire joint may be reduced in size as well.

The current rotator joint was designed for assembling axially, with components sliding into the base shell from the bottom. While this design properly secured parts, it did create difficulty in assembly. One possible way to simplify assembly would be to split the base shell in half, which would be screwed back together after internal parts are assembled. Though this may reduce the part strength, the stress analysis showed that the safety factor was quite large and may still be adequate if the shell is split.

The modularity of the joints may also be improved in future designs. The current system of collars and tubes, fixed with machine screws, is sturdy; however, quick release mechanisms could be added to allow the mating of joints even simpler. Additionally, aligned electrical contacts could be included, such that joints would be able to “click”

together, and be firmly secured both mechanically and electrically. These improvements would make for a truly modular joint.



### 10.3 Base Fixture

In order to properly secure the elevator and rotator joints to a workstation or other existing features, a base fixture should be designed. A preliminary structure was designed, as shown in Figure 98, but should be further developed.

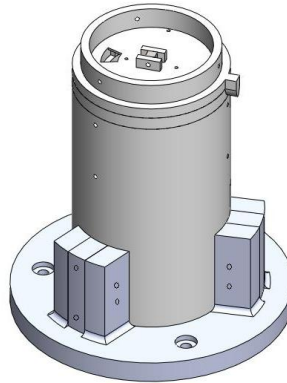


Figure 98: Base Fixture Proposed.

The fixture proposed includes three tabs to be mounted onto the joint via screw holes already present. These tabs would then be secured to the base fixture. The base fixture could be fixed to a flat surface or another robotic fixture.

### 10.4 Electronic Control Systems

There are several recommendations pertaining to the electronic control systems of the RoboJoint. Foremost would be to improve the board design and layout. Because, the scope of this project focused on prototyping the joint preliminary, a final board design was never created. It would be recommended that the final board utilize 4-layer construction. This fairly common board type uses two inner layers to provide power and ground, in addition to the traces placed on the top and bottom surfaces of the board. The layers are separated within the board by a dielectric, and interconnected by the use of conductive

vias, that physically attach exterior traces to the internal planes. This removes traces from the top and bottom sides of the board that had previously provide power and ground. The power plane, one of the internal layers, should carry the 12 volts the entire system requires. Because the H-bridge motor driver requires a large amount of current at 12 volts, designating the entire inner plane to be 12 volts will remove the need for the wide high current traces on the surface of the board. Because the components requiring 3.3 volts are located near each other, a centrally located voltage rectifier can be placed on the surface of the board to provide necessary power. Additionally, during the prototype phase, the traces along the edges of the board were often damaged or ripped because of the close tolerances between the joint body and the board perimeter. Ideally, more space could be left between the edge of the board and any traces. By removing the power and ground traces, space is also freed up to move the status LEDs to the top of the board. While these are not required, they are often useful in troubleshooting and amount to a fraction of the electronics cost. However, because they are currently placed on the underside of the board, it would require additional and costly work, if an automatic board loading machine was utilized during mass production, which may negate any value they may bring to the board.

Additionally, by removing traces and rearranging components to take advantage of a more efficient layout, the needed board area should be drastically reduced. This should allow for the fulfillment of the other recommendations in this section, particularly those relating to minimizing the joint's package size. Also, the board currently has a hole in the center of the board to accommodate the joint's motor. This was done to make the exterior housing as small as possible, however, if low profile connectors are utilized, placing the board underneath the motor may not add significant length.

A common board is used for the USB system controller, the elbow joint, and the rotator. The feasibility of modifying the common board or creating an additional board to accommodate an input/output module should be investigated. The current command set could be easily modified to send commands to such a board, as well as interpret received data. An I/O board would allow for integration into other systems, allow for an end effector to be attached to the joint, or for sensors to be integrated into the system, such as for positioning or feedback.

In the prototype, there are various connectors being utilized, ranging from power to programming, and data transmission. For production purposes, this should clearly be optimized. There should most likely be two separate wiring harnesses. One to interconnect the interior components and a second that provides external connectivity.

The interior wiring harness, should integrate the cabling for the encoder, motor, data(IR or hardwire), and power pass through. On the prototype board, these wires are either soldered directly to the board or use supplier's connector, as is the case of the US Digital encoder. This harness will most likely be connected on the unpopulated side of the board, to minimize potential interference with components. The second harness should provide data and power connectivity to the exterior of the case. Currently, this is being done with an RJ45 connector, which is both bulky and less than ideal because of the wire gauge used. Although, we got around this by combining multiple conductors in the RJ45 cable, an ideal solution would involve two larger gauge wires for power, accompanied by two small gauge wires for data transmission.

Another area of improvement would be the integral installation of limit switches. Due to manufacturing difficulties, it was decided not to integrate a COTS limit switch into the housing of the joint. In early iterations, a standard switch was simply glued to the exterior of the housing, and wired back into the controller. For the final prototype, custom plates were manufactured to serve as limit switches, as described in section 5.5.4. While these limit switches functioned properly, it would better serve production purposes to use a miniature limit switch recessed appropriately into the joint housing.

One feature, not fully implemented, but accounted for and included in the hardware design is the ability to measure the current draw of the motor. This functionality is provided by a voltage divider from the ground pin of the MOSFETs of the L298N H-bridge driver. Currently the output of this divider is routed to A/D capable pins of the dsPIC33FJ32MC302. By taking advantage of these measurements, the joint controller gains the capability to constantly monitor the change in current on the motor. From this information it should be possible to roughly estimate the load capacity on the joint, and to determine if a collision with another object has occurred, providing the controller the ability to automatically shutdown. Although not critical to the project, these features would provide valuable additional information.

A more involved improvement would be the creation of a coordinate system similar to that of industrial robots. Both of our joints refer to their position solely in terms of their respective plane, whereas industrial robots calculate their position in relation to a global 3-dimensional coordinate system. This makes programming and manipulation of the arm significantly simpler. However, because of the modular nature of the joint, and the fact that

the spacing and orientation of the joints in relation to each other can vary significantly between users, this is not at all a trivial task. Most likely, in addition to the calculations determining the relationship between the actual position and the relative coordinates, users may have to have an area to enter distances between joints or for the modules to somehow determine their relationship to each other on their own.

Lastly, the software and control interface have great potential for improvement. For testing and demonstration purposes a simple Visual Basic application was created to control the joint's movements. However, the directives are coded directly into the application. As a result there is no way for other applications to access or manipulate the joint. An API containing useful commands could be created to allow the creation of custom programs to control the joint, in addition to allowing the RoboJoint to be integrated into larger systems. This API would allow for direct control over the joint without necessary being familiar with the systems individual commands.

## 10.5 Parts/Manufacturing

A smaller motor with the necessary torque and speed requirements would be good if it could be found at a reasonable cost. It would help reduce overall package size, which is one of the outstanding qualities of the joints created in this MQP. Ultrasonic motors, for example, would be ideal as they are very small with high torque. More research on manufacturers and suppliers of ultrasonic motors would aid this project in the future.

In addition to decreased size, increased power would also make both joints more appealing to the end user. Increased power could be accomplished by using more powerful motors or motors with an increased gearbox ratio. This would necessitate an increase in torque, as well as speed, capacity of a motor.

Another improvement to the parts selection for the joints would be to use the same motor for both the rotator and the elbow, which would be beneficial for multiple reasons. In general a few standardized parts are more convenient than having many unique parts available. Motors could be purchased in larger batches which would reduce the individual unit price of each motor, and reducing the production cost of an individual joint. Individual inventories for the two different joints could be combined, reducing the amount needed at one time, again saving money. Using the same motor would be feasible because the elbow and the rotator had similar torque and speed requirements (assuming the 10:1 gear ratio was reintroduced into the rotator design, as mentioned in Section 10.2).

Outside of finding the perfect motor, both joints would also benefit in strength by press-fitting all parts with respect to the medium-drive interference requirements. As described in Section 6.1.4 press fits for a medium drive system would have been

significantly stronger than setscrews or pins. Limitations in manufacturing did not allow for the tight tolerance needed to achieve a medium drive press fit. The prototype also required ease of assembly and disassembly, and press fits would have been difficult to disassemble, therefore it was more reasonable, for the prototype, to use a set screw.

Additionally, the use of English unit parts would be more sensible and convenient than metric parts. Metric units were used after the motor was purchased because its shaft was measured in metric units and the team wanted all parts to have the same units. However, there were more options available and prices were typically more affordable with small English unit-based parts than with metric. Boston Gear, for example, had a number of small parts, from worm gears to right-angle gears, which would have worked better with the joint designs; however they were all in English units. McMaster-Carr also had a greater variety of parts in measured in English units that were also at a lower cost than Stock Drive Products/Sterling Instrument. Therefore all future purchases should be directed towards parts measured with English units.

We recommend waiting until a design appears to be nearly final before actually purchasing the parts needed. While waiting to purchase parts has its own difficulties, such as wait time for shipping, one of the challenges to identifying and buying parts was that they were chosen to meet the needs of one iteration, and then there would be significant changes in the next iteration that changed the initial logic and reasons behind selecting those parts. Many times this required retrofitting of already purchased parts to both the design and the actual prototype. This occurred with the worm for the elevator, where the design of iteration one did not require any machining, however iteration two brought

changes that required the integral shaft be turned down. Another example would be for the rotator, where in iteration one a 10:1 gear ratio existed with the worm and thus a motor was purchased that had 10 times less torque than was ultimately required. Iteration two, however, removed the worm gear with the 10:1 ratio; however the same motor was still incorporated into the design. Therefore, parts should be selected and incorporated into designs, but should not be purchased until a design appears to be in its final stages.

### **10.5.1 Elbow Joint**

A considerable improvement to the elbow joint would be to use larger miter gears. The size of the current miter gears was beneficial in that it reduced overall package size of the joint, however they proved to be difficult to both attach to the shaft of the worm and the play in the elbow coupler caused the teeth to jump once the torque placed on them reached a certain point.

The manufacturability of the worm proved to be very complicated, therefore one of the most important changes to the next elbow joint design would be to avoid using a worm with an integral shaft. A worm and separate shaft would reduce the manufacturing time and difficulty. Should any adjustments need to be made to attach the miter gear, they could be made to the shaft, which would have a relatively smaller diameter than the diameter of the shaft integral to the worm. This would decrease the amount of material removed, and subsequently reduce manufacturing cost. Ultimately, time and money would be saved by purchasing the worm and shaft separately.



### **10.5.2 Rotator Joint**

The only key improvement to the parts for the rotator joint would be to purchase a shaft made of a stronger material. Computer analysis of the shaft showed that it failed to meet the torque requirements, failing prior to reaching maximum torque. Therefore, a stronger, stainless steel material would need to be used.

### **10.6 Testing**

One very important aspect of robotics is accuracy. During background research it was found that many robotic joints were capable of accuracy within 0.01 degree. It was important to calculate and maximize the accuracy of the joints. Although a complete testing procedure was devised, the group unfortunately ran out of time for accuracy testing. However, in the future, proper accuracy tests are crucial for any robotic joint testing

Another key area of testing was product life. Although a complete testing procedure was devise, the group unfortunately ran out of time product life testing. However, in the future, proper product life test are crucial for any robotic joint testing.

## 11 Bibliography

1. **Carnegie Mellon University.** Carnegie Mellon University's Red Team Accepted To Compete in \$1 Million Desert Race for Robots. *DARPA*. [Online] Carnegie Mellon Media Relations, October 23, 2003. [Cited: April 29, 2009.] [http://www.cmu.edu/PR/releases03/031023\\_redteam.html](http://www.cmu.edu/PR/releases03/031023_redteam.html).
2. **iRobotics.** iRobot. *Our History - About iRobot*. [Online] [Cited: April 29, 2009.] <http://www.irobot.com/sp.cfm?pageid=203>.
3. **American Heritage Dictionary.** American Heritage Dictionary. [Online] Houghton Mifflin Company, 2000. <http://www.bartleby.com/61/>.
4. **VEX Robotics.** VEX Robotics. *about VEX Robotics*. [Online] 2009. <http://www.vexrobotics.com/>.
5. **Midmarket CIO Definitions.** Azimuth and Elevation. *Midmarket.com*. [Online] November 06, 2006. [Cited: October 13, 2008.] [http://searchcio-midmarket.techtarget.com/sDefinition/0,,sid183\\_gci838808,00.html](http://searchcio-midmarket.techtarget.com/sDefinition/0,,sid183_gci838808,00.html).
6. **Fox, Stuart.** Lock and Roll. *Popular Science*. October 2008, p. 41.
7. *Double Active Universal Joint (DAUJ)*. **Ryew, Sungmoo , and Hyoukryeol Choi.** 2001, IEEE Transactions on Robotics and Automation , pp. 290-300.
8. *Development of a robot finger for five-fingered hand using ultrasonic motors.* **Yamano, I., Takemura, K. and Maeno, T.** s.l. : IEEE, 2003. Intelligent Robots and Systems. pp. 2648-2653.
9. *Development of Modular Robotic Joint.* **Qing-xuan, Jia, Sun Han-xul, Song Jingzhou, and Cheng Tao.** 2006, 2006 IEEE International Conference on Industrial Informatics , pp. 827-32.
10. *Unidrive Modular Robot: Dynamics.* **Karbasi, Hamidreza, Amir Khajepour, and Jan Paul.** 2006, Journal of Dynamic Systems, Measurement, and Control , pp. 969-975.
11. **Choset, Howie.** Modular Snake Robots. *Biorobotics Laboratory*. [Online] 2008. [Cited: September 10, 2008.] <http://www.cs.cmu.edu/~biorobotics/projects/modsnake/>.
12. *Manipulability and redundancy control of robotic mechanisms.* **Yoshikawa, T.** 1985. Robotics and Automation. pp. 1004-1009.
13. **Amtec Robotics.** About Amtec Robots. *Amtec Robotics*. [Online] [Cited: October 10, 2008.] [http://www.amtec-robotics.com/ueber\\_amtec\\_robotics\\_en.html](http://www.amtec-robotics.com/ueber_amtec_robotics_en.html).
14. **Robotics Research Corporation.** Home. *Robotics Research Corpotation*. [Online] [Cited: October 10, 2008.] <http://www.robotics-research.com/>.
15. **Ulrich, N.** *D352050* United States of America, 1993.
16. *Robotic Joint Mechancism for Humanlike Motions.* **Ryew, Sungmoo , and Hyoukryeol Choi.** 2001, IEEE Transactions on Robotics and Automation, pp. 290-300.
17. *Trends in service robots for the disabled and the elderly.* **Kawamura, K and Iskarous, M.** s.l. : IEEE, 1994. Intelligent Robots and Systems . pp. 1647-1654.
18. *Workspace and Mobility of a Closed-Loop Manipulator.* **Bajpai, Atul.** 1985, The Internation Journal of Robotics Research, pp. 131-142.
19. *Accurate odometry and error modelling for a mobile robot.* **Chong, Kok Seng and Kleeman, L.** s.l. : IEEE, 1997. Robotics and Automation. pp. 2783-2788.
20. *Control of industrial robot with a fieldbus.* **Valera, A., et al.** s.l. : IEEE, 1999. Emerging Technologies and Factory Automation. pp. 1235-1241.
21. **Wikipedia contributors .** Network Topology. *Wikipedia*. [Online] [Cited: October 12, 2008.] [http://en.wikipedia.org/wiki/Network\\_topology](http://en.wikipedia.org/wiki/Network_topology).

22. **Freescale Semiconductor.** Robotic Arm. *Freescale Semiconductor*. [Online] [Cited: October 10, 2008.] <http://www.freescale.com/webapp/sps/site/application.jsp?nodeId=02nQXGcKzP>.

## Appendix A – Weighted Task Specifications

Task Specifications	Value	Weight	Ball Joint		Design 1		Design 2		Design 3		Design 4	
			score	points	score	points	score	points	score	points	score	points
<b>General</b>												
<b>Cost</b>	<\$1000	10		0		0		0		0		0
<b>Durability</b>	Cycle life TBD	7	1	7	4	28	2	14	2	14	3	21
<b>Maintenance</b>	Requires minimal technical knowledge to maintain	4	0	0	0	0	0	0	0	0	0	0
	No special tools required	0	0	0	0	0	0	0	0	0	0	0
	Minimal disassembly for regular maintenance	3	3	9	3	9	1	3	2	6	5	15
	Requires less than once per year	4	0	0	0	0	0	0	0	0	0	0
	See also Manufacturability				0		0		0		0	
<b>Materials</b>	Commercially available and stocked materials	8	2	16	4	32	1	8	1	8	3	24
<b>Manufacturable</b>	Preference will be given to standardized parts	7	2	14	4	28	1	7	1	7	3	21

	Minimize manufactured parts	5	0	0	0	0	0	0	0	0	0	0	0
	Utilizing inexpensive manufacturing techniques	5	0	0	0	0	0	0	0	0	0	0	0
<b>Modular</b>	At least attached to one other Daisy	10	3	30	5	50	5	50	5	50	5	50	50
	Attach to standard, industrial tools	0	0	0	0	0	0	0	0	0	0	0	0
<b>Ease of operation</b>	Hardware requires minimal technical knowledge to operate	7	0	0	0	0	0	0	0	0	0	0	0
	Software requires basic knowledge of programming languages	5	3	15	5	25	5	25	5	25	5	25	25
<b>Movement</b>	Azimuth joint must be able to rotate at least 360 deg	10	0	0	0	0	0	0	0	0	0	0	0
	Elbow and rotator must be less than 6 inches apart	0	0	0	0	0	0	0	0	0	0	0	0

	Precision must be within +/- 1 degree	6	0	0	0	0	0	0	0	0	0	0
	Angular velocity/acceleration should mimic human arm	6	0	0	0	0	0	0	0	0	0	0
	Joint sustains position without current draw	8	0	0	0	0	0	0	0	0	0	0
	DOF =2	10	0	0	0	0	0	0	0	0	0	0
	Infinite rotation	0	0	0	0	0	0	0	0	0	0	0
<b>Safety</b>	Under Normal Operating Conditions (NOC) user shall not sustain any injuries from using this device	10	0	0	0	0	0	0	0	0	0	0
	Under Normal Operating Conditions (NOC) robojoint shall not harm itself	10	0	0	0	0	0	0	0	0	0	0
<b>Power specifications</b>	Must run on a battery supply	10	0	0	0	0	0	0	0	0	0	0
	Torque: >2 ft-	9	0	0	0	0	0	0	0	0	0	0

	Ibs											
<b>Applications/Environment</b>	To Be Expanded		0	0	0	0	0	0	0	0	0	0
	Corrosion resistant and will adhere to industry standard		0	0	0	0	0	0	0	0	0	0
	Water resistant and will adhere to industry standard		0	0	0	0	0	0	0	0	0	0
	Water proof and will adhere to industry standard		0	0	0	0	0	0	0	0	0	0
<b>Dimensions</b>	Must be smaller than 12x6x6 inches		0	0	0	0	0	0	0	0	0	0
	Must weigh less than 25 pounds		0	0	0	0	0	0	0	0	0	0
<b>Total</b>				91		172		107		110		156

## Appendix B – Motor Selection Matrix

	Elevator	Rotator	
Required Torque	24000	18000	mNm
Required RPM	13	13	rpm
Gear Ratio	10	10	:1
Motor Torque	2400	1800	
Motor RPM	130	130	

Elevator	Motor Name	Motor Torque	Motor RPM	Required Gear Ratio (torque)	Required Gear Ratio (rpm)	With Torque Gear Ratio, RPM	Cost (USD)	Size (dia, mm)	Size (L, mm)	Search Tool:
1	Maxon, EC-max 40 Ø40 mm, brushless, 70 Watt (\$160 EUR)	85.1	8020	282.0211 516	616.9230 769	28.437583 33	(\$160 EUR)	32	58	<a href="http://productsearch.machinedesign.com/SpecSearch/Suppliers?QID=12283099&amp;Comp=17&amp;fc=1">http://productsearch.machinedesign.com/SpecSearch/Suppliers?QID=12283099&amp;Comp=17&amp;fc=1</a>
2	MicroMo, Permanent Magnet DC Motor -- GNM3125 , WITH GEARMOTOR: G2.6 , 4.8:36 ratio	480	4735	50	364.2307 692	94.7	?	58	96.5	<a href="http://www.micromo.com/uploadpk/GNM_31.pdf">http://www.micromo.com/uploadpk/GNM_31.pdf</a>
3	DOGA, Permanent Magnet DC Motor, Type	1500	240	16	18.46153 846	15	?	59.94	165.1	<a href="http://motion-controls.globalspec.com/SpecSearch/PartSpecs?VID=354591&amp;Comp">http://motion-controls.globalspec.com/SpecSearch/PartSpecs?VID=354591&amp;Comp</a>



	111 Series -- 111.9039.20.00 ; WITH GEARMOTOR: 12:1 ratio									=17&PartId={580babad-2058-42be-b308-126a1c15472b}&RegEvent=login
4	Anaheim Automation, BDPG-60-110-24V-3000-R168 Planetary Gearmotor	15980	15	1.501877 347	1.153846 154	9.9875	97.2	59.94	179.3	(with gearing) <a href="http://www.anaheimautomation.com/brush-dc-planetary-gear-motor.aspx">http://www.anaheimautomation.com/brush-dc-planetary-gear-motor.aspx</a>
5	ISL Productions Intl, DC Motor, RA-27 (04 & 05 Type), 77:1 ratio	28440	51	0.843881 857	3.923076 923	60.435	?	27.18	41.1	<a href="http://www.islproducts.com/prod/gear_motors.htm">http://www.islproducts.com/prod/gear_motors.htm</a>
6	MicroMo, PMDC Motor, 3257G-012CR, with planetary gearhead 38/1, 134:1 gear reduction	4500	5700	5.333333 333	438.4615 385	1068.75	?	32	57	<a href="http://www.micromo.com/uploadpk/3257_CR_MME.pdf">http://www.micromo.com/uploadpk/3257_CR_MME.pdf</a>
7	Merkle-Korff, PMDC, KF2500	5650	307	4.247787 611	23.61538 462	72.272916 67	?	39.6	4.567	<a href="http://www.merkle-korff.com/pdf/DC/kf2500.pdf">http://www.merkle-korff.com/pdf/DC/kf2500.pdf</a>
8	Beetle B231 Gearmotor 231:1 ratio (planetary)	2630	70	9.125475 285	5.384615 385	7.6708333 33	39.99	21.84	57.15	<a href="http://www.robotmarketplace.com/products/0-B231.html">http://www.robotmarketplace.com/products/0-B231.html</a>
9	ML-50 50:1 Geared Motor	2260	120	10.61946 903	9.230769 231	11.3	26.95	37	56	<a href="http://www.robotmarketplace.com/products/ML-50.html">http://www.robotmarketplace.com/products/ML-50.html</a>
<b>Rotator</b>	Motor Name	Motor	Motor	Required	Required	With				

		Torque	RPM	Gear Ratio (torque)	Gear Ratio (rpm)	Torque Gear Ratio, RPM				
1	MicroMo, Brushless DC-Servomotors, Series 1628 024B	2.6	65000	6923.076 923	5000	9.3888888 89	?	16	28	<a href="http://www.micromo.com/uploadpk/1628_B_MME.pdf">http://www.micromo.com/uploadpk/1628_B_MME.pdf</a>
2	MicroMo, Stepper Motor, 2 phase, AM2224-R3-ww-ee	26	15000	692.3076 923	1153.846 154	21.666666 67	?	22	37	<a href="http://www.micromo.com/uploadpk/AM_2224_R3.pdf">http://www.micromo.com/uploadpk/AM_2224_R3.pdf</a>
3	MicroMo, DC gearmotor, 012 SR IE2 (with 8:1 already built in gear ratio)	30	635	600	48.84615 385	1.0583333 33	?	26	19.1	<a href="http://www.micromo.com/uploadpk/2619_SR_MME.pdf">http://www.micromo.com/uploadpk/2619_SR_MME.pdf</a>
4	Maxon, EC-max 30 Ø30 mm, brushless, 40 Watt (\$120 EUR)	35	1500	514.2857 143	115.3846 154	2.9166666 67	?	30	42	<a href="http://shop.maxonmotor.com/maxon/assets_external/Katalog_neu/Downloads/Katalog_PDF/maxon_ec_motor/EC-max-programm/EC-max-30_272766_08_178_e.pdf">http://shop.maxonmotor.com/maxon/assets_external/Katalog_neu/Downloads/Katalog_PDF/maxon_ec_motor/EC-max-programm/EC-max-30_272766_08_178_e.pdf</a>
5	Maxon, A-max 32 Ø32 mm, Graphite Brushes, 15 Watt (\$120 EUR)	36	4670	500	359.2307 692	9.34	?	32	62.9	<a href="http://shop.maxonmotor.com/maxon/assets_external/Katalog_neu/Downloads/Katalog_PDF/maxon_dc_motor/A-max-programm/A-max-">http://shop.maxonmotor.com/maxon/assets_external/Katalog_neu/Downloads/Katalog_PDF/maxon_dc_motor/A-max-programm/A-max-</a>

										32_236643_08_123_e.pdf
6	Maxon, EC 22 Ø22 mm, brushless, 50 Watt (\$125.87)	37.2	22400	483.8709 677	1723.076 923	46.293333 33	?	22	62.5	<a href="http://shop.maxonmotor.com/ishop/article/article/201048.xml">http://shop.maxonmotor.com/ishop/article/article/201048.xml</a>
7	ISL Productions Intl, DC Motor, RA-27 (04 & 05 Type), 60:1 ratio	21570	65	0.834492 35	5	77.891666 67	?	27.1	35.9	<a href="http://www.islproducts.com/prod/gear_motors.htm">http://www.islproducts.com/prod/gear_motors.htm</a>
8	Merkle-Korff, PMDC, KF2500	5650	307	4.247787 611	23.61538 462	72.272916 67	?	39.6	116	<a href="http://www.merklekorff.com/pdf/DC/kf2500.pdf">http://www.merklekorff.com/pdf/DC/kf2500.pdf</a>
9	Beetle B231 Gearmotor 231:1 ratio (planetary)	2630	70	6.844106 464	5.384615 385	10.227777 78	39.99	21.84	57.15	<a href="http://www.robotmarketplace.com/products/0-B231.html">http://www.robotmarketplace.com/products/0-B231.html</a>
10	ML-50 50:1 Geared Motor	2260	120	7.964601 77	9.230769 231	15.066666 67	26.95	37	56	<a href="http://www.robotmarketplace.com/products/ML-50.html">http://www.robotmarketplace.com/products/ML-50.html</a>

## Appendix C – Calculations for Securing the Miter Gear

(Interference Fit, Set Screw, and Pin)

### Press Fit Calculations

$l_w := 0.007$	Length of contact btwn 2 surfaces
$r := 0.0015$	Nominal radius of the interference btwn parts
$\mu := 0.2$	Friction btwn 2 materials (cite)
$\Delta r := 0.0000156$	Diametral interference btwn parts
$E_o := 103 \cdot 10^9$	Modulus of elasticity for ISO 8/Brass
$E_i := 193 \cdot 10^9$	Modulus of elasticity for 18-8 steel
$r_o := 0.007$	Outside radius of hub
$\nu_o := 0.33$	Poisson's ratio, brass
$r_i := 0$	Inside radius (if shaft were hollow, but it's not so it = 0)
$\nu_i := 0.3$	Poisson's ratio, steel

$$T_w := \frac{\pi \cdot l_w \cdot \mu \cdot (2 \cdot \Delta r)}{\frac{1}{E_o} \left( \frac{r_o^2 + r^2}{r_o^2 - r^2} + \nu_o \right) + \frac{1}{E_i} \left( \frac{r^2 + r_i^2}{r^2 - r_i^2} - \nu_i \right)} \quad T = 11.78$$

### Setscrew Holding Power

According to Mark's Standard Handbook for Mechanical Engineers, 11th edition, the holding power of an M2 setscrew is approximately 0.179 Nm, significantly lower than the desired 2.4 or 2.2 Nm.

### Pin Calculations

$\tau := 2.75 \cdot 10^8$	Shear strength of a 1.5 mm dia pin, from Grainger (I think?)
$D := 0.0015$	Diameter
$r_p := \frac{D}{2}$	Radius
$A_w := \pi \cdot \frac{D^2}{4}$	Cross-sectional area of the pin
$T_p := \tau \cdot r_p \cdot A$	$T_p = 0.364$

## Appendix D – Full Testing Data

### *Rotator-Joint Test Results*

Test	Voltage	Load	Sound	Vibration	Deformation	Heat	15 cycle time (s)	average cycle time (s)	avg. 360deg time (s)	average current draw	peak current draw	Notes
<b>1</b>	3V	0g	slight creak from slip joint	none	slip joint wobbly	none	140	9.333333333	4.666666667	-	-	-
<b>2</b>	3V	250g	slight creak from slip joint	none	none- weight dampened wobble	none	150	10	5	-	-	-
<b>3</b>	3V	500g	increase in creak volume and duration, increase motor noise	some slipjoint vibration	none- weight dampened wobble	none	155	10.33333333	5.166666667	-	-	-
<b>4</b>	3V	750g	creak less, more grinding from slip joint	none	none	none	151	10.06666667	5.033333333	-	-	-
<b>5</b>	3V	1000g	creak less noticeable, more grinding of contacts	none	none	none	170	11.33333333	5.666666667	-	-	-

<b>6</b>	6V	0g	quiet, minimal grinding	none	none	none	70	4.666666667	2.333333333	100 mA	-	long pause between direction change - loose set screws
<b>7</b>	6V	250g	more creak and grinding	none	none	none	70	4.666666667	2.333333333	100 mA	-	long pause between direction change - loose set screws
<b>8</b>	6V	500g	more gear noise, more grinding	none	none	none	70	4.666666667	2.333333333	100 mA	-	long pause between direction change - loose set screws
<b>9</b>	6V	750g	grinding, gear noise	none	none	none	70	4.666666667	2.333333333	-	175mA	-
<b>10</b>	6V	1000g	significant grinding	vibration from slip-joint grinding	none	none	74	4.933333333	2.466666667	-	-	only 20 cycles, concerns of grinding
<b>11</b>	9V	0g	minimal	none	none	none	47	3.133333333	1.566666667	-	-	lot of play as direction changes- need to tighten

												set screws
<b>12</b>	9V	250g	rough slip joint	minimal	none	none	45	3	1.5	200 mA	-	-
<b>13</b>	9V	500g	rough slip joint	minimal, bit wobbly	none	none	45	3	1.5	-	-	-
<b>14</b>	9V	750g	rough slip joint	vibration from slip-joint grinding	none	none	48	3.2	1.6	-	-	-
<b>15</b>	9V	1000g	rough slip joint	minimal	none	none	46	3.066666667	1.533333333	-	-	-

### *Elbow-Joint Test Results*

Test	Voltage	Load	avg. 360deg time (s)	average current draw	Notes
<b>1</b>	3V	0g	4.67	-	-
<b>2</b>	3V	250g	5.00	-	-
<b>3</b>	3V	500g	5.17	-	-
<b>4</b>	3V	750g	5.03	-	-
<b>5</b>	3V	1000g	5.67	-	-
<b>6</b>	6V	0g	2.33	100 mA	long pause between direction change - loose set scrwes
<b>7</b>	6V	250g	2.33	100 mA	long pause between direction change - loose set scrwes
<b>8</b>	6V	500g	2.33	100 mA	long pause between direction change - loose set scrwes
<b>9</b>	6V	750g	2.33	175 mA	-
<b>10</b>	6V	1000g	2.47	-	only 20 cycles, concerns of grinding
<b>11</b>	9V	0g	1.57	-	lot of play as direction changes- need to tighten set screws
<b>12</b>	9V	250g	1.50	200 mA	-
<b>13</b>	9V	500g	1.50	-	-
<b>14</b>	9V	750g	1.60	-	-
<b>15</b>	9V	1000g	1.53	-	-



## Appendix E – Preliminary Information gathering:

### a. Measuring arm speed

- i. This was an experiment done to measure the average speed of human arm motion.
  1. Subjects were asked to start with their hand on a horizontal surface
  2. Using only their elbow joint they were to lift their hand to their face at a relaxed pace. Time records were kept to see how much time was needed to complete the maneuver. This was done five times.
  3. The angular velocities and accelerations were calculated and the averages became the base numbers that were to be used for analysis of the joints.

	Dist (Deg)	Time (s)	Ang Velo (Deg/s)	Ang Velo (Rad/s)	Ang Accel (Rad/s <sup>2</sup> )
#1	90	1.34	67.1642	1.1722	0.8748
#2	90	1.61	55.9006	0.9756	0.6060
#3	90	0.93	96.7742	1.6890	1.8162
#4	90	0.93	96.7742	1.6890	1.8162
#5	90	0.93	96.7742	1.6890	1.8162
		$\omega_{ave}$	1.4430	$\alpha_{ave}$	1.3859

# Appendix F – Vendor Spec Sheets (Electrical Systems Iteration 01) :

## MSP430F248

### MSP430x22x2, MSP430x22x4 MIXED SIGNAL MICROCONTROLLER

SLAS504B – JULY 2006 – REVISED JULY 2007

- Low Supply Voltage Range 1.8 V to 3.6 V
- Ultralow-Power Consumption
  - Active Mode: 270  $\mu$ A at 1 MHz, 2.2 V
  - Standby Mode: 0.7  $\mu$ A
  - Off Mode (RAM Retention): 0.1  $\mu$ A
- Ultrafast Wake-Up From Standby Mode in Less Than 1  $\mu$ s
- 16-Bit RISC Architecture, 62.5-ns Instruction Cycle Time
- Basic Clock Module Configurations:
  - Internal Frequencies up to 16 MHz With Four Calibrated Frequencies to  $\pm$ 1%
  - Internal Very-Low-Power Low-Frequency Oscillator
  - 32-kHz Crystal
  - High-Frequency Crystal up to 16 MHz
  - Resonator
  - External Digital Clock Source
  - External Resistor
- 16-Bit Timer\_A With Three Capture/Compare Registers
- 16-Bit Timer\_B With Three Capture/Compare Registers
- Universal Serial Communication Interface
  - Enhanced UART Supporting Auto-Baudrate Detection (LIN)
  - IrDA Encoder and Decoder
  - Synchronous SPI
  - I<sup>2</sup>C™
- 10-Bit, 200-kps A/D Converter With Internal Reference, Sample-and-Hold, Autoscan, and Data Transfer Controller
- Two Configurable Operational Amplifiers (MSP430x22x4 Only)
- Brownout Detector
- Serial Onboard Programming, No External Programming Voltage Needed Programmable Code Protection by Security Fuse
- Bootstrap Loader
- On Chip Emulation Module
- Family Members Include:
  - MSP430F2232: 8KB + 256B Flash Memory 512B RAM
  - MSP430F2252: 16KB + 256B Flash Memory 512B RAM
  - MSP430F2272: 32KB + 256B Flash Memory 1KB RAM
  - MSP430F2234: 8KB + 256B Flash Memory 512B RAM
  - MSP430F2254: 16KB + 256B Flash Memory 512B RAM
  - MSP430F2274: 32KB + 256B Flash Memory 1KB RAM
- Available in a 38-Pin Thin Shrink Small-Outline Package (TSSOP) and 40-Pin QFN Package
- For Complete Module Descriptions, Refer to the *MSP430x2xx Family User's Guide*

#### description

The Texas Instruments MSP430 family of ultralow-power microcontrollers consist of several devices featuring different sets of peripherals targeted for various applications. The architecture, combined with five low-power modes is optimized to achieve extended battery life in portable measurement applications. The device features a powerful 16-bit RISC CPU, 16-bit registers, and constant generators that contribute to maximum code efficiency. The digitally controlled oscillator (DCO) allows wake-up from low-power modes to active mode in less than 1  $\mu$ s.

The MSP430x22xx series is an ultralow-power mixed signal microcontroller with two built-in 16-bit timers, a universal serial communication interface, 10-bit A/D converter with integrated reference and data transfer controller (DTC), two general-purpose operational amplifiers in the MSP430x22x4 devices, and 32 I/O pins.

Typical applications include sensor systems that capture analog signals, convert them to digital values, and then process the data for display or for transmission to a host system. Stand-alone radio-frequency (RF) sensor front ends are another area of application.



Please be aware that an important notice concerning availability, standard warranty, and use in critical applications of Texas Instruments semiconductor products and disclaimers thereto appears at the end of this data sheet.

All trademarks are the property of their respective owners.

PRODUCTION DATA information is current as of publication date. Products conform to specifications per the terms of Texas Instruments standard warranty. Production processing does not necessarily include testing of all parameters.

 **TEXAS  
INSTRUMENTS**  
POST OFFICE BOX 655303 • DALLAS, TEXAS 75265

Copyright © 2007 Texas Instruments Incorporated

1

## MSP430x22x2, MSP430x22x4 MIXED SIGNAL MICROCONTROLLER

SLAS504B – JULY 2006 – REVISED JULY 2007

### MSP430x22x2 device pinout, DA package

TEST/SBWTK	1	38	P1.7/TA2/TDO/TDI
DVCC	2	37	P1.6/TA1/TDI
P2.5/Rosc	3	36	P1.5/TA0/TMS
DVSS	4	35	P1.4/SMCLK/TCK
XOUT/P2.7	5	34	P1.3/TA2
XIN/P2.6	6	33	P1.2/TA1
RST/NMI/SBWDIO	7	32	P1.1/TA0
P2.0/ACLK/A0	8	31	P1.0/TACLK/ADC10CLK
P2.1/TAINCLK/SMCLK/A1	9	30	P2.4/TA2/A4/VREF+/VeREF+
P2.2/TA0/A2	10	29	P2.3/TA1/A3/VREF-/VeREF-
P3.0/UCB0STE/UCA0CLK/A5	11	28	P3.7/A7
P3.1/UCB0SIMO/UCB0SDA	12	27	P3.6/A6
P3.2/UCB0SOMI/UCB0SCL	13	26	P3.5/UCA0RXD/UCA0SOMI
P3.3/UCB0CLK/UCA0STE	14	25	P3.4/UCA0TXD/UCA0SIMO
AVSS	15	24	P4.7/TBCLK
AVCC	16	23	P4.6/TBOUTH/A15
P4.0/TB0	17	22	P4.5/TB2/A14
P4.1/TB1	18	21	P4.4/TB1/A13
P4.2/TB2	19	20	P4.3/TB0/A12

### MSP430x22x4 device pinout, DA package

TEST/SBWTK	1	38	P1.7/TA2/TDO/TDI
DVCC	2	37	P1.6/TA1/TDI
P2.5/Rosc	3	36	P1.5/TA0/TMS
DVSS	4	35	P1.4/SMCLK/TCK
XOUT/P2.7	5	34	P1.3/TA2
XIN/P2.6	6	33	P1.2/TA1
RST/NMI/SBWDIO	7	32	P1.1/TA0
P2.0/ACLK/A0/OA0I0	8	31	P1.0/TACLK/ADC10CLK
P2.1/TAINCLK/SMCLK/A1/OA0I0	9	30	P2.4/TA2/A4/VREF+/VeREF+/OA1I0
P2.2/TA0/A2/OA0I1	10	29	P2.3/TA1/A3/VREF-/VeREF-/OA1I1/OA1I0
P3.0/UCB0STE/UCA0CLK/A5	11	28	P3.7/A7/OA1I2
P3.1/UCB0SIMO/UCB0SDA	12	27	P3.6/A6/OA0I2
P3.2/UCB0SOMI/UCB0SCL	13	26	P3.5/UCA0RXD/UCA0SOMI
P3.3/UCB0CLK/UCA0STE	14	25	P3.4/UCA0TXD/UCA0SIMO
AVSS	15	24	P4.7/TBCLK
AVCC	16	23	P4.6/TBOUTH/A15/OA1I3
P4.0/TB0	17	22	P4.5/TB2/A14/OA0I3
P4.1/TB1	18	21	P4.4/TB1/A13/OA1I0
P4.2/TB2	19	20	P4.3/TB0/A12/OA0I0



POST OFFICE BOX 655303 • DALLAS, TEXAS 75265

3

## TFDU4300

Vishay Semiconductors



## Infrared Transceiver Module (SIR, 115.2 kbit/s) for IrDA® Applications

### Description

The TFDU4300 is a low profile (2.5 mm) infrared transceiver module with independent logic reference voltage ( $V_{logic}$ ) for low voltage IO interfacing. It is compliant to the latest IrDA® physical layer standard for fast infrared data communication, supporting IrDA speeds up to 115.2 kbit/s (SIR) and carrier based remote control. The transceiver module consists of a PIN photodiode, an infrared emitter (IRED), and a low-power control IC to provide a total front-end solution in a single package.

This device covers an extended IrDA low power range of close to 1 m. With an external current control resistor the current can be adjusted for shorter ranges.

This Vishay SIR transceiver is built in a new smaller package using the experiences of the lead frame BabyFace technology.



The RXD output pulse width is independent of the optical input pulse width and stays always at a fixed pulse width thus making the device optimum for standard Endecs. TFDU4300 has a tri-state output and is floating in shut-down mode with a weak pull-up.

### Features

- Compliant to the latest IrDA physical layer specification (9.6 kbit/s to 115.2 kbit/s) and TV Remote Control, bi-directional operation included.
- Operates from 2.4 V to 5.5 V within specification over full temperature range from -30 °C to +85 °C
- Logic voltage 1.5 V to 5.5 V is independent of IRED driver and analog supply voltage
- Split power supply, transmitter and receiver can be operated from two power supplies with relaxed requirements saving costs, US Patent No. 6.157.476
- Extended IrDA Low Power range to about 70 cm
- Typical Remote Control range 12 m
- Low power consumption (< 0.12 mA supply current)



- Power shutdown mode (< 5  $\mu$ A shutdown current in full temperature range, up to 85 °C)
- Surface mount package, low profile (2.5 mm) - (L 8.5 mm  $\times$  H 2.5 mm  $\times$  W 2.9 mm)
- High efficiency emitter
- Low profile (universal) package capable of surface mount soldering to side and top view orientation
- Directly interfaces with various Super I/O and controller devices as e.g. TOIM4232
- Tri-state-receiver output, floating in shut down with a weak pull-up
- Compliant with IrDA background light specification
- EMI immunity in GSM bands > 300 V/m verified
- Lead (Pb)-free device
- Qualified for lead (Pb)-free and Sn/Pb processing (MSL4)
- Device in accordance with RoHS 2002/95/EC and WEEE 2002/96/EC

### Applications

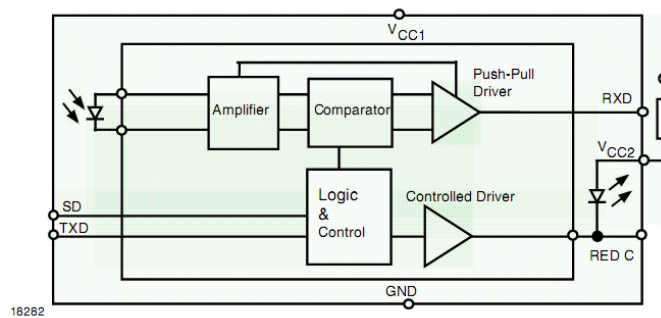
- Ideal for battery operated applications
- Telecommunication products (cellular phones, pagers)
- Digital still and video cameras
- Printers, fax machines, photocopiers, screen projectors
- Medical and industrial data collection
- Diagnostic systems
- Notebook computers, desktop PCs, Palmtop computers (Win CE, Palm PC), PDAs
- Internet TV boxes, video conferencing systems
- External infrared adapters (Dongles)
- Data loggers
- GPS
- Kiosks, POS, Point and Pay devices including IrFM - applications



**Parts Table**

Part	Description	Qty/Reel
TFDU4300-TR1	Oriented in carrier tape for side view surface mounting	750 pcs
TFDU4300-TR3	Oriented in carrier tape for side view surface mounting	2500 pcs
TFDU4300-TT1	Oriented in carrier tape for top view surface mounting	750 pcs
TFDU4300-TT3	Oriented in carrier tape for top view surface mounting	2500 pcs

**Functional Block Diagram**



**Pin Description**

Pin Number	Function	Description	I/O	Active
1	$V_{CC2}$ IRED Anode	Connect IRED anode directly to the power supply ( $V_{CC2}$ ). IRED current can be decreased by adding a resistor in series between the power supply and IRED anode. A separate unregulated power supply can be used at this pin.		
2	IRED Cathode	IRED Cathode, internally connected to the driver transistor		
3	TXD	This Schmitt-Trigger input is used to transmit serial data when SD is low. An on-chip protection circuit disables the LED driver if the TXD pin is asserted for longer than 300 $\mu$ s. The input threshold voltage adapts to and follows the logic voltage swing defined by the applied $V_{logic}$ voltage.	I	HIGH
4	RXD	Received Data Output, push-pull CMOS driver output capable of driving standard CMOS or TTL loads. During transmission the RXD output is inactive. No external pull-up or pull-down resistor is required. Floating with a weak pull-up of 500 k $\Omega$ (typ.) in shutdown mode. The voltage swing is defined by the applied $V_{logic}$ voltage	O	LOW
5	SD	Shutdown. The input threshold voltage adapts to and follows the logic voltage swing defined by the applied $V_{logic}$ voltage.	I	HIGH
6	$V_{CC1}$	Supply Voltage		
7	$V_{logic}$	$V_{logic}$ defines the logic voltage level of the I/O ports to adapt the logic voltage swing to the IR controller. The RXD output range is from 0 V to $V_{logic}$ , for optimum noise suppression the inputs- logic decision level is $0.5 \times V_{logic}$	I	
8	GND	Ground		

# Appendix G – Vendor Spec Sheets (Electrical Systems Iteration 02):

## PIC 16F876



# PIC16F87X

## 28/40-Pin 8-Bit CMOS FLASH Microcontrollers

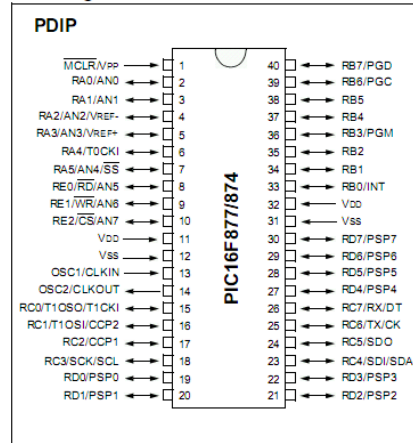
### Devices Included in this Data Sheet:

- PIC16F873
- PIC16F876
- PIC16F874
- PIC16F877

### Microcontroller Core Features:

- High performance RISC CPU
- Only 35 single word instructions to learn
- All single cycle instructions except for program branches which are two cycle
- Operating speed: DC - 20 MHz clock input  
DC - 200 ns instruction cycle
- Up to 8K x 14 words of FLASH Program Memory,  
Up to 368 x 8 bytes of Data Memory (RAM)  
Up to 256 x 8 bytes of EEPROM Data Memory
- Pinout compatible to the PIC16C73B/74B/76/77
- Interrupt capability (up to 14 sources)
- Eight level deep hardware stack
- Direct, indirect and relative addressing modes
- Power-on Reset (POR)
- Power-up Timer (PWRT) and  
Oscillator Start-up Timer (OST)
- Watchdog Timer (WDT) with its own on-chip RC  
oscillator for reliable operation
- Programmable code protection
- Power saving SLEEP mode
- Selectable oscillator options
- Low power, high speed CMOS FLASH/EEPROM  
technology
- Fully static design
- In-Circuit Serial Programming™ (ICSP) via two  
pins
- Single 5V In-Circuit Serial Programming capability
- In-Circuit Debugging via two pins
- Processor read/write access to program memory
- Wide operating voltage range: 2.0V to 5.5V
- High Sink/Source Current: 25 mA
- Commercial, Industrial and Extended temperature  
ranges
- Low-power consumption:
  - < 0.6 mA typical @ 3V, 4 MHz
  - 20 µA typical @ 3V, 32 kHz
  - < 1 µA typical standby current

### Pin Diagram

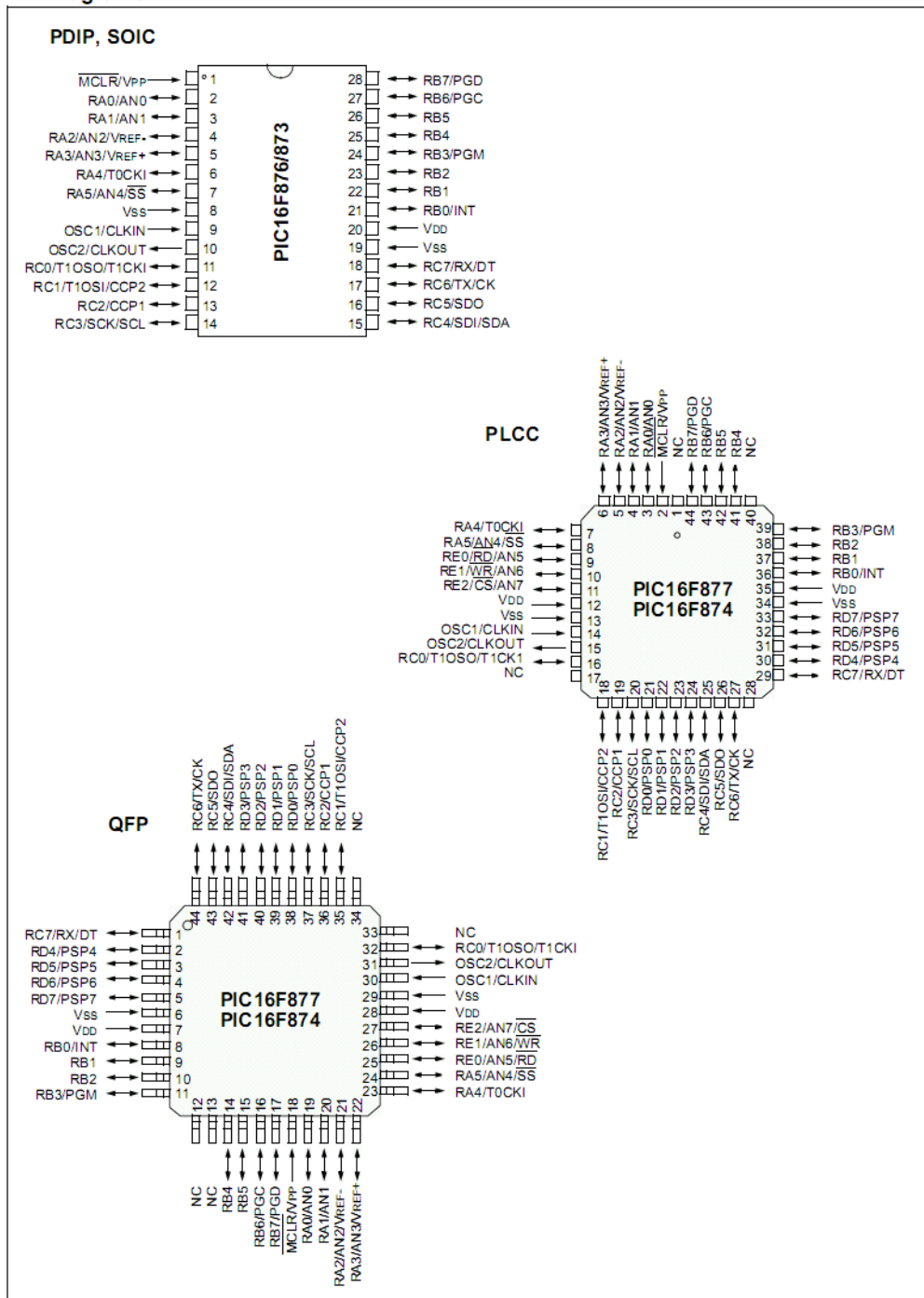


### Peripheral Features:

- Timer0: 8-bit timer/counter with 8-bit prescaler
- Timer1: 16-bit timer/counter with prescaler,  
can be incremented during SLEEP via external  
crystal/clock
- Timer2: 8-bit timer/counter with 8-bit period  
register, prescaler and postscaler
- Two Capture, Compare, PWM modules
  - Capture is 16-bit, max. resolution is 12.5 ns
  - Compare is 16-bit, max. resolution is 200 ns
  - PWM max. resolution is 10-bit
- 10-bit multi-channel Analog-to-Digital converter
- Synchronous Serial Port (SSP) with SPI™ (Master  
mode) and I<sup>2</sup>C™ (Master/Slave)
- Universal Synchronous Asynchronous Receiver  
Transmitter (USART/SCI) with 9-bit address  
detection
- Parallel Slave Port (PSP) 8-bits wide, with  
external RD, WR and CS controls (40/44-pin only)
- Brown-out detection circuitry for  
Brown-out Reset (BOR)

# PIC16F87X

## Pin Diagrams

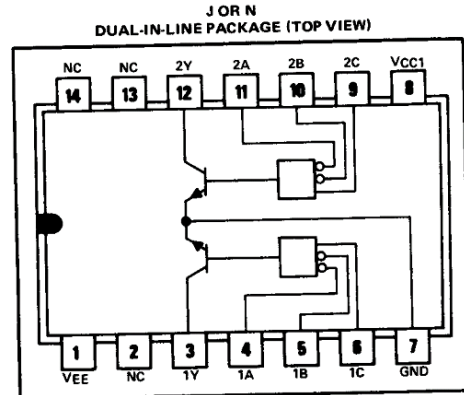


**INTERFACE  
CIRCUITS**

**TYPE SN75441  
DUAL ECL-COMPATIBLE PERIPHERAL DRIVER**

BULLETIN NO. DL-S 12479, DECEMBER 1976—REVISED AUGUST 1977

- Characterized For Use To 100 mA
- No Output Latch-Up at 20 V (After Conducting 100 mA)
- High-Speed Switching
- Positive OR Logic
- Versatile Interface Circuits for Use Between ECL and High-Current, High-Voltage Systems
- Inputs are Compatible with Series 10000 ECL and Other Similar ECL Families
- Standard Supply Voltages



NC—No internal connection

**description**

The SN75441 is a monolithic dual ECL-compatible peripheral driver and interface circuit. The device accepts standard input signals from ECL families and provides high-current and high-voltage output levels suitable for driving MOS and TTL circuits. Typical applications include high-speed logic buffers, line drivers, MOS drivers, and memory drivers.

The device has one in-phase and two out-of-phase ECL-compatible inputs per driver. By proper connections of the inputs, the SN75441 may be used three ways: positive-OR gate, differential ECL line receiver, or inverting gate. Some applications require one input per gate to be connected to an externally generated ECL reference voltage,  $V_{BB}$ .

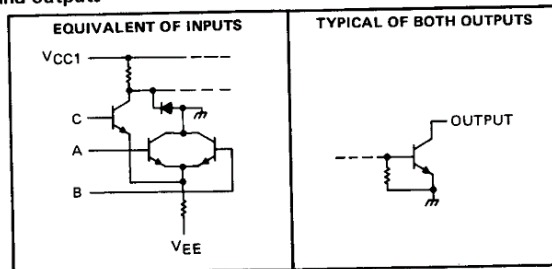
The SN75441 operates from two standard supplies, the TTL  $V_{CC}$  supply and the ECL  $V_{EE}$  supply, and is characterized for operation from 0°C to 70°C.

**FUNCTION TABLE**

	INPUTS			OUTPUT Y
	DIFFERENTIAL (More positive of A or B)—C		LOGIC LEVEL	
	A	B	C	
H ( $V_{ID} > 150$ mV)	H	L	L	H
	H	H	L	
? ( $-150$ mV $\leq V_{ID} \leq 150$ mV)	X	X	X	INDETERMINATE
L ( $V_{ID} < -150$ mV)	L	L	H	L

H = high level, L = low level, X = irrelevant  
See additional function tables in Figure 3.

**schematics of inputs and outputs**





# USDigital EP4 Optical Encoder



# E4P

OEM Miniature Optical Kit Encoder  
Page 1 of 8



## Description

The E4P miniature encoder is designed to provide digital quadrature encoder feedback for high volume applications with limited space constraints. The E4P version utilizes an innovative push-on codewheel which accepts shaft diameters of 1.5mm to .250".

The E4P encoder is the leader for high quantity OEM applications, but the E4 is the ideal choice when a set-screw codewheel encoder is required (see the E4 page).

The E4P miniature encoder base provides mounting holes for two #3-48, length 1/4" or two M2.5x.45mm, length 6mm screws on a .586" bolt circle. When mounting holes are not available, a pre-applied transfer adhesive (with peel-off backing) is available for "stick-on" mounting.

The encoder cover is easily snapped onto the base and is embossed with the connector pin-out.

The E4P series encoder can be connected by using a (high retention 4-conductor snap-in polarized 1.25mm pitch) connector. Mating cables and connectors (see the Cables / Connectors web page) are not included and are available separately.



## Features

- ▶ Miniature size
- ▶ Push-on hub - spring loaded collet design
- ▶ Minimum shaft length of .375"
- ▶ Fits shaft diameters of .059" to .250"
- ▶ Accepts +/- .020" Axial shaft play
- ▶ Off-axis mounting tolerance of .010"
- ▶ 100 to 360 cycles per revolution (CPR)
- ▶ 400 to 1440 pulses per revolution (PPR)
- ▶ Single +5V supply

## Related Products & Accessories

- ▶ CA-FC5-SH-MIC4 5-Pin Latching / 4-Pin Micro Shielded Cable (Base price \$15.18)
- ▶ CA-MD6-SS-MIC4 6-Pin Modular / 4-Pin Micro Silver Satin Cable (Base price \$11.53)
- ▶ CA-MIC4-SH-NC 4-Pin Micro / Unterminated Shielded Cable (Base price \$7.30)
- ▶ CA-MIC4-W4-NC 4-Pin Micro / Unterminated 4-Wire Discrete Cable (Base price \$6.80)
- ▶ CON-MIC4 4-Pin Micro Connector (Base price \$3.15)
- ▶ MCTOOL Centering Tool for E4, E4P, and E8P (Base price \$5.25)
- ▶ SPACER Spacer Tool (Base price \$0.95)

## Mechanical Drawing



1400 NE 136th Avenue  
Vancouver, Washington 98684, USA

info@usdigital.com  
www.usdigital.com

Local: 360.260.2468  
Toll-free: 800.736.0194

# Appendix H – Vendor Spec Sheets (Electrical Systems Final) :

18F2455



## PIC18F2455/2550/4455/4550

### 28/40/44-Pin High-Performance, Enhanced Flash USB Microcontrollers with nanoWatt Technology

#### Universal Serial Bus Features:

- USB V2.0 Compliant
- Low Speed (1.5 Mb/s) and Full Speed (12 Mb/s)
- Supports Control, Interrupt, Isochronous and Bulk Transfers
- Supports up to 32 endpoints (16 bidirectional)
- 1-Kbyte dual access RAM for USB
- On-chip USB transceiver with on-chip voltage regulator
- Interface for off-chip USB transceiver
- Streaming Parallel Port (SPP) for USB streaming transfers (40/44-pin devices only)

#### Power-Managed Modes:

- Run: CPU on, peripherals on
- Idle: CPU off, peripherals on
- Sleep: CPU off, peripherals off
- Idle mode currents down to 5.8  $\mu$ A typical
- Sleep mode currents down to 0.1  $\mu$ A typical
- Timer1 oscillator: 1.1  $\mu$ A typical, 32 kHz, 2V
- Watchdog Timer: 2.1  $\mu$ A typical
- Two-Speed Oscillator Start-up

#### Flexible Oscillator Structure:

- Four Crystal modes including High Precision PLL for USB
- Two External Clock modes, up to 48 MHz
- Internal oscillator block:
  - 8 user-selectable frequencies, from 31 kHz to 8 MHz
  - User-tunable to compensate for frequency drift
- Secondary oscillator using Timer1 @ 32 kHz
- Dual oscillator options allow microcontroller and USB module to run at different clock speeds
- Fail-Safe Clock Monitor
  - Allows for safe shutdown if any clock stops

#### Peripheral Highlights:

- High-current sink/source 25 mA/25 mA
- Three external interrupts
- Four Timer modules (Timer0 to Timer3)
- Up to 2 Capture/Compare/PWM (CCP) modules:
  - Capture is 16-bit, max. resolution 6.25 ns (Tcy/16)
  - Compare is 16-bit, max. resolution 100 ns (Tcy)
  - PWM output: PWM resolution is 1 to 10-bit
- Enhanced Capture/Compare/PWM (ECCP) module:
  - Multiple output modes
  - Selectable polarity
  - Programmable dead time
  - Auto-Shutdown and Auto-Restart
- Enhanced USART module:
  - LIN bus support
- Master Synchronous Serial Port (MSSP) module supporting 3-wire SPI™ (all 4 modes) and I<sup>2</sup>C™ Master and Slave modes
- 10-bit, up to 13-channels Analog-to-Digital Converter module (A/D) with programmable acquisition time
- Dual analog comparators with input multiplexing

#### Special Microcontroller Features:

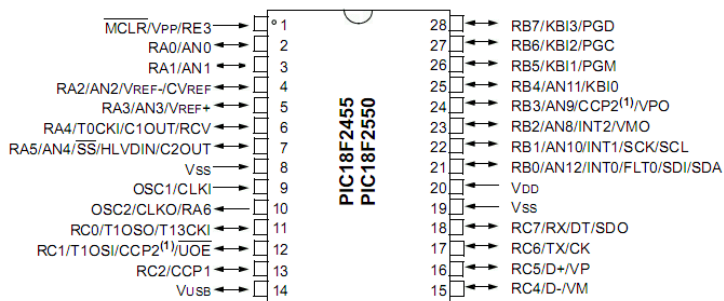
- C compiler optimized architecture with optional extended instruction set
- 100,000 erase/write cycle Enhanced Flash program memory typical
- 1,000,000 erase/write cycle Data EEPROM memory typical
- Flash/Data EEPROM Retention: > 40 years
- Self-programmable under software control
- Priority levels for interrupts
- 8 x 8 Single-Cycle Hardware Multiplier
- Extended Watchdog Timer (WDT):
  - Programmable period from 41 ms to 131s
- Programmable Code Protection
- Single-Supply 5V In-Circuit Serial Programming™ (ICSP™) via two pins
- In-Circuit Debug (ICD) via two pins
- Optional dedicated ICD/ICSP port (44-pin devices only)
- Wide operating voltage range (2.0V to 5.5V)

Device	Program Memory		Data Memory		I/O	10-bit A/D (ch)	CCP/ECCP (PWM)	SPP	MSSP		EAUSART	Comparators	Timers 8/16-bit
	Flash (bytes)	# Single-Word Instructions	SRAM (bytes)	EEPROM (bytes)					SPI™	Master I <sup>2</sup> C™			
PIC18F2455	24K	12288	2048	256	24	10	2/0	No	Y	Y	1	2	1/3
PIC18F2550	32K	16384	2048	256	24	10	2/0	No	Y	Y	1	2	1/3
PIC18F4455	24K	12288	2048	256	35	13	1/1	Yes	Y	Y	1	2	1/3
PIC18F4550	32K	16384	2048	256	35	13	1/1	Yes	Y	Y	1	2	1/3

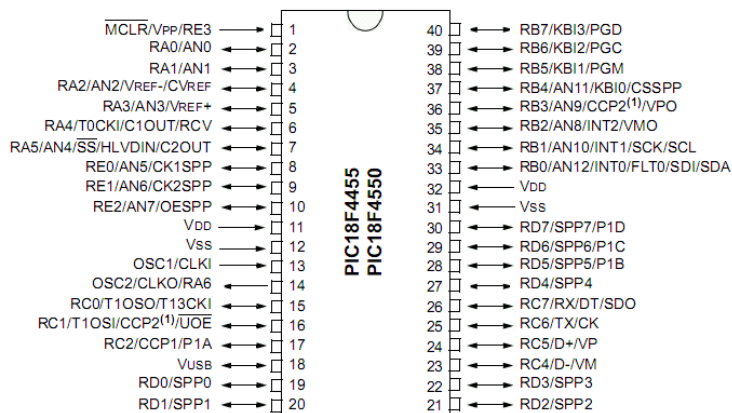
# PIC18F2455/2550/4455/4550

## Pin Diagrams

### 28-Pin PDIP, SOIC



### 40-Pin PDIP



Note 1: RB3 is the alternate pin for CCP2 multiplexing.



## dsPIC33FJ32MC302/304, dsPIC33FJ64MCX02/X04, AND dsPIC33FJ128MCX02/X04

### High-Performance, 16-bit Digital Signal Controllers

#### Operating Range:

- Up to 40 MIPS operation (at 3.0-3.6V):
  - Industrial temperature range (-40°C to +85°C)
  - Extended temperature range (-40°C to +125°C)

#### High-Performance DSC CPU:

- Modified Harvard architecture
- C compiler optimized instruction set
- 16-bit wide data path
- 24-bit wide instructions
- Linear program memory addressing up to 4M instruction words
- Linear data memory addressing up to 64 Kbytes
- 83 base instructions: mostly 1 word/1 cycle
- Two 40-bit accumulators with rounding and saturation options
- Flexible and powerful addressing modes:
  - Indirect
  - Modulo
  - Bit-Reversed
- Software stack
- 16 x 16 fractional/integer multiply operations
- 32/16 and 16/16 divide operations
- Single-cycle multiply and accumulate:
  - Accumulator write back for DSP operations
  - Dual data fetch
- Up to  $\pm 16$ -bit shifts for up to 40-bit data

#### Direct Memory Access (DMA):

- 8-channel hardware DMA
- Up to 2 Kbytes dual ported DMA buffer area (DMA RAM) to store data transferred via DMA:
  - Allows data transfer between RAM and a peripheral while CPU is executing code (no cycle stealing)
- Most peripherals support DMA

#### Timers/Capture/Compare/PWM:

- Timer/Counters, up to five 16-bit timers:
  - Can pair up to make two 32-bit timers
  - One timer runs as a Real-Time Clock with an external 32.768 kHz oscillator
  - Programmable prescaler
- Input Capture (up to four channels):
  - Capture on up, down or both edges
  - 16-bit capture input functions
  - 4-deep FIFO on each capture
- Output Compare (up to four channels):
  - Single or Dual 16-bit Compare mode
  - 16-bit Glitchless PWM mode
- Hardware Real-Time Clock/Calendar (RTCC):
  - Provides clock, calendar, and alarm functions

#### Interrupt Controller:

- 5-cycle latency
- 118 interrupt vectors
- Up to 53 available interrupt sources
- Up to three external interrupts
- Seven programmable priority levels
- Five processor exceptions

#### Digital I/O:

- Peripheral pin Select functionality
- Up to 35 programmable digital I/O pins
- Wake-up/Interrupt-on-Change for up to 21 pins
- Output pins can drive from 3.0V to 3.6V
- Up to 5V output with open drain configuration
- All digital input pins are 5V tolerant
- 4 mA sink on all I/O pins

#### On-Chip Flash and SRAM:

- Flash program memory (up to 128 Kbytes)
- Data SRAM (up to 16 Kbytes)
- Boot, Secure, and General Security for program Flash

---

**dsPIC33FJ32MC302/304, dsPIC33FJ64MCX02/X04, AND dsPIC33FJ128MCX02/X04**

---

**System Management:**

- Flexible clock options:
  - External, crystal, resonator, internal RC
  - Fully integrated Phase-Locked Loop (PLL)
  - Extremely low jitter PLL
- Power-up Timer
- Oscillator Start-up Timer/Stabilizer
- Watchdog Timer with its own RC oscillator
- Fail-Safe Clock Monitor
- Reset by multiple sources

**Power Management:**

- On-chip 2.5V voltage regulator
- Switch between clock sources in real time
- Idle, Sleep, and Doze modes with fast wake-up

**Analog-to-Digital Converters (ADCs):**

- 10-bit, 1.1 Msps or 12-bit, 500 Ksps conversion:
  - Two and four simultaneous samples (10-bit ADC)
  - Up to nine input channels with auto-scanning
  - Conversion start can be manual or synchronized with one of four trigger sources
  - Conversion possible in Sleep mode
  - $\pm 2$  LSB max integral nonlinearity
  - $\pm 1$  LSB max differential nonlinearity

**Audio Digital-to-Analog Converter (DAC):**

- 16-bit Dual Channel DAC module
- 100 Ksps maximum sampling rate
- Second-Order Digital Delta-Sigma Modulator

**Comparator Module:**

- Two analog comparators with programmable input/output configuration

**CMOS Flash Technology:**

- Low-power, high-speed Flash technology
- Fully static design
- 3.3V ( $\pm 10\%$ ) operating voltage
- Industrial and Extended temperature
- Low power consumption

**Motor Control Peripherals:**

- 6-channel 16-bit Motor Control PWM:
  - Three duty cycle generators
  - Independent or Complementary mode
  - Programmable dead time and output polarity
  - Edge-aligned or center-aligned
  - Manual output override control
  - One Fault input
  - Trigger for ADC conversions
  - PWM frequency for 16-bit resolution (@ 40 MIPS) = 1220 Hz for Edge-Aligned mode, 610 Hz for Center-Aligned mode
  - PWM frequency for 11-bit resolution (@ 40 MIPS) = 39.1 kHz for Edge-Aligned mode, 19.55 kHz for Center-Aligned mode
- 2-channel 16-bit Motor Control PWM:
  - One duty cycle generator
  - Independent or Complementary mode
  - Programmable dead time and output polarity
  - Edge-aligned or center-aligned
  - Manual output override control
  - One Fault input
  - Trigger for ADC conversions
  - PWM frequency for 16-bit resolution (@ 40 MIPS) = 1220 Hz for Edge-Aligned mode, 610 Hz for Center-Aligned mode
  - PWM frequency for 11-bit resolution (@ 40 MIPS) = 39.1 kHz for Edge-Aligned mode, 19.55 kHz for Center-Aligned mode
- 2-Quadrature Encoder Interface module:
  - Phase A, Phase B, and index pulse input
  - 16-bit up/down position counter
  - Count direction status
  - Position Measurement (x2 and x4) mode
  - Programmable digital noise filters on inputs
  - Alternate 16-bit Timer/Counter mode
  - Interrupt on position counter rollover/underflow

## dsPIC33FJ32MC302/304, dsPIC33FJ64MCX02/X04, AND dsPIC33FJ128MCX02/X04

---

### Communication Modules:

- 4-wire SPI (up to two modules):
  - Framing supports I/O interface to simple codecs
  - Supports 8-bit and 16-bit data
  - Supports all serial clock formats and sampling modes
- I<sup>2</sup>C™:
  - Full Multi-Master Slave mode support
  - 7-bit and 10-bit addressing
  - Bus collision detection and arbitration
  - Integrated signal conditioning
  - Slave address masking
- UART (up to two modules):
  - Interrupt on address bit detect
  - Interrupt on UART error
  - Wake-up on Start bit from Sleep mode
  - 4-character TX and RX FIFO buffers
  - LIN bus support
  - IrDA® encoding and decoding in hardware
  - High-Speed Baud mode
  - Hardware Flow Control with CTS and RTS
- Enhanced CAN (ECAN™ module) 2.0B active:
  - Up to eight transmit and up to 32 receive buffers
  - 16 receive filters and three masks
  - Loopback, Listen Only and Listen All
  - Messages modes for diagnostics and bus monitoring
  - Wake-up on CAN message
  - Automatic processing of Remote Transmission Requests
  - FIFO mode using DMA
  - DeviceNet™ addressing support
- Parallel Master Slave Port (PMP/EPSP):
  - Supports 8-bit or 16-bit data
  - Supports 16 address lines
- Programmable Cyclic Redundancy Check (CRC):
  - Programmable bit length for the CRC generator polynomial (up to 16-bit length)
  - 8-deep, 16-bit or 16-deep, 8-bit FIFO for data input

### Packaging:

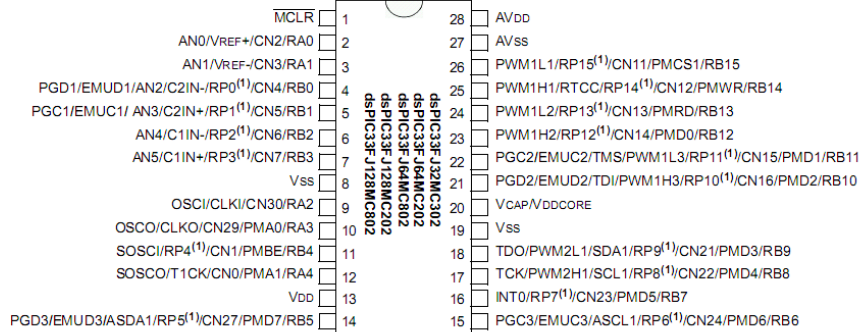
- 28-pin SDIP/SOIC/QFN-S
- 44-pin TQFP/QFN

<b>Note:</b> See the device variant table for exact peripheral features per device.
---

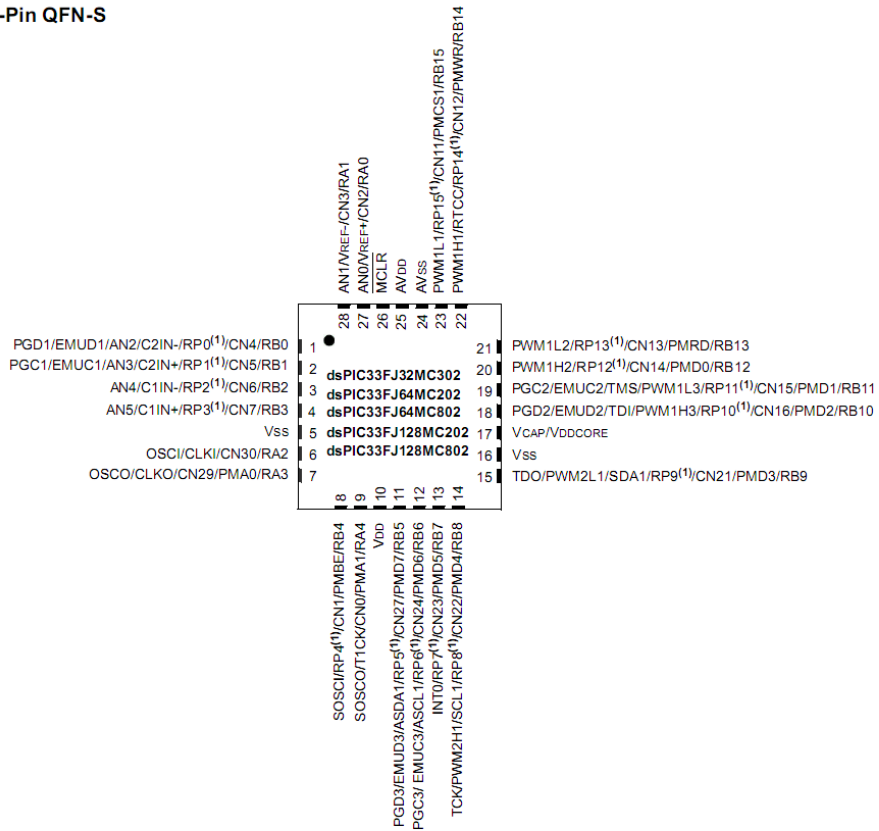
dsPIC33FJ32MC302/304, dsPIC33FJ64MCX02/X04, AND dsPIC33FJ128MCX02/X04

Pin Diagrams

28-Pin SDIP, SOIC



28-Pin QFN-S



Note 1: The RPx pins can be used by any remappable peripheral. See the table "dsPIC33FJ32MC302/304, dsPIC33FJ64MCX02/X04, and dsPIC33FJ128MCX02/X04 Controller Families" in this section for the list of available peripherals.

# L298 HBridge



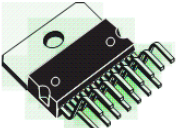
## L298

### DUAL FULL-BRIDGE DRIVER

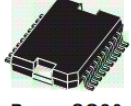
- OPERATING SUPPLY VOLTAGE UP TO 46 V
- TOTAL DC CURRENT UP TO 4 A
- LOW SATURATION VOLTAGE
- OVERTEMPERATURE PROTECTION
- LOGICAL "0" INPUT VOLTAGE UP TO 1.5 V (HIGH NOISE IMMUNITY)

#### DESCRIPTION

The L298 is an integrated monolithic circuit in a 15-lead Multiwatt and PowerSO20 packages. It is a high voltage, high current dual full-bridge driver designed to accept standard TTL logic levels and drive inductive loads such as relays, solenoids, DC and stepping motors. Two enable inputs are provided to enable or disable the device independently of the input signals. The emitters of the lower transistors of each bridge are connected together and the corresponding external terminal can be used for the con-



Multiwatt15

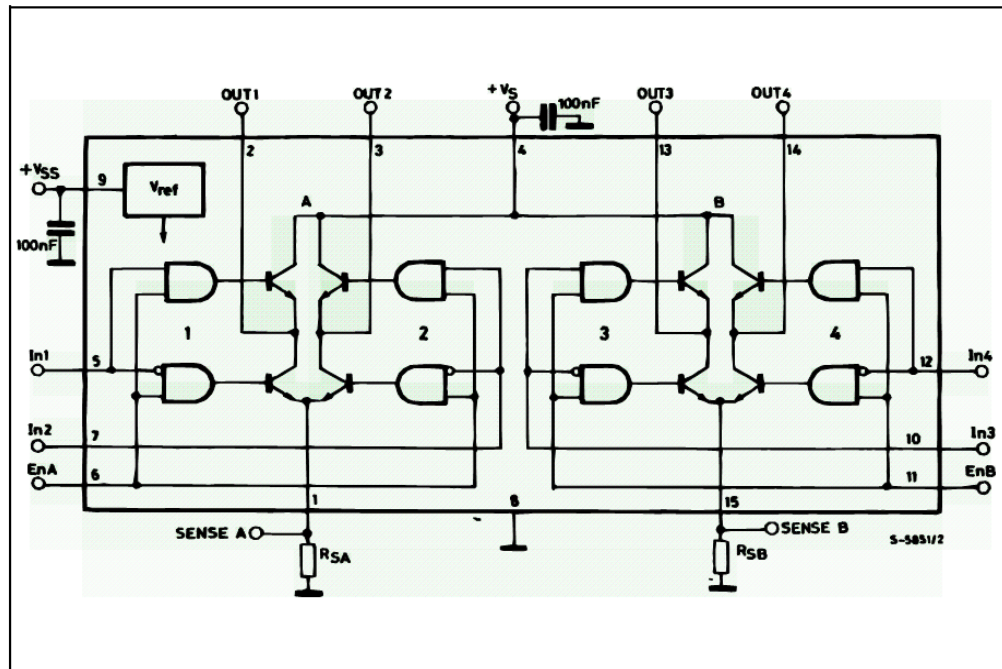


PowerSO20

**ORDERING NUMBERS :** L298N (Multiwatt Vert.)  
 L298HN (Multiwatt Horiz.)  
 L298P (PowerSO20)

nection of an external sensing resistor. An additional supply input is provided so that the logic works at a lower voltage.

#### BLOCK DIAGRAM



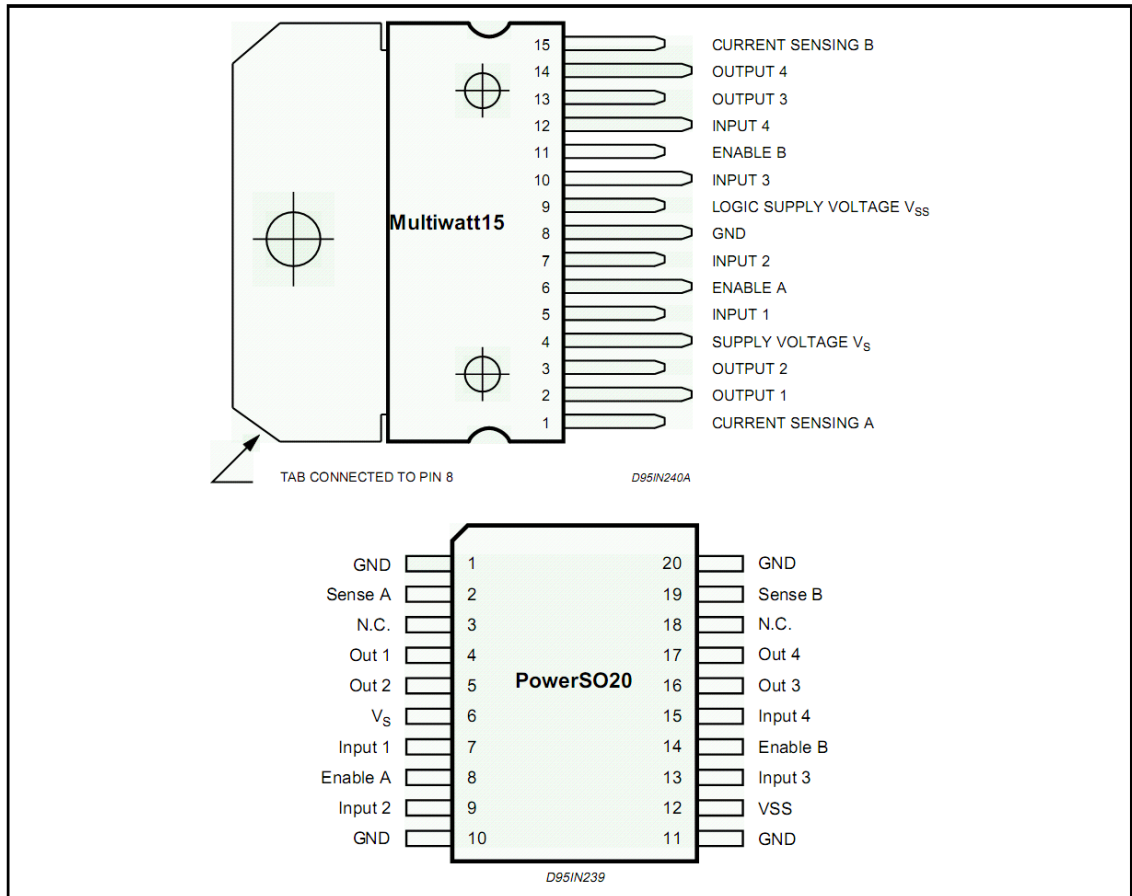


## L298

### ABSOLUTE MAXIMUM RATINGS

Symbol	Parameter	Value	Unit
$V_S$	Power Supply	50	V
$V_{SS}$	Logic Supply Voltage	7	V
$V_i, V_{en}$	Input and Enable Voltage	-0.3 to 7	V
$I_O$	Peak Output Current (each Channel)		
	- Non Repetitive ( $t = 100\mu s$ )	3	A
	- Repetitive (80% on -20% off; $t_{on} = 10ms$ )	2.5	A
	-DC Operation	2	A
$V_{sens}$	Sensing Voltage	-1 to 2.3	V
$P_{tot}$	Total Power Dissipation ( $T_{case} = 75^\circ C$ )	25	W
$T_{op}$	Junction Operating Temperature	-25 to 130	$^\circ C$
$T_{sig}, T_j$	Storage and Junction Temperature	-40 to 150	$^\circ C$

### PIN CONNECTIONS (top view)



### THERMAL DATA

Symbol	Parameter	PowerSO20	Multiwatt15	Unit
$R_{th j-case}$	Thermal Resistance Junction-case	Max.	3	$^\circ C/W$
$R_{th j-amb}$	Thermal Resistance Junction-ambient	Max.	13 (*)	$^\circ C/W$

(\*) Mounted on aluminum substrate

# MAXIM

## 350mA, 16.5V Input, Low-Dropout Linear Regulators

MAX1658/MAX1659

### General Description

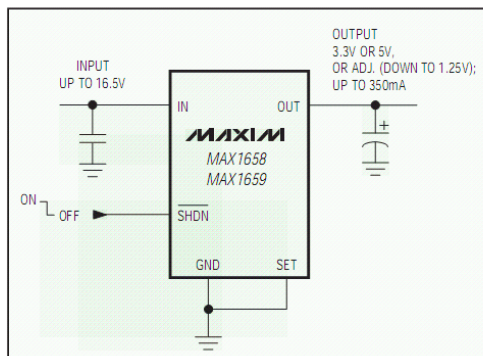
The MAX1658/MAX1659 linear regulators maximize battery life by combining ultra-low supply currents and low dropout voltages. They feature Dual Mode™ operation, which presets the output to 3.3V (MAX1658) or 5V (MAX1659), or permits it to be adjusted between 1.25V and 16V. The regulator supplies up to 350mA, with a typical dropout of 650mV for the MAX1658 and 490mV for the MAX1659. With their P-channel MOSFET pass transistor, these devices maintain a low quiescent current from zero output current to the full 350mA, even in dropout. They support input voltages ranging from 2.7V to 16.5V.

The MAX1658/MAX1659 feature a 1µA shutdown mode, reverse battery protection, short-circuit protection, and thermal shutdown. They are available in a special high-power (1.2W), 8-pin SO package designed specifically for compact applications.

### Applications

- Digital Cordless Phones
- PCS Phones
- Cellular Phones
- PCMCIA Cards
- Modems
- Hand-Held Instruments
- Palmtop Computers
- Electronic Planners

### Typical Operating Circuit



Dual Mode is a trademark of Maxim Integrated Products.

### Features

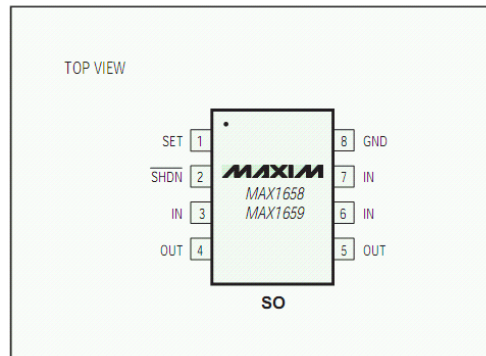
- ♦ Wide Input Voltage Range: 2.7V to 16.5V
- ♦ Low, 490mV Dropout at 350mA Output Current (MAX1659)
- ♦ 30µA Supply Current
- ♦ 1µA Max Shutdown Current
- ♦ High-Power (1.2W) 8-Pin SO Package
- ♦ Dual Mode Operation Output:
  - Fixed 3.3V (MAX1658)
  - Fixed 5.0V (MAX1659)
  - or Adjustable (1.25V to 16V)
- ♦ Thermal Overload Protection
- ♦ Current-Limit Protection
- ♦ Reverse Battery Protection

### Ordering Information

PART	TEMP. RANGE	PIN-PACKAGE
MAX1658C/D	0°C to +70°C	Dice*
MAX1658ESA	-40°C to +85°C	8 SO
MAX1659C/D	0°C to +70°C	Dice*
MAX1659ESA	-40°C to +85°C	8 SO

\*Dice are tested at  $T_A = +25^\circ\text{C}$ . DC parameters only.

### Pin Configuration



Maxim Integrated Products 1

For free samples & the latest literature: <http://www.maxim-ic.com>, or phone 1-800-998-8800.  
For small orders, phone 408-737-7600 ext. 3468.

## Appendix I – Code Listings :

### Iteration 02 – PIC16F876

```
//Compiler Generated Configuration Bits
__CONFIG(XT & WDTDIS & PWRTRDIS & BOREN & LVPEN & WRTEN &
DEBUGDIS & DUNPROT & UNPROTECT);
```

```
#include <stdio.h>
#include "usart.h"
```

```
//PORT definitions
#define LMT RB0 //Limit switch
#define ENCA RB4 //Encoder
#define ENCB RB5
#define DIR RC3 //H-Bridge Direction pin
```

```
//Crystal freq set to 8MHz for timing macros, UART baud generator
#define _XTAL_FREQ 8000000
```

```
//Variable Definitions, volatile variables accessible by interrupts, all used to do encoder
counts
```

```
volatile bit SENCA; //Encoder timing
volatile bit SENCB;
```

```
volatile unsigned int PENCA;
volatile unsigned int PENCB;
volatile unsigned int i;
```

```
//Additional Variable Definitions
unsigned int direction;
unsigned int time;
unsigned int speed;
unsigned int motorpwm;
unsigned int actspeed;
unsigned char input;
```

```
void startup(void){
    //TMR0 Interrupt enabled
    INTCON    = 0b00100000;

    //TMR0 enabled, WDT disabled
    OPTION   = 0b10001000;
```

```

    PIE1 = 0b00000000;
    TRISA= 0b00101111;
    TRISB= 0b11111011;
    TRISC= 0b00000000;

    //PWM Module Enabled, period set to 0xFF
    CCP1CON = 0b00001100;
    PR2 = 0b11111111;

    //TMR 2 enabled, prescaler 1:4, postscale 1:7
    T2CON = 0b00110101;

    //UART enabled, Asynch, 8bit, low-speed baud generator
    TXSTA = 0b00100000;
    RCSTA = 0b10010000;

    //Set Baud Rate to 9600bps
    SPBRG = 0b00011001;
}

void main(void){
    direction=0;
    time=0;
    speed=0;
    motorpwm=0;
    actspeed=0;

    init();

    init_comms(); // set up the USART, using uart.h include file
    PENCA=0; //reset encoder counters
    SENCA=0;
    // Output a message to prompt the user for a keypress
    // printf("\rPress a key and I will echo it back:\n");
    while(1){
        printf("\n");
        // Output a message to prompt the user for a keypress
        printf("\rChoose a Direction (1= Forward, 0 = Backwards):\n");
        while(1){
            direction = getch(); // read a response from the user
            printf("\r%c",direction);
            if(direction!=0x00)
                break;
        }
    }
}

```

```

    }
    printf("\n\rHow Long to Run?:\n");
    while(1){
        time = getch();// read a response from the user
        printf("\r%c",time);
        if(time!=0x00)
            break;
    }
    printf("\n\rEnter Speed (0-9) 0 is fastest\n");
    while(1){
        speed = getch();    // read a response from the user
        printf("\r%c",speed);
        if(speed!=0x00)
            break;
    }

    //motor speed will be speed x 10 +128 if backwards

    motorpwm = ((speed -48)* 255)/10;

    printf("\nPWM Rate:%d",motorpwm);
    printf("\ndirection:%d",direction);
//    CCPR1L=0;
//    CCPR2L=0;
    if(LMT){
        if(direction==48){
            CCPR1L = motorpwm;
            DIR=0;
        }

        else{
            CCPR1L = 255- motorpwm;
            DIR=1;
        }
    }
//CCPR2L = motorpwm;
//CCPR1L = motorpwm;
//T2CON    = 0b00000100;
//printf("\nPWMp:%d",motorpwm);
    time = (time-48)*1000;

    for(i=0;i<time;i++){
        __delay_ms(1);
    }

```

```

        DIR=1;
        CCPR1L = 0b11111111;

        printf("\nMotor Ran for %d seconds",(time/1000));
//      if(IENCA)
//          PENCA++;
        printf("\rFINAL POS[%u]",PENCA);

    }
}

void interrupt int(void){

    //TMR0 Interrupt
    if((TOIE)&&(TOIF)){
        RB0=ENCA;
        if(!LMT){ //Check to see if limit switch triggered
            DIR=1;
            CCPR1L = 0b11111111;
            printf("LIMIT TRIGGERED");
        }
        if(SENCA==0&&ENCA==1){ //check last state of encoder and
change, add to
counter if needed
            if(DIR)
                PENCA=PENCA+1;
            else
                PENCA=PENCA-1;
            SENCA=1;
            //      printf("\rPOS[%u]",PENCA);
        }
        else if(SENCA==1&&ENCA==0){
            SENCA=0;
        }
        TOIF=0; // clear event flag
    }
}
}

```

### Iteration 3 - PIC 18F2455

```
/** GENERIC MICROCHIP USB FIRMWARE FILES
#include "Compiler.h"
#include "HardwareProfile.h"
#include "GenericTypeDefs.h"
#include "USB/usb_device.h"
#include "USB/usb.h"
#include "USB/usb_function_generic.h"
#include "usb_config.h"
#include "usart.h"

#pragma config PLLDIV = 1
#pragma config CPUDIV = OSC1_PLL2
#pragma config USBDIV = 2
#pragma config FOSC = HS
//#pragma config FCMEM = OFF
#pragma config IESO = OFF
#pragma config PWRT = OFF
#pragma config BOR = ON
//#pragma config BORV = 21
#pragma config VREGEN = ON
#pragma config WDT = OFF
#pragma config WDTPS = 32768
#pragma config MCLRE = ON
#pragma config LPT1OSC = OFF
#pragma config PBADEN = OFF
#pragma config CCP2MX = ON
#pragma config STVREN = ON
#pragma config LVP = OFF
//#pragma config ICPRT = OFF
#pragma config XINST = OFF
#pragma config DEBUG = OFF
#pragma config CP0 = OFF
#pragma config CP1 = OFF
#pragma config CP2 = OFF
//#pragma config CP3 = OFF
#pragma config CPB = OFF
#pragma config CPD = OFF
#pragma config WRT0 = OFF
#pragma config WRT1 = OFF
#pragma config WRT2 = OFF
//#pragma config WRT3 = OFF
#pragma config WRTB = OFF
```

```

#pragma config WRTC = OFF
#pragma config WRWD = OFF
#pragma config EBTR0 = OFF
#pragma config EBTR1 = OFF
#pragma config EBTR2 = OFF
//#pragma config EBTR3 = OFF
#pragma config EBTRB = OFF

#pragma udata USB_VARIABLES=0x500

unsigned char OUTPacket[64];
unsigned char INPacket[64];

#pragma udata
BOOL blinkStatusValid;
USB_HANDLE USBGenericOutHandle;
USB_HANDLE USBGenericInHandle;
#pragma udata

static void InitializeSystem(void);
void USBDeviceTasks(void);
void UserInit(void);
void ProcessIO(void);
void BlinkUSBStatus(void);
void rx_handler(void);
char joints[32];
int posns[32];
char addr=0x00;
char posret=0x30;
char br=0xCC;
char flag=0;
char RX;
int i=0;
char data[64];
int c=0;

#pragma code rx_interrupt=0x8
void rx_int (void)
{
    _asm goto rx_handler _endasm
}
#pragma code
void rx_handler(void)

```



```

{
    RX=ReadUSART(); //Read usart
    TXREG='0xdd';
    if(RX==br){
        i=0;
        TXREG='c';
    }

    else if(i==1&&RX==addr){
        flag = 1;
        i=0;
    }

    data[i]=RX;
    i++;

    if(i>20)
        i=0;

    PIR1bits.RCIF = 0;
}

```

```

//////////MAIN FUNCTION//////////

```

```

void main(void){
    InitializeSystem();
    PORTA = 0x00;
    TRISA = 0x00;
    PORTC = 0x00;
    TRISC = 0x00;
    PORTB=0x00;
    TRISC=0x00;
    RCONbits.IPEN=1;
    IPR1bits.RCIP=1;
    INTCONbits.GIE=1;

```

```

joints[1]=0x11;

```

```

    OpenUSART(USART_TX_INT_OFF & USART_RX_INT_ON & USART_ASYNC_MODE &
USART_EIGHT_BIT & USART_CONT_RX & USART_BRGH_HIGH, 25);
    //putsUSART("Hello World!");
    PIE1bits.RCIE=1;
    // PORTB = 0b00000001;
    // putsUSART("UART INIT");

    while(1)
    {

        if(flag){ //process UART updates
            if(data[1]==posret){
                posns[data[2]]=data[3];
                putsUSART("DATA");
                putsUSART(data[3]);
                putsUSART(0xac);
            }
            //if address data
                //store address with type in array
            //if address term

            flag=0;

        }
        USBDeviceTasks(); //perform USB communications
        ProcessIO(); //update usb things

    }
}

static void InitializeSystem(void)
{
    ADCON1 |= 0x0F;

    USBGenericOutHandle = 0;
    USBGenericInHandle = 0;

    USBDeviceInit(); //usb_device.c.

```

```

}

void ProcessIO(void)
{
    if(!USBHandleBusy(USBGenericOutHandle))
    {
        switch(OUTPacket[0])
        {
            case 0x80: //Toggle LED(s) command from PC application.
                if(PORTAbits.RA4==1){
                    PORTAbits.RA4=0;
                    PORTAbits.RA5=0;
                }
                else{
                    PORTAbits.RA4=1;
                    PORTAbits.RA5=1;
                }

                break;

            case 0x30:
                WriteUSART(0xFF);//UNIT ID
                Delay100TCYx(50);
                WriteUSART(0x01);//COMMAND
                Delay100TCYx(50);
                WriteUSART(0x50);//VALUE

                INPacket[0]=0x15;
                INPacket[1]=0x48;

                break;

            default: //FWD

                // WriteUSART(0xFF);
                //Delay100TCYx(100); //FF AA 85 CC xx
                for (c=0;c<5;c++){
                    WriteUSART(0xFF); //SYNC
                    Delay100TCYx(50);
                }
        }
    }
}

```

```

        Delay100TCYx(50);
            WriteUSART(OUTPacket[1]); //UNIT ID
        Delay100TCYx(50);
            WriteUSART(OUTPacket[0]); //COMMAND
        Delay100TCYx(50);
            WriteUSART(OUTPacket[2]); //VALUE

        break;

    }

    USBGenericOutHandle =
    USBGenRead(USBGEN_EP_NUM,(BYTE*)&OUTPacket,USBGEN_EP_SIZE);
    USBGenericInHandle =
    USBGenWrite(USBGEN_EP_NUM,(BYTE*)&INPacket,USBGEN_EP_SIZE);
    }
}

#if 0
void __attribute__((interrupt)) _USB1Interrupt(void)
{
    #if !defined(self_powered)
        if(U1OTGIRbits.ACTVIF)
        {
            IEC5bits USB1IE = 0;
            U1OTGIEbits.ACTVIE = 0;
            IFS5bits USB1IF = 0;

            //USBClearInterruptFlag(USBActivityIFReg,USBActivityIFBitNum);
            USBClearInterruptFlag(USBIdleIFReg,USBIdleIFBitNum);
            //USBSuspendControl = 0;
        }
    #endif
}
#endif

void USBCBInitEP(void)
{

```

```

USBEnableEndpoint(USBGEN_EP_NUM,USB_OUT_ENABLED|USB_IN_ENABLED|USB_HANDSHAKE_ENABLED|USB_DISALLOW_SETUP);
    //
USBEnableEndpoint(2,USB_OUT_ENABLED|USB_IN_ENABLED|USB_HANDSHAKE_ENABLED|USB_DISALLOW_SETUP);
    //
USBEnableEndpoint(3,USB_OUT_ENABLED|USB_IN_ENABLED|USB_HANDSHAKE_ENABLED|USB_DISALLOW_SETUP);

        USBGenericOutHandle                                     =
USBGenRead(USBGEN_EP_NUM,(BYTE*)&OUTPacket,USBGEN_EP_SIZE);
        //                                     USBGenericOutHandle =
USBGenRead(2,(BYTE*)&OUTPacket1,USBGEN_EP_SIZE);
        //                                     USBGenericOutHandle =
USBGenRead(3,(BYTE*)&OUTPacket2,USBGEN_EP_SIZE);
    }

void USBCBSendResume(void)
{
    static WORD delay_count;

    USBResumeControl = 1;

    delay_count = 1800U;
    do
    {
        delay_count--;
    }while(delay_count);
    USBResumeControl = 0;
}

```

### Iteration 3 - dsPIC33FJ32MC302

```
#include <p33FJ32MC302.h>
#include <stdio.h>
#include <uart.h>
#include <libpic30.h>

_FBS(BSS_NO_FLASH & BWRP_WRPROTECT_OFF)
_FGS(GSS_OFF & GCP_OFF & GWRP_OFF)
_FOSCSSEL(FNOSC_FRC & IESO_OFF)
_FOSC(FCKSM_CSDCMD & IOL1WAY_ON & OSCIOFNC_ON & POSCMD_NONE)
_FWDT(FWDTEN_OFF & WINDIS_OFF & WDTPRE_PR128 & WDTPOST_PS32768)
//Set HPOL-OFF(Active Low),LPOL-ON(Active High)
_FPOR(PWMPIN_OFF & HPOL_OFF & LPOL_ON & FPWRT_PWR128 & ALTI2C_OFF)
_FICD(BKBUG_OFF & COE_OFF & JTAGEN_OFF & ICS_PGD1)
```

```
char RX;
//char * pi;
char data[24];
int i;
char addr=0x01;
char br=0xFF;
char flag=0;
```

```
void __attribute__((interrupt, no_auto_psv)) _U1RXInterrupt(void){
```

```
    //U1TXREG = U1RXREG;
    RX = U1RXREG;
    if(RX==br){
        i=0;
        //    U1TXREG='f';
    }

    else if(i==1&&RX==addr){
        flag = 1;
        i=0;
        //    data[0]=RX;
        //    U1TXREG='A';
    }

    data[i]=RX;
    i++;
```

```

        //    U1TXREG=i;

        if(i>20)
            i=0;

        IFS0bits.U1RXIF = 0;
    }

void __attribute__((__interrupt__, __shadow__)) _T1Interrupt(void)
{
    //check limit switch on RB10
    IFS0bits.T1IF = 0;
}

void putchUART1(char c){
    while (U1STAbits.UTXBF);
    U1TXREG=c;
}

void InitUART1() {

    U1MODEbits.UARTEN = 0;
    U1MODEbits.USIDL = 0;
    U1MODEbits.IREN = 0;

    U1MODEbits.UEN = 0;
    U1MODEbits.BRGH = 0;
    U1MODEbits.PDSEL = 0;
    U1MODEbits.STSEL = 0;

    U1BRG = 24;

    U1STAbits.UTXINV = 0;
    U1STAbits.UTXISEL0 = 0;
    U1STAbits.UTXBRK = 0;
    U1STAbits.UTXEN = 0;
    U1STAbits.URXISEL = 0;
    U1STAbits.ADDEN = 0;
}

```

```

    U1STAbits.RIDLE = 0;

    IFS0bits.U1TXIF = 0;
    IEC0bits.U1TXIE = 0;
    IFS0bits.U1RXIF = 0;
    IEC0bits.U1RXIE = 1;

    U1MODEbits.UARTEN = 1;

    U1STAbits.UTXEN = 1;

}

void StartPWM(void)
{
    PWMCON1bits.PMOD2=0;
    PWMCON1bits.PEN2L=1; //Enable PWM1L
    PWMCON1bits.PEN2H=1; //Enable PWM1H

    P1TCONbits.PTMOD=0;
    //P1TCONbits.PTCKPS=0;
    P1TCONbits.PTOPS=0;

    PTPER=0x7FFF;
    P1DC2=2046; //2046 -- max
    //delay(1000);
    P1TCONbits.PTEN=1;
}

int main(void) {
    //  RPINR14 = 0x0001;
    //  InitXTAL();
    RPINR18 = 0x07;           // Make Pin RP7 U1RX
    RPOR3bits.RP6R = 0x03;   // Make Pin RP6 U1TX
    //  TRISBbits.TRISB6=0;
    //  TRISBbits.TRISB6=0;
    //while(1){
    //  PORTBbits.RB6=1;
    //  PORTBbits.RB6=0;
    //}

    T1CONbits.TON = 0;

```



```

T1CONbits.TCS = 0;
T1CONbits.TGATE = 0;
T1CONbits.TCKPS = 0b00;
TMR1 = 0x00;
PR1 = 9;
IPC0bits.T1IP = 0x01;
IFS0bits.T1IF = 0;
IEC0bits.T1IE = 1;
T1CONbits.TON = 1;

    InitUART1(); // Initialize UART2 for 9600,8,N,1 TX/RX

//    TRISBbits.TRISB13=0;
//    PORTBbits.RB13=1;
//    TRISBbits.TRISB12=0;
//    PORTBbits.RB12=1;

//delay(50000);
//delay(50000);
//delay(50000);
//delay(50000);

//RB0, RB1 used for QEI
    RPINR14bits.QEA1R = 0x01;           // Make Pin RP7 U1RX
    RPINR14bits.QEB1R = 0x00;           // Make Pin RP7 U1RX
//    RPOR3bits.RP6R = 0x03; // Make Pin RP6 U1TX

ADPCFG = 0xffff;

MAX1CNT = 0xffff;
POS1CNT = 0x0000;

QEI1CONbits.UPDN = 1;
QEI1CONbits.QEIM = 0b101;

DFLT1CON = 0;

char fwd=0x85;

```

```

char stop=0x86;
char rvs=0x87;
char pos=0x50;

char cmd=0;
int value=0;

//PORTBbits.RB13=1;
//PORTBbits.RB12=1;

//StartPWM();
//      500000
//P1DC2=0;

StartPWM();
P1TCONbits.PTEN=1;
__delay32(20000);
P1DC2=2000;
while(1){
    //32768

    if(flag){
        __delay32(20000);
        cmd=data[1];
        value=data[2];
        putcharUART1(0xFF);
        putcharUART1(data[0]);
        putcharUART1(data[1]);
        putcharUART1(data[2]);
        putcharUART1(data[3]);

        if(data[1]==fwd){
            P1DC2=32768-(value*300);
            P1TCONbits.PTEN=1;
            putcharUART1('A');
            printf("%d",value);
        }

        else if(cmd==stop){//STOP
            P1TCONbits.PTEN=0;
            putcharUART1('B');
        }

        else if(cmd==rvs){//RVS
            P1DC2=32768+(value*300);
            P1TCONbits.PTEN=1;

```

```

        putcharUART1('C');
        printf("%d",value);
    }

    else if(cmd==pos){//query pos
        putcharUART1(0xFF);
        __delay32(200);
        putcharUART1(0x00);//UNIT ID
        __delay32(200);
        putcharUART1(0x30);//COMMAND
        __delay32(200);
        putcharUART1(addr);//VALUE
        __delay32(200);
        putcharUART1(POS1CNT>>8);//VALUE
        __delay32(200);
        putcharUART1(POS1CNT);//VALUE
        __delay32(200);

        putcharUART1(0xed);//VALUE
        printf("POS:%d",POS1CNT);
    }
    flag=0;
}

}

/* while (1){
    if(flag){
        cmd = data[2];
        value = data[3];

        if(cmd==fwd){ //FWD
            PORTBbits.RB13=0;
            P1DC2=23000;
        }
        else if(cmd==stop){ //STOP
            P1DC2=0;
            PORTBbits.RB13=1;
        }
        else if(cmd==rvs){ //RVS
            PORTBbits.RB13=1;
            P1DC2=0;
        }
    }
}

```

```

        else if(cmd==pos){ //Return POS
            putcharUART1(0xFF);
            putcharUART1(0x01);
            putcharUART1(0x30);
            putcharUART1(POS1CNT);
        }

        // printf("DATA0:%i\n",data[0]);
        // printf("DATA1:%i\n",data[1]);
        // printf("DATA2:%i\n",data[2]);
        // printf("DATA3:%i\n",data[3]);
        // printf("DATA4:%ixxx\n",data[4]);
        // U1TXREG=data[1];

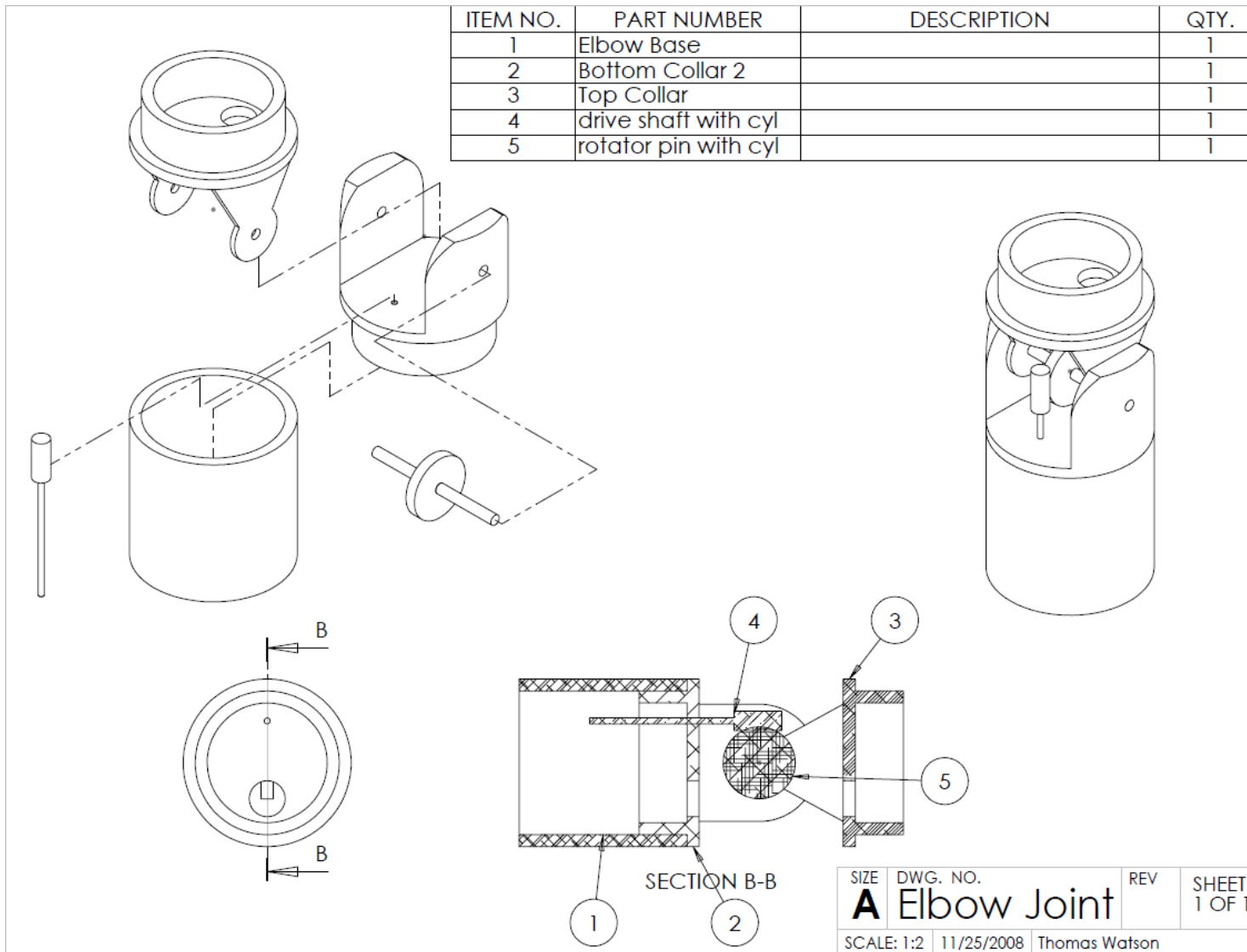
        flag=0;
    }

    // delay(50000);
    // delay(50000);
    // delay(50000);

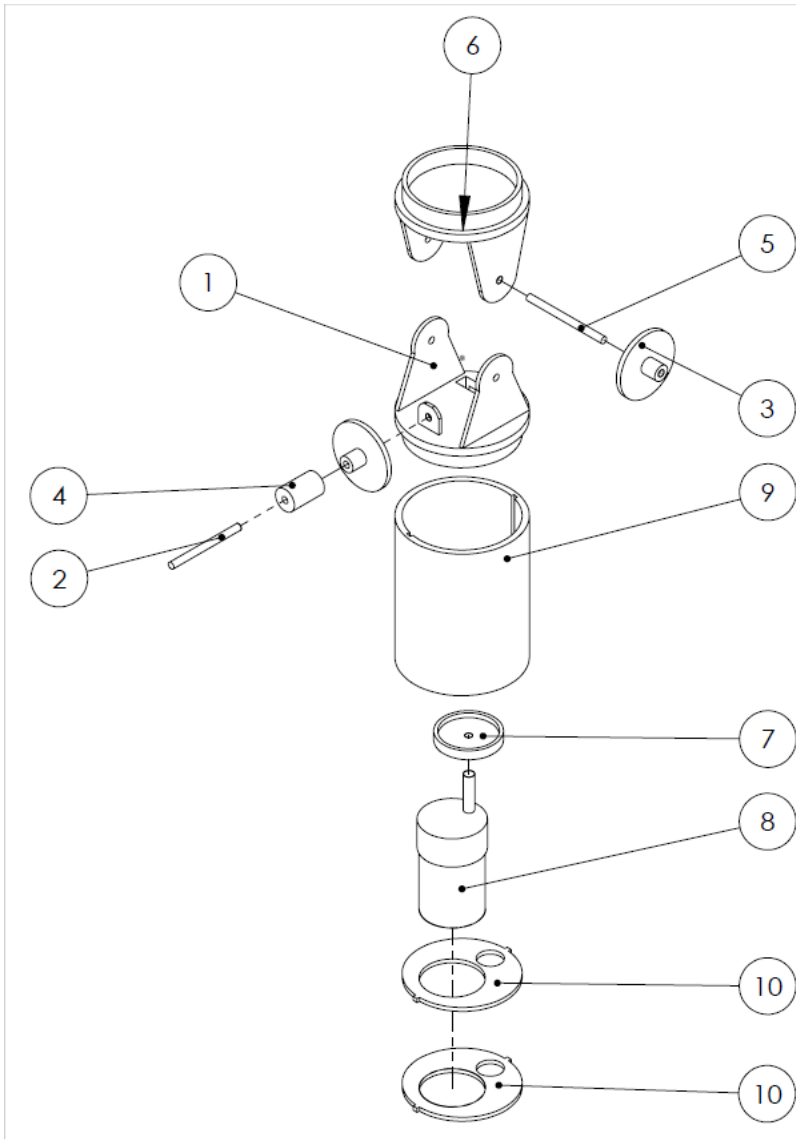
    //printf(P1DC2);
    // U1BRG++;
}
*/
}

```

## Appendix J - Elbow Joint Iteration 01 Exploded/Sectioned View

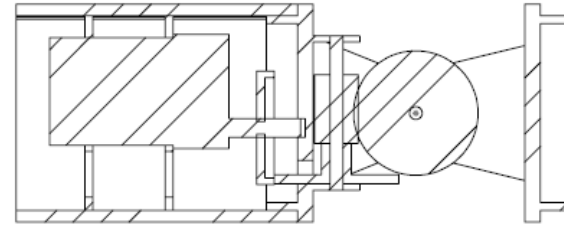
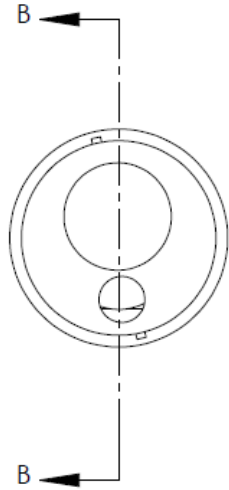


## Appendix K - Elbow Joint Iteration 02 Exploded/Sectioned View

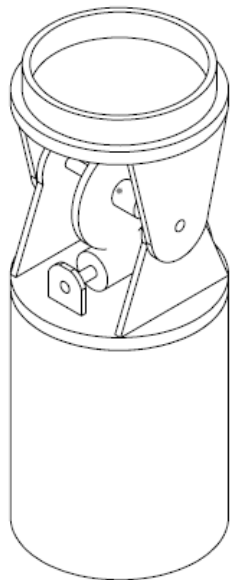


ITEM NO.	PART NUMBER	QTY.
1	Bottom Collar	1
2	shaft	1
3	large radial gear	2
4	Worm Gear	1
5	rotator pin	1
6	Driven Collar	1
7	Right Angle Gear	1
8	elbow motor	1
9	elbow sleeve	1
10	Motor mount 2	2

	NAME	DATE	Thomas Watson	
DRAWN	TBW	1/30/09	TITLE:	
CHECKED			ELBOW JOINT REVISION 4	
ENG APPR.				
MFG APPR.				
Q.A.				
DIMENSIONS ARE IN MILLIMETERS TOLERANCES: FRACTIONAL ± ANGULAR: MACH ± BEND ± TWO PLACE DECIMAL ± THREE PLACE DECIMAL ±			SIZE DWG. NO.	REV
			<b>A</b> Iteration 02 Assembly 12.10.08	<b>4</b>
SCALE: 1:3		WEIGHT:	PAGE 1	



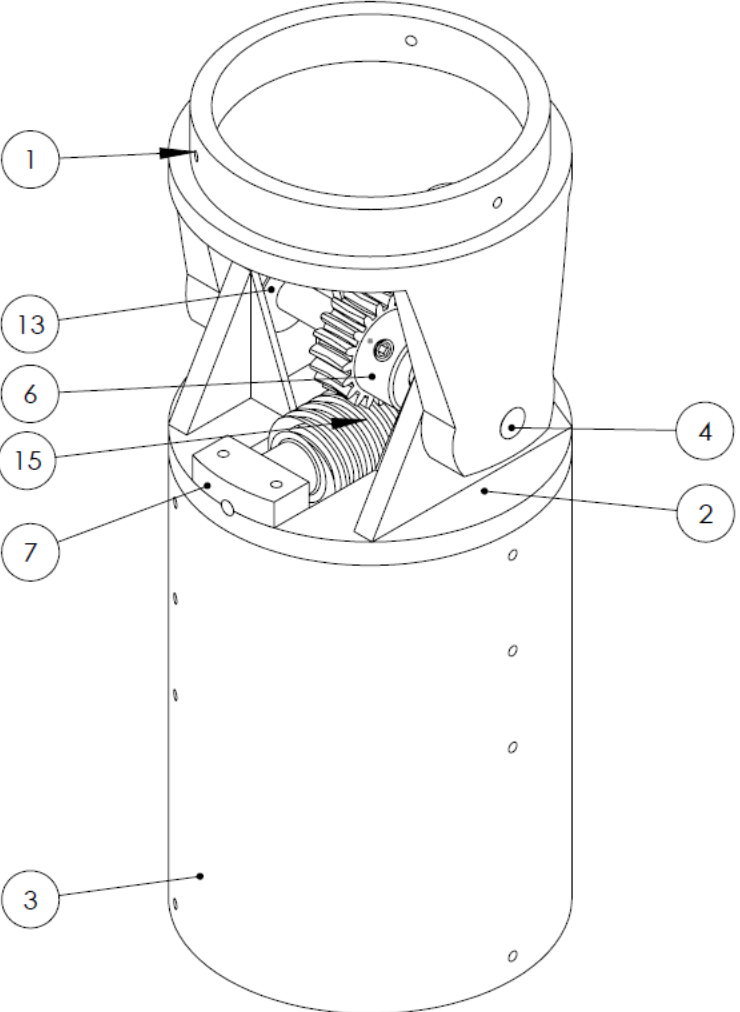
SECTION B-B  
SCALE 1 : 2



ITEM NO.	PART NUMBER	DESCRIPTION	QTY.
1	Bottom Collar	Re-designed so that it contains all driving components	1
2	anchored worm shaft	Shaft holds the worm gear and radial gear	1
3	rotator pin with cyl	This part is locked to the Driven Collar	1
4	Driven Collar		1
5	Drive gear	A 90 degree gear	1
6	motor	Based on preliminary dimensions of purchased motor	1

SIZE	DWG. NO.	REV	SHEET
<b>A</b>	<b>Elbow Joint</b>	02	1 OF 1
SCALE: 1:2	12/7/2008	Thomas Watson	

## Appendix L - Elbow Joint Iteration 03 Labeled Isometric View

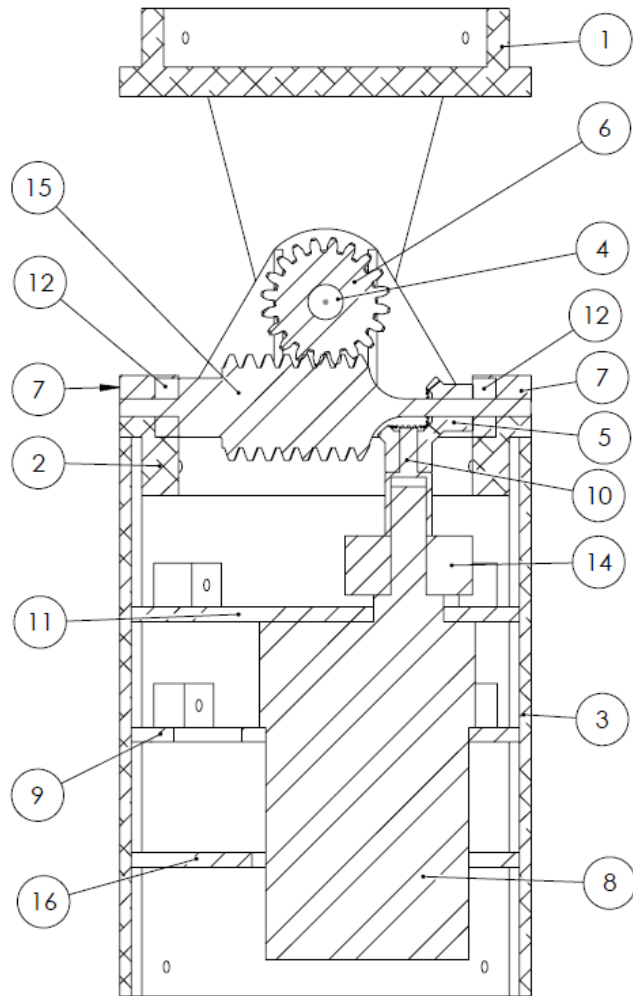


ITEM NO.	PART NUMBER	MATERIAL	QTY.
1	Driven Collar 1.28.2009	ABS	1
2	Bottom Collar	ABS	1
3	Elbow Sleeve 1.28.2009	ABS	1
4	Rotator Pin 1.28.2009	STEEL	1
5	Miter Gear	BRASS	2
6	Worm Gear Purchased 2	ACETYL	1
7	Drive Shaft Lock	ABS	2
8	Motor 1.28.2009	N/A	1
9	Motor Mount 1.28.2009	ABS	1
10	Elbow Coupler 1.28.2009	STEEL	1
11	Motor Mount Top 1.28.2009	ABS	1
12	3 mm Bearing	N/A	2
13	Bearing	N/A	2
14	encoder	N/A	1
15	Worm Machined	STEEL	1
16	PCB	N/A	1

	NAME	DATE	Thomas Watson	
DRAWN	TBW	1/30/09	TITLE:	
CHECKED			ELBOW JOINT REVISION 4	
ENG APPR.				
MFG APPR.				
Q.A.				
DIMENSIONS ARE IN MILLIMETERS TOLERANCES: FRACTIONAL ± ANGULAR: MACH ± BEND ± TWO PLACE DECIMAL ± THREE PLACE DECIMAL ±			SIZE <b>A</b>	DWG. NO. Iteration 03
			REV <b>4</b>	
			SCALE: 1:1	WEIGHT: PAGE 1



## Appendix M -Elbow Joint Iteration 03 Labeled Sectioned View

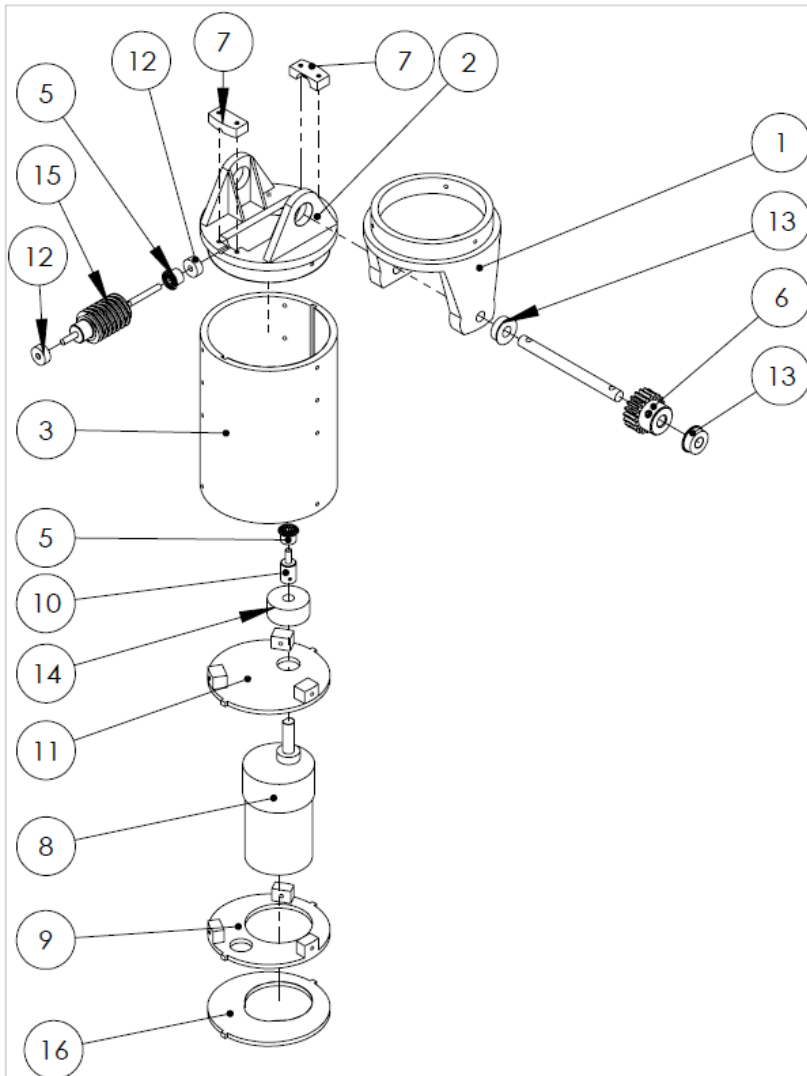


SECTION A-A  
SCALE 1 : 1

ITEM NO.	PART NUMBER	QTY.
1	Driven Collar 1.28.2009	1
2	Bottom Collar	1
3	Elbow Sleeve 1.28.2009	1
4	Rotator Pin 1.28.2009	1
5	Miter Gear	2
6	Worm Gear Purchased 2	1
7	Drive Shaft Lock	2
8	Motor 1.28.2009	1
9	Motor Mount 1.28.2009	1
10	Elbow Coupler 1.28.2009	1
11	Motor Mount Top 1.28.2009	1
12	3 mm Bearing	2
13	Bearing	2
14	encoder	1
15	Worm Machined	1
16	PCB	1

	NAME	DATE	Thomas Watson		
DRAWN	TBW	1/30/09	TITLE:		
CHECKED			ELBOW JOINT REVISION 4		
ENG APPR.			SIZE	DWG. NO.	REV
MFG APPR.			Iteration 03 Assembly Sectioned Side		4
Q.A.			SCALE: 1:4	WEIGHT:	PAGE 1
DIMENSIONS ARE IN MILLIMETERS TOLERANCES: FRACTIONAL: ± ANGULAR: MACH ± BEND ± TWO PLACE DECIMAL ± THREE PLACE DECIMAL ±					

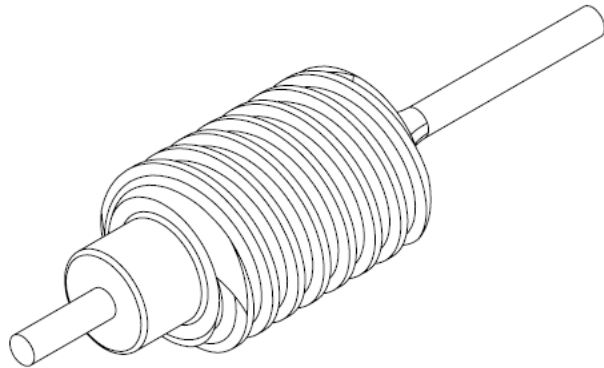
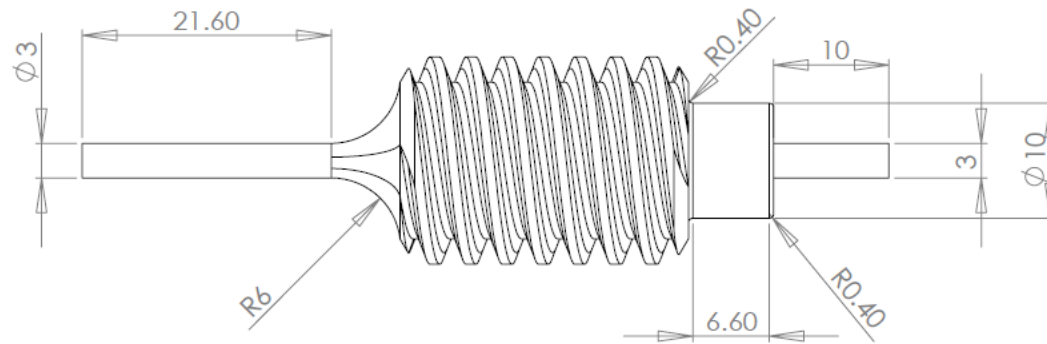
## Appendix N - Elbow Joint Iteration 03 Labeled Exploded View



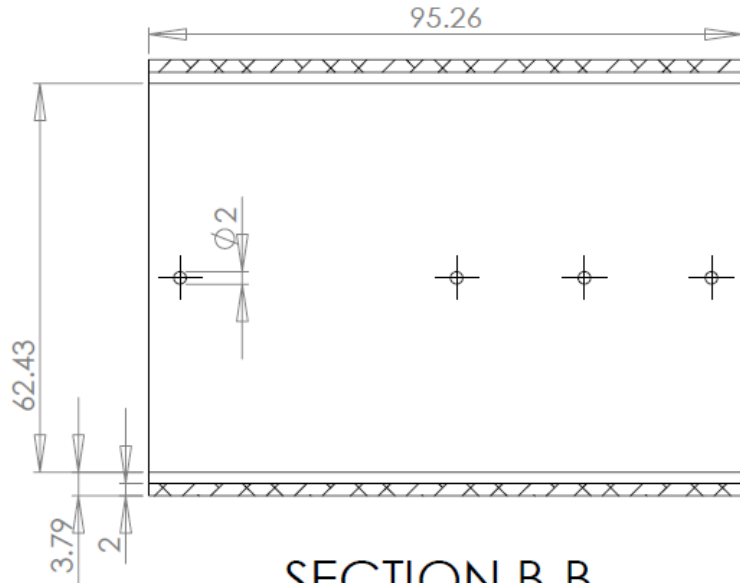
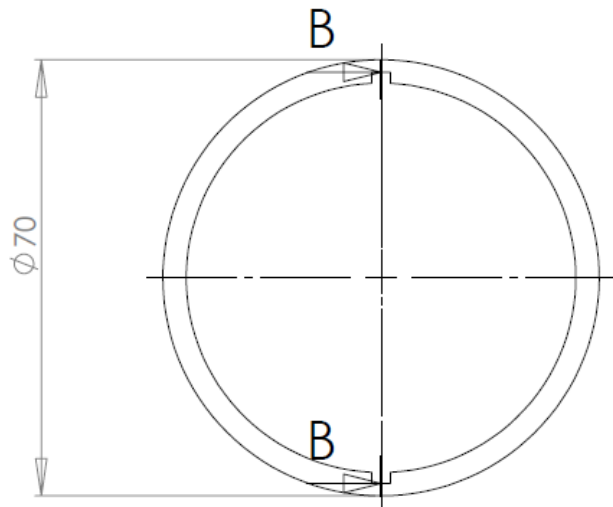
ITEM NO.	PART NUMBER	MATERIAL	QTY.
1	Driven Collar 1.28.2009	ABS	1
2	Bottom Collar	ABS	1
3	Elbow Sleeve 1.28.2009	ABS	1
4	Rotator Pin 1.28.2009	STEEL	1
5	Miter Gear	BRASS	2
6	Worm Gear Purchased 2	ACETYL	1
7	Drive Shaft Lock	ABS	2
8	Motor 1.28.2009	N/A	1
9	Motor Mount 1.28.2009	ABS	1
10	Elbow Coupler 1.28.2009	STEEL	1
11	Motor Mount Top 1.28.2009	ABS	1
12	3 mm Bearing	N/A	2
13	Bearing	N/A	2
14	encoder	N/A	1
15	Worm Machined	STEEL	1
16	PCB	N/A	1

	NAME	DATE	Thomas Watson		
DRAWN	TBW	1/30/09	TITLE:		
CHECKED			ELBOW JOINT REVISION 4		
ENG APPR.					
MFG APPR.					
Q.A.					
DIMENSIONS ARE IN MILLIMETERS TOLERANCES: FRACTIONAL ± ANGULAR: MACH ± BEND ± TWO PLACE DECIMAL ± THREE PLACE DECIMAL ±			SIZE <b>A</b>	DWG. NO. Iteration 03 EXPLODE	REV <b>4</b>
			SCALE: 1:3	WEIGHT:	PAGE 1

## Appendix O - Elbow Joint Iteration 03 Components

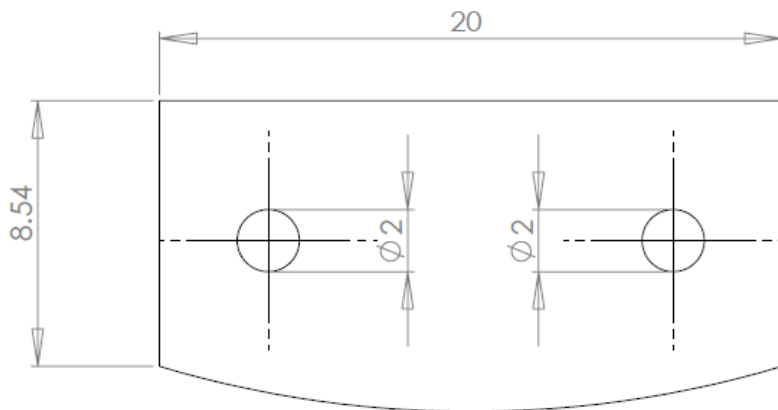
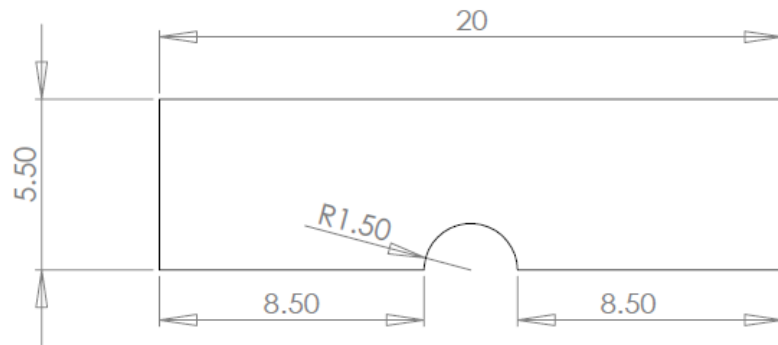


	NAME	DATE	Thomas Watson	
DRAWN	TBW	1/30/09	TITLE:	
CHECKED			ELBOW JOINT	
ENG APPR.			REVISION 4	
MFG APPR.				
Q.A.				
DIMENSIONS ARE IN MILLIMETERS TOLERANCES: FRACTIONAL $\pm$ ANGULAR: MACH $\pm$ BEND $\pm$ TWO PLACE DECIMAL $\pm$ THREE PLACE DECIMAL $\pm$			SIZE <b>A</b>	DWG. NO. Worm Machined
			REV <b>4</b>	
SCALE: 2:1		WEIGHT:	PAGE 1	

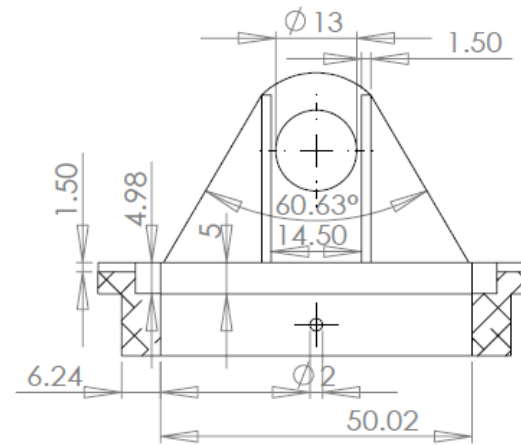
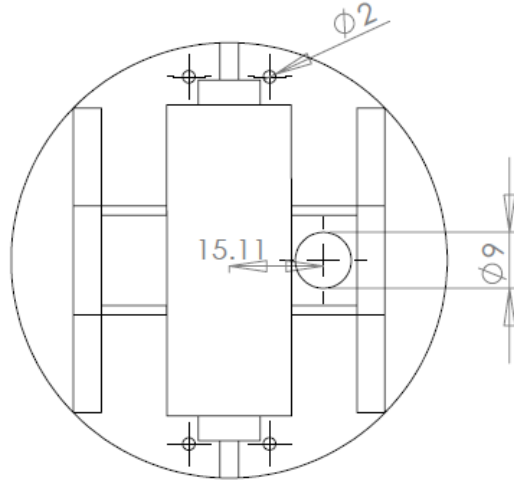
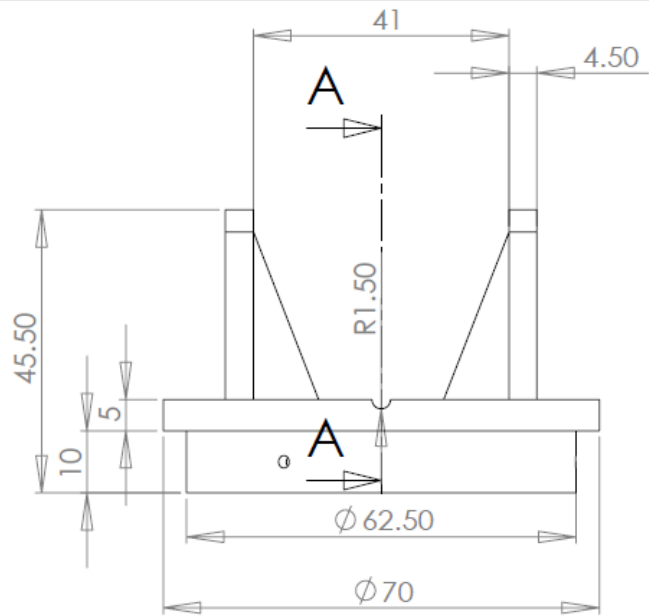


SECTION B-B  
SCALE 1 : 1

DRAWN	NAME	DATE	Thomas Watson		
TBW		1/30/09	TITLE:		
CHECKED			ELBOW JOINT		
ENG APPR.			REVISION 4		
MFG APPR.			SIZE	DWG. NO.	REV
Q.A.			A	Elbow Sleeve 1.28.2009	4
DIMENSIONS ARE IN MILLIMETERS TOLERANCES: FRACTIONAL $\pm$ ANGULAR: MACH $\pm$ BEND $\pm$ TWO PLACE DECIMAL $\pm$ THREE PLACE DECIMAL $\pm$			SCALE: 1:1	WEIGHT:	PAGE 1

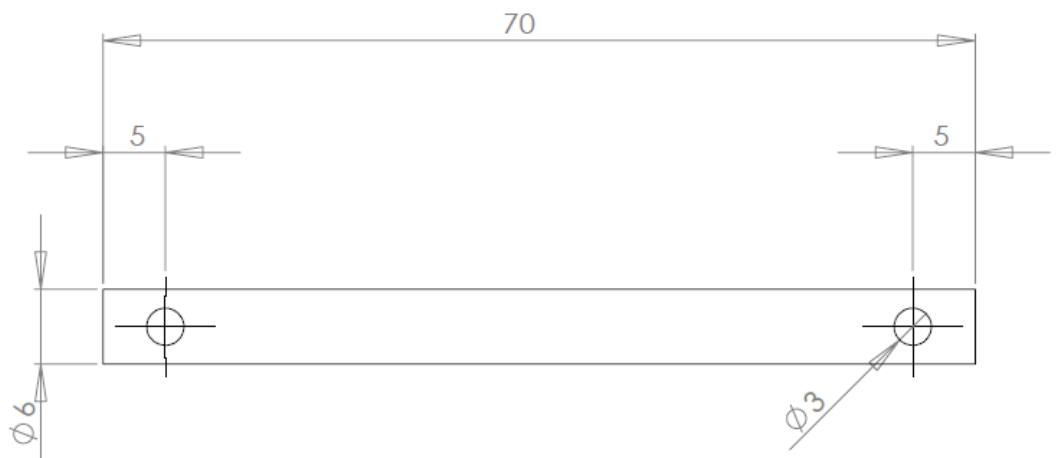


	NAME	DATE	Thomas Watson		
DRAWN	TBW	1/30/09	TITLE:		
CHECKED			ELBOW JOINT		
ENG APPR.			REVISION 4		
MFG APPR.			SIZE	DWG. NO.	REV
Q.A.			A	Drive Shaft Lock	4
DIMENSIONS ARE IN MILLIMETERS TOLERANCES: FRACTIONAL $\pm$ ANGULAR: MACH $\pm$ BEND $\pm$ TWO PLACE DECIMAL $\pm$ THREE PLACE DECIMAL $\pm$			SCALE: 5:1	WEIGHT:	PAGE 1

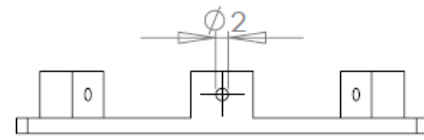
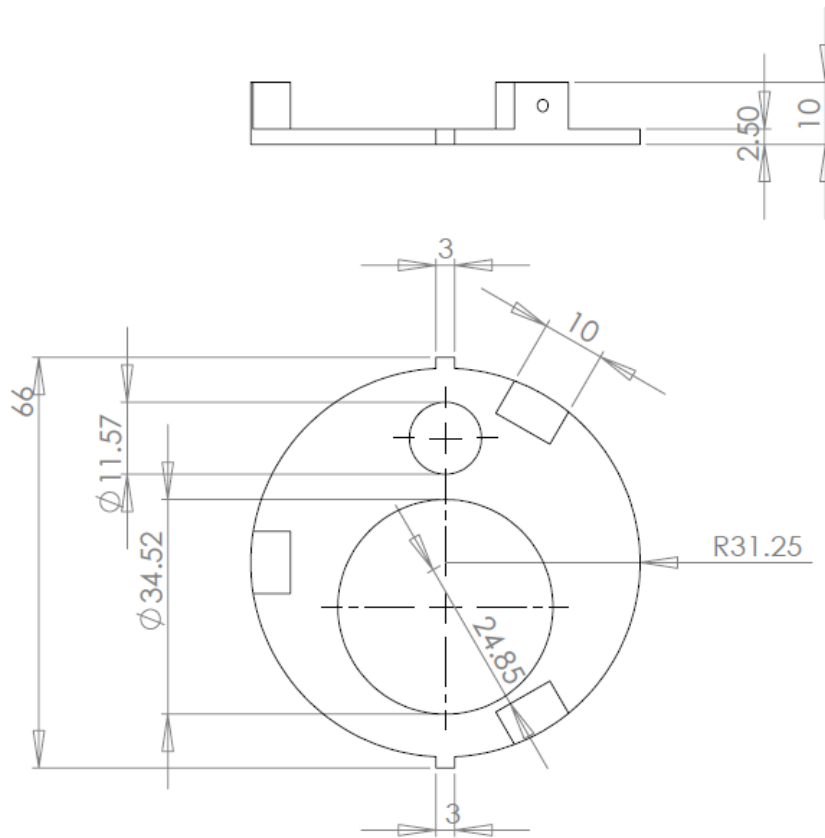


SECTION A-A  
SCALE 1 : 1

NAME	DATE	Thomas Watson		
DRAWN	TBW	1/30/09	TITLE:	
CHECKED			ELBOW JOINT	
ENG APPR.			REVISION 4	
MFG APPR.			SIZE	DWG. NO.
Q.A.			A	Bottom Collar 1.28.2009
DIMENSIONS ARE IN MILLIMETERS TOLERANCES: FRACTIONAL ± ANGULAR: MACH ± BEND ± TWO PLACE DECIMAL ± THREE PLACE DECIMAL ±			REV	4
			SCALE: 1:2	PAGE 1

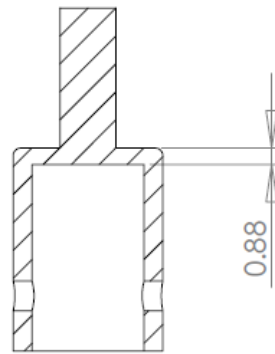


	NAME	DATE	Thomas Watson		
DRAWN	TBW	1/30/09	TITLE:		
CHECKED			ELBOW JOINT REVISION 4		
ENG APPR.					
MFG APPR.					
Q.A.					
DIMENSIONS ARE IN MILLIMETERS TOLERANCES: FRACTIONAL ± ANGULAR: MACH ± BEND ± TWO PLACE DECIMAL ± THREE PLACE DECIMAL ±			SIZE	DWG. NO.	REV
			A	Rotator Pin 1.28.2009	4
			SCALE: 2:1	WEIGHT:	PAGE 1

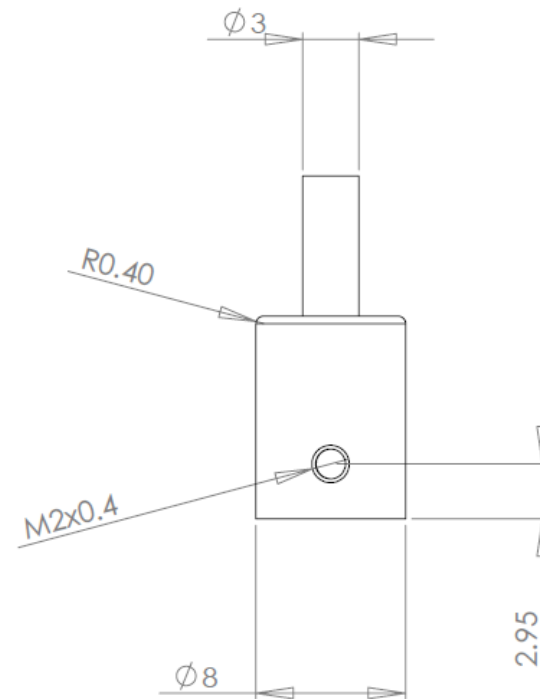
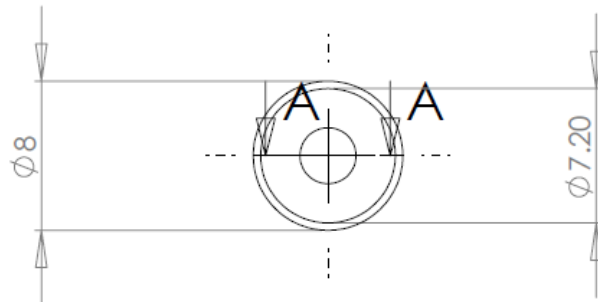


	NAME	DATE	Thomas Watson		
DRAWN	TBW	1/30/09	TITLE:		
CHECKED			ELBOW JOINT		
ENG APPR.			REVISION 4		
MFG APPR.			SIZE	DWG. NO.	REV
Q.A.			A	Motor Mount 1.28.2009	4
DIMENSIONS ARE IN MILLIMETERS TOLERANCES: FRACTIONAL ± ANGULAR: MACH ± BEND ± TWO PLACE DECIMAL ± THREE PLACE DECIMAL ±			SCALE: 1:1	WEIGHT:	PAGE 1

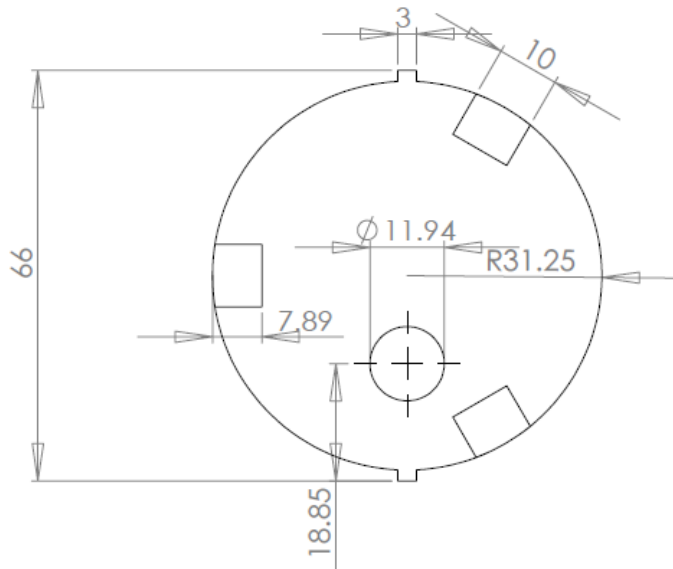
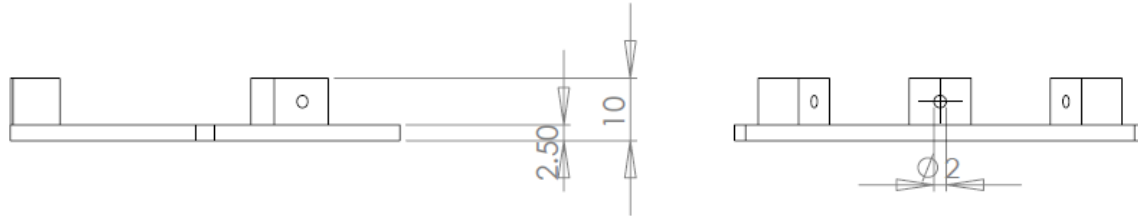




SECTION A-A  
SCALE 3 : 1

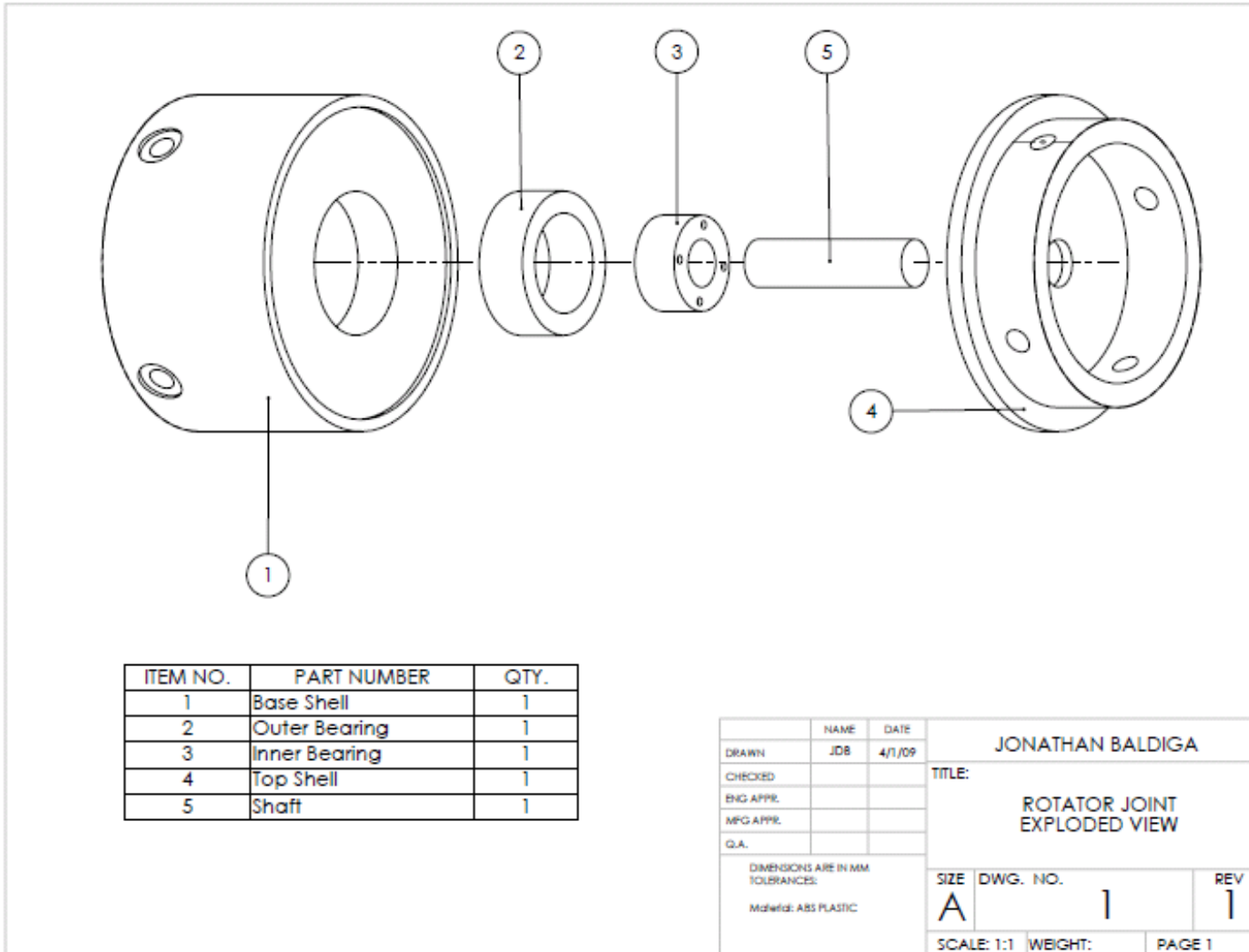


DRAWN	NAME	DATE	Thomas Watson		
TBW		1/30/09	TITLE:		
CHECKED			ELBOW JOINT		
ENG APPR.			REVISION 4		
MFG APPR.			SIZE	DWG. NO.	REV
Q.A.			A	Elbow Coupler 1.28.2009	4
DIMENSIONS ARE IN MILLIMETERS TOLERANCES: FRACTIONAL ± ANGULAR: MACH ± BEND ± TWO PLACE DECIMAL ± THREE PLACE DECIMAL ±			SCALE: 3:1	WEIGHT:	PAGE 1

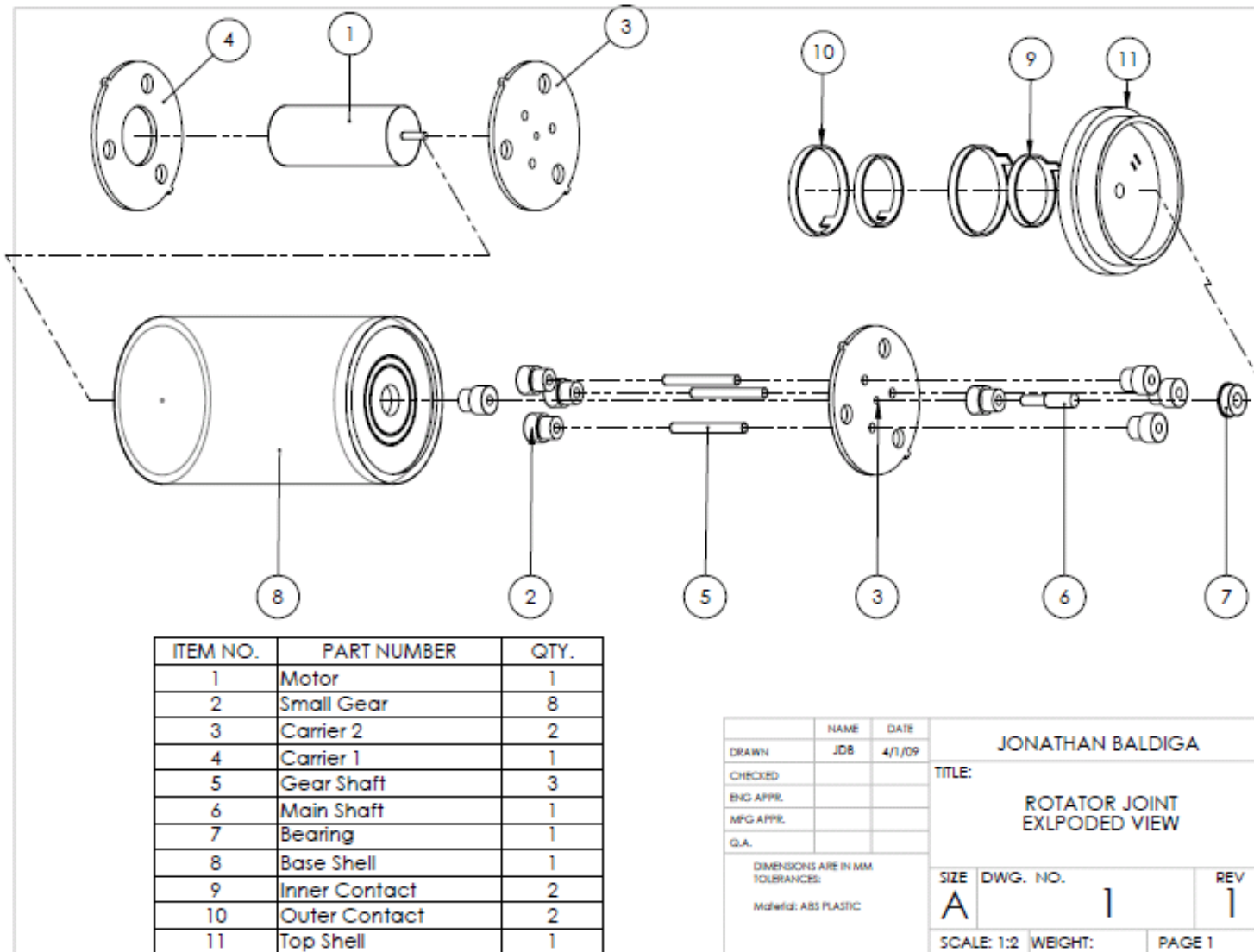


DRAWN	NAME	DATE	Thomas Watson		
CHECKED	TBW	1/30/09	TITLE:		
ENG APPR.			ELBOW JOINT		
MFG APPR.			REVISION 4		
Q.A.			SIZE	DWG. NO.	REV
DIMENSIONS ARE IN MILLIMETERS TOLERANCES: FRACTIONAL ± ANGULAR: MACH ± BEND ± TWO PLACE DECIMAL ± THREE PLACE DECIMAL ±			A	Motor Mount Top 1.28.2009	4
			SCALE: 1:1	WEIGHT:	PAGE 1

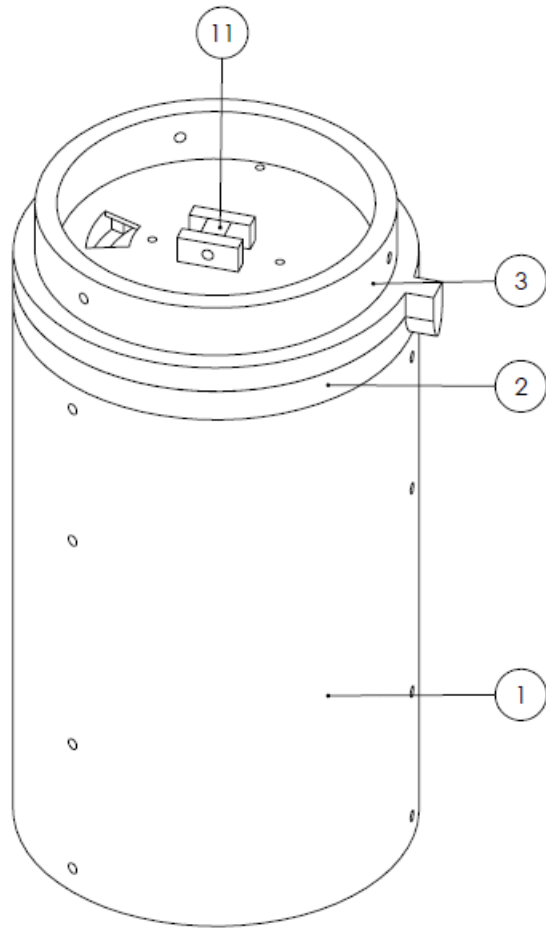
## Appendix P – Rotator Joint Iteration 01 Exploded View



## Appendix Q - Rotator Joint Iteration 02 Exploded View



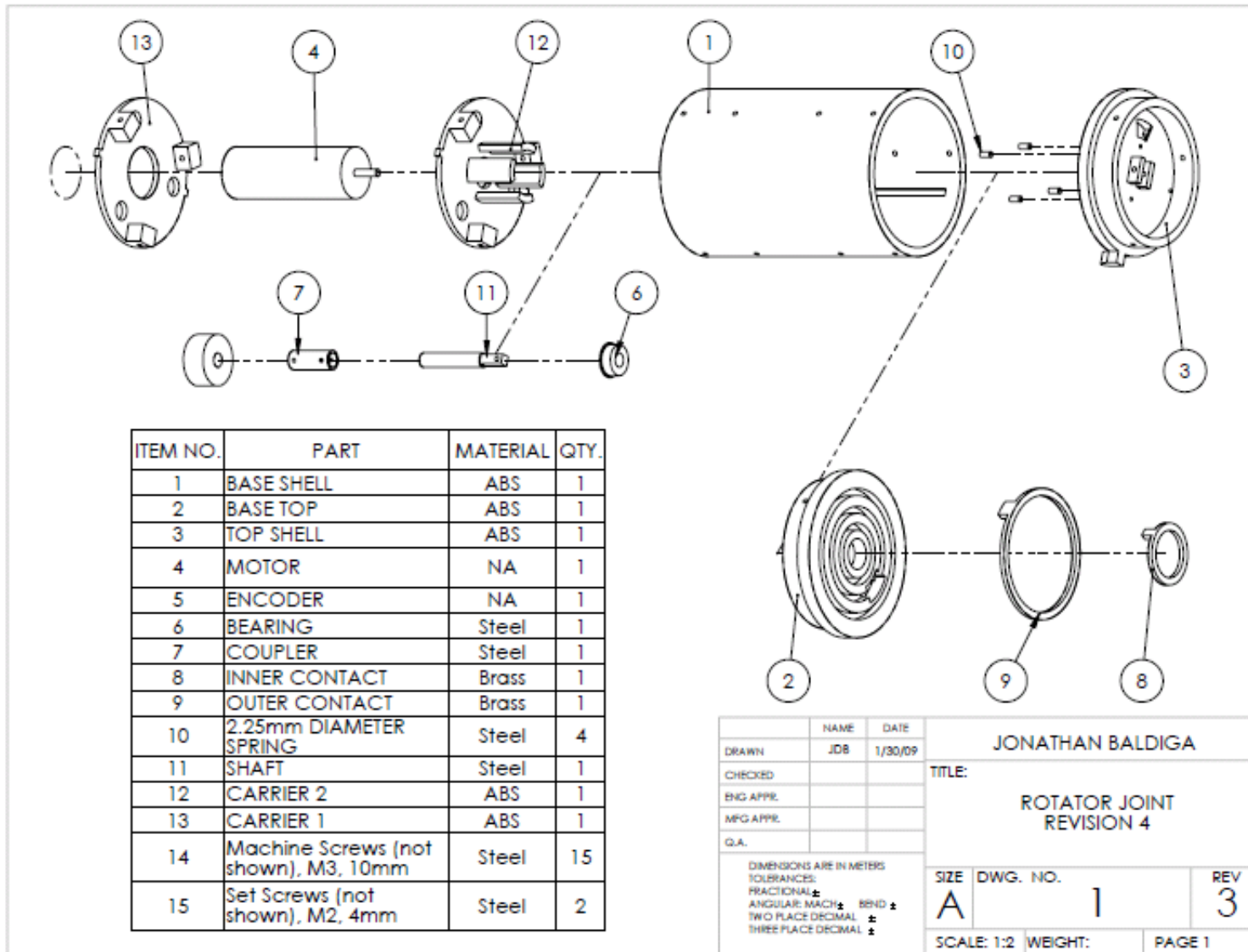
## Appendix R - Rotator Joint Iteration 03 Isometric View



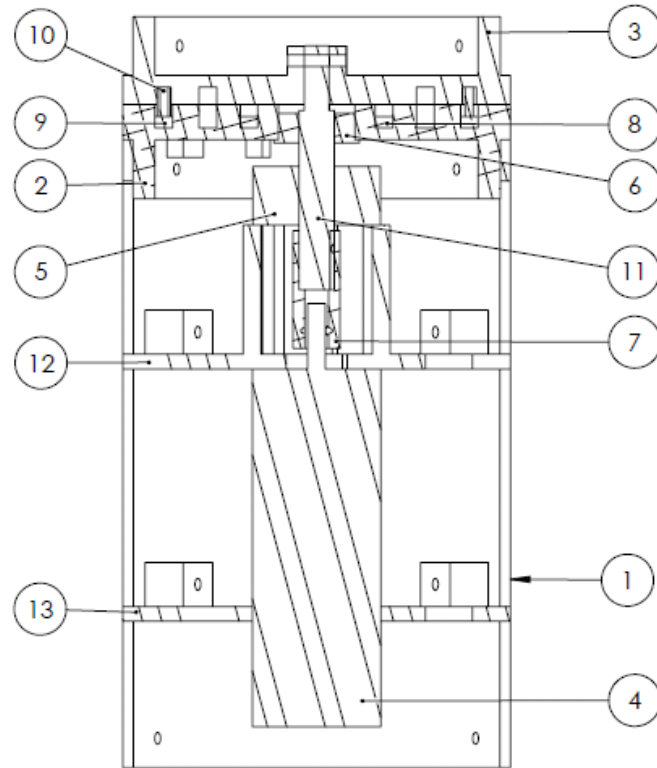
ITEM NO.	PART	MATERIAL	QTY.
1	BASE SHELL	ABS	1
2	BASE TOP	ABS	1
3	TOP SHELL	ABS	1
4	MOTOR	NA	1
3	ENCODER	NA	1
6	BEARING	Steel	1
7	COUPLER	Steel	1
8	INNER CONTACT	Brass	1
9	OUTER CONTACT	Brass	1
10	2.25mm DIAMETER SPRING	Steel	4
11	SHAFT	Steel	1
12	CARRIER 2	ABS	1
13	CARRIER 1	ABS	1
14	Machine Screws, M2, 10mm	Steel	15
15	Set Screws, M2, 4mm	Steel	2

	NAME	DATE	JONATHAN BALDIGA		
DRAWN	JDB	4/1/09	TITLE:		
CHECKED			ROTATOR JOINT ISOMETRIC VIEW		
ENG APPR.					
MFG APPR.					
Q.A.					
DIMENSIONS ARE IN MM TOLERANCES:			SIZE	DWG. NO.	REV
Material: ABS PLASTIC			A	2	3
			SCALE: 1:1	WEIGHT:	PAGE 1

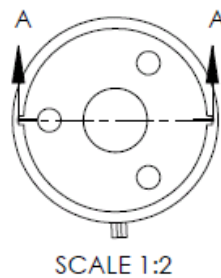
## Appendix S - Rotator Joint Iteration 03 Exploded View



## Appendix T - Rotator Joint Iteration 03 Section View



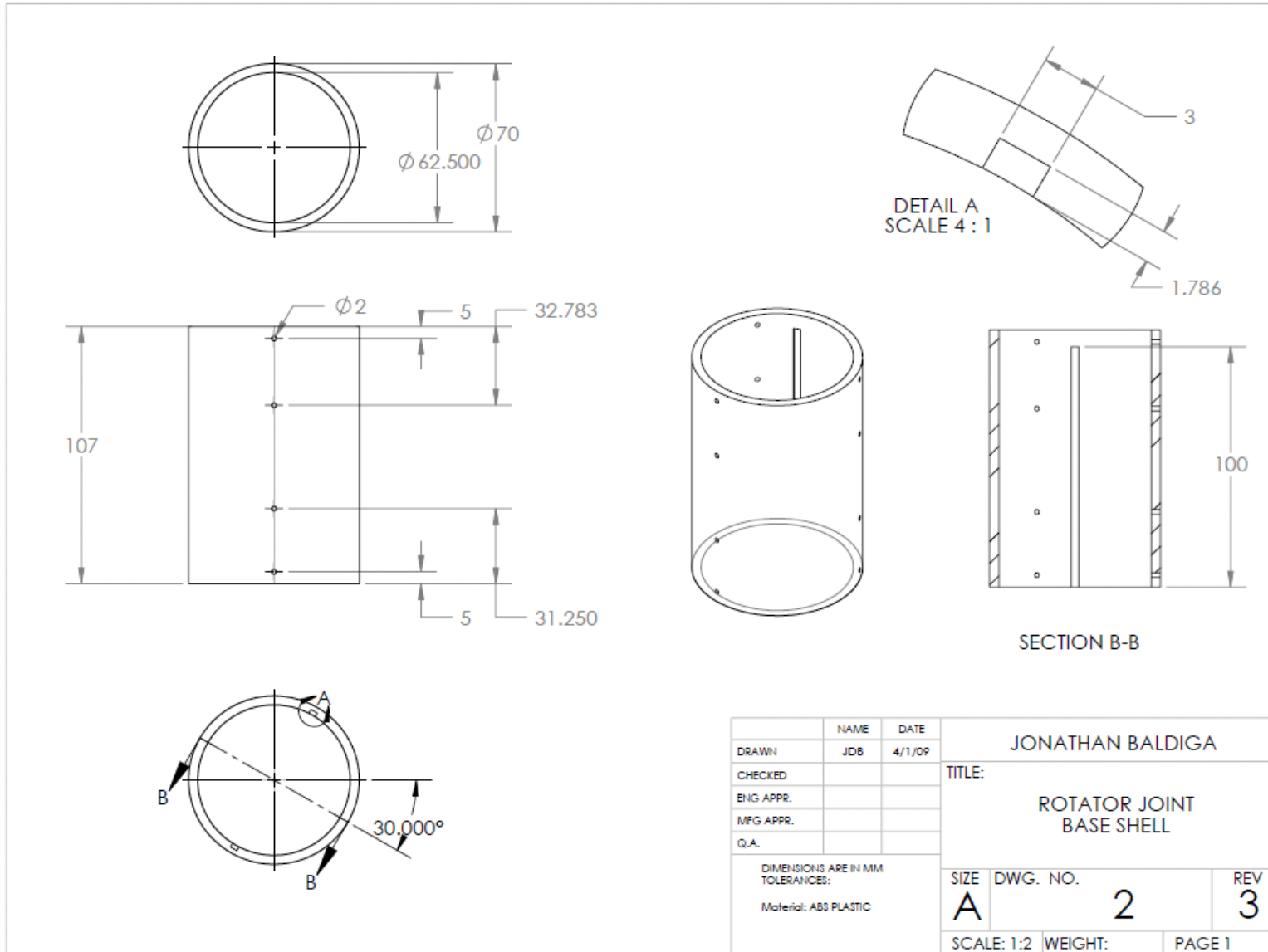
SECTION A-A  
SHEET SCALE



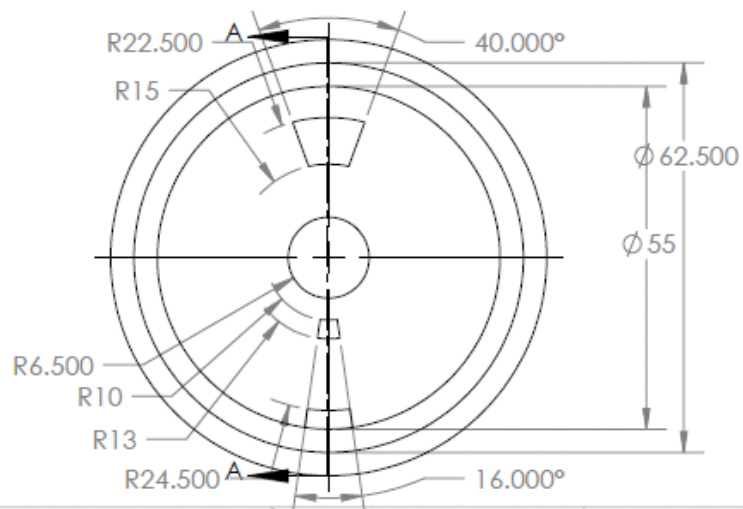
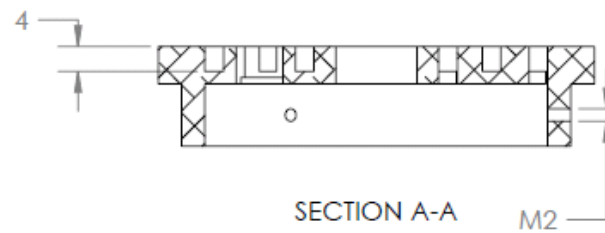
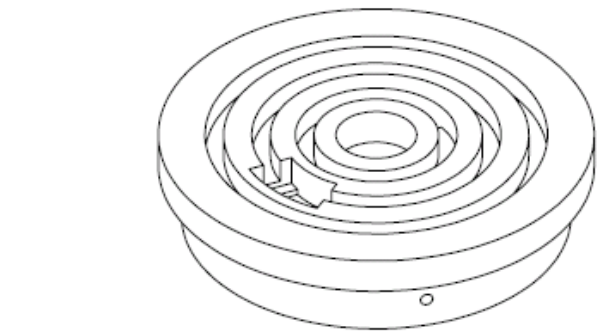
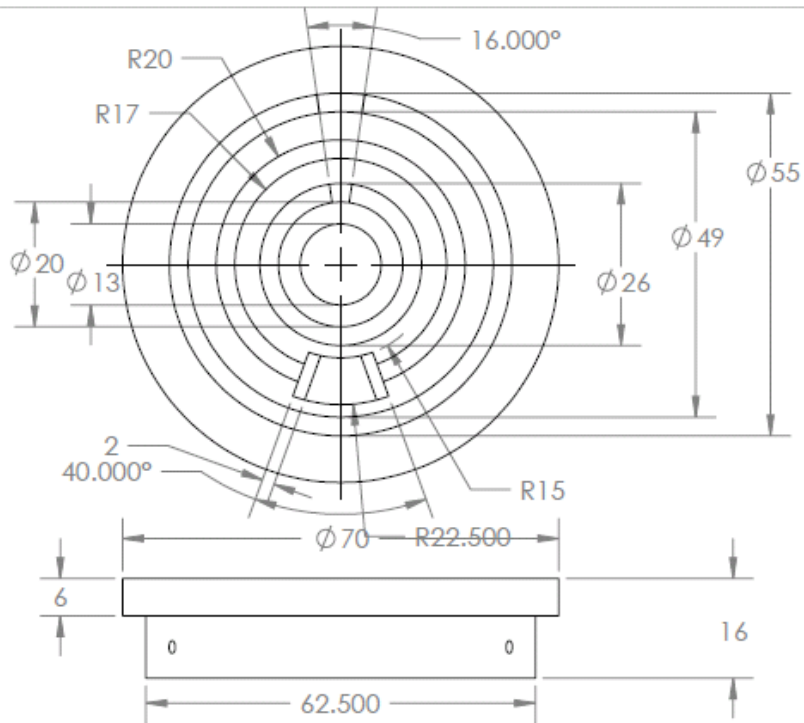
PART NO.	PART	MATERIAL	QTY.
1	BASE SHELL	ABS	1
2	BASE TOP	ABS	1
3	TOP SHELL	ABS	1
4	MOTOR	NA	1
5	ENCODER	NA	1
6	BEARING	Steel	1
7	COUPLER	Steel	1
8	INNER CONTACT	Brass	1
9	OUTER CONTACT	Brass	1
10	2.25mm DIAMETER SPRING	Steel	4
11	SHAFT	Steel	1
12	CARRIER 2	ABS	1
13	CARRIER 1	ABS	1
14	Machine Screws, M2, 10mm	Steel	15
15	Set Screws, M2, 4mm	Steel	2

	NAME	DATE	JONATHAN BALDIGA	
DRAWN	JDB	4/1/09	TITLE:	
CHECKED			ROTATOR JOINT SECTION VIEW	
ENG APPR.			SIZE	DWG. NO.
MFG APPR.			A	2
Q.A.			SCALE: 1:1	REV 3
DIMENSIONS ARE IN MM TOLERANCES: Material: ABS PLASTIC			WEIGHT:	PAGE 1

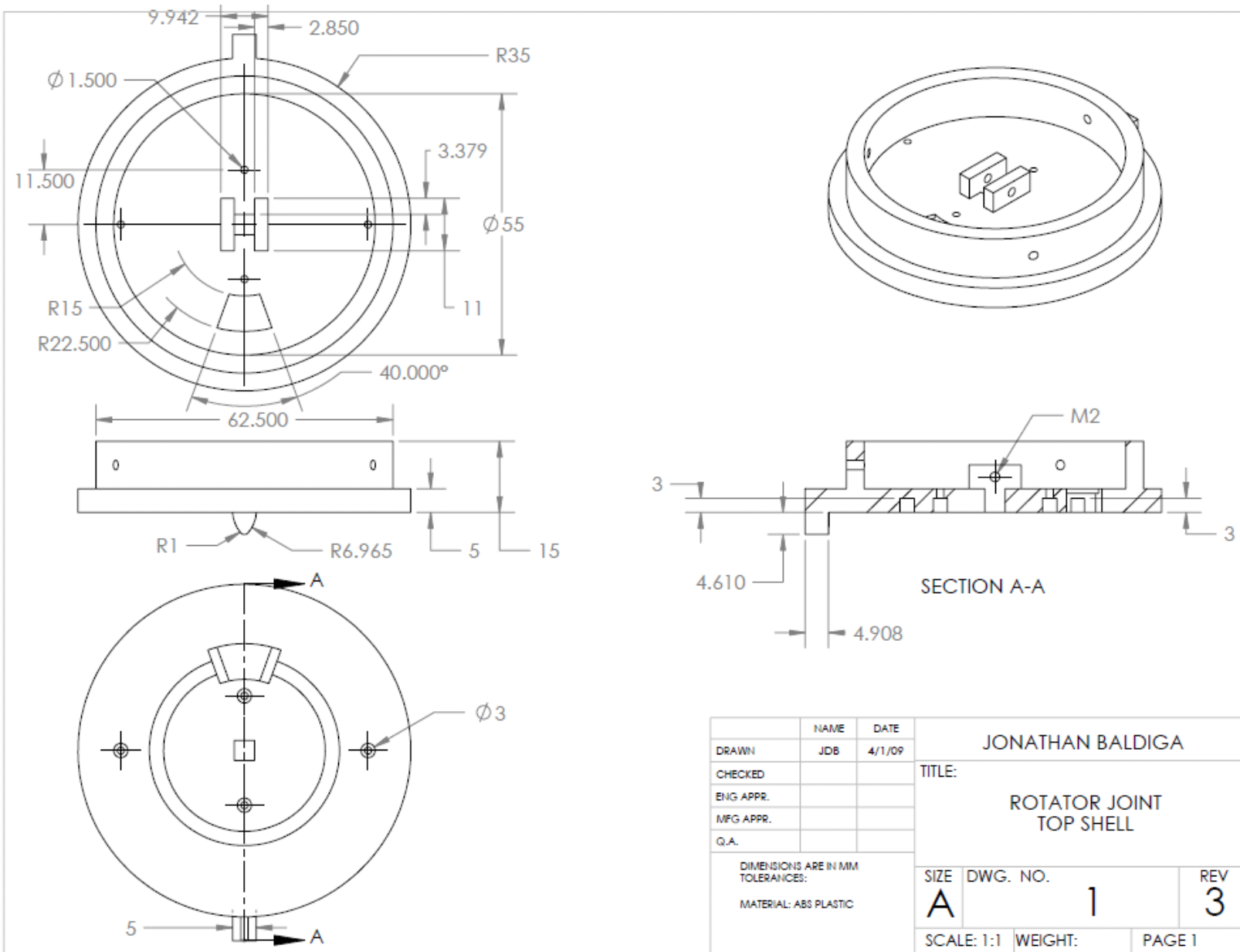
## Appendix U - Rotator Joint Iteration 03 Components

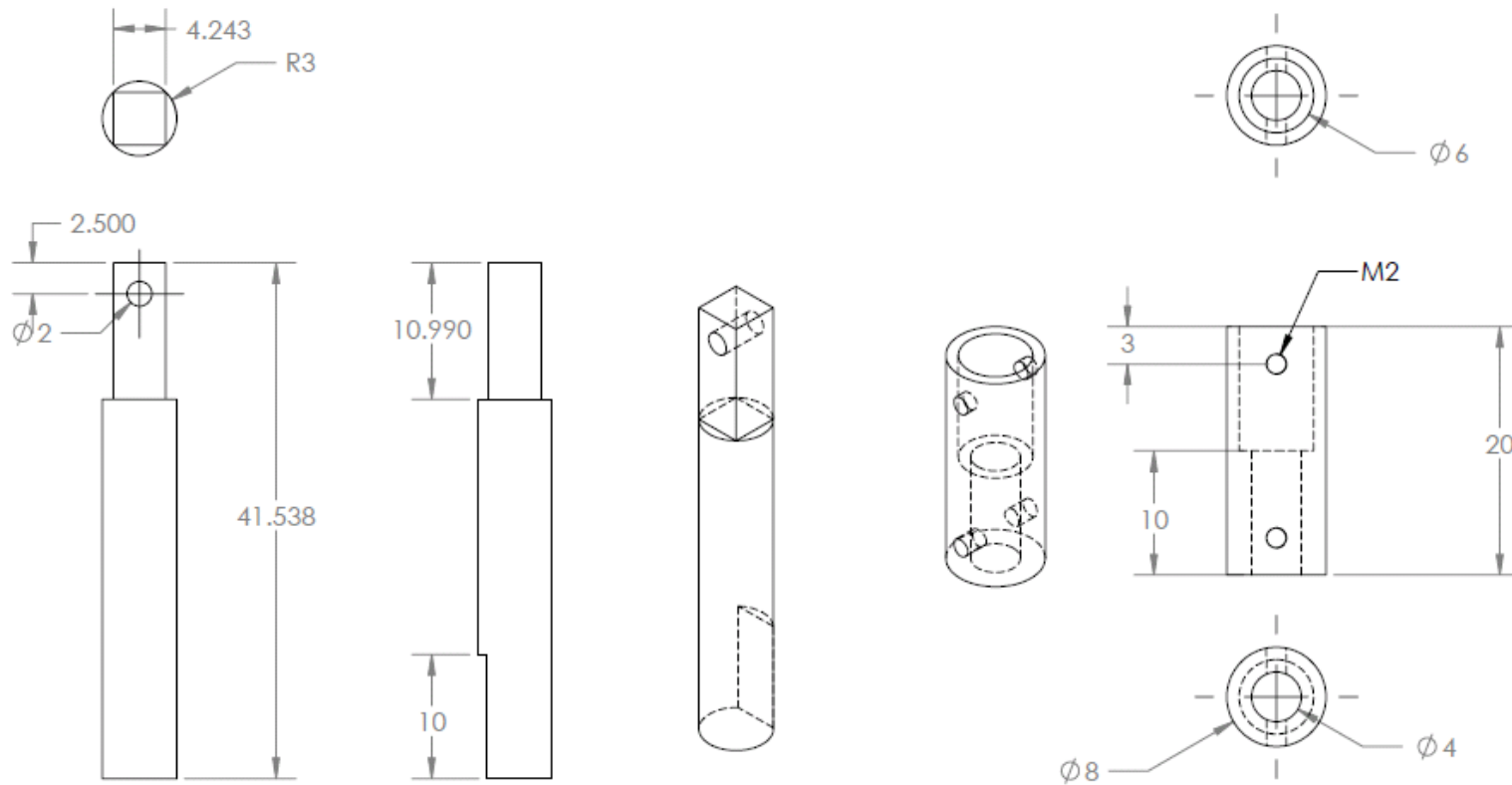






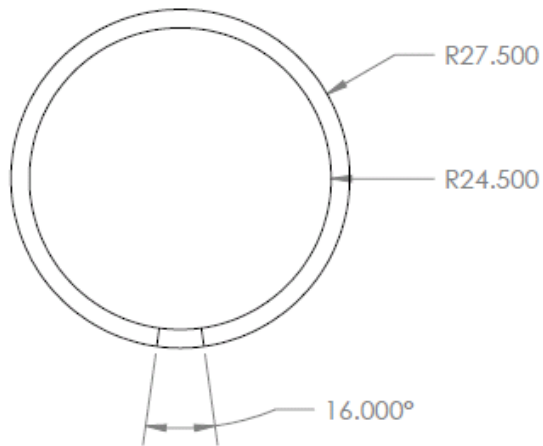
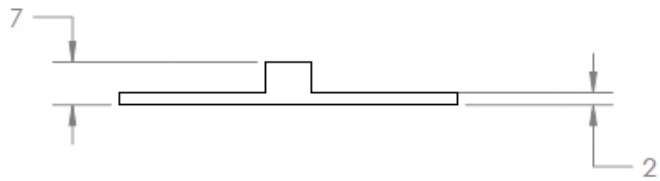
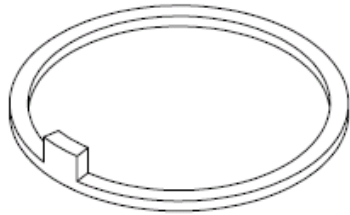
	NAME	DATE	JONATHAN BALDIGA	
DRAWN	JDB	4/1/09	TITLE:	
CHECKED			ROTATOR JOINT	
ENG APPR.			BASE TOP	
MFG APPR.				
Q.A.				
DIMENSIONS ARE IN MM TOLERANCES:			SIZE	DWG. NO.
MATERIAL: ABS PLASTIC			A	3
			SCALE: 1:1	REV
			WEIGHT:	3
			PAGE 1	



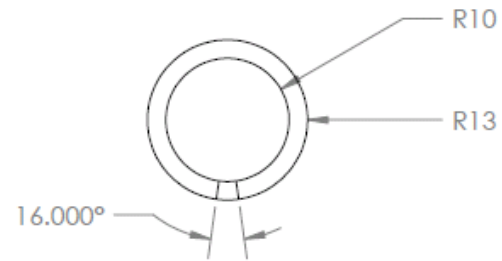
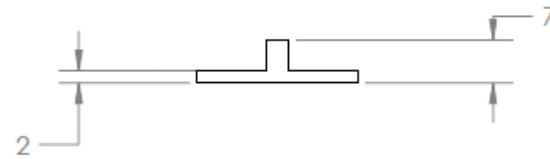
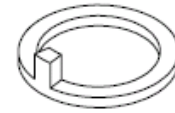


	NAME	DATE	JONATHAN BALDIGA		
DRAWN	JDB	4/1/09	TITLE:		
CHECKED			ROTATOR JOINT COUPLER & SHAFT		
ENG APPR.			SIZE	DWG. NO.	REV
MFG APPR.			A	5	3
Q.A.			SCALE: 2:1	WEIGHT:	PAGE 1
DIMENSIONS ARE IN MM TOLERANCES:					
MATERIAL: STEEL					

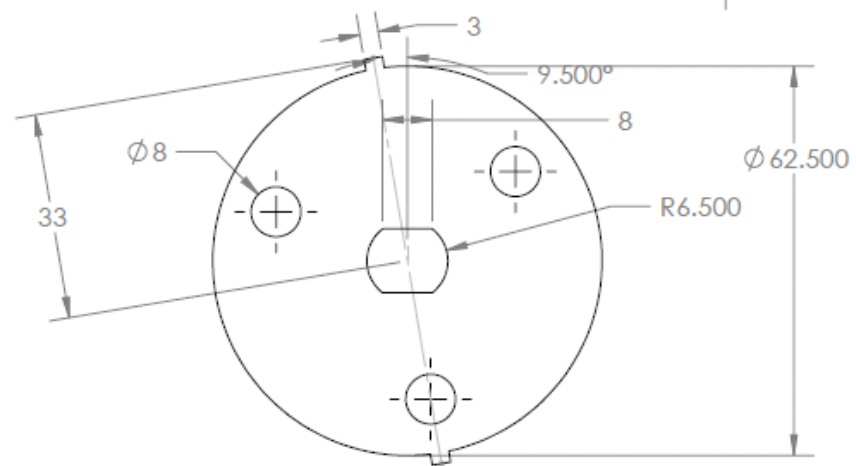
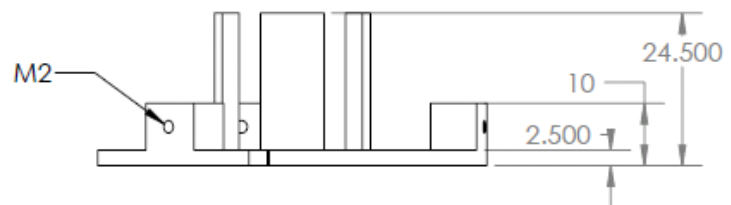
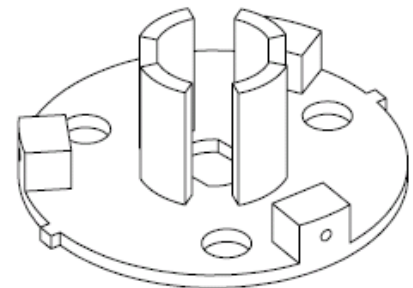
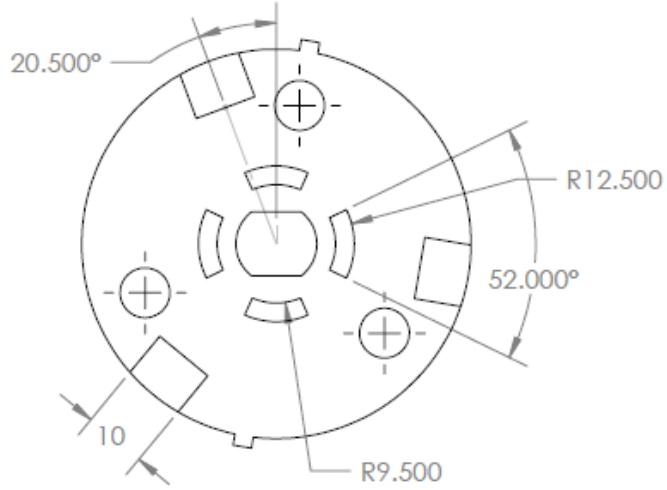
OUTER CONTACT



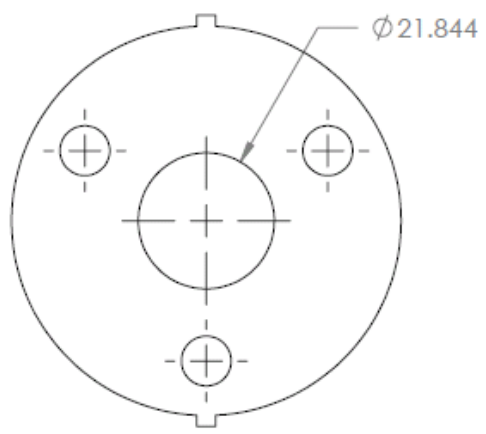
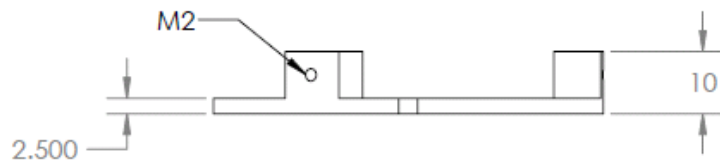
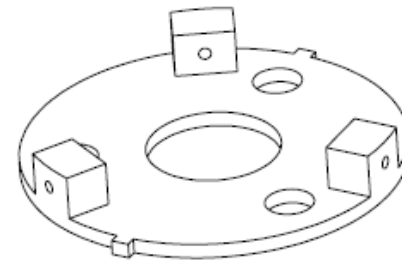
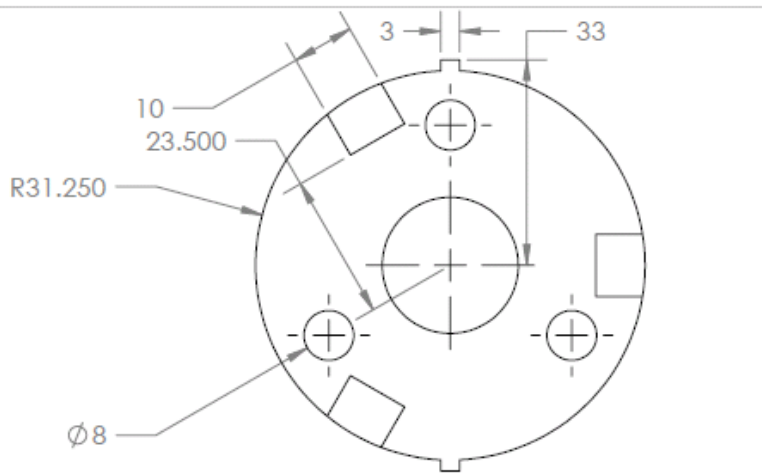
INNER CONTACT



	NAME	DATE	JONATHAN BALDIGA	
DRAWN	JDB	4/1/09	TITLE:	
CHECKED			ROTATOR JOINT	
ENG. APPR.			INNER AND OUTER CONTACTS	
MFG APPR.			SIZE	DWG. NO.
Q.A.			A	6
DIMENSIONS ARE IN MM TOLERANCES:			REV	3
MATERIAL: BRASS			SCALE: 1:1	WEIGHT: PAGE 1



	NAME	DATE	JONATHAN BALDIGA		
DRAWN	JDB	4/1/09	TITLE:		
CHECKED			ROTATOR JOINT CARRIER 2		
ENG APPR.			SIZE	DWG. NO.	REV
MFG APPR.			A	7	3
Q.A.			SCALE: 1:1	WEIGHT:	PAGE 1
DIMENSIONS ARE IN MM TOLERANCES:					
MATERIAL: ABS PLASTIC					



	NAME	DATE	JONATHAN BALDIGA	
DRAWN	JDB	4/1/09	TITLE:	
CHECKED			ROTATOR JOINT CARRIER 1	
ENG APPR.			SIZE	DWG. NO.
MFG APPR.			A	8
Q.A.			SCALE: 1:1	WEIGHT:
DIMENSIONS ARE IN MM TOLERANCES: MATERIAL: ABS PLASTIC			REV	3
			PAGE 1	

## Appendix V – Machining Process Calculation Sheet (WPI FSAE Team)

Process Table. Posted Version 3.5, 25Jan09

Process ID	Process	Unit Cost	Unit	Category	Tooling Required	Near Net Shape
1	None	\$ -				
2	Die Casting	\$ 4.00	kg	Basic Forming	Yes	Yes
3	Investment Casting	\$ 8.00	kg	Basic Forming		Yes
4	Plastic injection molding	\$ 2.75	kg	Basic Forming	Yes	Yes
5	Powder Metal Forming	\$ 3.00	kg	Basic Forming	Yes	Yes
6	Rapid Prototype - Stereo Lith.	\$ 32.00	kg	Basic Forming		Yes
7	Sand Casting	\$ 3.00	kg	Basic Forming	Yes	
8	Cure, Autoclave	\$ 50.00	m^2	Composite	Yes	
9	Cure, Oven	\$ 20.00	m^2	Composite	Yes	
10	Lamination, Manual	\$ 35.00	m^2	Composite		
11	Potting	\$ 0.50	cm	Composite		
12	Resin application, Infusion Molding	\$ 2.50	m^2	Composite		
13	Resin application, Manual	\$ 5.00	m^2	Composite		
14	Room Temperature Cure	\$ 10.00	m^2	Composite	Yes	
15	Attach Wire, Fork	\$ 0.25	unit	Electrical - Attach Wires		
16	Attach Wire, Quick connect terminal	\$ 0.10	unit	Electrical - Attach Wires		
17	Attach Wire, Ring	\$ 0.48	unit	Electrical - Attach Wires		
18	Attach Wire, Solder wire, bent	\$ 0.35	unit	Electrical - Attach Wires		
19	Attach Wire, Solder wire, not bent	\$ 0.52	unit	Electrical - Attach Wires		
20	Attach Wire, Terminated wire with screw	\$ 0.35	unit	Electrical - Attach Wires		
21	Attach Wire, Terminated wire with screw a	\$ 0.52	unit	Electrical - Attach Wires		
22	Attach Wire, Wire to screw	\$ 0.48	unit	Electrical - Attach Wires		
23	Attach Wire, Wire to screw with nut	\$ 0.65	unit	Electrical - Attach Wires		
24	Attach Wire, Wire to terminal block	\$ 0.35	unit	Electrical - Attach Wires		
25	Attach Wire, Wire wrap around terminal p	\$ 0.27	unit	Electrical - Attach Wires		
26	Install Cable Clamp (Zip Tie)	\$ 0.09	unit	Electrical - Bundle Install		
27	Wire Dressing (Install and route)	\$ 1.00	m	Electrical - Bundle Install		
28	Insert Bundle Into Tube or Sleeve	\$ 0.02	m	Electrical - Bundle Processing		
29	Install Adhesive Cable Clamp	\$ 0.19	unit	Electrical - Bundle Processing		
30	Lace	\$ 0.15	unit	Electrical - Bundle Processing		
31	Shrink Tube	\$ 0.15	cm	Electrical - Bundle Processing		
32	Taping Wire Bundle	\$ 0.04	m	Electrical - Bundle Processing		
33	Connector Install, Circular, Bayonet	\$ 0.11	unit	Electrical - Connections		
34	Connector Install, Circular, Friction	\$ 0.14	unit	Electrical - Connections		
35	Connector Install, Circular, Screw Thread	\$ 0.24	unit	Electrical - Connections		
36	Connector Install, Square, Friction	\$ 0.14	unit	Electrical - Connections		
37	Connector Install, Square, Latch/Snap-on T	\$ 0.17	unit	Electrical - Connections		
38	Connector Install, Square, Screw (x2)	\$ 0.50	unit	Electrical - Connections		

39	Connector Install, Square, Spring Clip	\$	0.20	unit	Electrical - Connections
40	Lay Wire - Control	\$	0.02	m	Electrical - Layout
41	Lay Wire - Power	\$	0.03	m	Electrical - Layout
42	Lay Wire - Signal	\$	0.02	m	Electrical - Layout
43	Crimp Wire	\$	0.17	unit	Electrical - Prep
44	Cut wire	\$	0.08	unit	Electrical - Prep
45	Strip Multi-Conductor	\$	0.13	wire(s)	Electrical - Prep
46	Strip Wire	\$	0.08	unit	Electrical - Prep
47	Tin Wire	\$	0.13	unit	Electrical - Prep
48	Connector Assembly, Crimp	\$	0.36	contacts	Electrical - Wire in Connector
49	Connector Assembly, Solder	\$	0.24	contacts	Electrical - Wire in Connector
50	Hand - Start Only	\$	0.12	unit	Fasteners
51	Hand, Loose <= 25.4 mm	\$	0.50	unit	Fasteners
52	Hand, Loose <= 6.35 mm	\$	0.25	unit	Fasteners
53	Hand, Loose > 25.4 mm	\$	0.75	unit	Fasteners
54	Hand, Tight <= 6.35 mm	\$	0.50	unit	Fasteners
55	Power Tool <= 25.4 mm	\$	0.25	unit	Fasteners
56	Power Tool <= 6.35 mm	\$	0.25	unit	Fasteners
57	Power Tool > 25.4 mm	\$	0.50	unit	Fasteners
58	Ratchet <= 25.4 mm	\$	0.75	unit	Fasteners
59	Ratchet <= 6.35 mm	\$	0.50	unit	Fasteners
60	Ratchet > 25.4 mm	\$	1.50	unit	Fasteners
61	Reaction Tool <= 25.4 mm	\$	0.25	unit	Fasteners
62	Reaction Tool <= 6.35 mm	\$	0.25	unit	Fasteners
63	Reaction Tool > 25.4 mm	\$	0.50	unit	Fasteners
64	Screwdriver < 1 Turn	\$	0.12	unit	Fasteners
65	Screwdriver > 1 Turn	\$	0.50	unit	Fasteners
66	Wrench <= 25.4 mm	\$	1.50	unit	Fasteners
67	Wrench <= 6.35 mm	\$	1.00	unit	Fasteners
68	Wrench > 25.4 mm	\$	2.00	unit	Fasteners
69	Sewing	\$	0.08	cm	Joining
70	Weld	\$	0.15	cm	Joining
71	Adjustment - Misc.	\$	5.00	unit	Labor
72	Aerosol Apply	\$	5.25	m^2	Labor
73	Assemble, >20 kg, Interference	\$	5.63	unit	Labor
74	Assemble, >20 kg, Line-on-Line	\$	3.75	unit	Labor
75	Assemble, >20 kg, Loose	\$	1.88	unit	Labor
76	Assemble, 1 kg, Interference	\$	0.19	unit	Labor
77	Assemble, 1 kg, Line-on-Line	\$	0.13	unit	Labor
78	Assemble, 1 kg, Loose	\$	0.06	unit	Labor



79 Assemble, 10 kg, Interference	\$	1.88	unit	Labor
80 Assemble, 10 kg, Line-on-Line	\$	1.25	unit	Labor
81 Assemble, 10 kg, Loose	\$	0.63	unit	Labor
82 Assemble, 15 kg, Interference	\$	2.81	unit	Labor
83 Assemble, 15 kg, Line-on-Line	\$	1.88	unit	Labor
84 Assemble, 15 kg, Loose	\$	0.94	unit	Labor
85 Assemble, 20 kg, Interference	\$	3.75	unit	Labor
86 Assemble, 20 kg, Line-on-Line	\$	2.50	unit	Labor
87 Assemble, 20 kg, Loose	\$	1.25	unit	Labor
88 Assemble, 3 kg, Interference	\$	0.56	unit	Labor
89 Assemble, 3 kg, Line-on-Line	\$	0.38	unit	Labor
90 Assemble, 3 kg, Loose	\$	0.19	unit	Labor
91 Assemble, 5 kg, Interference	\$	0.94	unit	Labor
92 Assemble, 5 kg, Line-on-Line	\$	0.63	unit	Labor
93 Assemble, 5 kg, Loose	\$	0.31	unit	Labor
94 Brake Bleed - Per Bleeder Valve	\$	2.50	unit	Labor
95 Brush Apply	\$	0.02	cm^2	Labor
96 Cut (scissors, knife)	\$	0.06	cm	Labor
97 Liquid Applicator Gun	\$	0.02	cm	Labor
98 Liquid Apply - Spot	\$	0.10	unit	Labor
99 Machining Setup, Change	\$	0.65	unit	Labor
100 Machining Setup, Install and remove	\$	1.30	unit	Labor
101 Suspension Setup - Solid Axle (per corner)	\$	4.50	unit	Labor
Suspension Setup-Independent Susp. (per				
corner)	\$	8.75	unit	Labor
103 Tape	\$	0.80	m	Labor
104 Drilled hole < 50.8 mm dia.	\$	0.70	hole	Material Removal
105 Drilled holes < 25.4 mm dia.	\$	0.35	hole	Material Removal
106 EDM - Plunge		\$0.30	cm^3	Material Removal
107 EDM - Wire	\$	0.20	cm	Material Removal
108 Grind, Cylindrical	\$	0.15	cm^2	Material Removal
109 Grind, Flat	\$	0.15	cm^2	Material Removal
110 Grind, Profile	\$	0.15	cm^2	Material Removal
111 Laser Cut	\$	0.10	cm	Material Removal
112 Lathe - Face, Finish	\$	0.04	cm^3	Material Removal
113 Lathe - Face, Rough	\$	0.04	cm^3	Material Removal
114 Lathe - Turn, Finish	\$	0.04	cm^3	Material Removal
115 Lathe - Turn, Rough	\$	0.04	cm^3	Material Removal
116 Mill - End, Finish	\$	0.04	cm^3	Material Removal

117 Mill - End, Rough	\$	0.04	cm <sup>3</sup>	Material Removal
118 Mill - Face, Finish	\$	0.04	cm <sup>3</sup>	Material Removal
119 Mill - Face, Rough	\$	0.04	cm <sup>3</sup>	Material Removal
120 Mill - Form Cutter	\$	0.10	cm	Material Removal
121 Non-metallic cutting <= 25.4 mm	\$	0.35	cut	Material Removal
122 Non-metallic cutting <= 50.8 mm	\$	0.70	cut	Material Removal
123 Non-metallic cutting <= 76.2 mm	\$	1.05	cut	Material Removal
124 Non-metallic cutting > 76.2 mm	\$	1.40	cut	Material Removal
125 Plasma Cutting	\$	0.10	cm	Material Removal
126 Reamed hole	\$	0.35	hole	Material Removal
127 Saw or tubing cuts	\$	0.40	cm	Material Removal
128 Tapping holes	\$	0.35	hole	Material Removal
129 Waterjet Cut	\$	0.10	cm	Material Removal
130 Sheet metal bends	\$	0.25	bend	Sheet Materials
131 Sheet metal punching	\$	0.03	cm <sup>2</sup>	Sheet Materials
132 Sheet metal shearing	\$	0.25	cut	Sheet Materials
133 Sheet metal stamping	\$	0.03	cm <sup>2</sup>	Sheet Materials
134 Tube bends	\$	0.75	bend	Tubing
135 Tube cut	\$	0.15	cm	Tubing
136 Tube end preparation for welding	\$	0.75	end	Tubing
137 Weld - Round Tubing	\$	0.38	cm	Tubing

## Appendix W – Detailed Cost Estimate (Elbow)

<b>Cost Estimate for Elbow Joint</b>								
<b>Purchased Parts</b>								
<b>Part</b>	<b>Supplier</b>	<b>ID</b>	<b>Price of 1</b>	<b>Price of 1000 units</b>	<b># parts needed</b>	<b>Cost of 1 of 1</b>	<b>Cost of 1 of 1000</b>	
Elevator Motor	RobotMarketPlace	ML50	\$26.95	\$26.95	1	\$26.95	\$26.95	
Shaft: 6mm	SDP-SI	A 7X 1M060075	\$4.44	\$3.08	1	\$4.44	\$3.08	
Bearings: 6mm bore	McMaster-Carr	7804K143	\$9.10	\$9.10	2	\$18.20	\$18.20	
Bearings: 3mm bore	SmallParts	632ZZ	\$6.00	\$6.00	1	\$6.00	\$6.00	
Miter gear	SDP-SI	A 1B 4MYK05020	\$15.73	\$11.33	2	\$31.46	\$22.66	
Worm	SDP-SI	A 1C 5MWK10RC	\$25.88	\$21.74	1	\$25.88	\$21.74	
Worm Gear	SDP-SI	A 1Z 6MWK10R020R	\$24.67	\$20.59	1	\$24.67	\$20.59	
Encoder	Mouser Electronics	N/A	\$56.25	\$56.25	1	\$56.25	\$56.25	
Passive Electrical Components	Mouser Electronics	N/A	\$3.00	\$2.00	1	\$3.00	\$2.00	
MCU	Mouser Electronics	579-PIC18F2455-I/SO	\$4.96	\$3.78	1	\$4.96	\$3.78	
H-Bridge	Mouser Electronics	511-L298P	\$5.87	\$5.87	1	\$5.87	\$5.87	
Voltage Regulator	Mouser Electronics	595-LP2951-33D	\$0.60	\$0.30	1	\$0.60	\$0.30	
<b>Grouped Parts</b>	<b>Supplier</b>	<b>ID</b>	<b>Price/pack (minimum)</b>	<b>Price/pack of 1000</b>	<b># packs needed</b>	<b># packs needed per 1000 parts</b>	<b>Cost of 1 of 1</b>	<b>Cost of 1 of 1000</b>
Screw: 10mm L Philips Pan Head M3	SmallParts	Phillips Pan Head Machine	\$5.50	\$55.00	1	19	\$5.50	\$1.05
Screw: 20mm L Philips Pan Head M3	SmallParts	Zinc Plated Steel Flat Head P	\$1.25	\$12.67	1	2	\$1.25	\$0.03
Set Screw	SmallParts	Metric Hex Socket Cup Point	\$1.96	\$261.40	1	4	\$1.96	\$1.05
<b>Purchased Subtotal</b>							<b>\$216.99</b>	<b>\$189.54</b>
<b>Manufactured Parts</b>								
<b>ABS Printing</b>	<b>Supplier</b>	<b>ID</b>	<b>Cost</b>	<b>Per unit</b>	<b>Quantity</b>	<b>Cost of 1 of 1</b>	<b>Cost of 1 of 1000</b>	
driven collar	N/A	N/A	0.27	cm^3	47.2	12.74	12.74	
bottom collar	N/A	N/A	0.27	cm^3	27.7	7.48	7.48	
plates	N/A	N/A	0.27	cm^3	20	5.40	5.40	
casing	N/A	N/A	0.27	cm^3	70	18.90	18.90	
<b>Machined</b>	<b>Supplier</b>	<b>ID</b>				<b>Cost of 1 of 1</b>	<b>Cost of 1 of 1000</b>	
Worm, Coupler, Pin	N/A	N/A				\$10.16	\$9.16	
<b>Printed Circuit Board</b>	<b>Supplier</b>	<b>ID</b>				<b>Cost of 1 of 1</b>	<b>Cost of 1 of 1000</b>	
Board	N/A	N/A				\$20.00	\$2.00	
<b>Manufactured Subtotal</b>						<b>\$74.69</b>	<b>\$55.69</b>	
<b>Total Production Cost</b>		1 of 1	1 of 1000					
		\$291.68	\$245.22					

## Appendix X – Detailed Cost Estimate (Rotator)

Cost Estimate for Rotator Joint								
Purchased parts								
Single Parts	Supplier	ID	Price per 1	Price per 1000 units	# parts needed		Cost of 1 of 1	Cost of 1 of 1000
Rotator Motor	RobotMarketPlace	Beetle B231 Gearmotor	\$39.99	\$39.99	1		\$39.99	\$39.99
Shaft: 6mm	SDP-SI	A 7X 1M060050	\$4.01	\$2.76	1		\$4.01	\$2.76
Bearings: 6mm bore	McMaster-Carr	7804K143	\$9.10	\$9.10	1		\$9.10	\$9.10
Encoder	Mouser Electronics		\$56.15	\$56.15	1		\$56.15	\$56.15
Passive Electrical Components	Mouser Electronics	N/A	\$3.00	\$2.00	1		\$3.00	\$2.00
IrDA Transceiver	Mouser Electronics	782-TDFU4300	\$3.65	\$2.12	1		\$3.65	\$2.12
MCU	Mouser Electronics	579-PIC18F2455-I/SO	\$4.96	\$3.78	1		\$4.96	\$3.78
H-Bridge	Mouser Electronics	511-L298P	\$5.87	\$5.87	1		\$5.87	\$5.87
Voltage Regulator	Mouser Electronics	595-LP2951-33D	\$0.60	\$0.30	1		\$0.60	\$0.30
Grouped Parts	Supplier	ID	Price/pack (minimum)	Price/pack of 1000	# packs needed	# packs needed per 1000 parts	Cost of 1 of 1	Cost of 1 of 1000
Screw: Philips Pan Head M3, 10l	SmallParts	Phillips Pan Head Machine	\$5.50	\$55.00	1	16	\$5.50	\$0.88
Set Screw	SmallParts	Metric Hex Socket Cup Point	\$1.96	\$261.40	1	2	\$1.96	\$0.52
Purchased Subtotal							\$134.79	\$123.47
Manufactured Parts								
ABS Printing	Supplier	ID	Cost	Per unit	Quantity		Cost of 1 of 1	Cost of 1 of 1000
driven collar	N/A	N/A	0.27	cm^3	25.05		6.76	6.76
bottom collar	N/A	N/A	0.27	cm^3	24.49		6.61	6.61
plates	N/A	N/A	0.27	cm^3	19.29		5.21	5.21
casing	N/A	N/A	0.27	cm^3	82.31		22.22	22.22
Machined Parts	Supplier	ID					Cost of 1 of 1	Cost of 1 of 1000
Coupler, Shaft	N/A	N/A					\$7.44	\$6.46
Printed Circuit Board	Supplier	ID					Cost of 1 of 1	Cost of 1 of 1000
Board	N/A	N/A					\$20.00	\$2.00
Manufactured Subtotal							\$68.25	\$49.27
Total Production Cost		1 of 1	\$203.04		1 of 1000			\$172.74